U.S. DEPARTMENT OF COMMERCE
National Technical Information Service

PB-260 088

KINETICS OF ALGAL SYSTEMS IN WASTE TREATMENT
LIGHT INTENSITY AND NITROGEN CONCENTRATION AS GROWTH-LIMITING FACTORS

CALIFORNIA UNIVERSITY, BERKELEY

PREPARED FOR
FEDERAL WATER POLLUTION CONTROL
ADMINISTRATION, WASHINGTON, D. C.

MAY 1968

002248

253052

PB 260 088

KINETICS OF ALGAL SYSTEMS IN WASTE TREATMENT

LIGHT INTENSITY AND NITROGEN CONCENTRATION AS GROWTH-LIMITING FACTORS

LIBRARY
FWPCA, Ohio Basin Region
4676 Columbia Pkwy. Cinti, O. 45226

REPRODUCED BY
NATIONAL TECHNICAL
INFORMATION SERVICE
U. S. DEPARTMENT OF COMMERCE
SPRINGFIELD, VA. 22161

SANITARY ENGINEERING RESEARCH LABORATORY
COLLEGE OF ENGINEERING
AND
SCHOOL OF PUBLIC HEALTH
UNIVERSITY OF CALIFORNIA
BERKELEY
SERL REPORT No. 68-4

197

C

BIBLIOGRAPHIC DATA SHEET	1. Report No.	2.	3. Recipient's Accession No. PB-260 088

4. Title and Subtitle
Kinetics of Algal Systems in Waste Treatment. Light Intensity and Nitrogen Concentration as Growth-Limiting Factors

5. Report Date
May 68

6.

7. Author(s) Gedalia Shelef, W. J. Oswald, and C. G. Golueke

8. Performing Organization Rept. No. SERL-68-4

9. Performing Organization Name and Address
California Univ., Berkeley. Sanitary Engineering Research Lab.

10. Project/Task/Work Unit No.

11. Contract/Grant No.

12. Sponsoring Organization Name and Address
Federal Water Pollution Control Administration, Washington, D. C.

13. Type of Report & Period Covered

14.

15. Supplementary Notes

16. Abstracts

Kinetic models describing the relationships between algal biomass production and both incident irradiance and the concentration of nitrogen were developed and tested under controlled laboratory conditions. The applicability of these models to the prediction and evaluation of the performance of algal systems in waste treatment received special attention. Of three models developed, the macroscopic model based on the exponential relationship between irradiance and algal specific growth rate at the microscopic level proved to be the one most compatible with the experimental results under the conditions of a chemostatic algatron reactor.

17. Key Words and Document Analysis. 17a. Descriptors

17b. Identifiers/Open-Ended Terms

*Algae
*Waste treatment
Nitrogen cycle
Tables(Data)
*Mathematical Models
Irradiation
Ecosystems
Light scattering
*Growth
Biomass

17c. COSATI Field/Group 13B

18. Availability Statement	19. Security Class (This Report) UNCLASSIFIED	21. No. of Pages 197p
	20. Security Class (This Page) UNCLASSIFIED	22. Price

KINETICS OF ALGAL SYSTEMS
IN WASTE TREATMENT

Light Intensity and Nitrogen Concentration
As Growth-Limiting Factors

by

Gedalia Shelef
W. J. Oswald
C. G. Golueke

Federal Water Pollution Control Administration
U. S. Department of the Interior
Grant No. 00975-01A1

May 1968

Sanitary Engineering Research Laboratory
College of Engineering
and
School of Public Health
Berkeley

SERL Report No. 68-4

ABSTRACT

Kinetic models describing the relationships between algal biomass production and both incident irradiance and the concentration of nitrogen were developed and tested under controlled laboratory conditions. The laboratory work was conducted with the use of continuous algal cultures at steady state in which selected strains of Chlorella pyrenoidosa constituted the experimental organisms. The applicability of these models to the prediction and evaluation of the performance of algal systems in waste treatment received special attention. These models can be applied also to other algal biomass production systems, such as those designed for protein production or for photosynthetic life support.

Three models describing the relationship between algal specific growth rate and irradiance were developed and evaluated: a) a model based on energy balance and/or a "zero order-first order" kinetic relationship; b) one based on the rectangular hyperbola function; and c) another based on the exponential function describing the relationship between the algal specific growth rate and irradiance. The models incorporate the spectral distribution of the light source as it affects the essential parameters — light conversion efficiency and light transmission in an optically dense algal suspension. Each of the models represents the interrelationship existing at steady state conditions between dilution rate, associated algal concentration, and the expected average net specific growth rate and net algal production at a given incident irradiance. The condition which permits algal growth and production to proceed at maximum level can be estimated analytically.

Of the three models, the macroscopic model based on the exponential relationship between irradiance and algal specific growth rate at the microscopic level proved to be the one most compatible with the experimental results under the conditions of a chemostatic algatron reactor.

The relationship between nitrate-nitrogen concentration and algal specific growth rate under conditions of light saturation in a continuous culture of Chlorella pyrenoidosa was determined by using both chemostatic and turbidostatic control. The Modified Exponential Function best described this relationship and the various parameters of this function were determined in the laboratory. The Modified Exponential Function was found also to be applicable in optically dense algal cultures in describing the relationship between nitrate-nitrogen concentration and the average net algal specific growth rate or net algal production.

Preceding page blank

TABLE OF CONTENTS

Page

ABSTRACT iii

LIST OF TABLES xi

LIST OF FIGURES xii

Chapter

I. INTRODUCTION 1

Advantages of Unicellular Algae in a Controlled System 1

Applications of Controlled Algal Systems 1

Use of Algae in Waste Treatment 1

Photosynthetic Oxygenation of Organic Wastes 2

Nutrient Removal 2

Use of Algal Culture for Proteinaceous Feedstuff Production 3

Use of Algal Systems for Life Support Systems 3

Light (Irradiance) and Nitrogen as the Limiting Factors in Algal Systems 4

Light 4

Nitrogen 4

Need for a Rational Approach in the Design and Evaluation of Algal Waste Treatment Systems 4

Objectives of the Research 5

General Objectives 5

Specific Objectives 6

Organization of Research 6

II. ENERGY BALANCE ON AN ALGAL SYSTEM 7

Introduction 7

Light Conversion Efficiencies of Algal Systems in Waste Treatment 7

Energy Balance Model 8

Basic Assumptions 8

Thermodynamic Efficiency, E_m 9

Preceding page blank

TABLE OF CONTENTS (Continued)

Chapter Page

Light Utilization Efficiency E_g 11

Incident Light Intensity. 18

Illuminance as Contrasted to Irradiance 18

Spectral Distribution of the Light Source 18

Transmitted and Absorbed Light by Algal Suspension 21

Decay 22

Endogenous Respiration 22

Formulation of the Energy Balance Model 23

III. KINETICS OF ALGAL GROWTH AND PRODUCTION WITH RESPECT TO LIGHT INTENSITY 26

Basic Assumptions 26

Algae Growth vs. Light Intensity at the Microscopic Level 26

Basic Mechanisms of Photosynthesis 27

"First Order—Zero Order" Type Kinetic Model (Model I) 28

The Rectangular Hyperbolic Model (Model II) 31

The Exponential Model (Model III) 33

Comparison Between the Various Kinetic Models on the Microscopic Level 34

Algae Growth and Production as Functions of Light Intensity at the Macroscopic Level 35

Macroscopic Model I — "First Order—Zero Order" Type 37

Macroscopic Model II (Based on the Rectangular Hyperbolic Microscopic Model) 43

Macroscopic Model III (Based on the Exponential Microscopic Model). 45

A Comparison Between the Various Macroscopic Models 46

IV. ALGAL GROWTH KINETICS WITH RESPECT TO NITROGEN CONCENTRATIONS . . 48

Introduction 48

Review of Literature 48

Nitrogen Cellular Content 48

Nitrogen Assimilation Mechanism 49

Algal Growth as a Function of Nitrogen Concentration in the Medium. 49

TABLE OF CONTENTS (Continued)

Chapter Page

Nitrogen Fixation 50

Nitrogen Aspects in Waste Treatment and Pollution Control 50

The Kinetic Model of Algal Growth and Nitrogen Removal with Respect to Nitrogen Concentration Under Light-Saturation Conditions 52

Basic Assumptions 52

Specific Growth Rate as a Function of Nitrogen Concentration 54

The Michaelis-Menten-Type Function 54

Moser's Function 56

Teissier's Exponential Function 56

The Modified Exponential Function 57

A Comparison Between Michaelis-Menten and the Modified Exponential Functions 59

Materials Balance of a Chemostatic or Turbidostatic Algal Continuous System 59

V. GROWTH AND PRODUCTION OF ALGAE IN SYSTEMS IN WHICH BOTH LIGHT AND NITROGEN ARE LIMITING 61

VI. EXPERIMENTAL METHODOLOGY 64

Experimental Organisms 64

Algal Growth Units 64

Chemostatic Growth Units 64

Turbidostatic Growth Unit 65

Chemostatic Algatron 71

Media and CO_2 75

Media 75

CO_2 Supply 75

Light 78

Light Sources 78

Iodine-Quartz Incandescent Lamps 78

High-Temperature Sodium Vapor Arc Lamps 78

Full Spectrum Fluorescent Lamps 78

TABLE OF CONTENTS (Continued)

Chapter Page

Light Measurements 80

Incident Irradiance 80

Spectral Distribution 80

Spectral Absorbence and Transmittance by the Algal Suspension 80

Total Light Transmitted by the Algal Suspension 80

Geometrical Distribution of Candle Power of the Light Source 80

Light Filters 82

Sampling and Analyses 82

Sampling 82

Solids Determination 82

Nitrogen Determinations 82

Chlorophyll Determinations 83

Criteria for Steady State Conditions 83

Computations 83

VII. EXPERIMENTAL RESULTS AND DISCUSSION 84

Light as a Growth-Limiting Factor 84

Application of the Theoretical Models to the Algatron 84

Experimental Results as Compared to the Theoretical Models 88

Light Transmission 88

Algal Growth and Production 93

Compatability of the Theoretical Models with the Experimental Results 93

Applicability of Model III 94

Discrepancies Between the Experimental Data and Model III 101

Light Sources Comparison 102

Nitrogen as a Growth-Limiting Factor 102

General Patterns 112

Growth Curves 112

TABLE OF CONTENTS (Continued)

Chapter Page

Yield Coefficient 113

Best Fit Kinetic Function 113

The Michaelis-Menten Equation 113

The Modified Exponential Function 114

Recommended Parameters for the Growth Curve 115

Specific Experiments 115

Experiment 1. Temperature 35°C 115

Experiment 2. Temperature 39.2°C 116

Experiment 3. Temperature 28.5°C 115

Experiment 4. Temperature 19°C 116

The Effect of Temperature 117

Nitrogen as the Growth-Limiting Factor in an Optically Dense Culture 117

Comparison with the Experiment on Growth as a Function of NO_3-N Under Light Saturation (Experiment 3). 120

Algal Systems Designed for Assimilative Removal of Nutrients 124

VIII. CONCLUSIONS 126

General Conclusions 126

Specific Conclusions 126

Kinetic Models with Respect to Light Intensity (Irradiance) 126

Kinetic Models with Respect to Nitrogen Concentration 127

Kinetic Model with Respect to Both Light and Nitrogen 127

IX. RECOMMENDATIONS 129

General 129

Specific 129

TABLE OF CONTENTS (Continued)

Chapter Page

APPENDICES 131

A. Nitrate Medium 133

B. Remarks on the Effect of Autocatalysis on the Order of Reaction in Microbial Propagation as Compared to Chemical Reactions 136

C. The Rectangular Hyperbola Function as it Applies to Various Kinetic Models of Microbial Propagations 138

D. The Mathematical Development of Macroscopic Model II 142

E. The Mathematical Development of Macroscopic Model III 144

F. Light Sources 146

G. Light Transmittance of Various Filters 159

H. Computer Programs 162

I. Glossary 172

REFERENCES 177

LIST OF TABLES

Table	Title	Page
I.	Important Dimensions of Various Components in the Algatron	71
II.	Irradiance and Spectral Distribution Input Data	89
III.	Summary of Experimental Results as Compared with Results on the Basis of Theoretical Kinetic Models of Algal Growth with Respect to Irradiance	94
IV.	A Summary of Kinetic and Statistical Parameters of the Experiments with Algal Growth with Respect to Nitrogen Concentration	111
V.	Summary of Experimental Results Attained with an Optically Dense Culture in which Nitrogen was Limiting	121
VI.	Composition of Modified Myers' Nitrate Medium	133
VII.	Formula of the Modified Arnon's Micronutrient Stock Solution	134
VIII.	Composition of SERL Nitrate Medium	134
IX.	General Characteristics of the Light Sources Used in the Study	147

LIST OF FIGURES

Figure	Title	Page
1.	Quantum Conversion as a Function of Wavelength	10
2.	Quantum Efficiency (E_q) as a Function of Wavelength (λ) for Various Values of Quantum Requirement ($1/\phi$)	12
3.	Relative Quantum Yield Coefficient Q_λ as a Function of Wavelength (λ)	13
4.	Irradiance Decay in Algal Suspension as a Function of Depth, Showing the Relationship Between the Efficiency of Light Utilization (E_s) and the Incident Irradiance (I_o)	15
5.	Efficiency of Light Utilization (E_s) and Total Light Conversion Efficiency (E_T) as a Function of Incident Irradiance (I_o) at Various Levels of Light Saturation Intensity (I_s)	17
6.	Gross Algae Production (P_a) as a Function of Incident Irradiance (I_o)	19
7.	Spectral Luminous Efficiency Curve and Relative Action Spectrum of Chlorella pyrenoidosa	20
8.	Specific Growth Rate (μ_x) as a Function of Irradiance (I_x) for Various Microscopic Kinetic Models	30
9.	Comparison Between Three Kinetic Models on the Microscopic Level	36
10.	Light Intensity Gradient Within an Algal Suspension	38
11.	Specific Growth Rate on the Microscopic Level (μ_x) as a Function of Algal Suspension Depth (x) When Incident Irradiance (I_o) is Applied at the Surface	39
12.	Gross Production of Algae (P_a) and Relative Average Specific Growth Rate ($\bar{\mu}$) as a Function of the Incident Irradiance (I_o), According to Various Macroscopic Kinetic Models	42
13.	The Relationship Between the Growth-Limiting Substrate Concentration (S_N) and Specific Growth Rate (μ), as Described by Michaelis-Menten Theorem	55
14.	The Relationship Between the Growth-Limiting Substrate Concentration (S_N) and Specific Growth Rate (μ), According to the Proposed "Modified Exponential Function"	58
15.	Schematic Flow Sheet of CSTR-Type Growth Unit	59
16.	Irradiance Gradient, Specific Growth Rate and Algal Production in Two Hypothetical Optically Dense Algal Cultures of Different Concentrations when Nitrogen Constitutes a Growth Limiting Factor	62

LIST OF FIGURES (Continued)

Figure Title Page

17. Diagrammatic Sketch of the Chemostat Growth Unit System . . . 66

18. Setup of Growth Units . . . 67

19. Diagrammatic Sketch of the Turbidostatic Growth Unit System . . . 68

20. The Turbidostatic Growth Unit with Optical Density Sensor . . . 69

21. Block Diagram of Density Regulating System . . . 70

22. Optical Density Sensor . . . 70

23. Algatron Prototype — Arrangement and Components . . . 72

24. The Algatron Chemostatic Unit . . . 73

25. The Algatron Drum (A), Showing the Iodine-Quartz Light Source with Water Jacket (B) . . . 74

26. Position of Algae Culture in Respect to Iodine-Quartz Light Source . . . 76

27. Position of Algae Culture in Respect to "Lucalox" Lamp . . . 77

28. Iodine-Quartz Lamps - Arrangement . . . 79

29. Arrangement for the Measurement of Total Light Transmitted by an Algal Suspension . . . 81

30. Light Transmission as a Function of Wavelength in a Suspension of *C. pyrenoidosa* . . . 90

31. The Light Extinction Coefficient, α_λ, as a Function of Wavelength in a Suspension of *C. pyrenoidosa* . . . 91

32. Total Extinction Coefficient, α_λ, as a Function of Concentration of *C. pyrenoidosa* at a Constant Culture Depth of 1.7 cm . . . 92

33. Algal Net Production as a Function of Dilution Rate (Iodine-Quartz Light Source) . . . 95

34. Algal Concentration in the Reactor as a Function of Dilution Rate (Iodine-Quartz Light Source) . . . 96

35. Algal Production as Related to Algal Concentration (Iodine-Quartz Light Source) . . . 97

36. Algal Net Production as a Function of the Dilution Rate ("Lucalox" Lamp as Light Source) . . . 98

37. Algal Concentration as a Function of the Dilution Rate ("Lucalox" Lamp as Light Source) . . . 99

38. Algal Production as Related to Algal Concentration ("Lucalox" Lamp as Light Source) . . . 100

LIST OF FIGURES (Continued)

Figure	Title	Page
39.	Algal Net Specific Growth Rate and Yield Coefficient as Functions of Nitrate Concentration (Experiment 1)	103
40.	Regression Analysis of the Modified Exponential Function, Using the Data Obtained in Experiment 1	104
41.	Algal Net Specific Growth Rate and Yield Coefficient as Functions of Nitrate Concentration (Experiment 2)	105
42.	Regression Analysis of the Modified Exponential Function, Using the Data Obtained in Experiment 2	106
43.	Algal Net Specific Growth Rate and Yield Coefficient as Functions of Nitrate Concentration (Experiment 3)	107
44.	Regression Analysis of the Modified Exponential Function, Using the Data Obtained in Experiment 3	108
45.	Algal Net Specific Growth Rate and Yield Coefficient as Functions of Nitrate Concentration (Experiment 4)	109
46.	Regression Analysis of the Modified Exponential Function, Using the Data Obtained in Experiment 4	110
47.	The Effect of Temperature on the Net Specific Growth Rate of C. pyrenoidosa with Respect to Nitrate Concentration	118
48.	The Effect of Temperature on Various Growth Kinetic Parameters of C. pyrenoidosa with Respect to Nitrate Concentration	119
49.	Nitrogen Concentration as a Growth-Limiting Factor in an Optically Dense Culture	122
50.	Titration Curves of Modified Myers' Nitrate Medium and SERI Nitrate Medium	135
51.	Spectral Energy Distribution of Iodine-Quartz Lamp	148
52.	Incident Irradiance Distribution at Culture Surface — Iodine-Quartz Lamp	149
53.	Vertical Relative Candle Power Distribution of Iodine-Quartz Lamps (With Water Jacket)	150
54.	Horizontal Relative Candle Power Distribution of Iodine-Quartz Lamps (With Water Jacket)	151
55.	Energy Spectral Distribution of the Lucalox Lamp	152
56.	Incident Irradiance Distribution at Culture Surface — Lucalox Lamp	153
57.	Vertical Relative Candle Power Distribution of the Lucalox Lamp	154
58.	Horizontal Relative Candle Power Distribution of the Lucalox Lamp	155

LIST OF FIGURES (Continued)

Figure	Title	Page
59.	Relative Energy Spectral Distribution of the Optima Fluorescent Lamp	156
60.	Energy Spectral Distribution of Solar Irradiation	157
61.	Energy Spectral Distribution of Sunlight	158
62.	Spectral Transmittance of Fish-Schurman Multilayer Interference Film Filters	160
63.	Spectral Transmittance of Optical Coating Wide-Band Hot Mirror Filter	161
64.	Spectral Internal Transmission of Schott Color Glass Filters . . .	161

I. INTRODUCTION

The photosynthetic reaction as it takes place in Chlorella pyrenoidosa, one of the more common and most thoroughly studied forms of green algae, may be expressed by the following stoichiometric equation, according to Oswald[1]:

$$NH_4^+ + 7.6\ CO_2 + 17.7\ H_2O \rightarrow C_{7.6}H_{8.1}O_{2.5}N + 7.6O_2 + 15.2\ H_2O + H^+ . \qquad (1\text{-}1)$$

The equation shows that in the photosynthetic reaction, oxygen is produced and a proteinaceous biomass is synthesized from a collection of inorganic materials, CO_2, and water. Moreover, a maximum net production of algal biomass will result in a maximum production of oxygen, maximum absorption of CO_2, and maximum assimilation of nutrients, i.e., maximum removal of these nutrients from the aqueous solution.

ADVANTAGES OF UNICELLULAR ALGAE IN A CONTROLLED SYSTEM

Algal culture as a means of crop production has many advantages over conventional agriculture which is the other controlled photosynthetic process. Perhaps the most important advantage of algal culture is the five- to fifteen-fold increase in areal yield on an energy basis over that obtained in conventional agriculture [2-4]. Other advantages of algal systems are as follows:

1. Algae have a high specific growth rate and continuous reproduction.
2. Algae have a high protein, fat, and vitamin content, and a minimum of unusable (as a feedstuff) structural material (xylem, fiber, cork, etc.).
3. Algae are grown in an aquatic environment in which optimum conditions of moisture can result in dense cultures.
4. A relatively dense algal suspension, highly efficient in respect to light energy utilization, can withstand high pressures and conditions of high acceleration, weightlessness, continuous pumping, turbulent mixing, and other conditions which may exist in mechanized reactors both on earth and in extraterrestrial applications.

APPLICATIONS OF CONTROLLED ALGAL SYSTEMS

The main advantage of algal culture results primarily from the simultaneous accomplishment of biomass production, oxygen production, CO_2 absorption, and nutrient utilization and removal associated with the photosynthetic reaction. Among the more important applications are protein production, waste treatment, and biogenerative life support systems. In this study the application in the field of waste treatment will be stressed with emphasis on assimilative algal nutrient removal. However, it should be noted that the basic techniques, engineering design, and scientific principles involved in algal systems in waste treatment are almost identical to the algal mass cultures designed for tasks other than waste treatment.

Use of Algae In Waste Treatment

In waste treatment, algal processes can be used as secondary treatment systems fed by organic wastes, as tertiary treatment for removal of soluble mineral nutrients, or as combined secondary-tertiary treatment where both the reduction of BOD as well as nutrient removal are objectives of the treatment.

Photosynthetic Oxygenation of Organic Wastes. The use of an algal-bacterial symbiotic culture system as a means of photosynthetic oxygenation in the aerobic oxidation of sewage was studied by Oswald and Gotaas [5-7] at the University of California (Berkeley) in the early 1950's. Their findings led to development of the concept of "high-rate" pond systems for waste treatment. The principal objectives of the high-rate pond system concept are BOD and algal nutrient removal, and the production of algal-biomass for use as an animal feedstuff.

BOD is removed through bacterial oxidation of the organic matter. The oxygen used by the bacteria can be produced by the algae. The application of the high-rate pond system solely as a means of BOD removal does not seem to be economically justified when conventional systems such as the activated sludge and the trickling filter are available. The reason is in the need for removing the algal biomass from the treated water before it can be discarded into receiving waters without giving rise to pollutional problems. The cost of removing the algae -- considering the present state of technology -- is prohibitive.

An apparent solution to the relatively high cost of removing the algae would be to process the biomass as a feedstuff and thereby have a product to sell. Money thus obtained could be used to defray the cost of harvesting. This possibility was explored in the University of California studies in which it was found by Hintz [8,9] that sewage-grown algae served as an excellent source of protein for the test animals, i.e., comparable to soybean oil meal for sheep and fish meal for swine.

The economic feasibility of the high-rate pond system depends upon the cost of producing the algae, its sales value, and the demand for the product. For the present, information on these aspects is incomplete.

Nutrient Removal. The removal of algae growth-promoting substances from waste effluents by mass cultures of algae under controlled conditions appears to be an effective method of nutrient removal. Experiments have shown that after a mass culture of algae has been grown on a waste effluent and the algae thus produced have been removed from the treated water, very little additional growth of algae can be supported by the water. Removal of a given amount of algal cellular material constitutes removal of a proportionate amount of nutrient. Depending upon the species of the algae and conditions under which they were grown, dried algae contain from 6% to 11% nitrogen and from 0.5% to 2% phosphorus [10,11].

The high content of nitrogen in algal biomass indicates that a substantial portion of the nitrogen removal from waste waters (and natural bodies of water) is by way of assimilation by the algae, i.e., conversion of soluble nitrogen into plant protein. Other minerals also can be removed. Bush for example [12] reports a reduction of approximately 40% in total soluble solids brought about by assimilation and precipitation of K^+, Ca^{++}, Mg^{++} $SO_4^=$, HCO_3^-, NO_3^-, NH_4^+, and $PO_4^\equiv$ following mass algal growth.

Biological stripping of algae growth-promoting substances includes the assimilative removal of micronutrients. The trace elements Mo, V, Co, Cu, Mn, Zn, and B have been demonstrated as being essential for the growth of algae [13]. In fact, one or more of them may be the limiting factor for the growth of phytoplankton and blooms in natural bodies of water [14].

Similar reasoning applies to the stripping of the more "exotic" growth stimulants such as vitamins and other biologically synthesized growth factors by the mass culture of algae. Among the vitamins, vitamin B_{12}, thiamine, and biotin have been shown to be essential to algal growth [15,16].

An evaluation of the economics of the use of a biological system involving the pregrowth of algal biomass solely for the removal of nutrients has yet to be made. It appears that the economic justification for the use of algae in nutrient removal will depend upon the recovery of algal biomass as a salable foodstuff.

It is possible to combine photosynthetic oxygenation for BOD removal and nutrient removal in one operation followed by the harvest of the algal biomass. Combined secondary-tertiary treatment has the advantages of reduced costs and increased algal yields — the latter due to an enhanced supply of CO_2 resulting from the bacterial degradation of the organic matter in the wastes. Thus far, studies on algal nutrient removal mostly have been limited. Experiments and observations ranging from laboratory- to full-scale treatment plants have been described by Parker [17], Bogan [18-20], Fitzgerald and Rohlich [21,22], Oswald et al. [23], Reid [24,25], Bush et al. [12], and others. To date, no studies on the kinetics of nutrient removal have been reported in the literature. This lack is one of the reasons for the dearth of rational design parameters for systems based on nutrient removal through the use of pregrown algal biomass.

Use of Algal Culture for Proteinaceous Feedstuff Production

Advantages in the use of algal systems for production of protein-rich feedstuffs as compared with conventional agriculture have resulted in focusing attention on the use of large-scale, controlled algal production systems. The possibility of using algal systems to meet at least a part of the protein shortage in developing countries such as India, Israel, Japan, and others is becoming recognized. As reported by Enebo [26] and Mitsuda [27], pilot-plant scale installations designed specifically for protein production with a surface area of 1/8 to 1/4 acre are currently in the preliminary stages of development in Czechoslovakia and Japan.

General features common to all algal mass culture systems are: 1) a controlled reactor illuminated primarily by sunlight; 2) a rapidly growing algal culture operated as a continuous culture; 3) a suspending medium containing mineral nutrients; 4) a provision for adding CO_2 to the culture; and 5) a means for harvesting and processing the algae.

Use of Algal Systems for Life Support Systems

The use of algae grown in mass culture under carefully controlled conditions is one of the types of life support systems proposed for prolonged space travel, space laboratories, and permanent extraterrestrial bases. The maximum dimensions of an algal photosynthetic reactor designed for a life support system is determined by its gas-exchange capacity, i.e., capacity for oxygen regeneration and CO_2 absorption. In addition to serving as gas exchangers, the reactor can function simultaneously as a device for organic waste treatment, nutrient removal, and water reclamation. The organic waste treatment function depends upon the symbiotic activity of algae and bacteria. The biomass, predominantly algal, may serve as an important food source. Thus the algal photosynthetic reactor can serve as an integrated life support system and in this respect it is unique as compared to regenerative processes which depend upon bacteria or on chemical and physical phenomena.

A detailed discussion of the complexities and technical ramifications of photosynthetic life support systems is beyond the scope of this presentation. Excellent reviews of the state of the art is contained in an article by Miller and Ward [28]. In brief, the major factors to be considered in arriving at a design for an algal photosynthetic reactor for a life support system are similar to those of an algal system designed for waste treatment. In both, light intensity, nutrient and organic loadings, and CO_2 supply are major factors, and the capacities of both are determined by the net production of the algal biomass through the photosynthetic process. Apparently the major difference between the two is that life support systems are of necessity more mechanized, and are more closely controlled as far as environmental conditions are concerned. This is in order to attain a maximum degree of efficiency, and a reduction insofar as is possible in volume, weight, and surface area requirements.

LIGHT (IRRADIANCE) AND NITROGEN AS THE LIMITING FACTORS IN ALGAL SYSTEMS

Many factors can be growth-limiting in an algal culture. Examples are light, CO_2, major nutrients, trace elements, vitamins, and other growth stimulants. Light and nitrogen were selected as the factors for consideration in this study for the following reasons.

Light. It can be assumed that algal growth in mass cultures is almost exclusively photolithotropic (autotrophic nutrition through photosynthesis). Because of this fact, light can be considered as the sole energy supply for an algal system. Consequently, light intensity is the determining factor for the system's maximum capacity, its physical dimensions, operational parameters, biomass concentrations, and biomass production.

Nitrogen. With production capacity determined by the energy supply, nitrogen, as well as any other essential nutrient, may be a limiting factor if its concentration is lower than the one needed to support the maximum growth possible from the energy source. The reason that nitrogen was selected for study as a nutritive limiting factor is that the concentration of nitrogen in domestic waste waters is relatively low in comparison to that of other essential nutrients, notably phosphorus. Thus, algae grown on domestic waste waters will usually reach the point of nitrogen starvation before any other nutrient becomes limiting.

Another reason why nitrogen is important as a limiting factor is the possible practical application of algal systems for the removal of nitrogen in various large-scale projects currently under study, viz., San Joaquin Valley Drainage Water System and the Greater Tel-Aviv (Israel) Waste Water Reclamation Project.

San Joaquin Valley drainage water ultimately will contain an estimated average of 21 mg/ℓ nitrogen (mostly in nitrate form). It has been suggested that such a high concentration of nitrogen could trigger and support heavy plankton blooms in the receiving waters of the Sacramento River Delta and the upper parts of San Francisco Bay. An algal system has been proposed by Oswald [29] as one means of the assimilative conversion of the nitrogen into algal biomass. The biomass would then be harvested, marketed, or otherwise disposed [30,31].

A large-scale waste water reclamation project for Greater Tel-Aviv is under design. This project is aimed at treating the waste water generated by more than a million people, recharging underground water with the treated waste water, and reusing the recharged water for domestic and irrigation uses. The treated wastes will have from 80 to 200 mg/ℓ of nitrogen as nitrate. Unless this nitrate is removed the quality of the reclaimed water will be lower than desirable. A large algal system designed for BOD removal and the assimilative removal of nitrogen and possibly the production of algae as a source of animal proteinaceous feedstuff has been proposed [29,32,33].

NEED FOR A RATIONAL APPROACH IN THE DESIGN AND EVALUATION OF ALGAL WASTE TREATMENT SYSTEMS

The complexity of algal systems in waste treatment together with a lack of sufficient data are major problems in the design of practical algal systems. Unfortunately, much of the available data is uninterpretable and cannot be generalized for practical use. Ostensibly missing are many of the basic parameters of biological processes such as concentration of biomass, specific growth rates, cellular substrate loading and removal coefficients, yield coefficients, energy-mass balances, etc., which could furnish a kinetic basis for application of the algal system.

The use of an empirical approach in the design of algal systems has resulted in the almost complete neglect of the biological processes involved and the driving forces of the key reactions. Thus it has been difficult to improve the performance or to understand the real potential and limitations of the process. The empirical approach has made it difficult for the engineer to apply the developments resulting from algal research in related fields. Valuable information on algae developed by algologists, plant biochemists, limnologists, and marine and aquatic biologists has not been considered adequately in the design of algal waste treatment plants. This is probably one of the reasons why the use of algal systems in waste treatment is still controversial.

An urgent need exists to develop a rational kinetic model of an algae system based upon biological kinetic parameters to develop and interpret research and field findings; hopefully to employ these data into improved process design.

A few attempts have been made to develop design parameters for algal systems in waste treatment. However, most of these parameters pertain to BOD removal in ponds in which the major biological activity was that of the aerobic bacterial phase. Hermann and Gloyna [34,35] developed a design method in which BOD loadings are related to temperature according to the Van't Hoff theory of biological systems. Their approach was used in practice for the design and prediction of performance of "facultative" (aerobic-anaerobic) ponds. The complex of bacterial and algal activities in ponds appears to be temperature dependent and since temperature levels to some extent are related to the average prevailing sunlight irradiance, the method has some merit in the prediction of performance of facultative ponds. According to calculations based on Hermann and Gloyna's method, the rate coefficient for BOD removal in facultative ponds is only slightly higher than that in fairly stagnant natural bodies of water.

A different approach has been suggested by Marais [36,37]. His approach was to describe and design facultative ponds in series. He designed his ponds to be continuously stirred tank reactors (CSTR), and assumed organic substrate removal to take place as a first-order reaction. The overall design criteria in Marais' approach agrees with Hermann and Gloyna's formulations, although Marias' design tends to be slightly conservative due to the application of an increased safety factor. The effect of light, as the determining factor of the capacity of the algal phase was given little consideration in Hermann and Gloyna's and in Marais' approach, and the basic parameters for the design of their systems were the detention period and volumetric and surface organic loadings.

A rational method for the design of "high-rate" algae ponds based on the overall conversion efficiency of available visible light energy at average daily light intensities has been proposed by Oswald _et al_. [6,38,39]. This method, which deals directly with the algal phase, is based _upon_ the light energy flux as the determining factor for the design of the system, and relates the performance of the algal system to the total net production of the algal biomass. This method constitutes an important step in the development and the application of a photosynthetic algal reactor for waste treatment as well as for other applications. A detailed discussion of Oswald's approach and the one proposed in this presentation is given in Chapter II.

As with any method, Oswald's method of high-rate pond design requires further refinement, especially with respect to limiting factors as they affect the growth rate and production of the algal system. Overall light conversion efficiency is an example of a parameter which, although measured by Oswald under various environmental conditions, is entered in the design equations on the basis of an empirical estimate.

OBJECTIVES OF THE RESEARCH

General Objectives

The general objective of the research work described herein was to develop and test a kinetic model for the mass culture of algae with respect to irradiance (light intensity) and to nitrogen concentrations.

Specific Objectives

The specific objectives were as follows:

a. To develop theoretical models for predicting and evaluating the performance of algal systems primarily dependent upon light energy flux (irradiance). Included in such models would be all pertinent factors, especially those related to the spectral distribution of the light.

b. To test the models in an experimental reactor to find the one most compatible with experimental findings.

c. To determine the conditions required for maximum net production of algal biomass and to relate these conditions to the process parameters.

d. To establish the kinetic relationship between growth of algae and nitrate-nitrogen concentrations with special reference to algal production systems and the assimilative removal of nitrogen by algal biomass.

e. To develop a kinetic model based upon both light intensity and nitrogen concentration, to permit optimization of the assimilative removal of nitrogen, and to test this model.

ORGANIZATION OF RESEARCH

The research consists of two major phases, namely the theoretical development of various kinetic models and the testing of the models in the laboratory. However, the two phases were carried on simultaneously and the theoretical models were influenced by information feedback from the laboratory work.

Both the theoretical and the experimental phases are presented in the following order: a) kinetics with respect to light intensity (irradiance); b) kinetics with respect to nitrogen concentration; and, c) kinetics with respect to both light intensity and nitrogen concentration.

The research covered by this report is the first phase of a comprehensive study concerned with the development of kinetic models for the mass culture of algae with respect to irradiance and to important nutrient factors. The research is sponsored by the Federal Water Pollution Control Administration of the U. S. Department of the Interior (Grant No. 00975-01A1).

II. ENERGY BALANCE ON AN ALGAL SYSTEM

INTRODUCTION

The energy balance of a photosynthetic system can be expressed in a simplified manner as follows:

$$\begin{array}{c}\text{Incident Light}\\ \text{Energy}\end{array} = \begin{array}{c}\text{Heat of Combustion}\\ \text{of the Organic Matter Produced}\\ \text{by Photosynthesis}\end{array} + \begin{array}{c}\text{Energy}\\ \text{Losses}\end{array} \qquad (2\text{-}1)$$

or as

$$\begin{array}{c}\text{Cellular Chemical}\\ \text{Energy}\end{array} = E_o \left[\begin{array}{c}\text{Incident Light}\\ \text{Energy}\end{array}\right] . \qquad (2\text{-}2)$$

E_o is the overall light conversion efficiency of photosynthesis. As far as algal cultures are concerned, E_o can be defined as the overall efficiency of conversion of the incident light energy into chemical energy stored in the algal cellular matter. The value of E_o indicates the conversion of light energy flux into net production of algal biomass. Values of E_o for higher and lower plants and their significance have been summarized by Rabinowitch [40,41]. Reported estimates of E_o for mass culture algal systems range from about 0.015 to 0.15.

Values approaching those of quantum efficiencies, i.e., from 0.15 to 0.30, have been reported for cultures grown under laboratory conditions in very thin suspension exposed to low light intensities [10,41,42]. For example, Kok [43] reports total efficiencies of 0.20 to 0.24 attained with the use of sodium light and a moderately concentrated culture. Such efficiencies are not significantly different from the theoretical quantum efficiency of sodium light.

Light Conversion Efficiencies of Algal Systems in Waste Treatment

Gotaas, Oswald, and Ludwig [5] reported E_o values ranging from 0.005 to 0.15 for an outdoor pilot-plant algal system in which conditions such as detention periods and depth of the pond markedly influenced the overall light conversion efficiency.

The effect of temperature, detention period, and light periodicity of E_o was investigated by Golueke [44] with the use of a high temperature strain of *Chlorella pyrenoidosa* grown on settled sewage under indoor laboratory conditions. His estimated values ranged from 0.10 to 0.19. Working with *Chlorella* fed with settled sewage, Oswald [38] observed values of E_o ranging from 0.003 to 0.07. A strong dependence on incident light intensity, nutrients, periodicity, detention period, and temperature was observed.

Oswald and Gotaas [6] assumed values of E_o from 0.02 to 0.05 in the design of high-rate ponds for photosynthetic oxygenation of wastes. Oswald [39] later proposed using an E_o value of between 0.03 to 0.05. With Oswald's method, the value of E_o times the average incident light irradiance is assumed to be proportional to the rate of algae production per unit area, which is assumed to be proportional to the rate of oxygen produced. According to Oswald's method, the value of E_o is a major factor in determining the dimensions and performance of a given algal system, once the average irradiance is known for a particular locality.

The use of overall light conversion efficiency has some advantages over the use of empiric or semiempiric methods in the design of ponds (cf. Chapter I). Nevertheless it suffers from the fact that the absolute values of E_o observed in a given series of experiments do not necessarily apply in situations in which conditions differ from those of the experiments. An indication of existence of this difficulty is found in the controversy that still exists regarding the proper value of E_o to be used. The method developed by Oswald is empirical because it relates the design parameters of an algal system to a given average light irradiance with the use of an empirical factor E_o.

Recent advances in the fundamental understanding of photosynthesis should make possible the development of a rational model by employing improved techniques in energy balances and by application of growth kinetics.

ENERGY BALANCE MODEL

Basic Assumptions

The energy balance model is based on the conservation of energy principle and the photosynthetic conversion of irradiated energy into chemical energy within the cellular material. Thus the following equation can be written as an expansion of Equations 2-1 and 2-2.

$$\begin{array}{c}\text{ALGAE}\\\text{NET}\\\text{PRODUCTION}\end{array} = \left(\begin{array}{c}\text{Energy-Mass}\\\text{Conversion}\\\text{Factor}\end{array}\right)\left(\begin{array}{c}\text{Thermodynamic}\\\text{Efficiency}\end{array}\right)\left(\begin{array}{c}\text{Light}\\\text{Utilization}\\\text{Efficiency}\end{array}\right) \times \left[\left(\begin{array}{c}\text{LIGHT}\\\text{IN}\end{array}\right) - \left(\begin{array}{c}\text{LIGHT}\\\text{OUT}\end{array}\right)\right] - \left[\begin{array}{c}\text{Respiration}\\\text{(Decay)}\end{array}\right] \quad (2\text{-}3)$$

or

$$P_{na} = \frac{1}{J}\left[E_m(\lambda)\right]\left[E_s(I_o, I_d, I_s)\right]\left[I_o(\lambda) - I_d\,(I_{o\lambda}, \alpha_\lambda, d, C_c)\right] - \left[D_R(C_c, d)\right] \quad (2\text{-}4)$$

in which P_{na} is the net production of dry algae per unit of illuminated surface area per unit of time (mg/cm^2-min); J, the chemical energy as measured by heat of combustion (cal/mg); E_m, the thermodynamic efficiency; E_s, the efficiency of light utilization within the illuminated suspension; I_o, the incident light intensity of the illuminated surface (cal/cm^2-min); $I_o(\lambda)$, the wavelength distribution of I_o and $I_{o\lambda}$ is the incident light intensity of a given wavelength band λ; I_d, the light intensity at the depth of the culture, d, (cal/cm^2-min) and α_λ the extinction coefficient; D_R, loss in production due to decay with units equivalent to P_{na}, i.e., mg/cm^2-min; and C_c, concentration.

The numerical value of J ranges from 5.2 to 6.3 [39,43,45], and is a very complicated function of the nutritive media and of the growth conditions. In this work, the value 5.5 cal/mg is used as an average workable constant, since that is the number recommended by Myers [46], Miller and Ward [47], and others.

An analysis of the various components of Equations 2-4 and 2-5, together with an attempt to formulate a workable materials balance model for the design and prediction of algal systems, follows.

Thermodynamic Efficiency, E_{T}

The basic reaction of photosynthesis as given by Rabinowitch [41] is:

$$CO_2 + 4H_2O \xrightarrow{n\,(h\nu)} CH_2O + 3H_2O + O_2 \qquad \Delta H = 112 \text{ k-cal/mole} \quad . \tag{2-5}$$

According to the equation, and based upon Einstein's law of photochemical equivalence and Planck's quantum theory, an integer number of quanta, n, are required to energize the photosynthetic reaction per molecule of CO_2 reduced or molecule of oxygen produced. Or by its definition, n einsteins are required to convert one mole of CO_2 into carbohydrate with the production of one mole of oxygen, assuming for the moment that the assimilatory quotient AQ is unity.

According to Planck, the energy content of each quantum E is given by the fundamental expression

$$E = h\,\nu \tag{2-6}$$

in which h is Planck's constant and equals 6.6255×10^{-27} erg-seconds [48], and ν is the frequency in sec^{-1} and

$$\nu = \frac{c}{\lambda} \tag{2-7}$$

in which c is the light velocity, and λ is the wavelength. Thus,

$$E = \frac{h\,c}{\lambda} \tag{2-8}$$

and the energy content of an einstein, U, is

$$U = N_A\,E = N_A\,\frac{h\,c}{\lambda} \tag{2-9}$$

in which N_A as Avogadro number ($N = 6.0225 \times 10^{23}$) [48]. The relationship expressed in Equation 2-9 is given graphically in Figure 1.

By using the energy content of a synthesized mole of carbohydrate as given in Equation 2-5; viz., $\Delta H = 112$ k-cal, and substituting for n, the conventional symbol for quantum requirement, $1/\phi$ (ϕ is the quantum yield); an expression for quantum efficiency E_q can be formulated as follows:

$$E_q = \frac{\Delta H}{1/\phi\ N_A\ E} = \frac{\Delta H\ \lambda}{1/\phi\ N_A\ h\ c} \quad . \tag{2-10}$$

Substituting numerical values for the constants, the expression becomes:

$$E_q = \frac{112\ (\text{k-cal/mole})\ \lambda\ (\text{m}\mu) \times 4.184 \times 10^{10}\ \text{erg/k-cal}}{1/\phi\ 6.0225 \times 10^{23} \times 6.6255 \times 10^{-27}\ (\text{erg-sec}) \times 3.0 \times 10^{17}\ \text{m}\mu/\text{sec}} \tag{2-11}$$

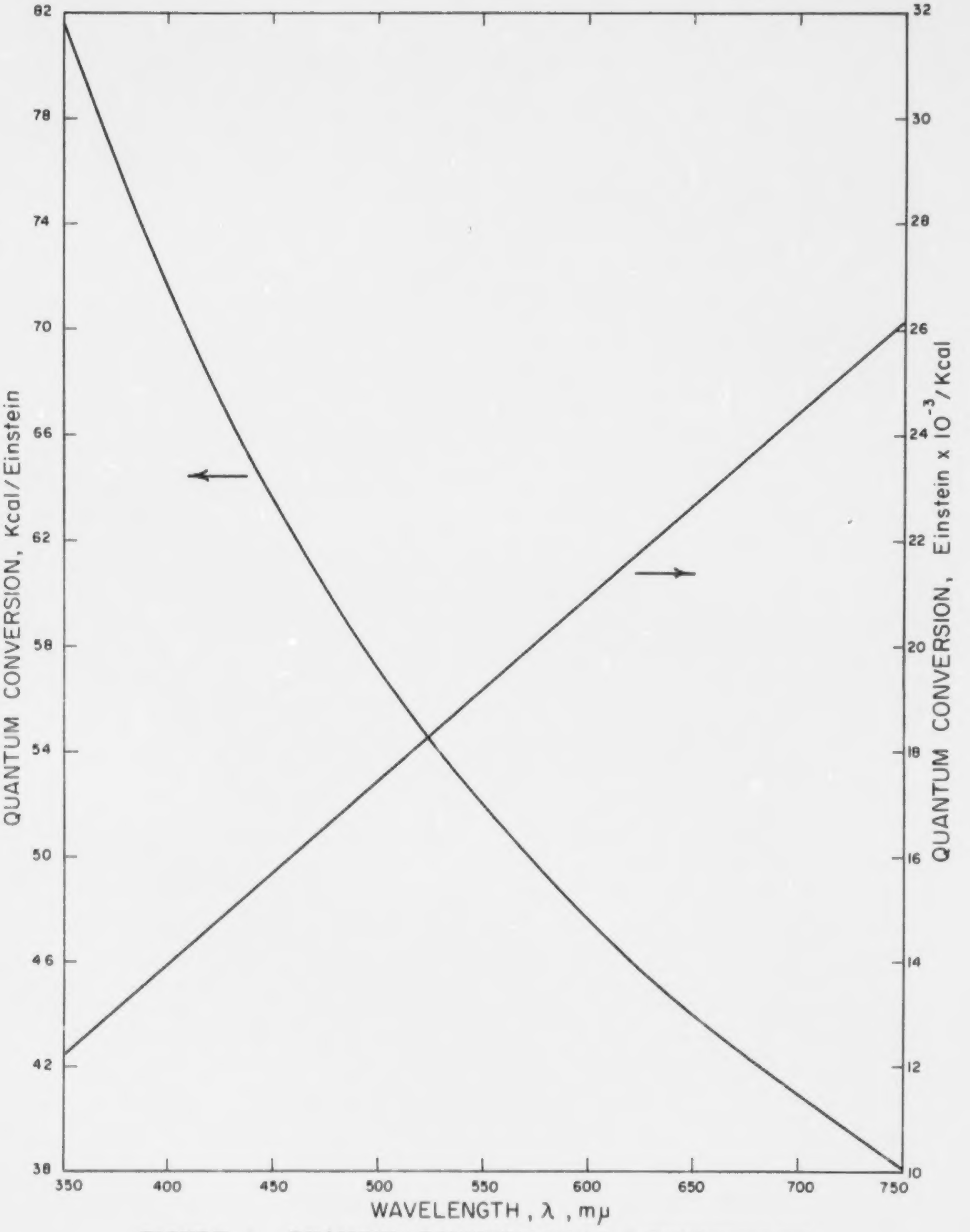

FIGURE 1. QUANTUM CONVERSION AS A FUNCTION OF WAVELENGTH

and

$$E_q = 0.00392 \frac{\lambda}{1/\phi} \quad . \tag{2-11A}$$

The relationship between the quantum efficiency and the wavelength for various values of $1/\phi$ is given in Figure 2.

The determination of the exact value of the quantum requirement in photosynthesis was a major objective of photosynthesis research during the five decades following the original experiments of Warburg and Negelein in 1922 [49]. The controversy as to the exact quantum requirement which existed during these decades stimulated much research which has been amply reported [41,50-52]. With only a few exceptions, the agreed upon value at present is 8 quanta per molecule of reduced CO_2 $(1/\phi = 8)$ [42,53,54]; therefore, it is the value which will be used in this analysis.

The thermodynamic efficiency, E_m, is a corrected form of the quantum efficiency E_q. This correction is based on the fact that there are relative differences in the efficiency of energy conversion that corresponds to particular wavelength regions within the visible light wavelength range of 400-700 mμ. This phenomenon was noted by Emerson and Lewis [55] in the early 1940's, and it has been related to the reduced efficiency of the cartenoid pigments and other accessory pigments as compared to that of chlorophyll. This phenomenon can be defined as the apparent action spectrum in relatively dense suspensions of algae in which most of the light is being absorbed by the suspension, thus both the true action spectrum of the particular algae and the adsorption spectrum of its suspension are considered [41,56].

The wavelength dependent coefficient required for the correction of E_q is denoted by Q_λ and its relative value is given in Figure 3, in which data compiled by Emerson and Lewis [55] are replotted. In accordance with this qualification, the equation for E_m becomes:

$$\boxed{E_m = Q_\lambda E_q} \quad . \tag{2-12}$$

Inasmuch as Q_λ and E_q are strongly dependent on wavelength, the information contained in Figures 2 and 3 is used to determine the value of E_m. Thus, the E_m value for $\lambda = 400$ mμ and a quantum efficiency of $1/\phi = 8$ would be:

$$E_m = 0.906 \times \frac{3.92 \times 10^{-3} \times 400}{8} = 0.178 \quad .$$

If $\lambda = 680$ mμ, the E_m would be:

$$E_m = 0.997 \frac{3.92 \times 10^{-3} \times 680}{8} = 0.333 \quad .$$

As these numbers show, the efficiency in the red portion of the spectrum (680 mμ) is almost twice that in the violet region (400 mμ).

Light Utilization Efficiency, E_s

The efficiency of light utilization as it appears in the energy balance model is based on the simplified assumption that up to a certain light intensity I_s, the photosynthetic machinery of an algal cell can convert light energy with an efficiency equal to the thermodynamic efficiency discussed above. Saturation light

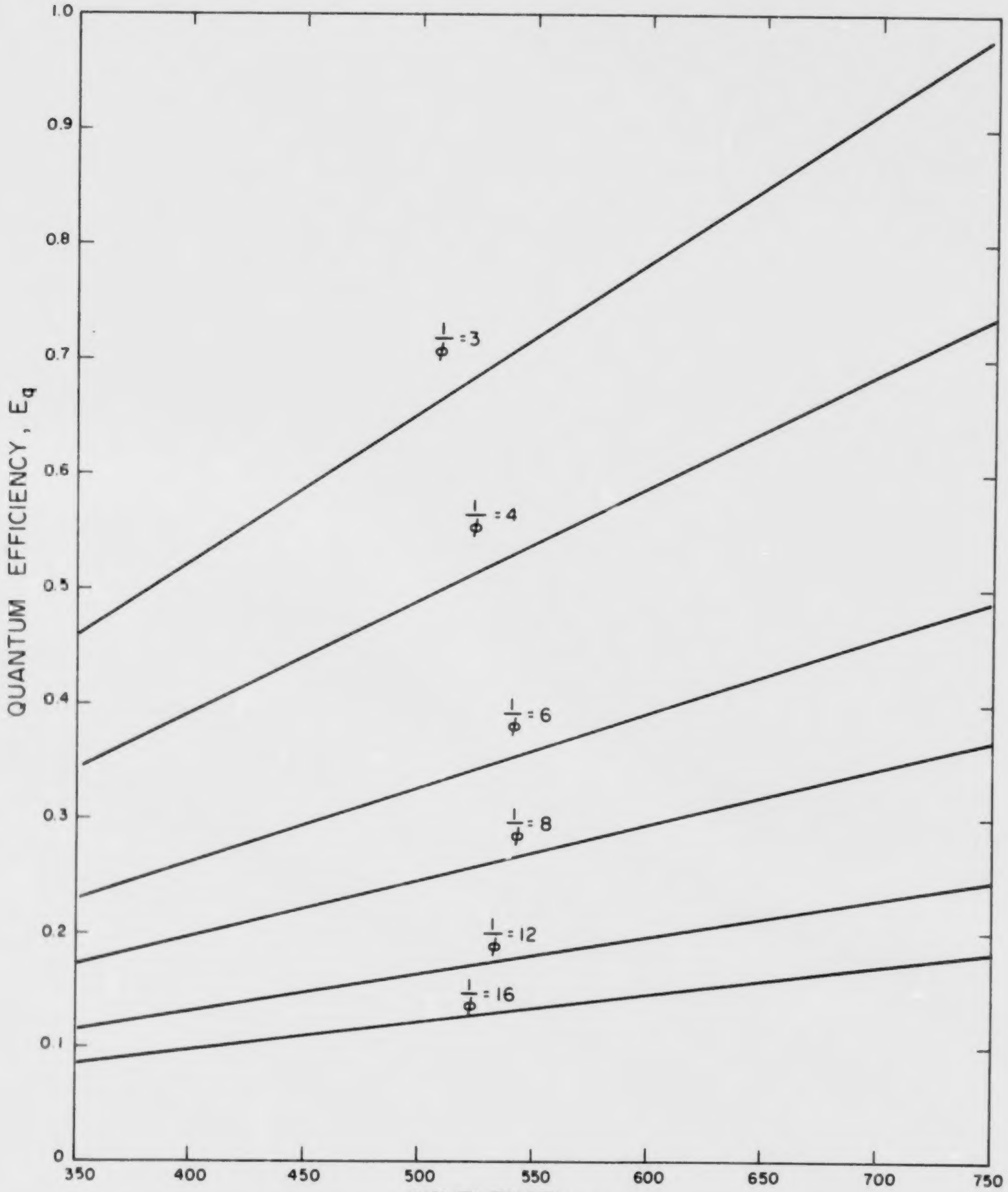

FIGURE 2. QUANTUM EFFICIENCY (E_q) AS A FUNCTION OF WAVELENGTH (λ) FOR VARIOUS VALUES OF QUANTUM REQUIREMENT ($1/\phi$)

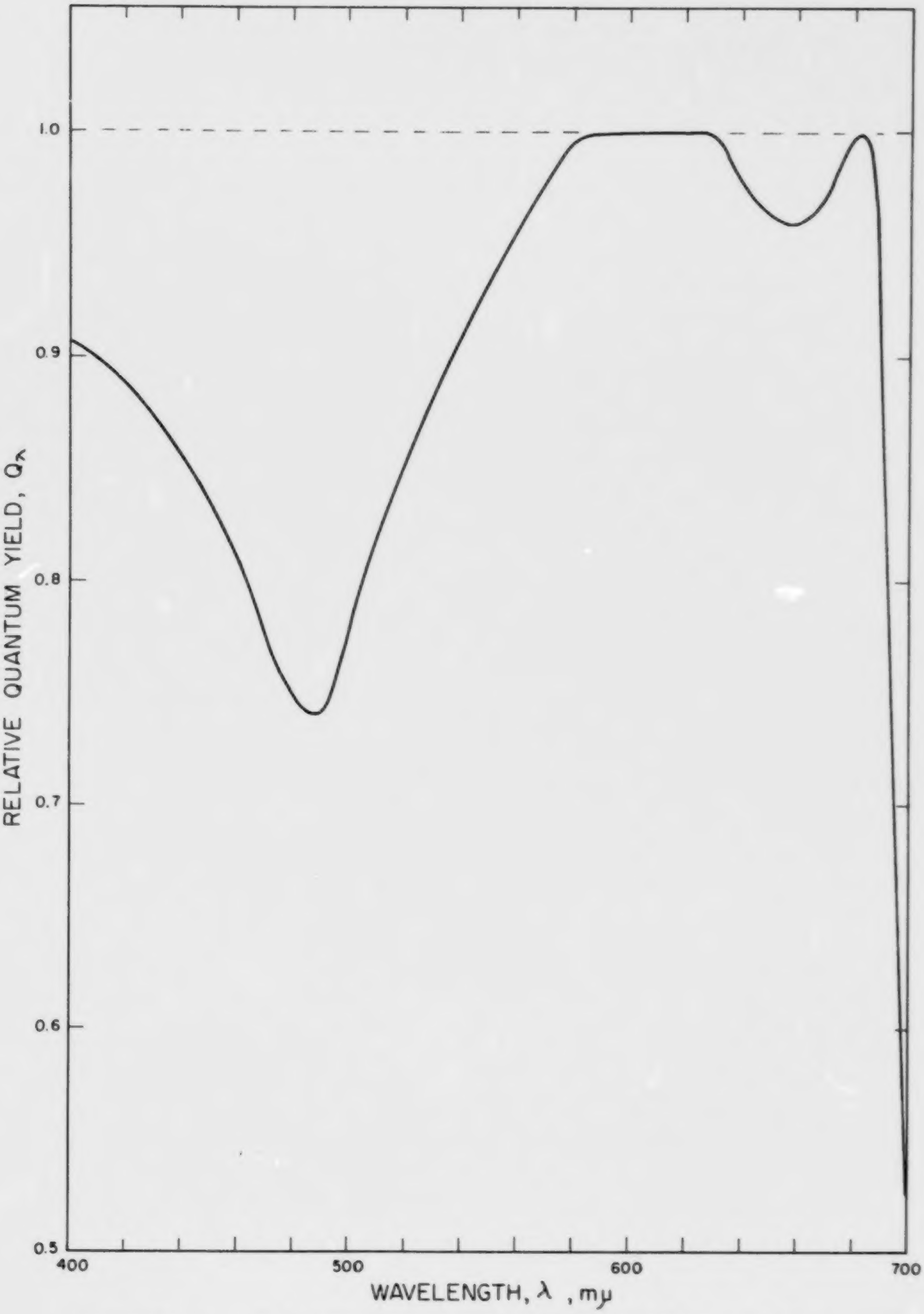

FIGURE 3. RELATIVE QUANTUM YIELD COEFFICIENT Q_λ AS A FUNCTION OF WAVELENGTH (λ). (BASED ON DATA COMPILED BY EMERSON AND LEWIS [55])

intensity (I_s) is the maximum intensity that can be accommodated by the photosynthetic apparatus. When the prevailing intensities are higher than saturation, the excess light is not used, and the photosynthetic activity proceeds at a constant level corresponding to that of I_s. With these assumptions, I_s is the only parameter determining E_s, and its value depends upon the genetic characteristics of the algae and the temperature. These assumptions were formulated by Bush [57] and have served as a basis for predicting efficiencies by several authors [6,38,46,58]. Figure 4 illustrates graphically the assumption which led to the mathematical formulation of the Bush Equation

$$E_s = \frac{I_s}{I_o}\left(\ln \frac{I_o}{I_s} + 1\right) \quad .$$

It appears that Bush has not published the mathematical derivation of his equation; thus, it is derived herein on the basis of the foregoing assumptions. Using information obtained from Figure 4 (Curve A) and assuming the applicability of the Beer-Lambert Law,

$$\frac{dI}{dx} = - \alpha \, C_c \, I_x \quad . \tag{2-13}$$

Here I_x denotes the light intensity at any depth x, α is the extinction coefficient, and C_c is the concentration of the algal suspension. Transposing Equation 2-13 will yield,

$$dx = - \frac{1}{\alpha \, C_c} \frac{dI}{I_x} \quad . \tag{2-14}$$

The light utilization efficiency can be defined (cf. Figure 4) as:

$$E_s = \frac{[\text{Total Light Applied}] - [\text{Unutilizable Light } (I_x > I_s)]}{[\text{Total Light Applied}]} \tag{2-15}$$

thus,

$$E_s = \frac{\int_{x=0}^{x=\infty} I_x \, dx - \int_{x=0}^{x_s} (I_x - I_s) \, dx}{\int_{x=0}^{x=\infty} I_x \, dx} \quad . \tag{2-16}$$

By substituting Equation 2-14 and changing boundary limits, the equation becomes

$$E_s = \frac{\frac{1}{(-\alpha C)} \int_0^{I_o} dI - \frac{1}{(-\alpha C)} \int_{I_s}^{I_o} (I_x - I_s) \frac{dI}{I_x}}{\frac{1}{(-\alpha C)} \int_0^{I_o} dI} \tag{2-17}$$

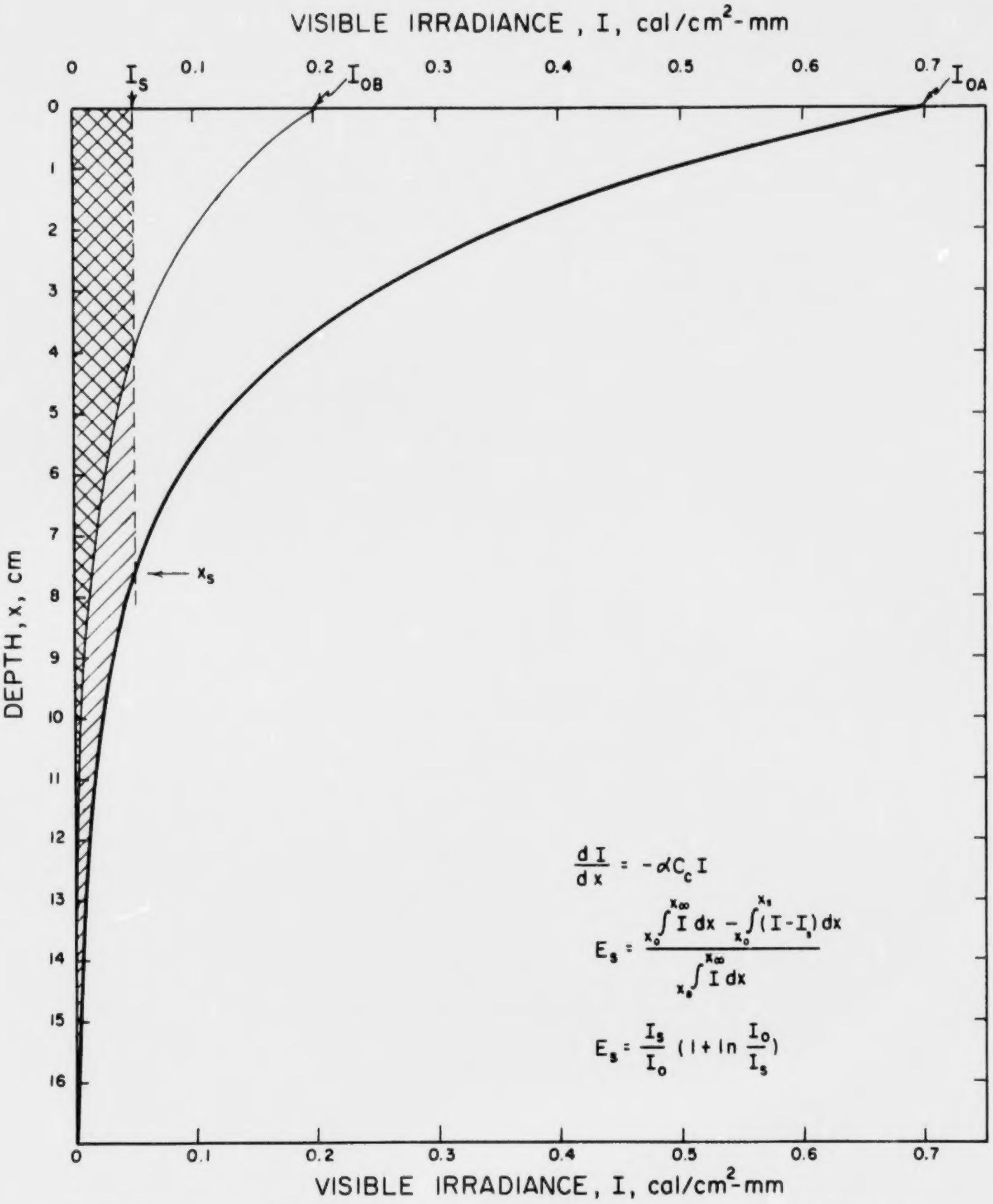

FIGURE 4. IRRADIANCE DECAY IN ALGAL SUSPENSION AS A FUNCTION OF DEPTH, SHOWING THE RELATIONSHIP BETWEEN THE EFFICIENCY OF LIGHT UTILIZATION (E_s) AND THE INCIDENT IRRADIANCE (I_o)

or

$$E_s = \frac{\int_0^{I_o} dI - \int_{I_s}^{I_o} dI + I_s \int_{I_s}^{I_o} \frac{dI}{I_x}}{\int_0^{I_o} dI} \quad . \qquad (2\text{-}18)$$

Finally, with the performance of the integration

$$E_s = \frac{I_o - (I_o - I_s) + I_s \ln (I_o/I_s)}{I_o} \quad .$$

The mathematical derivation is complete with the formulation of the Bush Equation:

$$\boxed{E_s = \frac{I_s}{I_o}\left(\ln \frac{I_o}{I_s} + 1\right)} \; . \qquad (2\text{-}19)$$

As can be deduced from Equation 2-19 and Figure 4, E_s increases significantly with increase in I_s.

Because of limitations associated with the boundary limits, the equation is applicable only to values of $I_o \geq I_s$. According to the assumptions which lead to the Bush Equation, whenever $I_o < I_s$, E_s is unity.

Figure 4 illustrates the gain in efficiency accomplished by using a soft incident light intensity (Curve B) as compared with the use of a strong incident intensity (Curve A). Curve A corresponds to incident light intensity of full sunlight. The application of such a high light intensity results in a rather low efficiency of utilization (E_s = 0.10 - 0.30).

The total efficiency E_T can be defined as the product of E_m and E_s, thus

$$\boxed{E_T = E_m \, E_s} \; . \qquad (2\text{-}20)$$

In Figure 5 is illustrated the relationship between Equations 2-19 and 2-20. In the figure both E_s and E_T are plotted as functions of the incident irradiance I_o at various values of I_s. E_m is assumed to be 0.2.

Assuming that all of the light is absorbed by the culture and neglecting respiration and decay, then, from Equation 2-4, the gross production of dry algae will be

$$\boxed{P_a = \frac{1440 \text{ (min/day)}}{J \text{ (cal/mg)}} E_T \, I_o \text{ (cal/cm}^2\text{-min)}} \qquad (2\text{-}21)$$

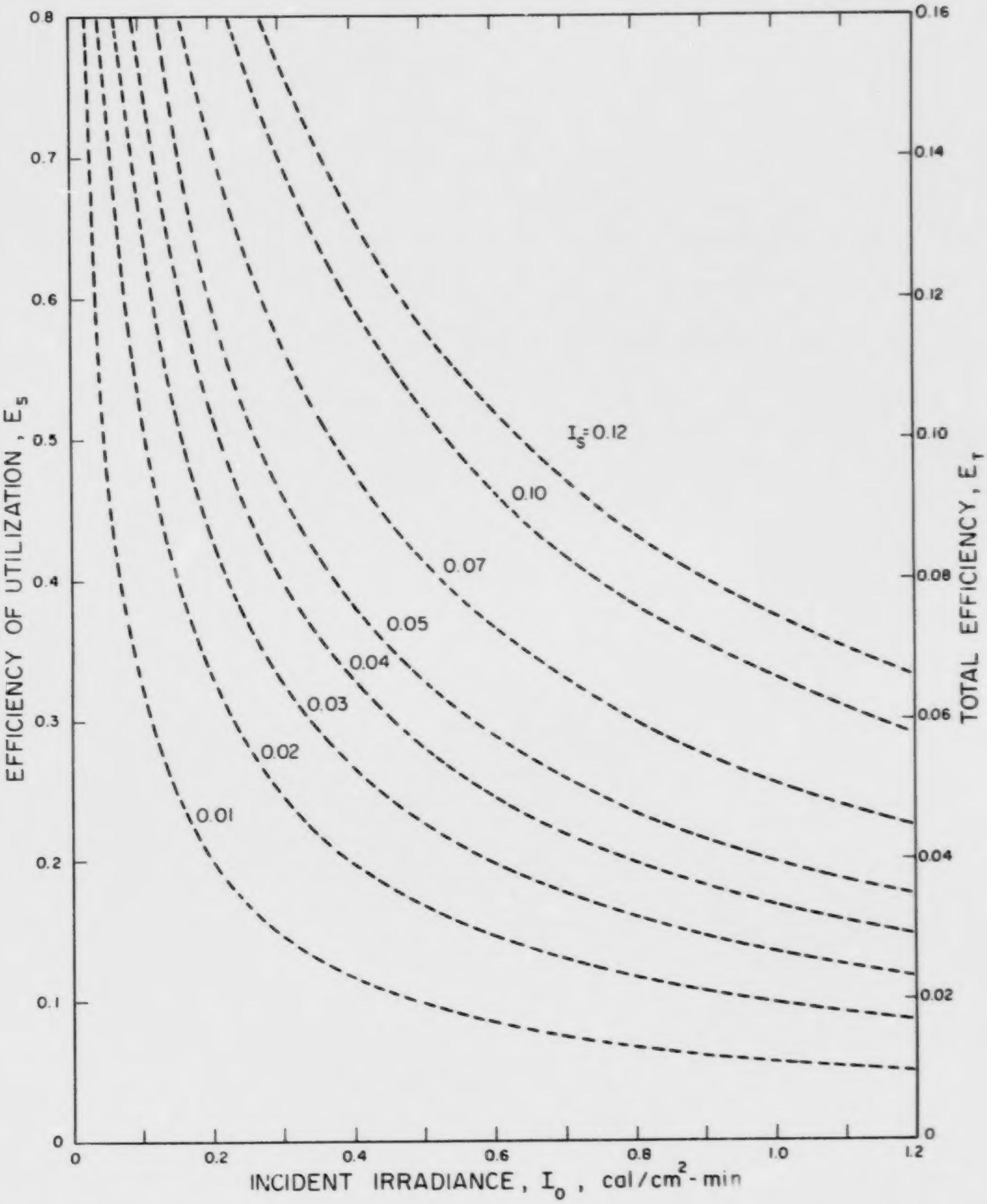

FIGURE 5. EFFICIENCY OF LIGHT UTILIZATION (E_s) AND TOTAL LIGHT CONVERSION EFFICIENCY (E_T) AS A FUNCTION OF INCIDENT IRRADIANCE (I_o) AT VARIOUS LEVELS OF LIGHT SATURATION INTENSITY (I_s)

in which P_a is in mg of dry algae per cm^2 of illuminated surface per day.* In Figure 6 is illustrated the computed form of Equation 2-21 as a function of the incident irradiance, I_o, at various levels of I_s and for two values for E_m. Here, again, the strong effect of both I_o and I_s are clearly seen.

The strong dependence of E_s and P_a on the incident irradiance as expressed in Equation 2-19 and Figures 4, 5, and 6 is a major factor in the design of algal systems. The fact that light energy utilization is increased so substantially with reduction in light intensity (I_o), has led to the application of various techniques aimed either at reducing the incident irradiance or at increasing the surface area of algae suspensions exposed to a given light source.

Incident Light Intensity

Illuminance as Contrasted to Irradiance. The responses of green plants (including algae) and the human eye to light are alike in the sense that both react to irradiation of the wavelength range 400 to 700 mμ, and both are not sensitive to irradiation below or above this range. However, within the visible wavelength range, the relative effect of the spectral distribution of light on the luminous efficiency of the eye differs from that on the photosynthetic reaction. Shown in Figure 7 are the differences between the response of the human eye, as defined by the standard spectral luminous efficiency curve for photic vision [59], and the response of the photosynthetic efficiency as defined by the relative action spectrum of Chlorella pyrenoidosa [60]. As is shown in the figure, the two responses are contrasting each other in that the response in photosynthesis is pronounced at wavelengths at which the response in vision is very limited. The difference between responses of the human eye and the photosynthetic system to spectral distribution is an explanation of why units of illuminance such as foot-candle, lux, phot, etc., presently in use for describing light intensities as they are related to vision and which are standardized by the standard photic vision curve (Figure 7) are not adequate for measuring light intensities as related to photosynthesis. Units of irradiance (radiant flux density at a surface) such as watts per cm^2, cal per cm^2 per minute, ergs per cm^2 per minute are the only meaningful ones as far as photosynthetic energy conversion is concerned. Therefore units of irradiance were the only types used in this presentation.

Spectral Distribution of the Light Source. The spectral distribution of the light source is a major factor in a quantitative growth-light model of algal systems. Its inclusion in the model is necessary because of both the physiological effect of particular regions of the light spectrum on the photosynthetic apparatus as well as the physical effect of differential absorption of light by the algal suspension.

Figures 51, 55, and 59 in Appendix F show the spectral distribution of the various light sources used in this work, whereas Figures 60 and 61 illustrate the spectral distribution of sunlight and its seasonal variations.

The models proposed in this work include the spectral distribution as a major parameter, thus the incident irradiance I_o is defined as the integral of its corresponding wavelength bands as follows:

$$I_o = \int_{\lambda=400}^{\lambda=700} I_{o\lambda} \, d\lambda \quad . \qquad (2\text{-}22)$$

---

*In many other cases P_a is expressed in units of g/m^2-day.

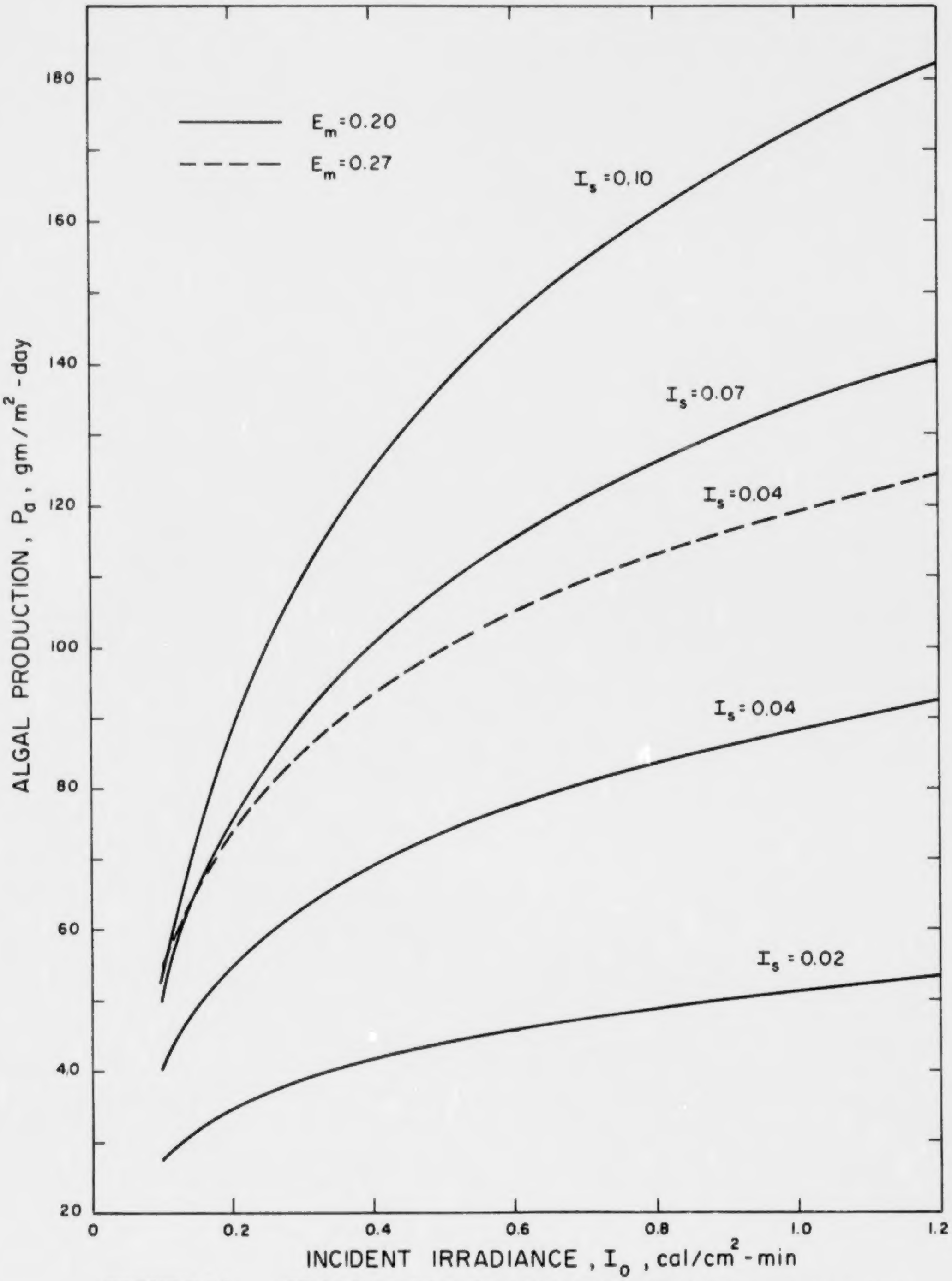

FIGURE 6. GROSS ALGAE PRODUCTION (P_a) AS A FUNCTION OF INCIDENT IRRADIANCE (I_o)

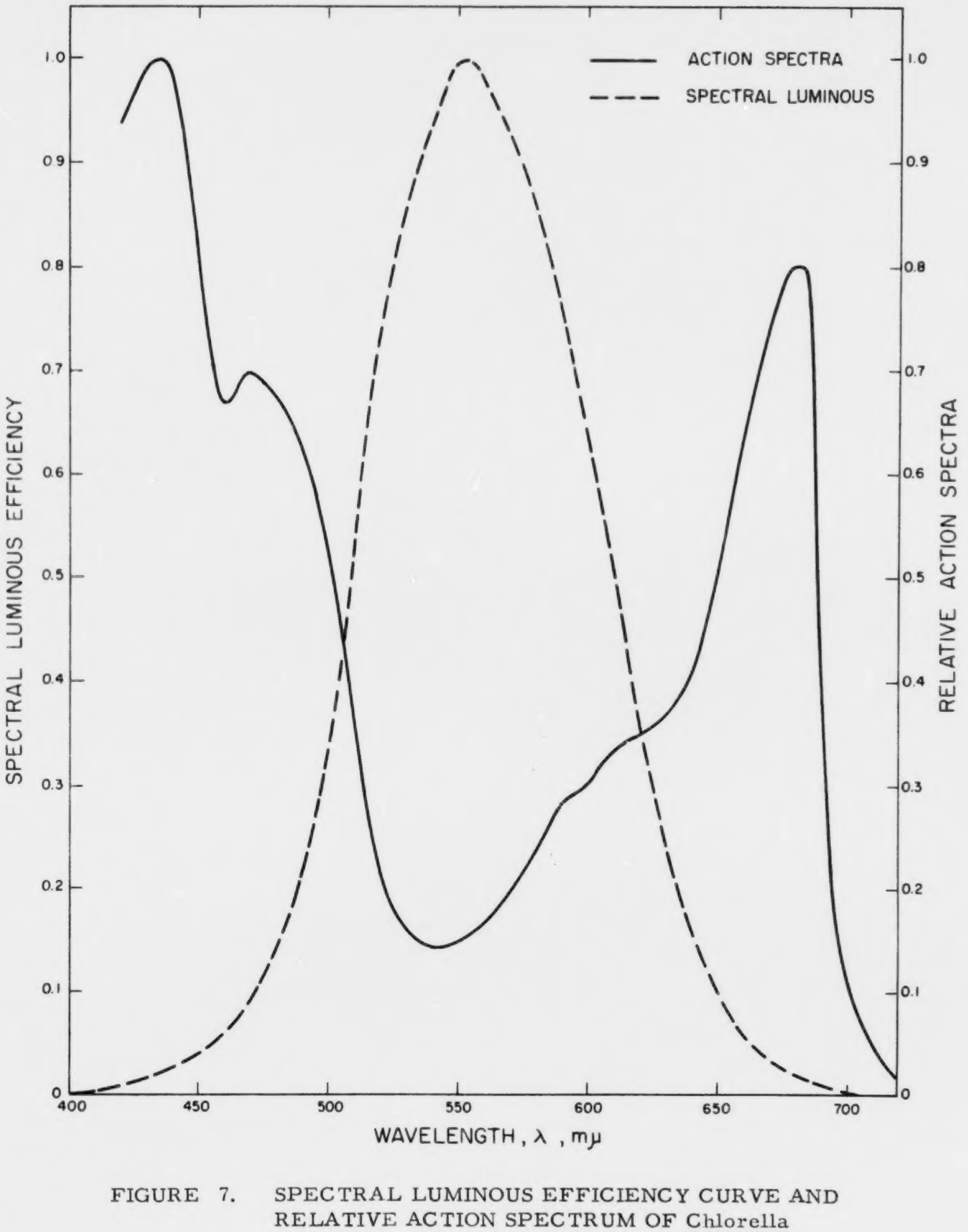

FIGURE 7. SPECTRAL LUMINOUS EFFICIENCY CURVE AND RELATIVE ACTION SPECTRUM OF Chlorella pyrenoidosa [61,62]

The spectral distribution is given as the function of the relative energy with the corresponding wavelength, as

$$I_{o\lambda} = I_o \frac{I_{\lambda R}}{R_t} \tag{2-23}$$

in which

$$R_t = \int_{\lambda=400}^{\lambda=700} I_{\lambda R}\, d\lambda \quad . \tag{2-24}$$

R_t is the area enclosed under the relative energy spectral distribution, which in turn is a constant for a particular light source. $I_{\lambda R}$ denotes the relative energy corresponding to a specific incremental wavelength band.

Transmitted and Absorbed Light by Algal Suspension

Beer-Lambert's Law expressed in its simplest form as

$$\boxed{\frac{I_x}{I_o} = e^{-\alpha C_c x}} \quad ,$$

has been applied in the calculation of the light intensity gradient in algal suspension on the assumption that it is applicable to polychromatic light [4,6,7,8]. However, Beer-Lambert's Law is applicable only to monochromatic light. Due to the differential absorption of algae with respect to wavelength, this law, in its simple form, is not applicable to algal cultures receiving polychromatic light. This limitation applies to most of the work which has been or is being done with algal cultures. Except in special studies, polychromatic light usually is used as the source of illumination. Simple observation of an algal suspension, however, will demonstrate the fact that green-yellow light (500-600 mμ) is preferentially transmitted by an algal suspension exposed to white light.

The significant discrepancy resulting from the application of the Beer-Lambert Law in situations involving polychromatic light in algal suspension was observed and reported by Tamiya [63], Myers and Graham [64], Oswald [39], Willard [65], and others. Most of these researchers noticed the dependence of the extinction coefficient, α, on the value of the product of the concentration and depth (C_c x), in which α decreased as (C_c x) increased. This phenomenon was found to be more pronounced in situations where light intensities were measured as illuminance rather than irradiance, because of the high relative weight of the green-yellow wavelength range on the spectral luminous efficiency curve (Figure 7).

This discrepancy resulting from the use of Beer-Lambert Law is regarded by Myers [46] and Oswald [39] as a major obstacle in the formation of a quantitative model for algal systems. The only way to overcome limitation is by incorporation of the light source spectral distribution and the wavelength-dependent absorption of light into the quantitative model. Thus

$$I_{x\lambda} = I_{o\lambda}\, e^{-\alpha_\lambda C_c x} \qquad (2\text{-}25)$$

or

$$I_{d\lambda} = I_{o\lambda}\, e^{-\alpha_\lambda C_c d} \qquad (2\text{-}26)$$

and

$$I_d = \int_{\lambda=400}^{\lambda=700} I_{o\lambda}\, e^{-\alpha_\lambda C_c d}\, d\lambda \qquad (2\text{-}27)$$

and from Equations 2-22 and 2-23,

$$I_d = \frac{I_o}{R_t} \int_{\lambda=400}^{\lambda=700} I_{\lambda R}\, e^{-\alpha_\lambda C_c d}\, d\lambda \qquad (2\text{-}28)$$

in which I_d is the light intensity at depth d of the reactor and which constitutes the light lost in its passage through the system, and $I_{d\lambda}$ is its respective value for an incremental wavelength.

The integrated form of the extinction coefficient, symbolized as α_t, is defined as

$$\alpha_t = \frac{1}{C_c\, d} \ln \frac{I_o}{I_d} \quad . \qquad (2\text{-}29)$$

As previously explained, α_t is dependent on the product (C_c d). It should be used only when (C_c d) is constant. When (C_c d) is not constant, the individual values of α_λ should be incorporated into the model in their nonintegrated form.

Decay

Decay is the loss or disappearance of cellular material and its inclusion is necessary to make a complete materials balance on the system. It can be defined as any loss of algal mass due to respiration and lysis.

Endogenous Respiration. Photosynthesis and endogenous respiration are included in the same overall equation.

Since respiration is related to light, the relationship between the respiration and irradiance must be included in a quantitative model based upon light intensity. The relationship between the respiration rate and light has been observed frequently in higher plants. Thomas and Hill [66] working with sugar beets noted a large increase in respiration during the day as compared to night-time activity. They report the value of respiration for actively multiplying parts of the plants in the light was between 11% – 15% of the gross daily rate of photosynthesis, and only 6% – 8% of the total during darkness. They also reported differences in the respiration rate corresponding to the degree of activity and growth of the tissues. The highest rate of respiration was found to be in the growing tops and roots of the plants.

In research with *Chlorella pyrenoidosa*, Cramer and Myers [67] noted a marked increase in respiration upon illuminating the algae culture. In addition Cramer and Myers found that a relationship exists between light intensity and degree of respiration. They estimated the rate of respiration to be between 10% – 15% of photosynthesis after 24 hours of light. They also established the relationship between light intensity and the availability of carbohydrates produced by photosynthesis as energy sources for respiration. Kandler and Sironval [68] observed a 250% increase in the respiration rate with the application of extremely high light intensities (about 10,000 ft-candles). However Brown [69,70], working with *Chlorella* and *Anabaena*, found that excessively strong light inhibited respiration although at intermediate light levels, respiration did increase with increase in intensity.

Kok [43] observed the effect of light intensity and the respiration rate, and determined the rate of respiration under continuous light to be between 10% – 20% of the gross photosynthetic rate. The steady state level in prolonged darkness was found to be from 2% – 3% of the total mass per day (0.02 – 0.03 day^{-1}).

Thus far, the best data on respiration as related to light have been reported by Hoch and his co-workers [71,72]. Working with green and blue-green algae they found a relationship between light intensities and the rate of respiration, as well as one between wavelength and respiration. In experiments involving green algae under continuous illumination they observed steady state respiration rates of between 12% – 13% of the gross photosynthetic rate in moderate and high irradiance levels. They found the steady state values for respiration after a moderately prolonged period of darkness (few days) to be between 2% and 3% of the gross photosynthetic rate. The relationship between light intensities and past history of the cells in regard to illumination and the respiration rate was reported also by Bassham *et al*.[54]. Working with *Chlorella pyrenoidosa*, Bassham found the steady state respiration rate to be about one-eighth of the gross photosynthetic rate for an irradiance of 1.5 mW/cm^2 (0.21 cal/cm^2-min) or greater.

Based on the foregoing data, an average value equivalent to 12.5% of the gross photosynthetic rate was assigned to the endogenous respiration rate. An assumed constant value for respiration rate has been suggested in the past for models of photosynthetic systems. An assumed constant respiration coefficient was proposed by Tsuchiya *et al*. [73] for algal mass cultures and by Steele [74] and by Riley [75] for models predicting primary productivity of phytoplankton in natural aquatic environments. The decay rate for the model herein is based on respiration alone, and is assumed to be an average constant of $K_d = 0.125$ per day. Thus the respiration decay term D_R per unit of illuminated surface area at algal concentration C_c (mg/ℓ) and depth d (cm) will be

$$\boxed{D_R = 10^{-3} K_d C_c d} \qquad (2\text{-}30)$$

in which D_R is expressed in mg of dry algae/cm^2-day.

Formulation of the Energy Balance Model

Referring to the basic Equations 2-3 and 2-4 and substituting the detailed relationships for each factor, namely Equations 2-11, 2-12, 2-19 and 2-21, then for monochromatic light the gross production of algae per unit of light-exposed surface area will be as follows:

$$P_a = \frac{0.00392 \times 1440}{J\ 1/\Phi}\ I_{o\lambda}\ Q_\lambda\ \lambda\left[\frac{I_s}{I_o}\left(\ln\frac{I_{o\lambda}}{I_s}+1\right) - \frac{I_s}{I_{o\lambda}\ e^{-\alpha_\lambda C_c d}}\left(\ln\frac{I_{o\lambda}\ e^{-\alpha_\lambda C_c d}}{I_s}+1\right)\right] . \qquad (2\text{-}31)$$

Or by substituting Equation 2-26, the expression becomes:

$$P_a = \frac{0.00392 \times 1440}{J\ 1/\Phi}\ I_{o\lambda}\ Q_\lambda\ \lambda\left[\frac{I_s}{I_{o\lambda}}\left(\ln\frac{I_{o\lambda}}{I_s}+1\right) - \frac{I_s}{I_{d\lambda}}\left(\ln\frac{I_{d\lambda}}{I_s}+1\right)\right] . \qquad (2\text{-}32)$$

For polychromatic irradiance $I_o(\lambda)$ given in cal/cm^2-min (cf. Equations 2-22 and 2-28), the gross production of algae per unit of light-exposed surface area (mg of dry algae/cm^2-day) will be as follows:

$$P_a = \frac{0.00392 \times 1440}{J\ 1/\Phi}\left[\frac{I_s}{I_o}\left(\ln\frac{I_o}{I_s}+1\right)\int_{\lambda=400}^{\lambda=700} Q_\lambda\ \lambda\ I_{o\lambda}\ d\lambda - \frac{I_s}{I_d}\left(\ln\frac{I_d}{I_s}+1\right)\int_{400}^{700} Q_\lambda\ \lambda\ I_{o\lambda}\ e^{-\alpha_\lambda C_c d}\ d\lambda\right] \qquad (2\text{-}33)$$

in which I_d is as defined by Equation 2-28. Substituting Equation 2-23 for $I_{o\lambda}$ and rearranging results in

$$P_a = \frac{5.645}{J\ 1/\Phi\ R_t}\ I_o\left[\frac{I_s}{I_o}\left(\ln\frac{I_o}{I_s}+1\right)\int_{\lambda=400}^{\lambda=700} Q_\lambda\ \lambda\ I_{\lambda R}\ d\lambda - \frac{I_s}{I_d}\left(\ln\frac{I_d}{I_s}+1\right)\int_{400}^{700} Q_\lambda\ \lambda\ I_{\lambda R}\ e^{-\alpha_\lambda C_c d}\ d\lambda\right] . \qquad (2\text{-}34)$$

The computerized form of this equation as it is applied to the reactor system is given in Chapter VII and Appendix H. The term $I_s/I_d(\ln I_d/I_s + 1)$ is a multiplier of the light loss through penetration because in the development of Equation 2-19 the integration was performed to the limit of $x = \infty$. As was true in Equation 2-19, this term is valid only for $I_d \geq I_s$, while for $I_s > I_d$ it should be equal to unity. In practice the ideal situation is one in which I_d is as small as possible, (i.e., close to or less than I_s); thus, the term will not be significant in dense cultures. However, in cultures which are not dense and which are exposed to relatively strong light, the term becomes quite significant.

From Equations 2-30 and 2-32, the net production will be

$$\boxed{P_{na} = P_a - 10^{-3} K_d C_c d} \qquad (2\text{-}35)$$

and the average specific growth rate of the system $\bar{\mu}$, expressed in units of day^{-1} will be

$$\boxed{\bar{\mu} = \frac{10^3 P_a}{C_c d}} \; . \qquad (2\text{-}36)$$

Similarly, the average net specific growth rate of the system will be

$$\boxed{\bar{\mu}_n = \bar{\mu} - K_d} \; . \qquad (2\text{-}37)$$

III. KINETICS OF ALGAL GROWTH AND PRODUCTION WITH RESPECT TO LIGHT INTENSITY

BASIC ASSUMPTIONS

A kinetic model of microbial propagation with respect to a growth-limiting substrate can be based on two assumptions:

1. The growth rate of a culture is proportional to the rate of consumption of substrate.

2. The specific growth rate of a culture is some function of the substrate concentration.

The assumptions were proven to be applicable for heterotrophic bacterial cultures grown on organic substrate as well as for algae with respect to inorganic nutrients.

If light intensity is considered to be analogous to substrate concentration, and the utilization of light energy to the consumption of substrate, then the two assumptions can be used as a basis for a kinetic model of algal production in relation to light energy. The resulting kinetic model is more complex than the one based on substrate. The reasons are:

1. Light is an instantaneously dissipated "substrate."

2. Due to the attenuation of the light beam, light intensity is not uniform within an optical path of finite length in a reactor. Therefore, an intensity gradient, analogous to a "concentration gradient" exists in most algal systems.

Assumption 1 is the basis of the light energy balance described in Chapter II. Assumption 2 can be defined for algal cultures as follows: The rate of photosynthesis, which is proportional to the rate of photolithotrophic growth of algal biomass, is some function of light intensity. Thus in general,

$$\mu = \frac{dC_c}{C_c\, dt} = f(I) \quad . \qquad (3\text{-}4)$$

ALGAE GROWTH VS. LIGHT INTENSITY AT THE MICROSCOPIC LEVEL

The rate of photosynthesis (R_x) for a given increment of depth (dx) is proportional to the concentration (C_c) of the light energy absorber (algae in this study), and is a function of the incremental light intensity (I_x) at depth x. Hence,

$$R_x = C_c \, f(I_x) \quad . \qquad (3\text{-}5)$$

Since the photolithotrophic growth of algae is proportional to its rate of photosynthesis, then,

$$R_x = k \frac{dC_c}{dt} \tag{3-6}$$

and

$$\mu_x = \frac{dC_c}{C_c\,dt} = f(I_x) \quad . \tag{3-7}$$

The relationship described in Equation 3-7 is the key to kinetic models of algal systems and the mathematical formulation of the above function must be used.

Few attempts have been made to formulate this function on a postulated mechanism for the conversion of light energy into cellular material. Attempts to verify such mechanisms experimentally have met with varying degrees of success. To understand the various mathematical expressions which have been formulated, a review of the basic mechanism of photosynthesis is presented.

Basic Mechanisms of Photosynthesis

The postulated mechanism of conversion of light energy into organic matter is based on two or more consecutive reactions. A simplified example of a photosynthetic reaction which can be carried on *in vitro* is Hill's reaction in which an inorganic metal serves as the electron acceptor while H_2O is the electron donor. This electron transfer mechanism is driven by light energy and results in the evolution of molecular oxygen and in a reduced metal.

An example of Hill's reaction with isolated chloroplasts in which a ferric salt serves as the electron acceptor (ferric oxalate was originally used [40]) can be written as follows:

$$4Fe^{+++} + 2H_2O \xrightarrow{light} 4Fe^{++} + 4H^{+} + O_2 \quad . \tag{3-8}$$

This reaction is analogous (though simplified) to the *in vivo* photosynthesis in which CO_2 is the terminal electron acceptor rather than Fe^{+++}.

A simple mechanism scheme was proposed for Hill's reaction by Lumry and Rieske [76]. It contains two basic reactions,

$$C \xrightarrow{k_s I} C^* \tag{3-9}$$

$$H_2O + C^* \xrightarrow{k_D} C + \left\{OH\right\} + \left\{H\right\} \quad . \tag{3-10}$$

The free radicals produced in the second step are assumed to react very rapidly as follows:

$$\left\{H\right\} + \text{oxidant} \xrightarrow{rapid} \text{reduced oxidant} \tag{3-11}$$

$$4\left\{OH\right\} \xrightarrow{rapid} O_2 + 2H_2O \quad . \tag{3-12}$$

In this scheme, C and C* represent respectively the unactivated and activated "sensitizers" or "trapping centers for excitation energy" — an assemblage of pigment molecules, or an enzyme associated with such an assemblage, which absorb excitation energy. K_S and K_D are the rate constants of the reactions. Reaction (3-9) is a photoelectric one requiring light and is practically independent of temperature. Subsequent reactions are enzymatic and chemical, are temperature dependent, and can be carried on in the dark.

As for in vivo photosynthesis, the mechanism is more complex. Here, CO_2 is fixed, serves as an electron acceptor, and is fed into a rather complicated biochemical cycle by way of a path which involves a multitude of enzymatic activities [77]. Several mechanism schemes have been proposed by Rabinowitch [41], Tamiya [78] and Kok [79]. Fortunately, examination of kinetic models derived from the various mechanisms shows that a final model would not differ much from the one derived on the basis of the basic mechanism proposed by Lumry and Rieske [76] for Hill's Reaction.

"First Order-Zero Order" Type* Kinetic Model (Model I)

The "first order-zero order" type of kinetic model is based upon the assumption that the rate of photosynthesis is proportional to the light intensity, I_x, until a maximum rate is attained at a certain light intensity, I_s; and that thereafter the rate remains constant at a maximum level regardless of any increase in I_x. Referring to Equations 3-5, 3-6, and 3-7, it can be shown that for $I_x \leq I_s$:

$$\mu_x = f(I_x) = K_1 I_x \qquad (3\text{-}13)$$

and for $I_x \geq I_s$:

$$\mu_x = K_o \quad . \qquad (3\text{-}14)$$

Here, K_o and K_1 denote various constants. The functions 3-13 and 3-14 can be referred to as first-order and zero-order propagations, respectively (cf. Appendix B).

Referring to the photosynthesis mechanism scheme delineated above, the first order-zero order kinetic model implies that the rate of the temperature-independent photoelectric reaction (excitation) as it appears in Equation 3-9 is directly proportional to the microscopic light intensity. The biochemical utilization of the excitation energy and the regeneration of the unactivated photoelectrical apparatus operate concurrently until maximum capacity is reached. This maximum capacity is constant, and it is reached at the levels of irradiance which corresponds to light saturation, I_s. Furthermore the saturation capacity determines the maximum rate of photosynthesis and correspondingly the maximum specific growth rate. Taking Hill's Reaction mechanism as an example, the rate of the photosynthetic reaction can be defined as:

$$R_x = k_D C^* \quad . \qquad (3\text{-}15)$$

---

*For remarks on the "order of reaction" in nonautocatalytic microbial propagations, and their analogy to the order of reaction in chemical reactions, please refer to Appendix B.

Since the pool of unactivated "sensitizer" or "trapping center," C, can be assumed as a constant, then for $I \leqq I_s$

$$C^* = k_s \, I \tag{3-16}$$

and

$$R_x = k_s' \, I \quad . \tag{3-17}$$

The microscopic specific growth rate, μ_x, which is proportional to the rate of photosynthesis, then becomes:

$$\mu_x = K_1 \, I_x \tag{3-18}$$

while for $I \geqq I_s$,

$$C^* = \text{Const} = k \, C_t \tag{3-19}$$

where

$$C_t = C + C^* \tag{3-20}$$

and

$$\mu_x = K_o = \hat{\mu}_x \quad . \tag{3-21}$$

Here, k_D, k_s, k_s', K, and K_o denote various constants, and $\hat{\mu}_x$ denotes the microscopic maximum specific growth rate which is temperature and species dependent. It can also be shown that K_1 is the slope of the curve $\Delta \mu_x / \Delta I_x$ [cf. Figure 8 (I)], and

$$\hat{\mu}_x = K_1 \, I_s \quad .$$

On the basis of Equation 3-9, i.e., $C \xrightarrow{k_s I} C^*$, it is reasonable to assume that at low levels of light intensity, k_s represents that portion of light energy which is utilizable by the photosynthetic apparatus. Thus

$$k_s = \gamma \, \phi \, I$$

in which γ is the fraction of light absorbed by the particular photosynthetic pigment system while ϕ is the quantum efficiency which is a function of the wavelength and practically independent of temperature. Equation 3-9, therefore, should be written as:

$$C \xrightarrow{\gamma \, \phi \, I} C^* \tag{3-23}$$

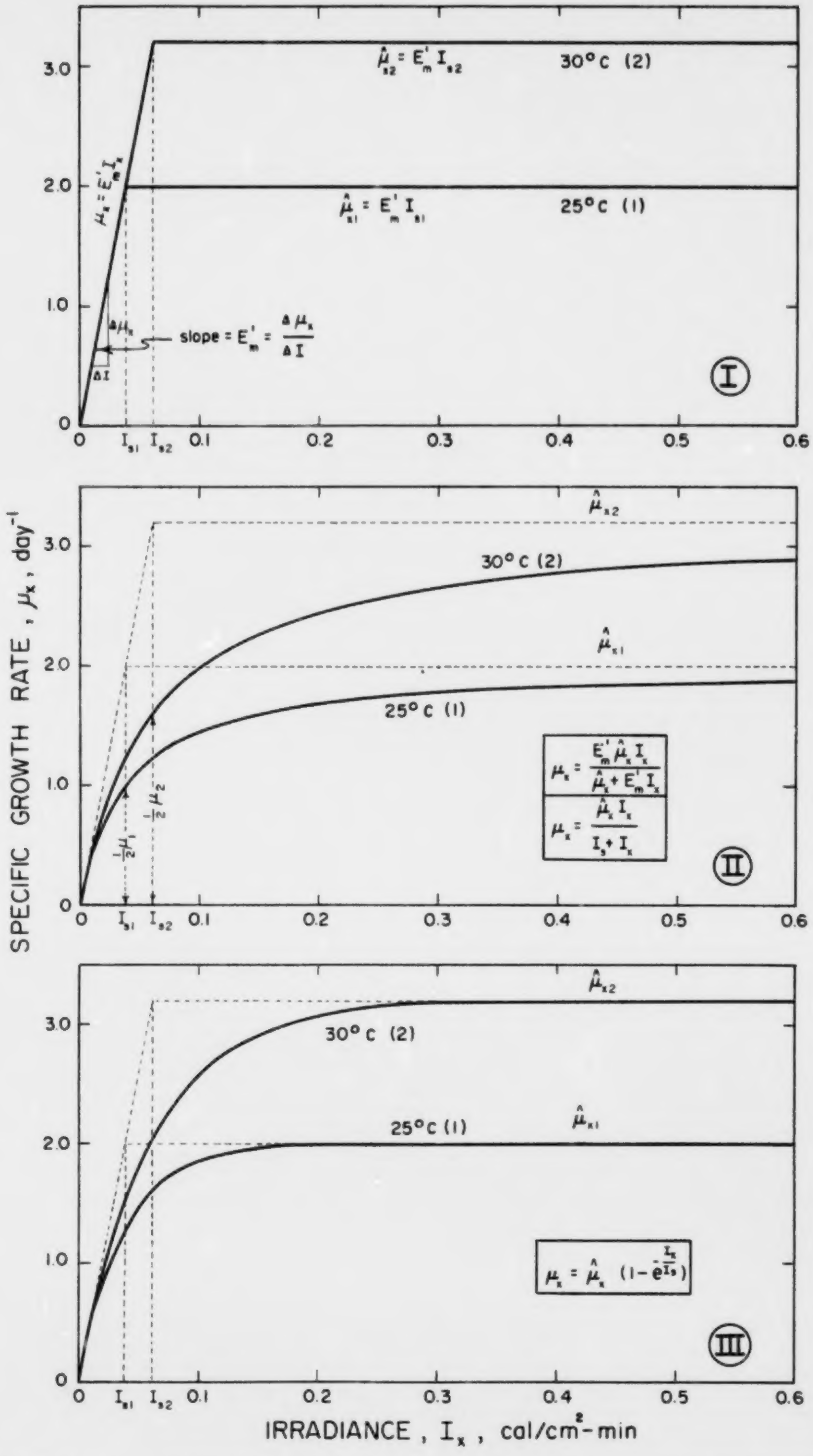

FIGURE 8. SPECIFIC GROWTH RATE (μ_x) AS A FUNCTION OF IRRADIANCE (I_x) FOR VARIOUS MICROSCOPIC KINETIC MODELS

and for $I \leq I_s$

$$C^* = \gamma \, \phi \, I_s \quad .$$

Transferring the above to terms of rate of photosynthesis on a microscopic level and converting ϕ to E_m, the thermodynamic efficiency of light utilization in photosynthesis is

$$R_x = E_m \, I_x \quad . \qquad (3\text{-}24)$$

E_m represents the maximum light conversion efficiency attained experimentally in diluted algal suspension illuminated at a low light intensity.

From Equation 3-24, and again for $I_x \leq I_s$

$$\boxed{\mu_x = E_m' \, I_x} \qquad (3\text{-}25)$$

in which

$$E_m' = \frac{k_n}{J} E_m \qquad (3\text{-}26)$$

where k_n is a time-dimension constant which is equal to 1440 min/day. Relating light intensity (usually expressed in cal/cm^2-min) to specific growth rate (g/g-day), the value of k_n/J is approximately 265.5 (cal^{-1} min cm^2 day^{-1}). Thus, when $I \geq I_s$

$$\boxed{\mu_x = \hat{\mu}_x = E_m' \, I_s} \quad . \qquad (3\text{-}27)$$

A careful consideration of the above kinetic model reveals its similarity to the energy balance model presented in Chapter II. This similarity becomes clearer when the model is considered on the macroscopic level. A graphic illustration of the model is presented in Figure 8 (I).

The Rectangular Hyperbolic Model (Model II)*

Considering Equations 3-9 and 3-10, and with the correction in Equation 3-23, one obtains

$$C \xrightarrow{\gamma \, \phi \, I_x} C^* \qquad (3\text{-}23)$$

---

*For a discussion of the various rationales in applying the rectangular hyperbola for the formulation of kinetic models of microbial propagations, please refer to Appendix C.

and

$$H_2O + C^* \xrightarrow{k_D} C + \left\{OH\right\} + \left\{H\right\} \quad . \qquad (3\text{-}10)$$

The fraction γ of the light intensity I is absorbed either by C or C*, and conversion occurs with a quantum efficiency Φ only when C is excited, so

$$\frac{d[C]}{dt} = - \frac{d[C^*]}{dt} = k_D\,[C^*] - \gamma\,\Phi\,I\,\frac{[C]}{[C] + [C^*]} \quad . \qquad (3\text{-}28)$$

Assuming that

$$[C] + [C^*] = [C_t] \qquad (3\text{-}29)$$

and the rate of photosynthesis equals k_D C* and becomes maximal when all of C is excited (i.e., $[C^*] = [C_t]$), then at steady state

$$\frac{d[C]}{dt} = - \frac{d[C^*]}{dt} = 0 = k_D\,[C^*] - \gamma\,\Phi\,I\,\frac{[C]}{[C_t]} \qquad (3\text{-}30)$$

and

$$[C^*] = \frac{\gamma\,\Phi\,I\,[C_t]}{k_D\,[C_t] + \Phi\,I} \quad . \qquad (3\text{-}31)$$

Therefore, using Equation 3-24

$$R_x = \frac{E_m\,I_x\,k_D\,[C_t]}{k_D\,[C_t] + E_m\,I_x} \qquad (3\text{-}32)$$

and

$$\mu_x = \frac{E_m'}{k_D}\,\frac{I_x\,k_D\,[C_t]}{[C_t] + E_m\,I_x} \quad . \qquad (3\text{-}33)$$

If the constants are rearranged and $\hat{\mu}_x$ is assumed proportional to C_t, then

$$\boxed{\mu_x = \frac{\hat{\mu}_x\,E_m'\,I_x}{\hat{\mu}_x + E_m'\,I_x}} \quad . \qquad (3\text{-}34)$$

Thus the microscopic specific growth rate μ_x is a rectangular hyperbolic function of the microscopic light intensity I_x and two constants $\hat{\mu}_x$ and E_m'.

By definition, $E_m' = d[f(I)]/dI$ at low intensity levels (i.e., the linear range) and is not temperature dependent; this constant can be determined experimentally. E_m' is proportional to the maximum thermodynamic efficiency, which in turn is related directly to quantum efficiency. Research on the quantum efficiencies in photosynthesis is extensive; thus, the magnitude of the coefficient E_m' can be estimated with reasonable accuracy. The coefficient $\hat{\mu}_x$ is highly temperature and species dependent and must be determined experimentally by growing algae under optimal conditions with ample light. However, the relationship

$$\hat{\mu}_x = E_m' \, I_s \qquad (3\text{-}27)$$

still holds, provided I_s is defined as the light intensity corresponding to the interception point of $E_m' = \Delta\mu/\Delta I_{(low)}$ and the asymptotic straight line $\hat{\mu}_x$ [cf. Figure 8 (II)]. The determination of appropriate values for I_s (temperature and species dependent) has been the subject of extensive research by many groups. As with E_m', the value of $\hat{\mu}_x$ can be estimated from available scientific data and by experiment.

Substituting Equation 3-27 into 3-34 and rearranging yields the expression

$$\boxed{\mu_x = \frac{\hat{\mu}_x \, I_x}{I_s + I_x}} \; . \qquad (3\text{-}35)$$

Equation 3-35 is shown graphically in Figure 8 (II).

Equation 3-35 is identical with the Michaelis-Menten equation. The similarity of the two equations is illustrative of the high degree of versatility in the application of the rectangular hyperbolic curve to the description of biological activities. This subject is discussed in detail in Appendix C.

Exponential Model (Model III)

In this model it is assumed that the relationship between C*, R_x, and μ_x and the light intensity I_x can be described best by an exponential function. Thus

$$\boxed{\mu_x = \hat{\mu}_x \left(1 - e^{-I_x/I_s} \right)} \; . \qquad (3\text{-}36)$$

Equation 3-36 is illustrated in Figure 8 (III).

An exponential function was proposed by Brackett [80] as an empirical approximation of his experimental results. He suggested the function

$$R_x = \hat{R}_x \left(1 - e^{-k \, I_x} \right) \qquad (3\text{-}37)$$

in which $\hat{R}_x$ is the maximum rate of photosynthesis as measured by oxygen evolution.

A curve similar to Equation 3-36 appeared to be the best fit of the experimental data of Van Oorschot [4], Kok [79], and in the later work that of Kok and Businger [81]. A similar relationship has been proposed for bacterial propagation by Teissier [82].

Rewriting Equation 3-36 as

$$\mu_x = \hat{\mu}_x \left(\frac{e^{I_x/I_s} - 1}{e^{I_x/I_s}} \right) \qquad (3\text{-}38)$$

and substituting e^{I_x/I_s} with its expression as a Taylor series,

$$e^{I_x/I_s} = 1 + \frac{I_x}{I_s} + \frac{1}{2!}\left(\frac{I_x}{I_s}\right)^2 + \frac{1}{3!}\left(\frac{I_x}{I_s}\right)^3 + \frac{1}{4!}\left(\frac{I_x}{I_s}\right)^4 + \ldots \qquad (3\text{-}39)$$

one can see that whenever $I_x/I_s \ll 1$,

$$e^{I_x/I_s} \cong 1 + \frac{I_x}{I_s} \quad .$$

Therefore (from Equation 3-38)

$$\mu_x = \hat{\mu}_x \left(\frac{I_x/I_s}{1 + I_x/I_s} \right)$$

or

$$\mu_x = \frac{\hat{\mu}_x \, I_x}{I_s + I_x} \qquad (3\text{-}35)$$

which is the same function used in Model II. However, if $I_x \gg I_s$, then Equation 3-36 becomes $\mu_x = \hat{\mu}_x$ similar to that of Equation 3-27 in Model I.

Comparison Between the Various Kinetic Models on the Microscopic Level

Although the relationships of the rate of photosynthesis and specific growth rate to light intensity has been investigated by many researchers, especially with respect to Chlorella, a conclusion on the best kinetic model has yet to be reached. A prerequisite for a study of this relationship is that the investigation be done with very dilute suspensions of algae maintained in thin films in which the cells are arranged, as far as is possible, in a monocellular layer so as to minimize mutual shading. If this condition is not met, the findings would be one of a macroscopic rather than a microscopic relationship, since the various cells would have been exposed to differing light intensities.

Research of this type has been carried on mostly by biochemists involved in photosynthesis in the elucidation of the mechanism and pathway of photosynthetic reactions. Such an investigation is beyond the scope of this study. However, the macroscopic model can be developed by integrating the microscopic functions of growth vs. light intensities throughout the depth of the culture (and hence throughout the light intensity gradient as it occurs).

In Figure 9 are shown the overlapping theoretical curves of the three models (I, II, and III) described earlier. The same constants are used for each. Although the three models are almost identical for very low and for the very high values of I_x; they depart significantly for intermediate light intensities between 0.025 to 0.3 cal/cm^2-min. The departure at the intermediate range is extremely significant, since this is the range of light intensity encountered in natural sunlight and artificial illumination.* Moreover, light within this particular range of intensity is utilized efficiently.

As mentioned previously, no agreement exists as to the best kinetic model for the function. For instance, with the exception of a minute curvature near the intersection of $\mu_x = \hat{\mu}_x$ and $\mu_x = E_m' I_x$, the data obtained by Sorokin et al. [83-85] in experiments involving the use of Chlorella pyrenoidosa (strain 71105) fit a pattern similar to that postulated in Model I. The Bush Equation (cf. Chapter II) recommended by Myers [46] for use in predicting algal production, also is based essentially on the same assumptions as Model I.

Tamiya et al. have demonstrated repeatedly the validity of Model II [86,87]. This model also corresponds to the kinetics of the Hill reaction described earlier [76,88]. Moreover, Model II is based on the kinetic interpretation of a rational mechanism scheme. This model was used by Miller et al. [89] in his experiments involving the applications of flashing light, as well as for the theoretical model for algal suspensions in turbulent systems exposed to intermittent light proposed by Fredrickson and his co-workers [90]. As was mentioned earlier, the data of Brackett [80], Van Oorschot [4], Kok and his co-workers [79,81] were found to be fit best by the exponential function of Model III.

Despite the significant variations between Models I, II, and III, considerable agreement exists with respect to their constant parameters E_m', $\hat{\mu}_x$, and consequently, I_s, inasmuch as $I_s = \hat{\mu}_x/E_m'$. The agreement stems from the fact that the three models do coincide in their representation of situations involving low light intensities and those concerned with very high intensities. In the former situation, the determination of E_m' is based upon the slope of the light curve at very low intensities; in the latter, all curves approach $\hat{\mu}_x$. This agreement is very important because E_m', $\hat{\mu}_x$, and I_s also are parameters in the macroscopic models.

ALGAE GROWTH AND PRODUCTION AS FUNCTIONS OF LIGHT INTENSITY AT THE MACROSCOPIC LEVEL

Any macroscopic model of growth of algae must be based on the integration of microscopic growth as it occurs at all depths of a culture. Thus, the model considers mutual shading and the gradient of light intensity, and thereby is applicable to real situations, i.e., systems consisting of many multicellular layers. Therefore three macroscopic models have been developed on the basis of the three microscopic functions described above. These models are: Model I - "First Order—Zero Order" type, Model II - based on a rectangular hyperbolic relationship, and Model III - based on the exponential function.

---

*In analogous kinetic models of bacterial propagation with respect to concentration of soluble organic substrate in waste treatment, it is possible that in most systems, the concentration levels are quite small and at the "linear" zone of curve. Thus, variations between kinetic models similar to the above will be very small, since in this range the differences between the various models are almost negligible. As is explained in the text, this situation does not exist in algal systems with respect to light intensities.

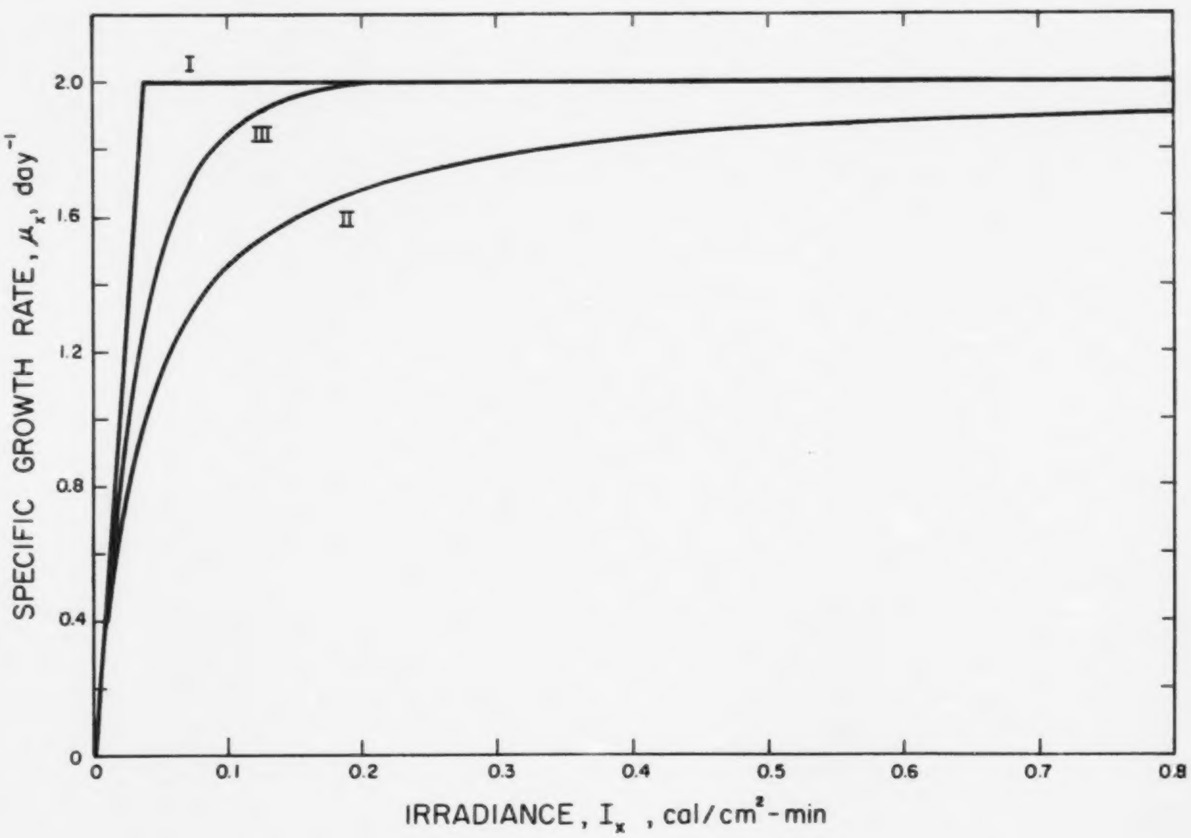

FIGURE 9. COMPARISON BETWEEN THREE KINETIC MODELS ON THE MICROSCOPIC LEVEL

A step common to the development of the three models is the equation expressing total production per unit of surface area. Since the microscopic production of algae, P_x, is equal to μ_x times the concentration C_c, then from Equation 3-7

$$P_x = C_c \; \mu_x = C_c \; f(I_x) \quad . \qquad (3\text{-}40)$$

The total production per unit surface area, therefore, becomes

$$P_a = C_c \int_{x=o}^{x=d} \mu_x \; dx = C_c \int_{x=o}^{x=d} f(I_x) \; dx \quad . \qquad (3\text{-}41)$$

If it is assumed that for monochromatic light the light intensity gradient follows the Beer-Lambert law (expressed as $I_x = I_o \; e^{-\alpha \; C_c \; x}$) then Equation 3-41 would become

$$P_a = C_c \int_{x=o}^{x=d} f\left(I_o \; e^{-\alpha \; C_c \; x} \; dx\right) \quad . \qquad (3\text{-}42)$$

An illustration of Equation 3-42 is given in Figures 10 and 11.

Since most algal systems are mixed continuously by mechanical means and/or by bubbling of CO_2, the question may arise as to whether or not the integration implied by Equation 3-42 is allowable. It appears that considerations concerning mixing by conventional means may be neglected, because the impact of light on the algal cell and the response of the cell to light are practically instantaneous. As summarized by Kamen [91], the phenomena of quantum absorption and light conversion occurs within a time scale of an order of magnitude of 10^{-15} to 10^{-9} seconds; while the consequent photochemical reactions are completed within 10^{-9} to 10^{-3} seconds. Consecutive biochemical reactions such as CO_2 assimilation and biosynthesis require a longer time period, namely from 10^{-4} to 1 second. The validity of this reasoning is demonstrated by the findings of Fredrickson _et al_. [90]. After applying a thorough-going theoretical treatment to the random movement of algal cells in an intensely stirred illuminated reactor, they proved that the effect of stirring is very limited in a system undergoing conventional mixing with random movement of cells. The effect of mixing becomes significant only under conditions of extreme turbulence (Powell [92]) or when the cells change their position with respect to light in a synchronized manner (Miller [89]) and within a time scale of the order of magnitude of the light reactions given above. In short, conventional mixing of a type that would fit the definition of a continuously stirred tank reactor (CSTR) as applied to chemical and biochemical reactions, would exert a negligible effect insofar as the assumption implied by Equation 3-42 is concerned.

The remaining steps involved in developing a model differ according to the microscopic function used.

Macroscopic Model I - "First Order—Zero Order" Type

Model I for growth and production on the macroscopic level is developed through a few steps in addition to the common step described in the previous

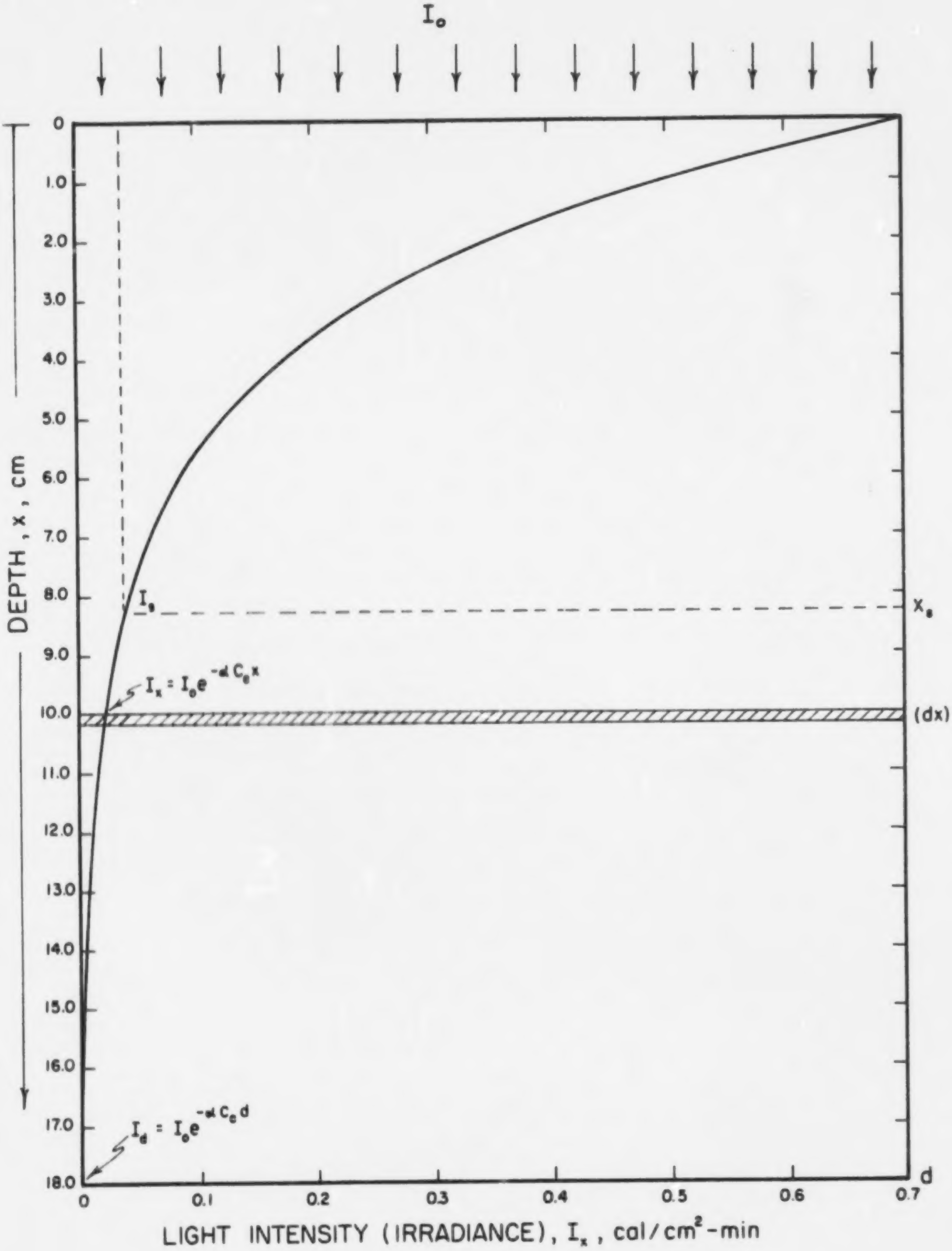

FIGURE 10. LIGHT INTENSITY GRADIENT WITHIN AN ALGAL SUSPENSION

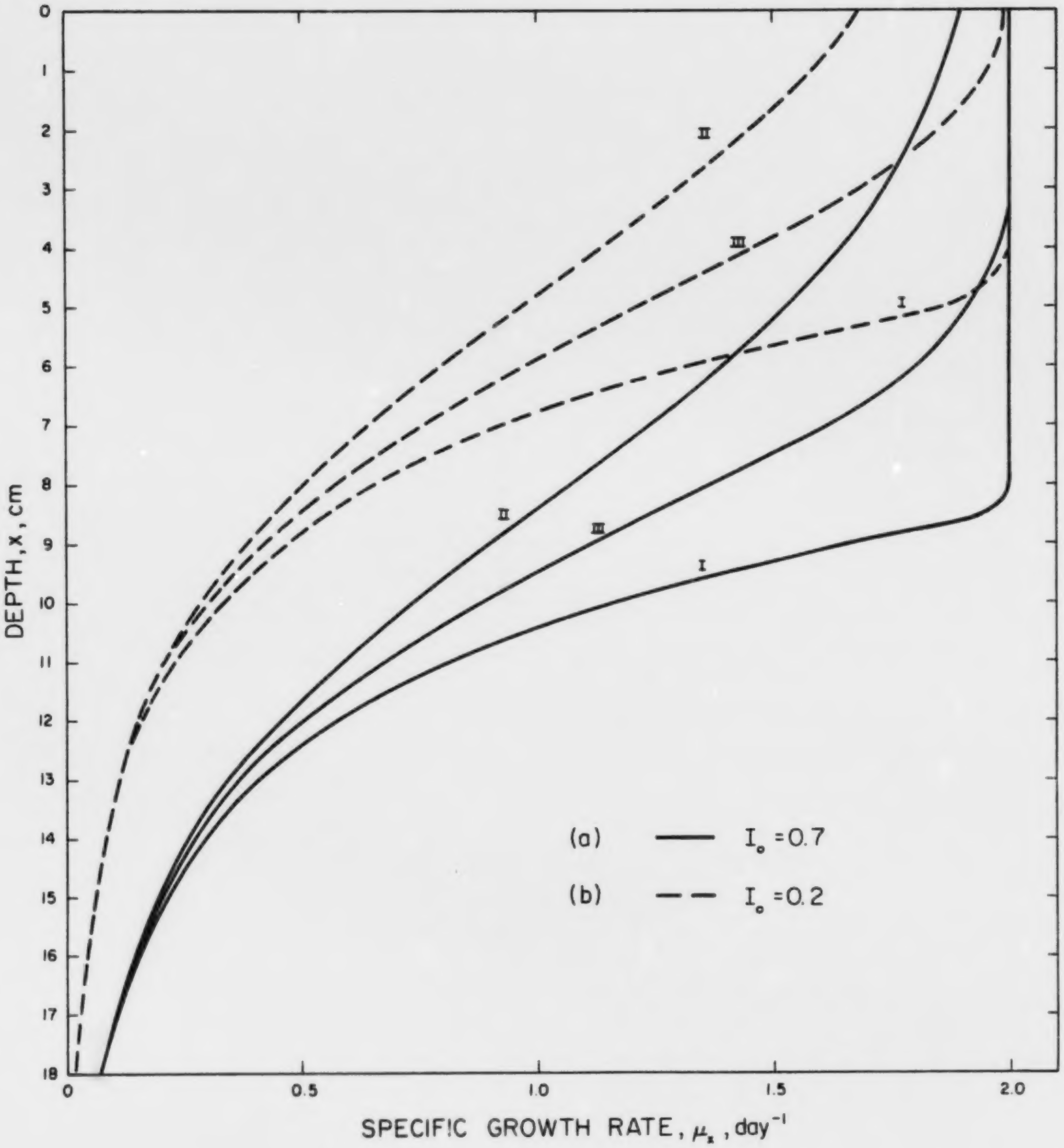

FIGURE 11. SPECIFIC GROWTH RATE ON THE MICROSCOPIC LEVEL (μ_x) AS A FUNCTION OF ALGAL SUSPENSION DEPTH (x) WHEN INCIDENT IRRADIANCE (I_o) IS APPLIED AT THE SURFACE

paragraphs. Using the formula for Model I of the microscopic level for $I_x \geq I_s$, namely

$$\mu_x = \hat{\mu}_x = E_m' \, I_s \qquad (3\text{-}27)$$

and that for $I_x \leq I_s$, namely

$$\mu_x = E_m' \, I_x \qquad (3\text{-}25)$$

in the integration described in Equations 3-41 and 3-42 with reference to Figures 10 and 11 is performed to arrive at an expression for gross production, P_{a_1} which is

$$P_{a_1} = \int_o^{x_s} C_c \, E_m' \, I_s \, dx + \int_{x_s}^{d} C_c \, E_m' \, I_o \, e^{-\alpha C_c x} \, dx \quad . \qquad (3\text{-}43)$$

Letting

$x_s' = \alpha \, x_s,$

$d' = \alpha \, d,$

$x' = \alpha \, x,$

and performing the integrations results in the expression

$$P_{a_1} = C_c \, E_m' \, I_s \, x_s' + E_m' \, I_o \left[-e^{-C_c d'} + e^{-C_c x_s'} \right] \quad . \qquad (3\text{-}44)$$

Since

$$I_s = I_o \, e^{-C_c x_s'}$$

or

$$e^{-C_c x_s'} = \frac{I_s}{I_o}$$

or

$$x_s' = \frac{1}{C_c} \ln \frac{I_o}{I_s} \quad ,$$

then by substituting in Equation 3-44, the equation for P_{a_1} becomes

$$P_{a_1} = E_m' \, I_s \ln \frac{I_o}{I_s} + E_m' \, I_o \left[\frac{I_s}{I_o} - e^{-C_c d'} \right] . \qquad (3\text{-}45)$$

Rearranging and substituting α d for d', the final form becomes:

$$\boxed{P_{a_1} = E_m' \left[I_s \left(\ln \frac{I_o}{I_s} + 1 \right) - I_o \, e^{-\alpha C_c d} \right]} \; . \qquad (3\text{-}46)$$

The expression 3-46 is representative of the area enclosed by the curves Ia and Ib in Figure 11, and is given as a function of I_o in Figure 12 (Curve I).

The similarity between Equation 3-46 and that developed with the use of the Energy Balance Model (Equation 2-31) is apparent. The only difference is the addition of the term

$$\frac{I_s}{I_o \, e^{-\alpha C_c d}} \left(\ln \frac{I_o \, e^{-\alpha C_c d}}{I_s} + 1 \right)$$

in Equation 2-31, or of its simplified form

$$\frac{I_s}{I_d} \left(\ln \frac{I_d}{I_s} + 1 \right)$$

in Equation 2-32.

In real systems, I_d will be reduced to a minimum level to minimize light losses. Thus when $I_s \cong I_d$, the above terms will be equal to unity and Equation 3-46 would be identical with Equations 2-31 and 2-32. A significant difference between the two models occurs only if the systems are very dilute and shallow and are exposed to a relatively strong incident light. Needless to say, such systems are impractical.

With respect to polychromatic light sources, a treatment similar to that used in the Energy Balance Model (Chapter II) can be applied to Equation 3-46. Thus,

$$E_m = \frac{3.92 \times 10^{-3}}{1/\phi} \int_{\lambda=400}^{700} Q_\lambda \, \lambda \, \frac{I_{\lambda R}}{R_t} \, d\lambda$$

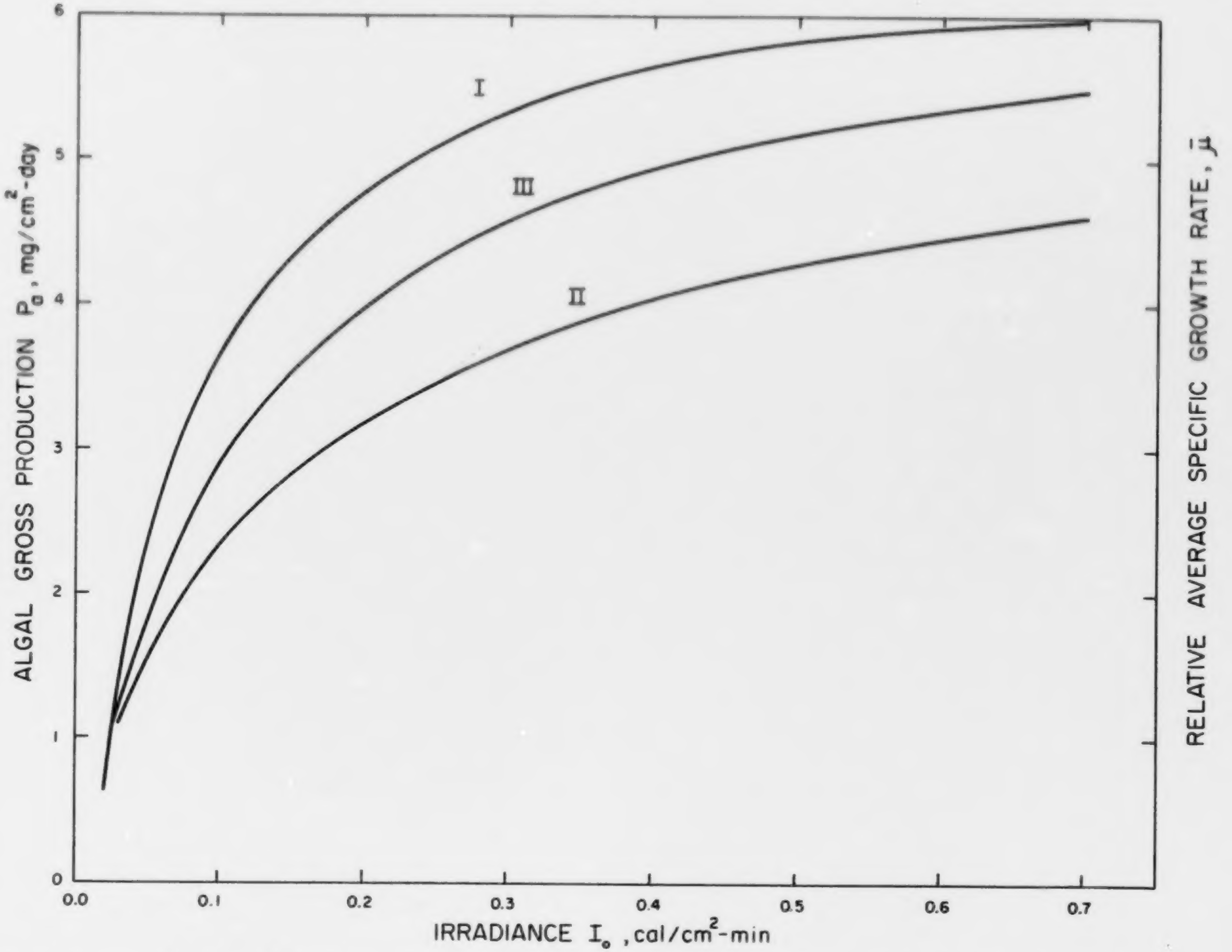

FIGURE 12. GROSS PRODUCTION OF ALGAE (P_a) AND RELATIVE AVERAGE SPECIFIC GROWTH RATE ($\bar{\mu}$) AS A FUNCTION OF THE INCIDENT IRRADIANCE (I_o), ACCORDING TO VARIOUS MACROSCOPIC KINETIC MODELS

in which

$$R_t = \int_{\lambda=400}^{700} I_{\lambda R}\, d\lambda$$

$$E_m' = \frac{3.92 \times 10^{-3} \times 1440}{J\ 1/\phi\ R_t} \int_{400}^{700} Q_\lambda\, \lambda\, I_{\lambda R}\, d\lambda$$

and the complete kinetic model based on Equation 3-46 will be:

$$\boxed{P_{a_1} = \frac{5.645}{J\ (1/\phi)\ R_t} \left[I_s \left(\ln \frac{I_o}{I_s} + 1 \right) \int_{\lambda=400}^{\lambda=700} Q_\lambda \lambda I_{\lambda R} d\lambda - I_o \int_{\lambda=400}^{\lambda=700} Q_\lambda \lambda I_{\lambda R} e^{-\alpha_\lambda C_c d}\, d\lambda \right]} \tag{3-47}$$

in which P_{a_1} is in mg of dry algae/cm^2-day. The computerized form of this equation applied to a reactor is given in Chapter VII and Appendix H.

The net production per unit of illuminated area will be:

$$\boxed{P_{na_1} = P_{a_1} - 10^{-3}\, K_d\, C_c\, d} \quad . \tag{3-48}$$

Both P_{a_1} and P_{na_1} are expressed in units of mg of dry algae cm^2-day. The average specific growth rate of the system, $\bar{\mu}$, will be:

$$\boxed{\bar{\mu}_1 = \frac{10^3\, P_{a_1}}{C_c\, d}} \tag{3-49}$$

and the average net specific growth rate:

$$\boxed{\bar{\mu}_{n_1} = \bar{\mu}_1 - K_d} \tag{3-50}$$

Macroscopic Model II (Based on the Rectangular Hyperbolic Microscopic Model)

Macroscopic Model II can be developed as follows: Using the final formula of Model II for the microscopic level described on page 33, namely,

$$\mu_x = \frac{\hat{\mu}_x I_x}{I_s + I_x} \qquad (3\text{-}35)$$

and making the integration described in Equations 3-41 and 3-42 leads to the following:

$$P_{a_2} = \int_{x=o}^{d} C_c \frac{\hat{\mu}_x I_o e^{-\alpha C_c x}}{I_s + I_o e^{-\alpha C_c d}} dx \quad . \qquad (3\text{-}51)$$

Finally, performing the integration of Equation 3-51 (cf. Appendix D) we arrive at:

$$\boxed{P_{a_2} = E_m{}' I_s \ln \frac{I_s + I_o}{I_s + I_o e^{-\alpha C_c d}}} \quad . \qquad (3\text{-}52)$$

This expression corresponds to the area enclosed by the curves IIa and IIb in Figure 11, and is given as a function of I_o in Figure 12 (Curve II).

The expression utilizing polychromatic light becomes

$$\boxed{P_{a_2} = \frac{5.645 I_s}{J\ 1/\phi\ R_t} \int_{\lambda=400}^{700} Q_\lambda\ \lambda\ I_{\lambda R} \left[\ln \frac{I_s + I_o}{I_s + I_o e^{-\alpha_\lambda C_c d}} \right] d\lambda} \qquad (3\text{-}53)$$

in which P_{a_2} is expressed in units of mg of dry algae/cm^2-day. The computerized form of Equation 3-53 applied to a reactor is given in Chapter VII and in Appendix H.

Using the same approach as in Model I, then,

$$\boxed{P_{na_2} = P_{a_2} - 10^{-3} K_d C_c d} \qquad (3\text{-}54)$$

also

$$\boxed{\bar{\mu}_2 = \frac{10^3 P_{a_2}}{C_c d}} \qquad (3\text{-}55)$$

and

$$\boxed{\bar{\mu}_{n_2} = \bar{\mu}_2 - K_d} \quad . \qquad (3\text{-}56)$$

Macroscopic Model III (Based on the Exponential Microscopic Model)

Repeating Equation 3-36, the basic equation of Model III on the microscopic level as described on page 33, which is

$$\mu_x = \hat{\mu}_x \left(1 - e^{-I_x/I_s} \right),$$

and performing the integration described in Equations 3-41 and 3-42 the following expression is obtained

$$P_{a_3} = C_c \, \hat{\mu}_x \int_{x=0}^{d} \left(1 - e^{-(I_0/I_s) e^{-\alpha C_c x}} \right) dx \qquad (3\text{-}57)$$

or

$$P_{a_3} = C_c \, \hat{\mu}_x \, d - C_c \, \hat{\mu}_x \int_{0}^{d} e^{-(I_0/I_s) e^{-\alpha C_c x}} \, dx \quad . \qquad (3\text{-}58)$$

Finally, performing the integration (cf. Appendix E) we arrive at,

$$\boxed{P_{a_3} = E_m' \, I_s \left[\alpha \, C_c \, d + E_i\left(\frac{I_0}{I_s}\right) - E_i\left(\frac{I_0}{I_s} e^{-\alpha C_c d}\right) \right]} \qquad (3\text{-}59)$$

in which E_i is the exponential integral defined as follows:

$$E_i\left(\frac{I_0}{I_s}\right) = \int_{I_0/I_s}^{\infty} \frac{e^{-t'}}{t'} \, dt' \qquad \left(\left| \arg \frac{I_0}{I_s} \right| < \pi \right) \qquad (3\text{-}60)$$

in which t' is a dummy variable of integration. The expression $E_i(I_0/I_s)$ can be solved by the following series [93].

$$E_i\left(\frac{I_0}{I_s}\right) = -\gamma' - \ln \frac{I_0}{I_s} - \sum_{n=1}^{\infty} \frac{(-1)^n \, (I_0/I_s)^n}{n \, n!} \qquad (3\text{-}61)$$

in which γ' is Euler's Constant ($\gamma' = 0.5772 \ . \ . \ .$).

Similar expressions as in Equations 3-60 and 3-61 can be applied to $E_1(I_o/I_s\ e^{-\alpha\ C_c\ d})$. Equation 3-60 can be also solved by performing a Gausian integration as is reported in Chapter VII and Appendix H.

Equation 3-59 corresponds to the area enclosed by the curves IIIa and IIIb Figure 11 and is given as a function of I_o in Figure 12.

For polychromatic light, Equation 3-59 will be

$$\boxed{P_{a_3} = \frac{5.645\ I_s}{J\ 1/\Phi\ R_t} \int_{\lambda=400}^{\lambda=700} Q_\lambda \lambda I_{\lambda R} \left[\alpha_\lambda\ C_c\ d + E_1\left(\frac{I_o}{I_s}\right) - E_1\left(\frac{I_o}{I_s}\ e^{-\alpha_\lambda\ C_c\ d}\right)\right] d\lambda} \quad . \tag{3-62}$$

Here, again, P_{a_3} is in units of mg of dry algae/cm^2-day. The computerized form of this equation applied to a reactor is given in Chapter VII and in Appendix H.

Using the same approach as in Models I and II,

$$\boxed{P_{na_3} = P_{a_3} - 10^{-3}\ K_d\ C_c\ d} \quad ; \tag{3-63}$$

also

$$\boxed{\bar{\mu}_3 = \frac{10^3\ P_{a_3}}{C_c\ d}} \tag{3-64}$$

and

$$\boxed{\bar{\mu}_{n_3} = \bar{\mu}_3 - K_d} \quad . \tag{3-65}$$

A Comparison Between the Various Macroscopic Models

In Figure 12 are illustrated the three macroscopic models in terms of both P_a and relative $\bar{\mu}$ for an algae reactor in which 95% of the light is absorbed by a culture, i.e., in which

$$\frac{I_d}{I_o} = e^{-\alpha\ C_c\ d} = 0.05 \quad .$$

All of the kinetic parameters are the same in the three models, i.e.,

$$I_s = 0.038 \text{ cal/cm}^2\text{-min}$$

and

$$E_m' = 52.5 \ (\text{day}^{-1} \text{ cal}^{-1} \text{ cm}^2\text{-min}) \quad .$$

The differences between the three models with respect to absolute production per unit area per unit of incident light intensity, relative values of production, and average specific growth rate in various ranges of light intensities, are quite significant. The differences in the ranges of I_o between 0.15 and 0.4 cal/cm^2-min are especially important, since it is within this range that most algal systems are illuminated by natural or by artificial light.

The basic form of Model I (Equation 3-46) is similar to that of the Energy Balance Model (Equation 2-31) described above. Under the assumptions involved in constructing Figure 12, i.e., $I_d/I_o = 0.05$, these two models are essentially identical.

Model II as given in Equation 3-52 differs slightly from the one developed by Tamiya [63], because of the different parameters used by Tamiya. However, both models have similar characteristics. An approach similar to that of Tamiya was followed by Tsuchiya et al. [73]. Here, again, the model is based on the integration of the rectangular hyperbola function used to describe both bacterial and algal growth, even though in the case of algae, the validity of this function remains in question [41].

Owing to its mathematical complexity, Model III, as expressed in Equation 3-62, has not been used to predict the performance of algal systems. However, its mathematical complexity does not constitute an obstacle if an electronic computer is used. Similarly, an electronic computer would be needed to utilize kinetic models of systems based on polychromatic light in which the light spectral distribution and the extinction coefficient, α, for each wavelength band should be computed (Equations 3-47, 3-53, and 3-62).

IV. ALGAL GROWTH KINETICS WITH RESPECT TO NITROGEN CONCENTRATIONS

INTRODUCTION

The models concerned with irradiance are satisfactory for use in the design of algal systems in which nutrient removal is of little concern. As for reactors designed for the removal of nutrients such as nitrogen, the relationship between algal growth and the nutrient concentration of the medium also must be determined. This is necessary to estimate proper nutrient loadings, nutrient removal rates, and the quality of the effluent. It should be noted that the effect of the nutrient as a limiting factor is secondary in importance in the design of a reactor, since the overall maximum capacity of a given reactor (and thus its optimal dimensions) will be determined largely by the primary energy source, namely light. However, with the system's capacity as determined by light, a particular nutrient can constitute a limiting factor, and as such determine the growth of the algae. This is in accordance with Liebig's classical "Law of the Minimum" and Blackman's classical concept of "Limiting Factors."

The isolation of nitrogen as a limiting factor can be done by supplying ample light to a given system while varying the supply of nitrogen. The light would have to be applied at saturation level throughout the reactor. This could be accomplished by using an extremely low algal concentration and very strong incident light. A system designed to meet such conditions would be very inefficient in terms of algal production per unit of area and hence would be impractical.

REVIEW OF LITERATURE

Nitrogen is an essential element in algal nutrition in that it constitutes a major part of the chlorophyll, nucleic acids, amino acids, and the proteins of the algae cell. Protein is a major constituent of unicellular algae; it is primarily a reproductive unit, constituting about 50% of the total cell mass. Because of its importance, the relationship between algae and nitrogen has received much attention in the literature [94-98]. In this investigation, however, only those works which are pertinent to the kinetic model proposed herein are discussed.

Nitrogen Cellular Content

The relationship between nitrogen concentration of the aqueous solution and that of the algal cells is important because nitrogen content of the cells determines the yield and removal coefficients.

Variations in protein and nitrogen content in algae according to the availability of nitrogen in the suspending medium were summarized by Parsons *et al*. [99] for selected marine algae. They found that the ratio of protein to total carbon in the algae studies was relatively fixed within a range of 1:1 and 1.5:1; and that variation in protein content due to nitrogen starvation was much less in marine algae than in freshwater algae.

Spoehr and Milner [100] working with *Chlorella pyrenoidosa* (freshwater algae) observed variations in N content of 1.2% to 14%, depending upon conditions of growth and degree of nitrogen starvation. They reported a variation in protein content ranging from 9% to 58%, depending upon degree and length of nitrogen starvation. Krauss [101] reports that during 14 days of growth in a nitrogen deficient medium, the nitrogen content of cells in a culture of *Scenedesmus* sp. decreased from 7.5% of the dry weight to 2.07%, and that the major portion of the nitrogen was in the form of protein. Tamiya [87], working with *Chlorella ellipsoida*, observed the differences in the nitrogen contents of cells in various stages of development and in various growth conditions. Thus, he found that "dark" cells contained from 7.0% to 9.5% N (dry weight) while "light" cells contained from 5.2% to 5.7%. Nihei et al. [102] reported similar results.

In studies involving Monodus subterraneus, Fogg [103] investigated the effect of nitrogen starvation on the cellular nitrogen content and growth of the organisms. He found that the protein and chlorophyll began to decline abruptly within a few days after the supply of nitrogen was cut off. The decline in protein was paralleled by a decrease in growth rate which continued until all growth ceased when the nitrogen content of the cells had dropped to 3%.

In studies on the effects of nitrogen on Microcystis aeruginosa, Gerloff and Skoog [104,105] found that a slow decrease in nitrogen content of the cells occurred as the nitrogen concentration in the media was reduced. The reduction in nitrogen was accompanied by only a small decrease in algal yield. However, when the concentration of nitrogen in the medium was reduced to 3 to 5 mg/ℓ, a rather abrupt reduction in growth took place, which was followed by sharp reduction in nitrogen content. The cellular concentration of nitrogen at this time was 3%, as compared to the 8% concentration of cells grown in medium in which nitrogen was not limiting. Gerloff and Skoog suggested that the cellular N and P content could serve as an indicator of the nutrient level and availability in oligotrophic and eutrophic lakes. In later studies, Gerloff and Krombholz [106] found a similar relationship existing in higher forms of aquatic plants.

Nitrogen Assimilation Mechanism

A knowledge of the mechanism of nitrate assimilation makes it possible to estimate the character of a kinetic model. As reported by Nicholas [107], a chain of consecutive enzymatic activity is required in the incorporation of NO_3-N into cellular material. This chain starts with the enzyme nitrate-permease, an enzyme required for the "pumping" and penetration of the nitrate ion into the cell. Once in the cell, a succession of reductase enzymes takes part in the reduction of a NO_3 ion to a form ready for incorporation into an amino acid. Nicholas [107] proposes a mechanistic model that includes four consecutive enzymatic steps as follows:

$$HNO_3 \xrightarrow[2[H]]{\substack{\text{nitrate}\\ \text{reductase}}} HNO_2 \xrightarrow[2[H]]{\substack{\text{nitrite}\\ \text{reductase}}} H_2N_2O_2 \xrightarrow[2[H]]{\substack{\text{hyponitrite}\\ \text{reductase}}} NH_2OH \xrightarrow[2[H]]{\substack{\text{hydroxylamine}\\ \text{reductase}}} NH_3 \, .$$

It has been suggested that the last step be omitted, since organic-N may be formed directly from hydroxylamine [61]. The mechanism proposed by Nicholas could explain the differences which exist between assimilation and removal rate of nitrate and those of other more reduced forms of nitrogen. It is possible that a unique kinetic relationship may exist for each major source of nitrogen.

Algal Growth as a Function of Nitrogen Concentration in the Medium

Relatively few investigations have utilized the relationship between algal growth and nitrogen concentration. Myers [62] using a continuous culture technique, could show no differences in growth rates which could be attributed to varying NO_3-N concentration within the range of 15 mg/ℓ to 340 mg/ℓ. Jones [108], growing Carteria sp. in various nitrate nitrogen concentrations in a continuous culture, found that a specific growth rate equal to 25% of the maximum could be maintained at a concentration of NO_3-N as low as 0.125 mg/ℓ. Jones also demonstrated the interrelationship between light intensity and nitrogen concentration. Caperon [109] in a kinetic study of the effect of nitrogen concentration on the growth of the marine alga Isochrysis galbana used both chemostatic continuous cultures and batch cultures. By assuming the general pattern of the Michaelis-Menten-Monod type kinetic model, he determined the kinetic constants necessary to define the model.

Rodhe [110] found that at least 5 mg/ℓ of nitrogen were required for the maximum growth of Scenedesmus quadricanda, a major species in outdoor mass culture of algae. Osterlind [111] working with the same species found that 0.1 to 5 mg/ℓ ammonia nitrogen or 10 to 50 mg/ℓ nitrate nitrogen provided good growth. Gerloff et al. [112] working with Coccochloris peniosystis showed that at nitrogen concentra- up to 6.8 mg/ℓ growth was greatly dependent on the nitrogen supply, while at higher concentrations, nitrogen was not limiting. In a later work, with Microcystis aeruginosa [104,105], Gerloff and Skoog found that maximum growth was attained with 8.0 mg/ℓ nitrogen; and that a marked decrease occurred at lower concentrations. The effect brought about by the utilization of the intracellular pool of nitrogenous metabolites or stored nutrients for algal growth at low external nutrient concentrations was observed by Williams [113] with continuous cultures and by Jewell [114] with batch cultures.

Ketchum [115] reports that the optimum nitrogen concentration for several algae was proven to be from 5 to 17 mg/ℓ. He also found that ammonium became toxic to Chlorella pyrenoidosa at concentrations of 31.5 mg/ℓ and higher.

Nitrogen Fixation

Some species of blue-green algae (e.g., species of Anabaena, Cylindrospermum, and Nostoc) are capable of fixing atmospheric molecular nitrogen when other sources of nitrogen are not available or their concentrations are extremely low [116,117]. The unavailability of other sources is a prerequisite for fixation.

Nitrogen Aspects in Waste Treatment and Pollution Control

Due to the relatively high content of nitrogen in algae and the importance of nutrient removal, the possible application of mass cultures of algae for nitrogen removal has attracted some attention. A few modest research investigations of this subject have been made ranging from laboratory-scale to pilot-scale outdoor treatment plants. Most of the work included studies on the percent reduction of nitrogen with reference to the detention period, and the quality of algae-free effluent. Only very few works consider algal growth per se, and rarely have researchers attempted to make a nitrogen materials balance on the system.

A few of the more pertinent works on algae with respect to nitrogen can be summarized as follows:

Oswald and Gotaas [3], working with high-rate algal ponds designed for photosynthetic oxygenation (i.e., for BOD removal), observed the relationship between sewage nitrogen and growing algae, and suggested a general formulation for this relationship as

$$C_c = 10N$$

in which C_c is the algal concentration and N is the nitrogen concentration of the influent. They assumed that approximately 80% of the N was being removed by algal assimilation and that the average nitrogen content of the algal biomass is approximately 8%.

Fitzgerald and Rolich [21,22] reported the reduction of ammonia-nitrogen from N values of up to 40 mg/ℓ to as low as 2 mg/ℓ in algal stabilization systems.

They also reported a 60% removal of organic nitrogen. Nitrate-nitrogen concentrations were negligible in their facultative ponds; in fact, the nitrate concentration increased at times in the effluent as a result of nitrification of incoming ammonia-nitrogen.

Neel et al. [118] state that in experiments on the treatment of raw sewage by means of experimental lagoons, they were able to attain from 94% to 98% of removal of the incoming nitrogen. They also found that at waste loadings less than 40 pounds of BOD per acre per day, photosynthetic activity in the lagoons was influenced by the concentration of available nitrogen. Bush et al. [12] reporting on the use of algae for the removal of dissolved solids from waste water, stated that removal efficiencies ranged from 63% to 90% for ammonia-N, 27% to 60% for nitrate-N, and 32% to 74% for organic-nitrogen.

Hermann [119] evaluated the performance and determined the N removal efficiency of a pilot-scale algal system designed for BOD removal. He arrived at an empirical equation based on his results as follows

$$Y_p = 0.97 - 0.032\ L_N$$

and

$$Y_e = 0.97\ L_N - 0.032\ L_N^2$$

in which Y_p is the performance of the pond as far as the effluent nitrogen concentrations are concerned expressed as a decimal fraction of a unity, Y_e is the efficiency of nitrogen removal, and L_N is the nitrate-nitrogen loadings in mg/ℓ per day. His studies revealed that at loadings greater than 15 mg/ℓ per day of nitrate-N, the efficiency of nitrate reduction declined to less than 50%. Golueke, Oswald, and Gee [120] further investigated the nitrogen regimen in outdoor pilot ponds fed with settled sewage to which were added doses of nitrogen sources in the form of anhydrous ammonia, urea, and sodium nitrate. The mutual effect of nitrogen loadings, nitrogen concentrations, and detention periods on algal yield and nitrogen removal efficiency were investigated. The preference of ammonia as compared to nitrate assimilation was observed, and the need of the algae to adapt themselves to nitrate sources was demonstrated. Nitrogen appeared to be limiting when the ammonia-nitrogen concentration in the pond was less than 12 to 16 mg/ℓ inasmuch as the addition of nitrogen under such a condition increased the algal yields as much as 60%.

Witt [121] in studies on algal culture of sewage treatment plant effluent observed a preferential absorption of ammonia in comparison to nitrate when both forms of nitrogen were present. He concluded that under optimum conditions a 20- to 24-hour detention period would suffice for near complete removal of nitrogen from secondary treatment plant effluent.

Gaur et al. [122] using continuous cultures of Oscillatoria grown on sewage and skim milk found that the nitrogen concentration determined the rate of growth of the culture at short detention periods (1-4 days); whereas very little dependence was noted at longer detention periods. Reid and Assenzo [24] growing attached algal slimes on sewage treatment plant effluent (prevalent genera--Microspora, Synedra, Oscillatoria, and Chlorella) found first-order nitrogen uptake rates between 0.017 and 0.072 ($\log_{10}$) per hour at 20°C. These rates were a function of the design of the reactor, light intensities, and types of algae.

Gates [123] found that the growth rates of Oscillatoria grown in controlled cultures fed by a biologically treated sewage (secondary effluent) were a function of the total inorganic nitrogen concentrations in the culture feed. He observed the existence of a critical range of nitrogen concentration within which the nitrogen concentration directly influenced the culture growth rate. He also noted that the quantity of inorganic nitrogen extracted from the waste was a function of the inorganic nitrogen in the culture influent. From these studies Gates predicted that with multiple exposure of the waste to algal culture of varying densities, it might be possible to attain 98% extraction of the inorganic nitrogen present in waste treatment plant effluent.

The absence of a theoretical kinetic model approach to algal processes with respect to nutrients by the workers cited above limits the interpretation of the observed data of the development of an appropriate kinetic model.

THE KINETIC MODEL OF ALGAL GROWTH AND NITROGEN REMOVAL WITH RESPECT TO NITROGEN CONCENTRATION UNDER LIGHT-SATURATION CONDITIONS

Basic Assumptions

The two assumptions fundamental to the kinetic description of algal growth which were discussed in Chapter III with respect to light intensity are also applicable to the kinetic model to be developed in this section. They are:

1. The specific growth rate of a culture is some function of the growth-limiting substrate concentration, thus

$$\mu = \frac{d\ C_c}{C_c\ dt} = f(S_N) \qquad (4\text{-}1)$$

in which S_N is the concentration of a particular nitrogenous compound expressed as N.

2. The growth rate of a culture is proportional to the rate of consumption (or removal) of the growth-limiting substrate, thus

$$\frac{dC_c}{dt} = Y\ \frac{-dS_N}{dt} \qquad (4\text{-}2)$$

in which Y is the yield coefficient defined as the mass of cells produced per unit of mass of limiting substrate utilized (or removed by assimilation). The expression $-dS_N/dt$ can be approximated by $\Delta S_N/\Delta t$ in which $\Delta S_N = S_{No} - S_{N1}$ The terms S_{No} and S_{N1} correspond to the initial and final nitrogen concentrations, respectively, and in a continuous culture Δt is equal to the mean residence time of the reactor θ. Thus,

$$\frac{d\ C_c}{dt} = Y\ \frac{S_{No} - S_{N1}}{\theta} \qquad (4\text{-}3)$$

and

$$\mu = \frac{d\ C_c}{C_c\ dt} = Y\ \frac{S_{No} - S_{N1}}{C_c\ \theta} \qquad (4\text{-}4)$$

and if we define

$$q = \frac{S_{No} - S_{N_1}}{C_c \, \theta}$$

then

$$\mu = Yq \qquad (4\text{-}5)$$

in which q is defined as the substrate removal velocity, i.e., the mass of substrate (in this case nitrogen) removed per unit of biomass per unit of time.

If all the nitrogen constituting the limiting substrate is removed by assimilation (i.e., no precipitation and volatilization taking place), then the yield coefficient Y is the inverse of the nitrogen content of the produced cells N_c and

$$Y = \frac{1}{N_c} \quad . \qquad (4\text{-}6)$$

Due to the decrease in the nitrogen content of algal cells cultured under conditions of nitrogen starvation (cf. Page 48), the yield coefficient is not a constant, and it is dependent upon the nitrogen concentration – at least within a limited range of S_N. Thus

$$Y = f(S_N) \qquad (4\text{-}6A)$$

and Equation 4-5 becomes

$$\mu(S_N) = Y(S_N)\, q(S_N) \quad . \qquad (4\text{-}7)$$

Therefore, assumption No. 2 is not entirely valid as far as the model to be presented herein is concerned.

Knowing the function $Y(S_N)$, one could apply it to a situation such as that described by Equation 4-7, in which case a rather complicated kinetic model would result. However, values for $Y(S_N)$ are not available in the literature; nor can they be elucidated from the experimental results of work done as a part of this research. Values of N_c obtained in this experiment with low nitrogen concentrations were not consistent. Fortunately, Y appears to be a constant at slightly higher nitrogen concentrations (approx. 1 mg/ℓ and higher). These concentrations are of the order that would occur in the practical application of the mass culture of algae for nutrient removal and/or algae production. For nitrogen concentrations within certain limits (approx. 1 mg/ℓ to approx. 15 mg/ℓ for Chlorella sp.) Equations 4-2, 4-3, 4-4, and 4-5 do apply, and assumption No. 2 should be modified as follows: "At concentrations of a growth-limiting nutrient above a certain minimum and lower than a certain maximum, the growth rate of a culture is proportional to the rate of consumption (or removal) of the growth-limiting substrate."

It should be noted that the function $Y(S_N)$ is important in situations involving low concentrations of a growth-limiting substrate corresponding to marginal growth rate. Therefore, this function should be considered when the nutrient concentration is lower than optimum, such as is the case in natural bodies of water and in long-term batch cultures.

Specific Growth Rate as a Function of Nitrogen Concentration

Referring to assumption No. 1, the appropriate function $\mu = f(S_N)$ in Equation 4-1 must be developed.

Information reported previously indicates that a hyperbolic or "diminishing return" type of relationship exists between nitrogen concentration and algal growth. It appears reasonable to use an approach similar to that used for bacterial growth.

The Michaelis-Menten-Type Function. The rectangular hyperbola is the function most commonly used in expressing the relationship between microbial growth and the concentration of rate-limiting nutrient or energy supply. This relationship is based upon the Michaelis-Menten equation which was developed to describe rate of enzyme reaction as a function of concentration of substrate; and which was observed empirically by Monod [124,125] to describe adequately the growth of bacteria in continuous flow chemostat studies. This equation has the following form:

$$\boxed{\mu = \frac{\hat{\mu}\, S_N}{K_s + S_N}} \qquad (4\text{-}8)$$

in which K_s is the substrate concentration at one-half the maximum growth rate (i.e., $\mu = \hat{\mu}/2$).

The relation between μ and S_N is shown in Figure 13(A). A linear relation between $1/\mu$ and $1/S_N$ is found when one uses the reciprocal form of Equation 4-8 as follows,

$$\boxed{\frac{1}{\mu} = \frac{K_s}{\hat{\mu}}\frac{1}{S_N} + \frac{1}{\hat{\mu}}} \quad . \qquad (4\text{-}9)$$

The constants K_s and $\hat{\mu}$ can be obtained graphically. This relationship is illustrated in Figure 13(B).

In addition to being relatively simple, the Michaelis-Menten equation is based upon general enzyme-substrate reaction or surface controlled reactions (Langmuir Adsorption Isotherm). (A discussion of the wide applicability of the rectangular hyperbola to various postulated reaction mechanisms is presented in Appendix C.)

The Monod and Michaelis-Menten Equation for the kinetic description of microbial growth on growth-limiting substrates was confirmed by Herbert [126,127], Northam [128] and others. It is now generally accepted by microbiologists and engineers working with continuous bacterial systems involving either pure or mixed cultures. In sanitary engineering for example, descriptions of kinetic systems making use of the Michaelis-Menten equation have been proven to be valid in experiments with bacterial systems — aerobic [129-131], and anaerobic [132-135] — which were concerned with use of various energy-source substrates. A summary of the applications of the Monod model in bacterial biological waste treatment has been given by Pearson [136].

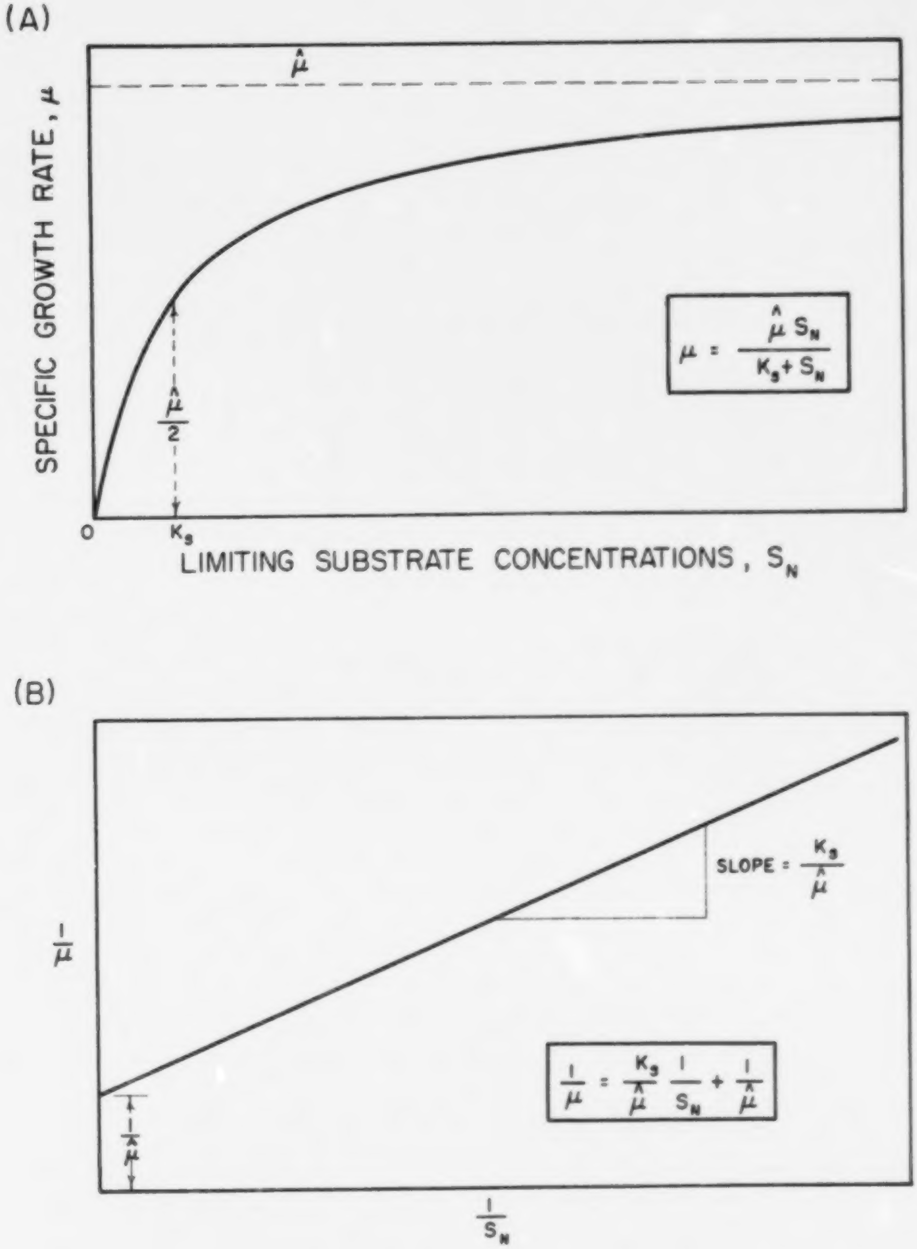

FIGURE 13. THE RELATIONSHIP BETWEEN THE GROWTH-LIMITING SUBSTRATE CONCENTRATION (S_N) AND SPECIFIC GROWTH RATE (μ), AS DESCRIBED BY MICHAELIS-MENTEN THEOREM

Caperon [109] found that the function $\mu(S_N)$ in the culture of the marine algae *Isochrysis galbana* with nitrate-N as the limiting factor can be described with a general hyperbolic-type pattern. Although his results did not fit exactly the pattern of a rectangular-hyperbola, he preferred to use the Michaelis-Menten equation to describe them because of its universality. Thus he found the parameters K_s and $\hat{\mu}$ by linear regression (of rather scattered data) to be 2.13 and 2.38 micro-gram-atom per liter as N for K_s (for two different runs under the same applied conditions) and 0.333 hr^{-1} and 0.531 hr^{-1} for $\hat{\mu}$ (for the two experimental runs as above). Due to scattered data within each run and the differences in results between the runs, a precise description of the function $\mu(S_N)$ cannot be made from Caperon's experiments.

Attempts to describe the growth rate of *Chlorella pyrenoidosa* (Emerson and TX 71105 strain) as a function of nitrate-N concentration with a Michaelis-Menten relationship have proven unsuccessful. An explanation of the inapplicability of the Michaelis-Menten equation to a situation in which nitrate-N is the limiting nutrient may be in the complexity of the various enzymatic sequences involved in nitrate assimilation (cf. page 73).

Moser's Function. Various mathematical relationships other than the rectangular hyperbola have been proposed for describing the function $\mu(S_N)$. Among them is one developed by Moser [137] which would fit a nonrectangular hyperbola more closely than it would one which is rectangular. It is:

$$\mu = \frac{\hat{\mu}\, S_N^n}{K_s + S_N^n} \quad . \tag{4-10}$$

This equation can be reduced to Monod-Michaelis-Menten expression (Equation 4-8) when n=1.

Teissier's Exponential Function. Teissier [82] in his work with bacterial populations, proposed the use of an exponential relationship similar to the one that was used in describing algal growth with respect to light intensity (Model III, page 45). His equation has the following form

$$\boxed{\mu = \hat{\mu}\left(1 - e^{-S_N/K_s}\right)} \tag{4-11}$$

in which K_s has the same value as in Equation 4-8.

The relation of Equation 4-11 to Equation 4-8 can be shown by rewriting it as

$$\mu = \frac{\hat{\mu}\left(e^{S_N/K_s} - 1\right)}{e^{S_N/K_s}} \tag{4-12}$$

and substituting for e^{S_N/K_s} its Taylor series (cf Equation 3-57). It is apparent that whenever $S_N/K_s \ll 1$, the first two terms of its Taylor series can be used to approximate e^{S_N/K_s}, i.e., by $1 + S_N/K_s$. Substituting these two terms of Taylor series into Equation 4-12, then when $S_N/K_s \ll 1$,

$$\mu = \frac{\hat{\mu}\, S_N}{K_s + S_N}$$

which is equivalent to Equation 4-8.

The Modified Exponential Function. Moser's equation did not fit the experimental results in this presentation nor did the original Teissier equation. The equation which best fit the data was found to be an exponential of the following general form

$$\mu = \hat{\mu}\left(1 - e^{-kS_N}\right) \qquad (4\text{-}13)$$

in which k is a constant dependent on temperature and on genetic characteristics. Possibly a better way to express Equation 4-13 is a "Modified Exponential Function" as follows:

$$\boxed{\mu = \hat{\mu}\left(1 - e^{-S_N/K_A}\right)} \qquad (4\text{-}14)$$

in which K_A is a constant corresponding to a specific concentration of the growth-limiting substrate. It also can be related to a given proportion of the maximum growth rate in a fashion similar to K_s but without necessarily relating it to $\hat{\mu}/2$. Equation 4-14 can be rewritten as

$$\mu = \hat{\mu}\, \frac{e^{S_N/K_A} - 1}{e^{S_N/K_A}} \qquad (4\text{-}14A)$$

and when $K_A = S_N$ from Equation 4-14A

$$\mu = \hat{\mu}\, \frac{e - 1}{e} = 0.632\ \hat{\mu} \quad . \qquad (4\text{-}14B)$$

Thus, K_A is equal to the value of S_{N1} which corresponds to a specific growth rate of 0.632 $\hat{\mu}$.

Equation 4-14 is illustrated in Figure 14 (A). Equation 4-14 can be transformed to the following logarithmic function:

$$\boxed{\log \frac{\hat{\mu}}{\hat{\mu} - \mu} = \frac{0.4343}{K_A}\, S_N} \quad . \qquad (4\text{-}15)$$

Equation 4-15 is illustrated in Figure 14 (B). Once the value of $\hat{\mu}$ is known, then the value of K_A can be found by performing a linear regression on the logarithmic function (cf. Appendix H).

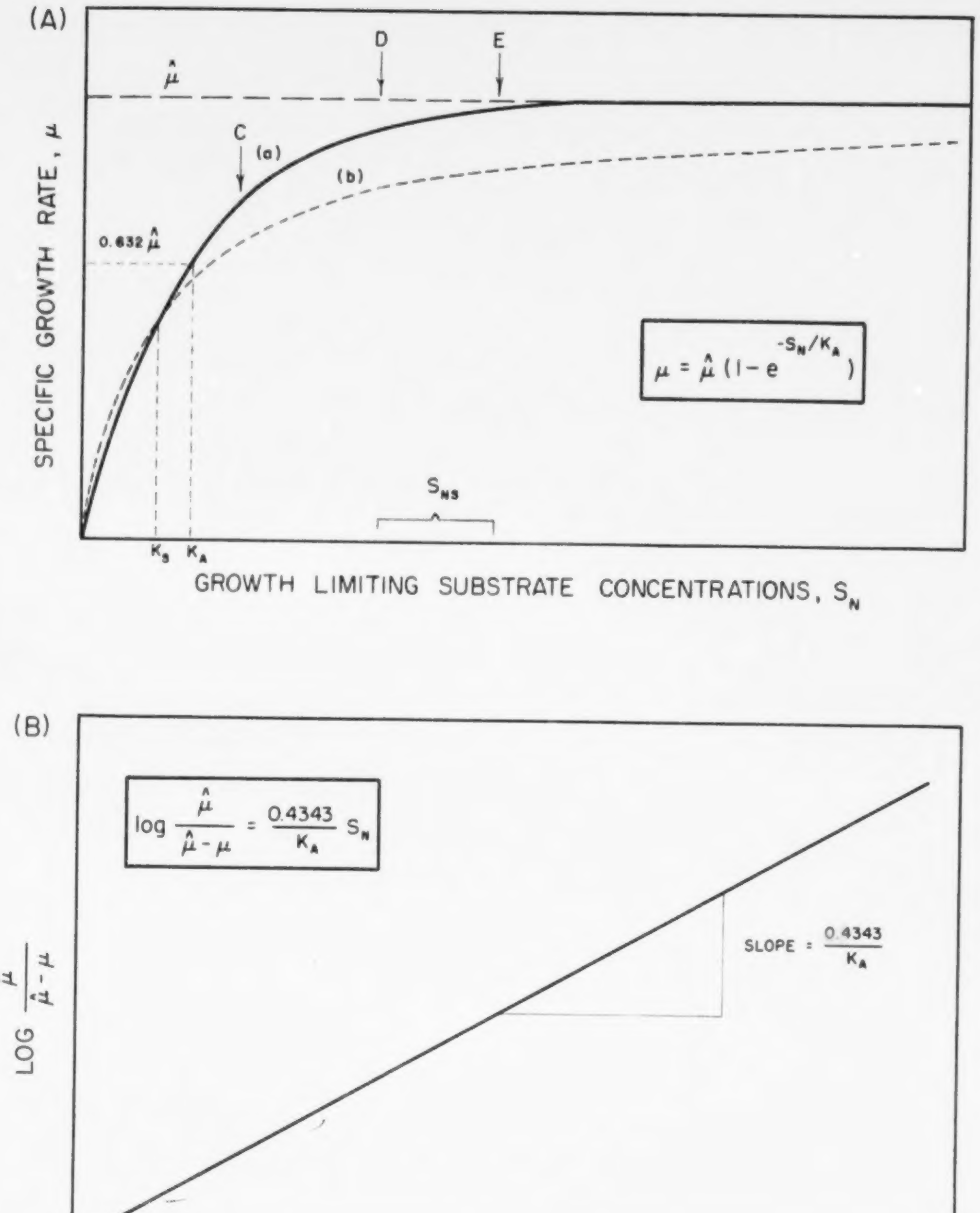

FIGURE 14. THE RELATIONSHIP BETWEEN THE GROWTH-LIMITING SUBSTRATE CONCENTRATION (S_N) AND SPECIFIC GROWTH RATE (μ), ACCORDING TO THE PROPOSED "MODIFIED EXPONENTIAL FUNCTION"

A Comparison between Michaelis-Menten and the Modified Exponential Functions. In Figure 14 (A) is illustrated the comparison between the proposed kinetic relationship as expressed in Equation 4-14 (Curve A) and the Michaelis-Menten relationship expressed in Equation 4-8 (Curve B), in which both curves have the same value for $\hat{\mu}$ and K_s. The similarity between the two curves for values of $S_N \leq K_s$ should be noted.

Materials Balance of a Chemostatic or Turbidostatic Algal Continuous System

Algal systems generally are nonrecycle systems insofar as biomass separation and recycle are concerned. This is due not only to the technical difficulty associated with cell separation and recycle but also due to the fact that it would tend to reduce the net growth of the system. The relatively high cost of separation of unicellular algae also is an important deterrent. Any recirculation of concentrated biomass would necessitate the provision of a separator in addition to that needed for harvesting, and therefore should be avoided if possible.

The following materials balance on biomass can be written for a nonrecycle CSTR-type (Figure 15) in which the effluent is assumed to have the same concentrations of substrate and biomass as those in the reactor:

$$V \frac{d\,C_c}{dt} = Q\,C_{co} + V\,C_c\,\mu - V\,K_d\,C_c - Q\,C_c \qquad (4\text{-}16)$$

in which V is the volume of the reactor, Q is the flow rate, and K_d is the decay coefficient.

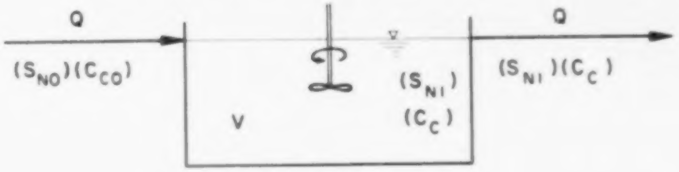

FIGURE 15. SCHEMATIC FLOW SHEET OF CSTR-TYPE GROWTH UNIT (NO RECYCLING OF BIOMASS)

Assuming that the influent media is free of algae, i.e., $C_{co} = 0$, then at steady state, in which $dC_c/dt = 0$, the following equation is the result:

$$\frac{Q}{V} = \mu - K_d \quad . \qquad (4\text{-}17)$$

In other words the dilution rate Q/V is equal to the net specific growth rate, μ_n, when

$$\mu_n = \mu - K_d \quad . \qquad (4\text{-}17A)$$

Substituting Equation 4-5 for μ in Equation 4-17 results in

$$\frac{Q}{V} = Yq - K_d \quad . \tag{4-18}$$

Assuming that $\mu(S_N)$ is best represented by Equation 4-14, then

$$q = \frac{\hat{\mu}}{Y}\left(1 - e^{-S_N/K_A} \right) \tag{4-19}$$

or

$$\frac{S_{No} - S_{N1}}{C_c \, \theta} = \frac{\hat{\mu}}{Y}\left(1 - e^{-S_N/K_A} \right) \tag{4-20}$$

and

$$\frac{Q}{V} = \hat{\mu}\left(1 - e^{-S_N/K_A} \right) - K_d \quad . \tag{4-21}$$

The value for K_d, the decay rate, could not be estimated experimentally using Equation 4-18 because the yield coefficient was not constant for all values of S_N and the data for $\mu(S_N)$ at low values of S_N were scattered. Moreover, the constant value of $K_d = 0.125 \text{ day}^{-1}$ assumed in the kinetic models with respect to light, could not be used to estimate the value of K_d in the nitrogen materials balance. This is because $K_d = 0.125 \text{ day}^{-1}$ was based on assumed energy and mass losses by endogenous respiration, i.e., light energy utilized directly in the respiration cycle or energy attained by utilization of stored carbohydrates and lipids. No significant nitrogen consumption or losses are expected to be associated with the endogenous respiration. Proteins are assumed to be only slightly affected by endogenous respiration. In fact the protein content of cells increases during respiration in the dark as reported by Tamiya [87] and Nihei et al. [102]. Insofar as the assimilative removal of nitrogen and/or net algal production are concerned, the value of μ_n is the one of practical significance rather than μ. Consequently, the values of μ and $\hat{\mu}$ in the various equations in this chapter were estimated by the net values of the specific growth rate (i.e., μ_n and $\hat{\mu}_n$) which in turn were determined experimentally.

Thus the following equations can be developed from Equations 4-17 and 4-17A,

$$\boxed{\frac{Q}{V} \cong \hat{\mu}_n\left(1 - e^{-S_N/K_A} \right)} \tag{4-22}$$

and

$$\frac{Q}{V} = \mu_n \cong Y\,q \quad . \tag{4-23}$$

V. GROWTH AND PRODUCTION OF ALGAE IN SYSTEMS IN WHICH BOTH LIGHT AND NITROGEN ARE LIMITING

For optimum performance of a photosynthetic reactor the algal concentration should be relatively high and the culture dense to absorb all the light. Light conversion efficiency and production of algal biomass per unit of illuminated surface or per unit of reactor volume increase substantially in cultures having relatively high concentrations of algae and absorbing maximum amounts of light. This relationship is illustrated in Figure 16 in which are shown light absorption, specific growth rate, and net specific growth rate as a function of concentration of a culture grown in a simple rectangular reactor at depth d and incident irradiance I_o. The algal concentration of the culture in the A series of curves is assumed to be 400 mg/ℓ; and that in the B series to be 200 mg/ℓ. Sections A_1, A_2, B_1, and B_2 of the figure describe the distribution of light intensities within the cross section of the reactor; and sections A_3 and B_3, the microscopic specific growth rate according to the three models described in Chapter III. On the basis of the respective macroscopic kinetic models (cf. Chapter III), gross algal production dependent on light alone is proportional to the area confined by curves I, II, and III in A and B. The net specific growth rate of the algae taking into consideration respiration and decay at an assumed constant rate, K_d, is shown in sections A_4 and B_4. (The latter illustration is an example only of Model III.) The net surface algae production when light is the limiting factor is proportional to the area confined by the A-D portion of the curve minus the area confined by the portion D-E in sections A_4 and B_4 of the figure. The area confined by the D-E portion represents the net loss of biomass in the part of the culture in which light intensities are below that of compensation intensity, I_b*. It should be noted that although light is deficient in the lower strata of the culture when the algal concentration is 400 mg/ℓ (A series in Figure 16), useful light is lost by light penetrating and leaving the culture when the concentration is at 200 mg/ℓ (B series in Figure 16). Obviously the ideal situation is one in which in a given reactor the concentration of algae is such that the compensation intensity, I_b, is reached precisely at the bottom of the reactor (i.e., when $d = d_b$). Sections A_5 and B_5 of Figure 16 show the yields to be expected at algal concentrations of 400 mg/ℓ and 200 mg/ℓ as contrasted with the maximum yield that would be obtained if $d_o = d$. Judging from the similarity between amounts of the expected yields and that of the maximum attainable, the levels of concentration selected for examples A and B were not far from the "ideal."

Whenever the nitrogen concentration in an algal reactor is such that it exerts a limiting effect on specific growth rate, a situation arises in which both light and nitrogen limit the growth of algae, but each in separate regions of the reactor. For example, if the nitrogen concentration S_N is at a level corresponding to a particular specific growth rate, μ_N' (point "C" in Figure 14), i.e., in this example at 0.75 of its maximum, the macroscopic growth rate of the algae will be limited by μ_N' as indicated by the dashed line B-C in section A_3, B_3, A_4, and B_4 in Figure 16. Similarly the expected algal production for the proposed Models I, II, and III will be decreased in proportion to the area confined by points A-B and C. The net production, then, will be proportional to the shaded area defined by points B, C, and D minus the shaded area defined by the D-E in section A_4 in Figure 16. The effect of such a nitrogen-limiting condition on total net algal production, and in this case, on removal of nitrogen by assimilation, is indicated by the shaded areas in sections A_5 and B_5 of Figure 16.

---

*Compensation Intensity, I_b, is defined as the level of light intensity at which oxygen produced in photosynthesis is equal to that used in endogenous respiration. Thus no oxygen exchange is noticeable. The value of I_b is approximated as being between 0.01 and 0.05 cal/cm^2-min and is dependent on the environmental conditions, past history of the cells, and genetic characteristics. No agreement has been reached yet on the exact value of I_b for Chlorella sp., for example.

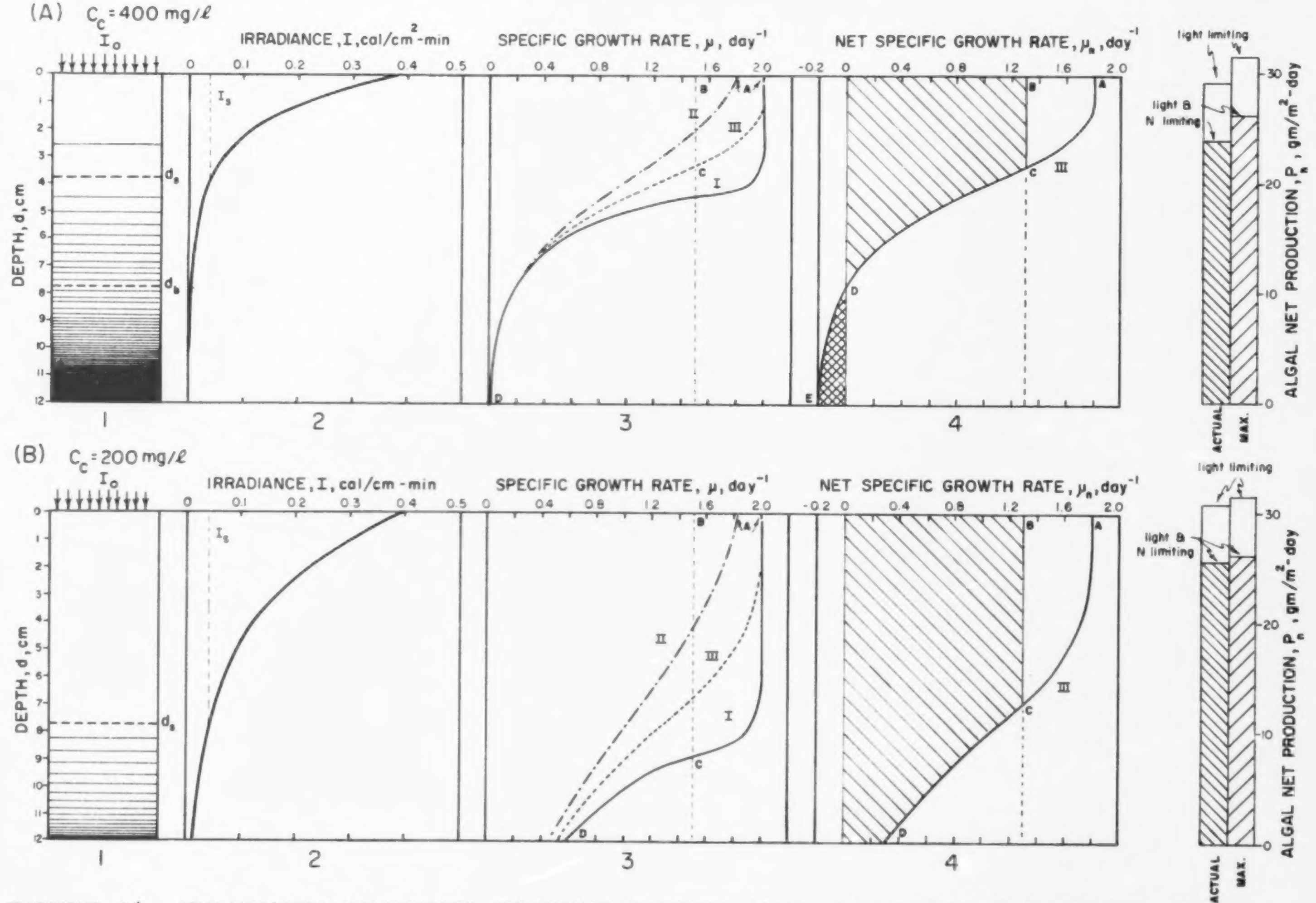

FIGURE 16. IRRADIANCE GRADIENT, SPECIFIC GROWTH RATE, AND ALGAL PRODUCTION IN TWO HYPOTHETICAL OPTICALLY DENSE ALGAL CULTURES OF DIFFERENT CONCENTRATIONS WHEN NITROGEN CONSTITUTES A GROWTH-LIMITING FACTOR

The mathematical development of the function corresponding to the difference between the integrals representing the appropriate areas in sections A_4 and B_4 in Figure 16 is a very complicated one, and can be done only on the basis of trial and error with the computerized form of the function. Moreover, such an approach was proved impractical when dealing with algal growth units such as those used in this study. This was because of the geometrical arrangement of the growth units and the geometrical distribution of the incident irradiance on the culture surface. Hence, a more simplified empirical approach to describe the relationship between algal growth and production in an optically dense culture was used based on the experimental results. This approach is described and discussed in Chapter VII.

Judging from the information given in Figures 14 and 16, an optimum level of nitrogen concentration for algae production and the assimilative removal of nitrogen would be one within the D-E portion of the curve in Figure 14; that is, one which will permit maximum growth and yet result in an effluent having a low nitrogen concentration. This concentration level is designated by S_{NS}*. At nitrogen concentration levels (S_N) which are less than those at point D in Figure 14, algal production will drop sharply. Although optimal for algae growth, an S_N beyond point E will be accompanied by an unnecessary increase in the nitrogen concentrations of effluent and, of course, a consequent decrease in the efficiency of nitrogen removal.

---

*Later in this study S_{NS} is defined as the value of S_{N1} corresponding specifically to $\mu = 0.9\ \hat{\mu}$.

VI. EXPERIMENTAL METHODOLOGY

EXPERIMENTAL ORGANISMS

Two strains, Emerson and TX 71105 (developed by Sorokin and co-workers), of the species of *Chlorella pyrenoidosa* were selected as the major groups of experimental organisms to be used in the work reported herein. The Emerson strain was used in experiments in which the temperature was maintained at levels between 20°C and 30°C. Strain TX 71105 was used in those experiments in which the temperature was kept at a level higher than 30°C. One of the reasons for selecting the species *Chlorella pyrenoidosa* was its rapid growth rate and capacity for production. Another was the fact that it is quite commonly encountered in mass cultures of algae and in natural algal systems. Use of the species in mass cultures and its ofttimes predominance in natural situations are due to the rapid growth rate of the members of the species. Traditionally, *Chlorella pyrenoidosa* has been regarded as a good representative of unicellular green algae. Moreover, its characteristics rather closely resemble those of widespread species of unicellular green algae, as for example, *Chlorella vulgaris* and *Scenedesmus* spp. [138]. The Emerson and Sorokin strains were selected for study because many of their characteristics are well known and have been reported in the literature.

Adaptation to low concentrations of nitrogen did not enter into the decision on the types of organisms to be used. In fact, the original isolation of *Chlorella pyrenoidosa* was from moist rich soils apparently having a high nitrogen content, while the inocula used in the present studies were obtained from stock cultures maintained on nitrogen-rich media over a number of years. However, since a species of *Chlorella* most likely will be the major organism in practical algal biomass production systems, the influence of nitrogen availability and concentration of nitrogen on its growth and production rate is a very important consideration in the design of such systems.

Pure cultures of the two strains of *Chlorella pyrenoidosa* were obtained from the Biodynamics Laboratory of the University of California (Berkeley) and from the U.S. Air Force School of Aerospace Medicine, Brooks Air Force Base, Texas. Stock cultures were kept on agar slants under bacteria-free conditions. However, no special precautions were taken to maintain the cultures free of bacteria while growing in the environmental growth chambers. The stock cultures were subcultured at four-week intervals to maintain genetic characteristics.

ALGAL GROWTH UNITS

Three types of growth units were used in the course of the experimental work. The first was a one-liter continuous chemostatic type of growth unit; the second, a one-liter continuous turbidostatic type; and the third, a 9.7-liter algatron (continuous chemostatic spin-type reactor). The chemostatic and the turbidostatic growth units were employed in the development of the kinetic model with respect to nitrogen. The algatron was used to obtain data needed for the kinetic models concerned with light intensity.

Chemostatic Growth Units

Except for certain minor modifications, the five chemostatic growth units used in the experiments were the same in design and operation as those described by Oswald [38,139,140]. They were constructed of cylindrical pyrex culture tubes 70 cm in length and 5.5-cm inside diameter; culture volume of the individual tubes was approximately one liter. Each tube was equipped so that a predetermined amount of medium could be added each 30-minute interval throughout the course of an experimental run. The contents of the tube were maintained in a continuously stirred condition by bubbling a mixture of CO_2 and air through the reactor.

Constant and continuous light intensity was applied unilaterally to each culture by four (per culture) 30-watt full-spectrum fluorescent lamps*. To provide light saturation conditions throughout the cross section of the culture, the suspended solids concentration of the culture usually was kept at less than 130 mg/ℓ. Light saturation was attained by imposing conditions which would result in the irradiance penetrating through the culture to be equal to or more than 0.05 cal/cm^2-min.

The temperature of the cultures in the units was maintained at the desired level (±0.7°C) by passing water held at a suitable temperature through a "cold finger" inserted in each tube.

Each tube was equipped with two outlets so that it could be operated as a turbidostatic growth unit when desired. Advantage was taken of this feature in the initial period of runs in which the conditions to be imposed were such that an inordinate length of time would be required for a culture to reach steady state if grown under chemstatic conditions.

Schematic sketches of the units and their appurtenances are shown in Figures 17 and 18. Additional information is supplied in Appendix F.

Turbidostatic Growth Unit

A turbidostat is characterized by the maintenance of a steady state, predetermined population density accomplished by means of a photoelectric control. The photoelectric system regulates the population density by controlling the frequency and volume of dosage of medium and hence the dilution rate as determined by the amount of light penetrating a sample of the culture. A turbidostatic control system has marked advantages over a chemostatic control system with respect to the time required to reach steady state conditions following a change in the experimental conditions. It also permits a greater degree of precision in control of the culture than is possible with chemostat.

The turbidostatic growth unit system used in this study consisted of a turbidostat and growth vessel. The turbidostat and the vessel controlled by it are shown in Figures 19 and 20. The vessel was identical in design and interchangeable with the vessels used in the chemostatic system. The turbidostat, a two-channel unit, was assembled and constructed by the personnel of the Lawrence Radiation Laboratory of the University of California specifically for work with unicellular algae in photosynthetic studies. One of the channels was used exclusively for the turbidostatic system. The second was used interchangeably and temporarily with one or the other of the vessels of the chemostatic system.

In preliminary experiments it was found that monitoring of scattered light provided a better control of algae concentration in terms of weight of biomass (i.e., concentration as mg material per liter of volume) than did that of optical density. Consequently, a scattered light sensor was used in the experiments to be described. An optical density sensor is strongly influenced by the pigment content of the biomass (primarily chlorophyll) while a scattered light sensor is more reactive to the concentration of biomass as expressed by total suspended solids or to the number of cells per unit of volume. However, the latter is somewhat influenced by the cell size distribution.

A block diagram of the turbidostatic system used in the study is shown in Figure 21, and the components of the sensor, in Figure 22. The sensor as set up

---

*"Optima" type manufactured by the Duro-Test Co., North Bergen, N. J.

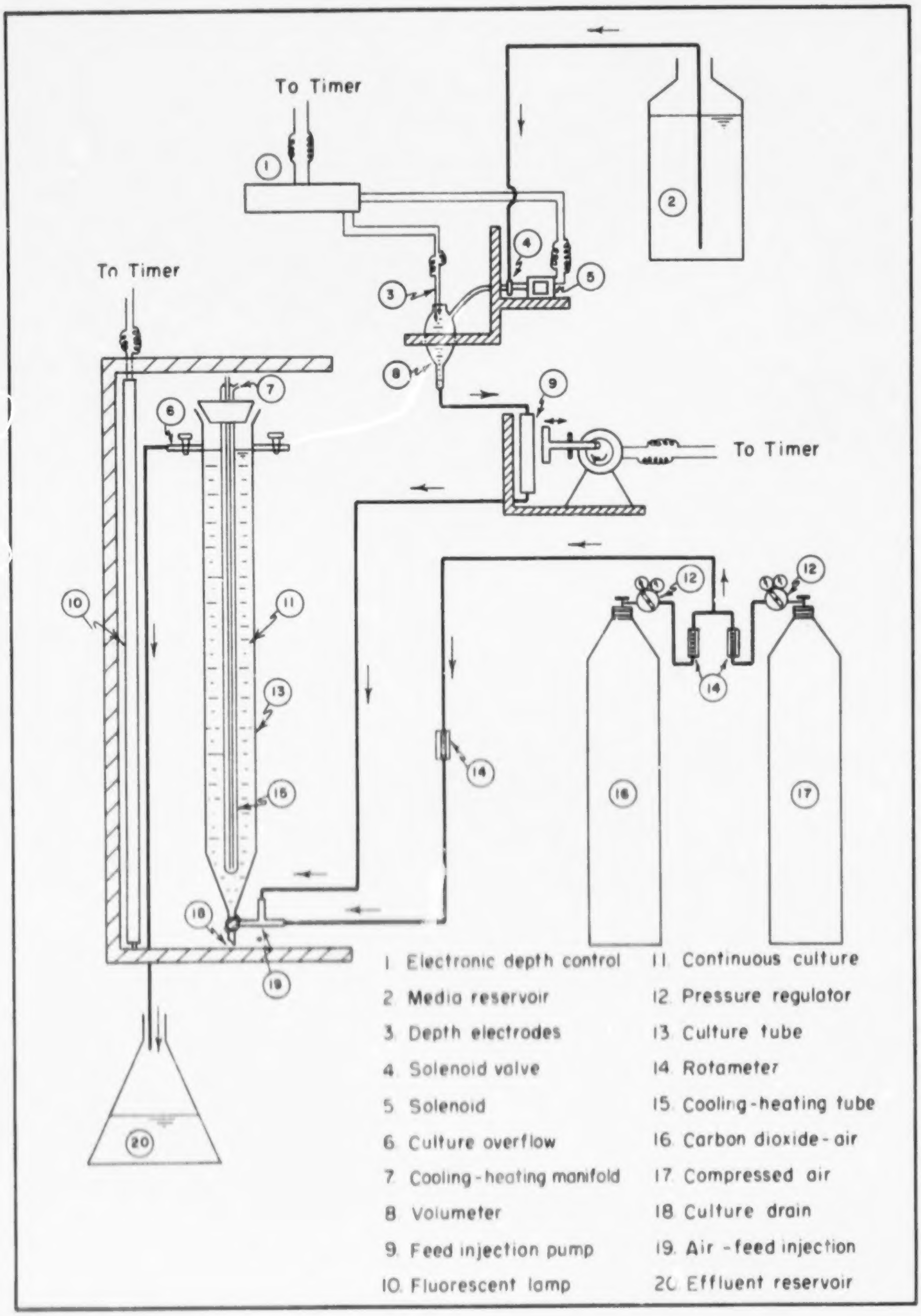
To Timer
To Timer
To Timer
1. Electronic depth control
2. Media reservoir
3. Depth electrodes
4. Solenoid valve
5. Solenoid
6. Culture overflow
7. Cooling-heating manifold
8. Volumeter
9. Feed injection pump
10. Fluorescent lamp
11. Continuous culture
12. Pressure regulator
13. Culture tube
14. Rotameter
15. Cooling-heating tube
16. Carbon dioxide-air
17. Compressed air
18. Culture drain
19. Air-feed injection
20. Effluent reservoir

FIGURE 17. DIAGRAMMATIC SKETCH OF THE CHEMOSTATIC GROWTH UNIT SYSTEM

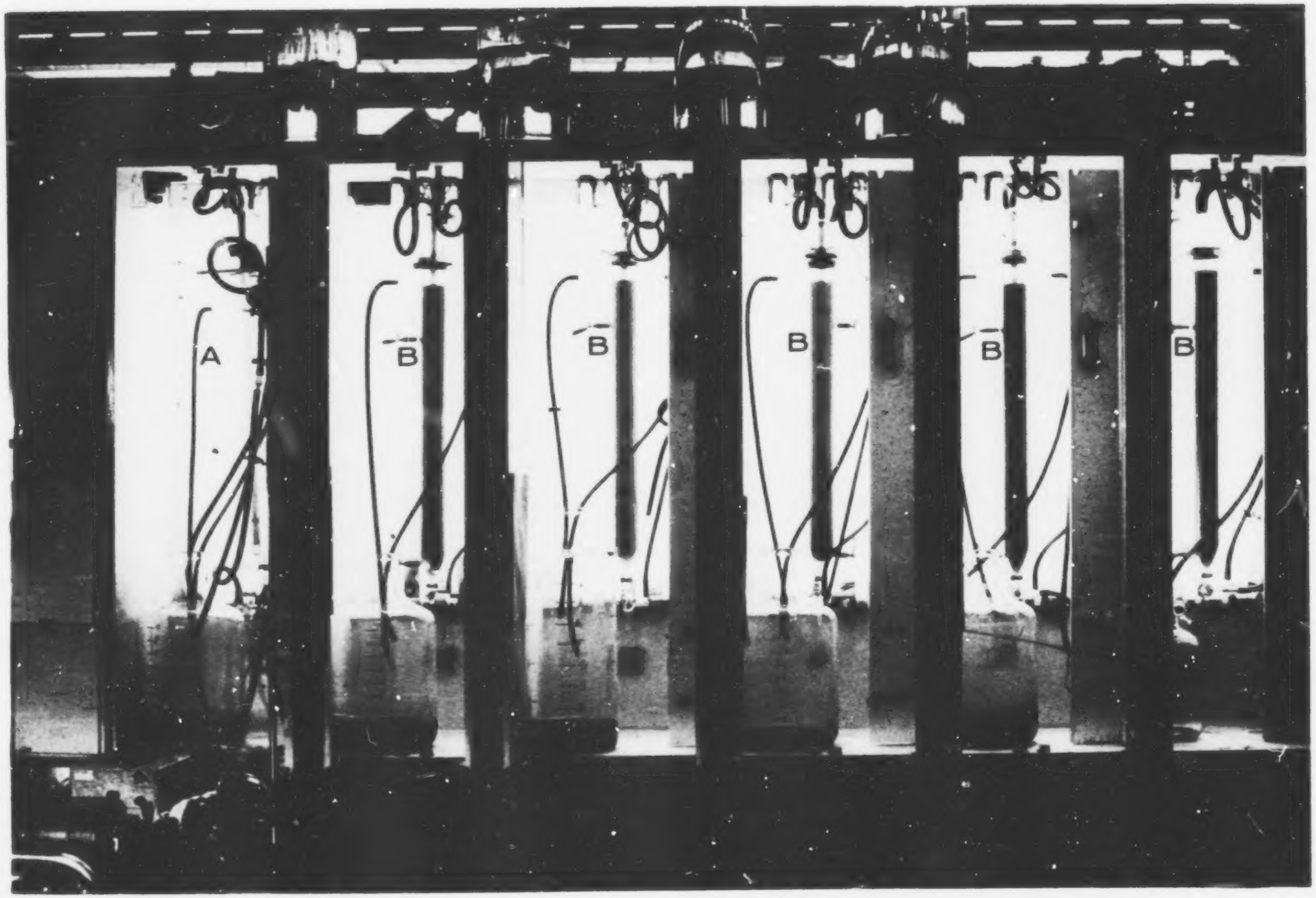

FIGURE 18. SETUP OF GROWTH UNITS. (A) TURBIDOSTATIC GROWTH UNIT. (B) CHEMOSTATIC GROWTH UNITS.

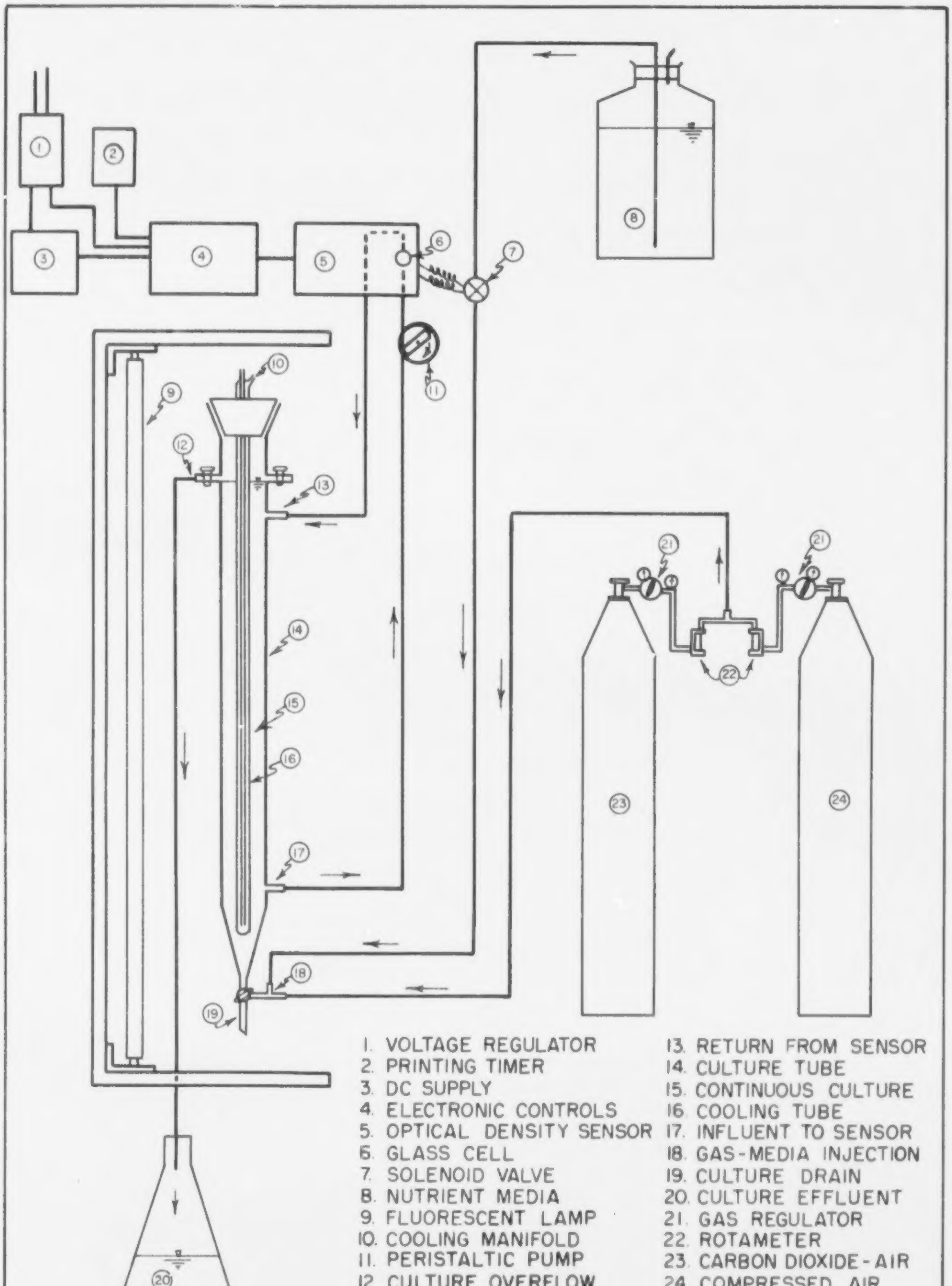
1. VOLTAGE REGULATOR
2. PRINTING TIMER
3. DC SUPPLY
4. ELECTRONIC CONTROLS
5. OPTICAL DENSITY SENSOR
6. GLASS CELL
7. SOLENOID VALVE
8. NUTRIENT MEDIA
9. FLUORESCENT LAMP
10. COOLING MANIFOLD
11. PERISTALTIC PUMP
12. CULTURE OVERFLOW
13. RETURN FROM SENSOR
14. CULTURE TUBE
15. CONTINUOUS CULTURE
16. COOLING TUBE
17. INFLUENT TO SENSOR
18. GAS-MEDIA INJECTION
19. CULTURE DRAIN
20. CULTURE EFFLUENT
21. GAS REGULATOR
22. ROTAMETER
23. CARBON DIOXIDE-AIR
24. COMPRESSED AIR

FIGURE 19. DIAGRAMMATIC SKETCH OF THE TURBIDOSTATIC GROWTH UNIT SYSTEM

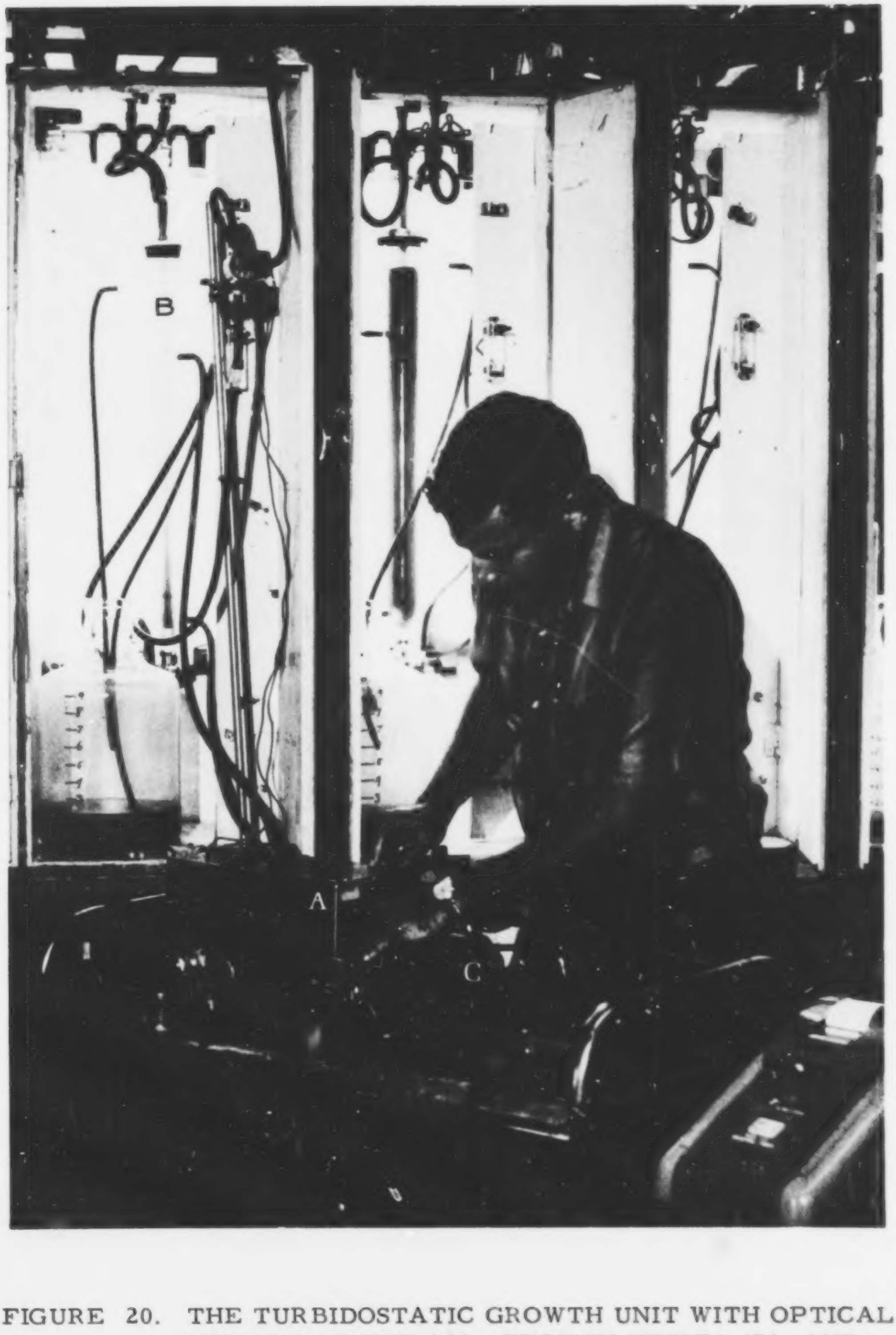

FIGURE 20. THE TURBIDOSTATIC GROWTH UNIT WITH OPTICAL DENSITY SENSOR (A), GROWTH VESSEL (B), AND PERISTALTIC PUMP (C)

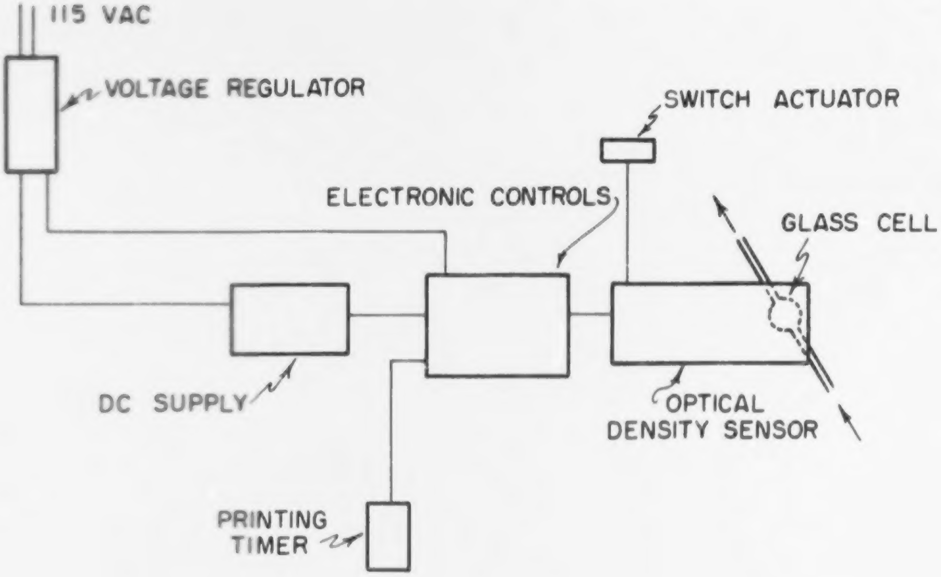
115 VAC
VOLTAGE REGULATOR
SWITCH ACTUATOR
ELECTRONIC CONTROLS
GLASS CELL
DC SUPPLY
OPTICAL DENSITY SENSOR
PRINTING TIMER

FIGURE 21. BLOCK DIAGRAM OF DENSITY REGULATING SYSTEM

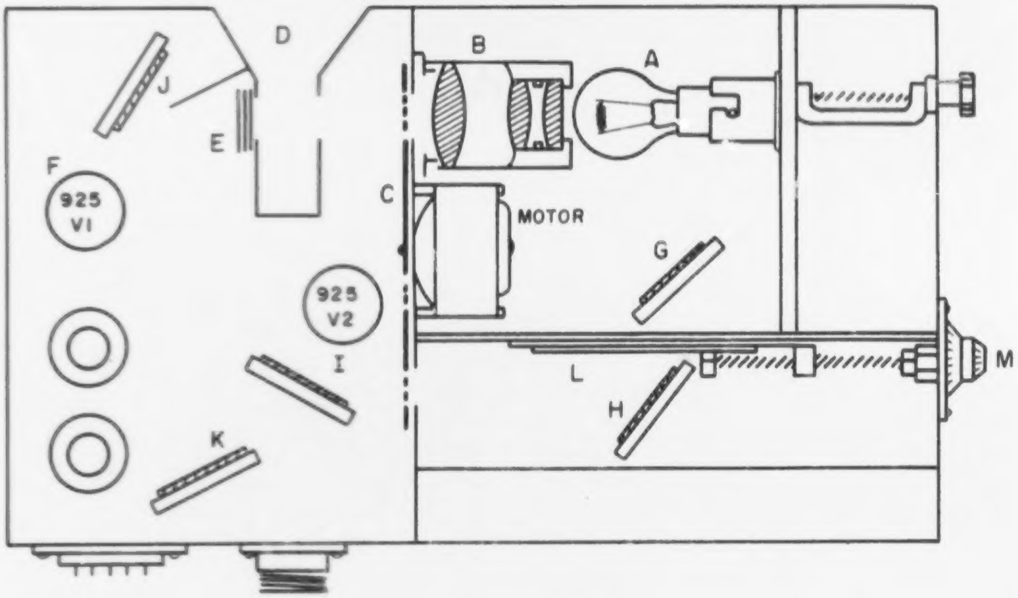
D
B
A
J
E
F
925 V1
C
MOTOR
G
925 V2
I
L
M
H
K

FIGURE 22. OPTICAL DENSITY SENSOR

to respond to optical density consists of a light probe, light source, a set of lenses, mirrors, light chopper, a sliding reference grating, phototube, and related switches, relays, and other equipment. A light beam transmitted through an algal suspension flowing through the light probe passes through an infrared filter, a color filter (to transmit red light only), and an amber-colored glass before being received by the photocell. The sensor is made to respond to light scattering by removing filters and reorienting a shield. The glass probe is made of glass tubing flattened at the middle portion so that the probe assumes a pancake-like configuration having two flat parallel surfaces.

In operating the sensory system, a portion of the algal culture is passed continuously through a glass probe inserted in the optical sensor head. As soon as the photo diode senses a preset density in the probe, a switch and solenoid valve is activated. The solenoid valve opens and fresh nutrient is added to the culture, thereby diluting it. When the preset density is reached, the solenoid valve closes again. In using a conventional growth vessel, the algal culture is circulated through the glass probe by means of a peristaltic pump.

Chemostatic Algatron

The algatron (spin-type reactor) was developed at the University of California by Oswald et al. and its construction, characteristics, and operation are described in detail in the literature [141-144]. Its principal characteristics are described in Table I and in Figures 23, 24, and 25. The reciprocating mixer, optical sensor (8 and 9 in Figure 23), and the outside light source were not used in the experiments reported herein. The unit used in the present study was equipped to inject medium into the cultures at preset intervals ranging from 15 to 35 minutes.

TABLE I

IMPORTANT DIMENSIONS OF VARIOUS
COMPONENTS IN THE ALGATRON

Components	Dimensions
Algatron Drum	
Diameter	61 cm
Radius	30.5 cm
Height	30.5 cm
Circumference	192 cm
Motor, RPM	1725
Drum, RPM	210
Radial Acceleration	15.1 x g
Linear Velocity	672 cm/sec
Culture (film)	
Height	30.5 cm
Depth - average	1.71 cm
maximum	2.72 cm
minimum	0.7 cm
Surface Slope	1:15.1
Volume	9700 mℓ
Liquid-Air Surface Area	5750 cm^2
Specific Liquid-Air Surface	0.594 cm^{-1}

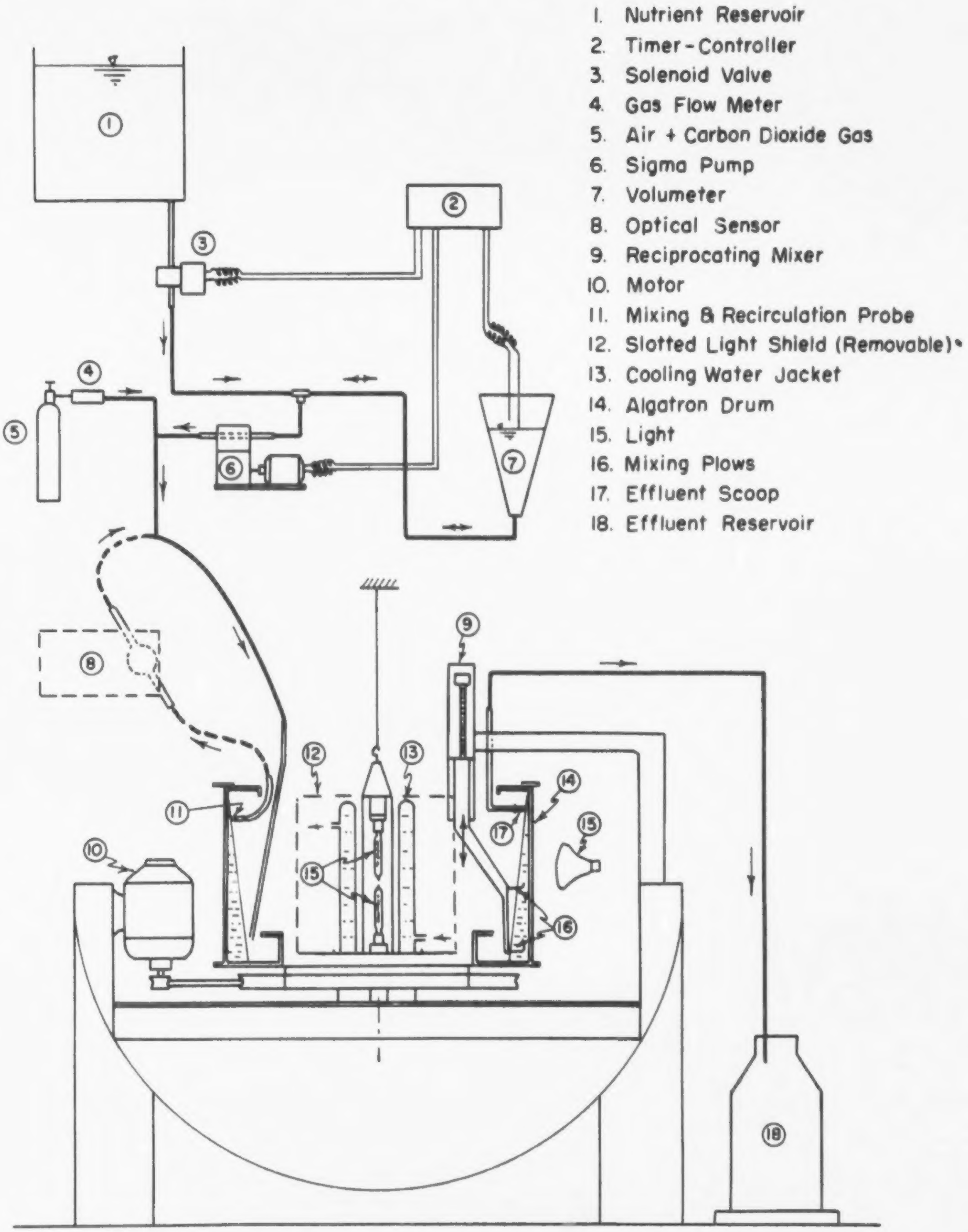

1. Nutrient Reservoir
2. Timer - Controller
3. Solenoid Valve
4. Gas Flow Meter
5. Air + Carbon Dioxide Gas
6. Sigma Pump
7. Volumeter
8. Optical Sensor
9. Reciprocating Mixer
10. Motor
11. Mixing & Recirculation Probe
12. Slotted Light Shield (Removable)
13. Cooling Water Jacket
14. Algatron Drum
15. Light
16. Mixing Plows
17. Effluent Scoop
18. Effluent Reservoir

FIGURE 23. ALGATRON PROTOTYPE – ARRANGEMENT AND COMPONENTS

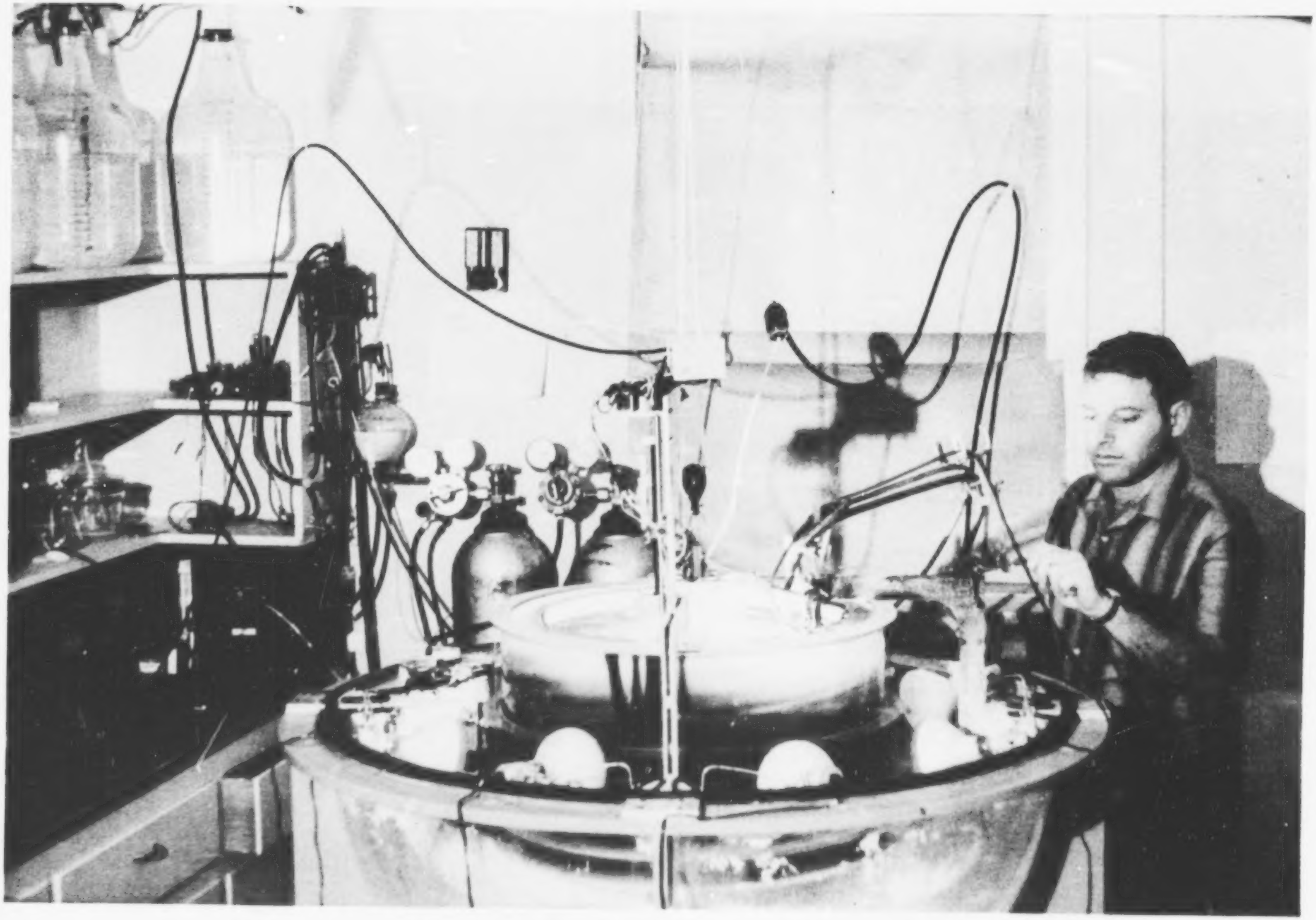

FIGURE 24. THE ALGATRON CHEMOSTATIC UNIT

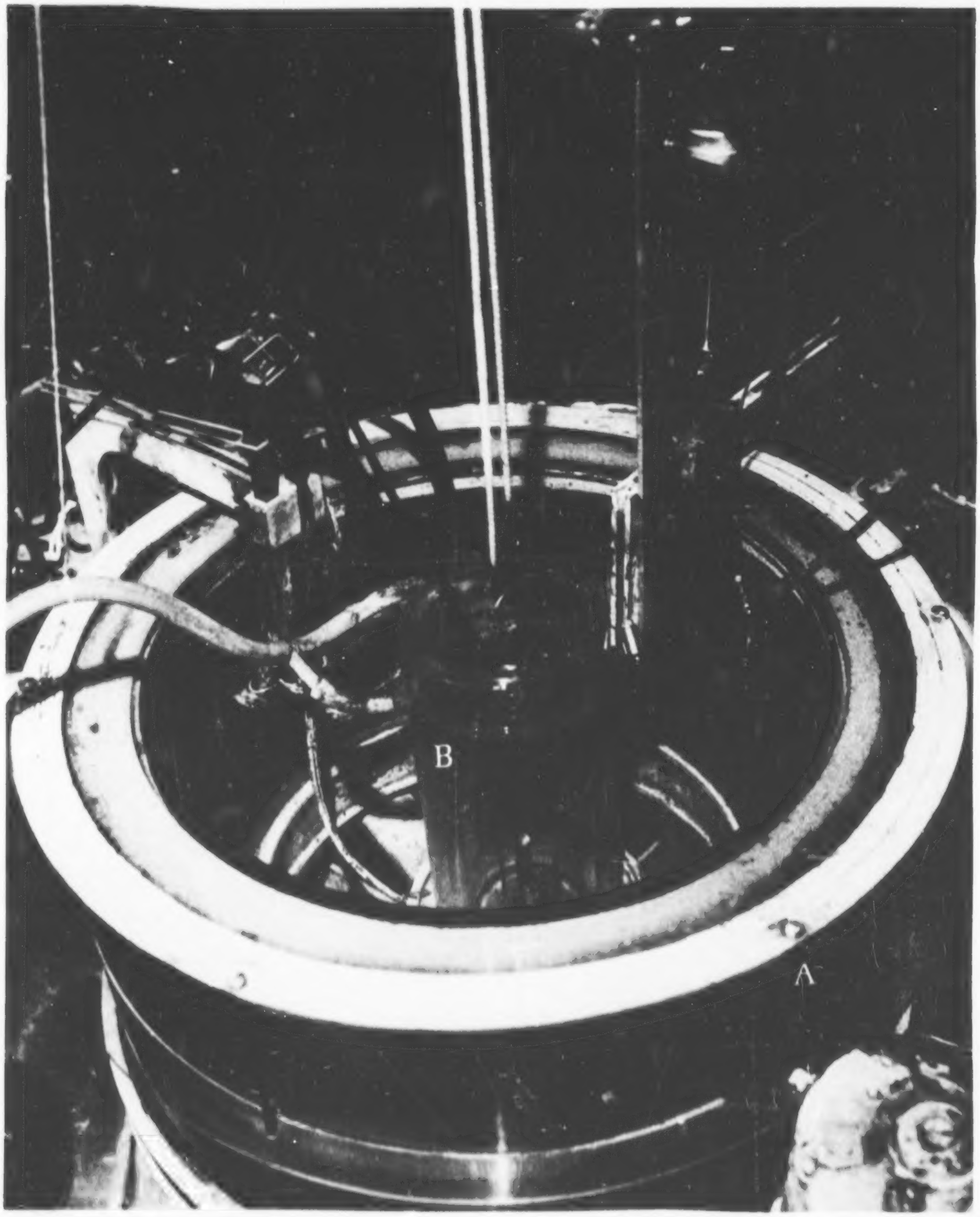

FIGURE 25. THE ALGATRON DRUM (A), SHOWING THE IODINE-QUARTZ LIGHT SOURCE WITH WATER JACKET (B)

Use was made of the algatron system because of the following inherent advantages of the system: a) It is larger than conventional laboratory growth units; thus it can be controlled more accurately. b) Conditions are provided which are highly favorable to maximum growth and production without interference of growth-limiting factors not deliberately imposed. These conditions are an extensive culture surface exposed to light, relatively thin layer of culture, large liquid-air interface, and complete mixing. c) The central location of the light source within the cylindrical configuration of the culture reactor makes it possible to measure light distribution accurately, and provides a geometrical light-culture arrangement not possible with the conventional culture unit. The arrangement also facilitates the use of many important light sources that cannot be applied to horizontal rectangular units without a great sacrifice of uniformity of irradiance distribution.

Limitations of the model of the algatron employed in this research are as follows: a) The culture had a surface slope of 1:15.1 due to the ratio between the radial acceleration and gravity. This surface slope is illustrated in Figures 26 and 27. It resulted in a nonuniform light path through the culture, thereby complicating the computation of theoretical models developed on the basis of the algatron. It also is a distortion of the classical pattern of outdoor algal systems, which in most cases are horizontal ponds with a uniform depth. b) The unit lacked a thermostatic temperature control. The temperature was maintained through a combination of heating with infrared lamps and ventilation. Despite the crudity of the temperature control, the temperature fluctuation was only ±1°C. c) Because of a heavy loss of water from the system through evaporation, distilled water had to be continuously added to the culture to maintain its volume.

Two types of light sources were used in the study, namely: Sylvania 500-watt Iodine-Quartz lamps (two lamps) and a G.E. 400-watt "Lucalox" lamp. These light sources are described in detail later in this Chapter and in Appendix F.

MEDIA AND CO_2

Media

The Modified Myers' Nitrate Medium [145], commonly used in algal mass cultures, was selected for this study. The composition of this medium is given in Appendix A. However during the course of preliminary studies it was found that the above medium did not provide the optimum nutrient conditions needed. Although the Modified Myers' Medium supported good growth, the lag time was rather long due to the low pH of the medium. As a result of experimentation, an optimal medium with nitrate as the nitrogen source was developed. It is basically a modification of the Modified Myers' Medium. It will be referred to as SERL-Nitrate medium. Because of the probable future application of the SERL medium in continuous algal culture, detailed description of its composition is given in Appendix A.

Obviously, in tests in which nitrogen was to constitute a limiting factor, its relative concentration in the media was reduced according to the particular experimental design.

CO_2 Supply

The concentration of CO_2 is an important factor because it is a source of carbon, but also because it has marked influence on the pH of a culture. In the present studies, air enriched with CO_2 (1%) was supplied to the turbidostatic and chemostatic growth units. This level is within the reported optimal range of 0.5 to 1.5% [140, 146, 147]. Gas was supplied in excess in order to provide proper mixing and insure an adequate supply of CO_2. Adequacy of CO_2 was checked by alkalinity tests and daily pH determinations. Pure CO_2 was supplied to the culture in the algatron by injection into the internal recirculation stream. It was found that

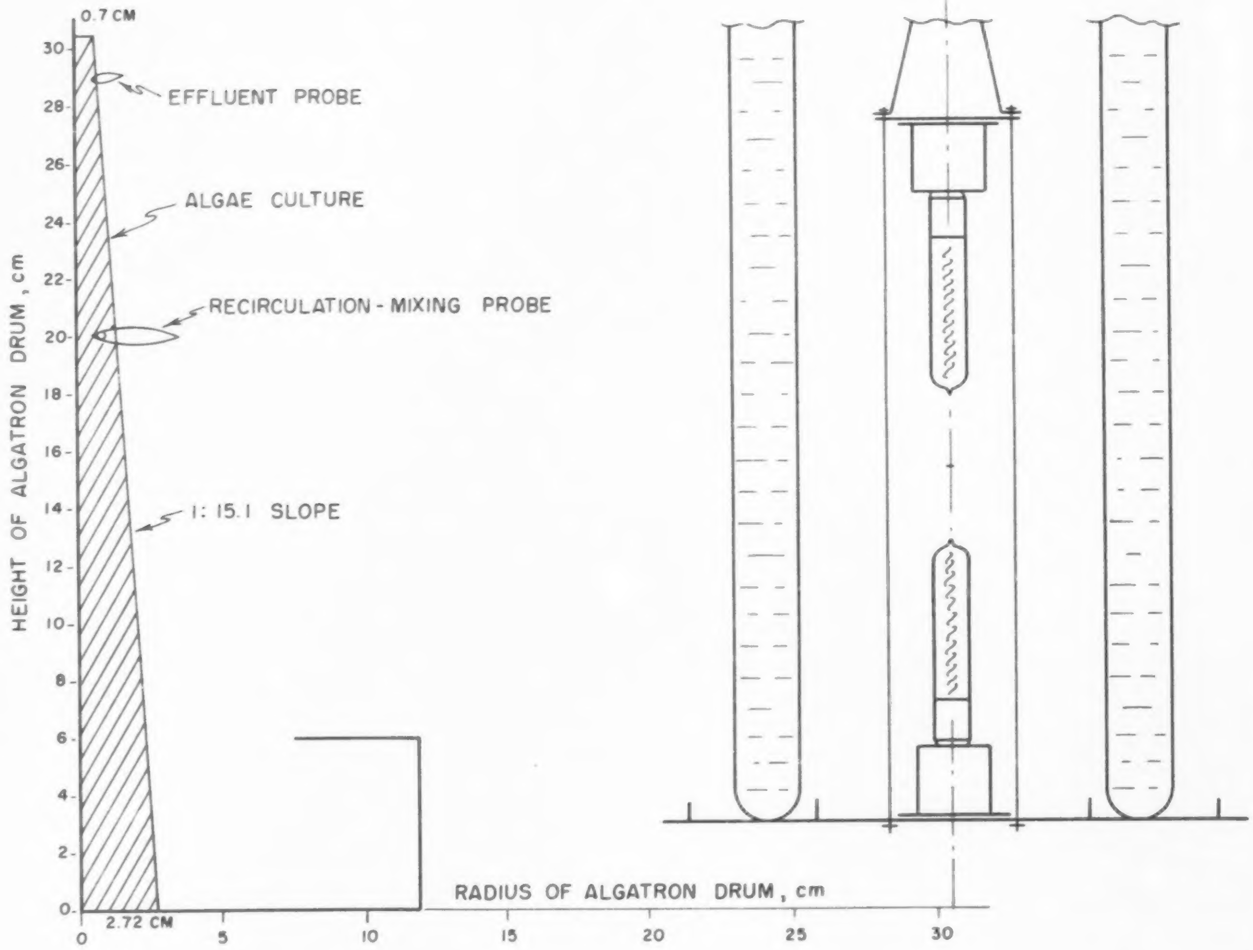
0.7 CM
EFFLUENT PROBE
ALGAE CULTURE
RECIRCULATION - MIXING PROBE
1: 15.1 SLOPE
HEIGHT OF ALGATRON DRUM, cm
30
28
26
24
22
20
18
16
14
12
10
8
6
4
2
0
2.72 CM
0
5
10
15
20
25
30
RADIUS OF ALGATRON DRUM, cm

FIGURE 26. POSITION OF ALGAE CULTURE IN RESPECT TO IODINE-QUARTZ LIGHT SOURCE

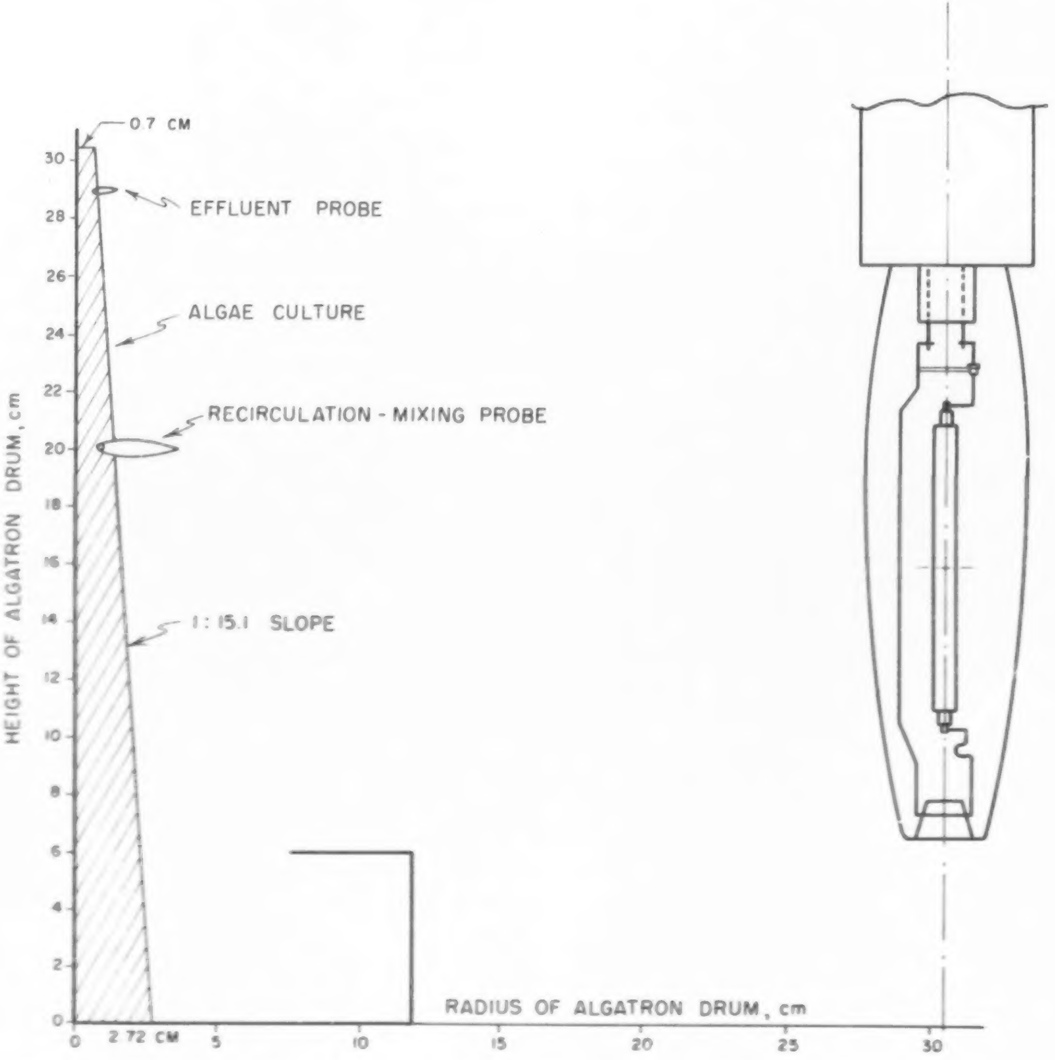
0.7 CM
EFFLUENT PROBE
ALGAE CULTURE
RECIRCULATION - MIXING PROBE
1 : 15.1 SLOPE
HEIGHT OF ALGATRON DRUM, cm
30
28
26
24
22
20
18
16
14
12
10
8
6
4
2
0
2.72 CM
5
10
15
20
25
30
RADIUS OF ALGATRON DRUM, cm

FIGURE 27. POSITION OF ALGAE CULTURE IN RESPECT TO "LUCALOX" LAMP

due to the large liquid-air interface, equilibrium with the atmosphere in the algatron drum was reached rapidly at a level which resulted in pH levels of 6.8 ± 0.2. The total amount of CO_2 to be supplied was predetermined as being 2.5 times the carbon requirement of the growing algal biomass according to experience gathered in the preliminary studies.

LIGHT

Since light intensity (irradiance) was made the major growth-limiting factor, and since wavelength distribution is a major parameter in the proposed kinetic models, accuracy in determining the specific characteristics of the light source and in measuring the light energy was an essential factor in the successful conduct of the research.

Light Sources

As mentioned previously, three types of light sources were used in the investigation: a) Iodine-Quartz incandescent lamps, b) high-temperature sodium vapor arc lamps, and c) full-spectrum fluorescent lamps.

(a) Iodine-Quartz Incandescent Lamps. Two 500-watt lamps of the tungsten-halogen type (Sylvania Co.) were used in the experiments with the algatron. The color-temperature of the lamps was approximately 3000°K. Because of the relatively large infrared emission, a pyrex water cooling jacket had to be installed around it (cf. Figure 28). The relative energy spectral distribution, incident irradiance distribution on the culture surface, and the vertical and horizontal candle power distribution of the light from this source are given in Appendix F, Figures 51, 52, 53, and 54, respectively. Other characteristics of the light source are summarized in Table VIII.

(b) High-Temperature Sodium Vapor Arc Lamps. A 400-watt "Lucalox" lamp (General Electric Co.) was used in the algatron experiments. This lamp is a newly introduced high-temperature, high-pressure sodium vapor type of lamp. Since it is a high-temperature, high-pressure lamp, its spectral distribution is wider than that of the regular type of sodium lamp. Its main characteristics are a high energy-to-light conversion efficiency (approximately 25%), relatively low emission of energy at the infrared and ultraviolet ranges of the spectrum (no special cooling was necessary), and a relatively high irradiance within the yellow-orange spectral range. The mounting of the lamp in relation to the culture is shown in Figure 27. The energy spectral distribution, incident irradiance distribution of the culture surface, and the vertical and horizontal candle power distribution are given respectively in Figures 55, 56, 57, and 58 of Appendix F. Other characteristics of the light source are summarized in Table VIII of Appendix F.

(c) Full-Spectrum Fluorescent Lamps. As stated earlier, four 30-watt Optima lamps (Duro-Test Co.) were used for each of the six chemostatic and turbidostatic growth units. Since these growth-units were not used in the studies concerned with irradiance kinetics, it was not necessary to explore thoroughly the irradiance characteristics of the lamps. The spectral distribution is given in Figure 59 of Appendix F. Other characteristics of the light sources are summarized in Table VIII of Appendix F.

Each light source was "broken in" for a period of 120 hours prior to use to allow it to reach a constant level of energy emission.

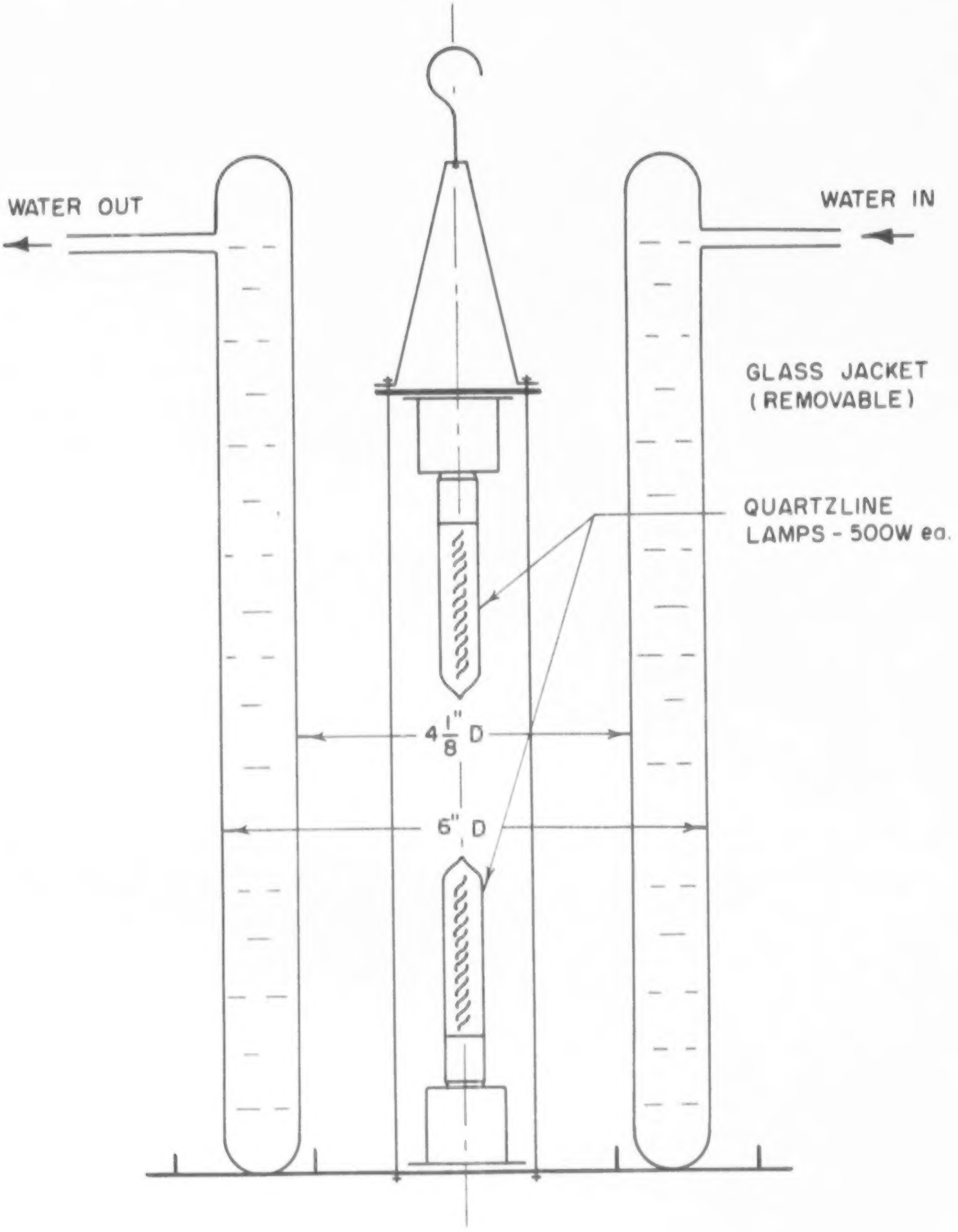
WATER OUT
WATER IN
GLASS JACKET (REMOVABLE)
QUARTZLINE LAMPS - 500W ea.
$4\frac{1}{8}$" D
6" D

FIGURE 28. IODINE-QUARTZ LAMPS – ARRANGEMENT

Light Measurements

Incident Irradiance. Incident irradiance, I_o, was measured with the use of a YSI-Kettering Radiometer, Model 65, supplemented with appropriate filters (Appendix G) to eliminate the radiation below and above the visible range. The incident irradiance at the surface of the culture was measured repeatedly at intervals of 1 cm in order to construct the distribution of incident irradiance for the various light sources (cf. Figures 52 and 56 in Appendix F). The incident irradiance, I_o, was measured, reported, and computed in the theoretical models in terms of units of calories per square centimeter per minute.

Spectral Distribution. The original spectral distribution was supplied by the manufacturers (Figures 51, 55, and 59 in Appendix F). During the course of the experiment, it was checked for consistency with the use of a monochromatic radiometer consisting of a Bausch and Lomb high-intensity grading monochrometer, a reader thermopile, and a Keithley microvoltmeter. Information on the spectral distribution was needed in the determination of $I_{R\lambda}$ with respect to irradiance in the kinetic models. A comparison between the spectral distribution of light sources applied in the experimental work and that of sunlight can be made by consulting Figures 51, 55, 59, 60, and 61 in Appendix F. The last named two figures are concerned with the spectral distribution of sunlight [148].

Spectral Absorbence and Transmittance by the Algal Suspension. Measurement of spectral absorbence and transmittance was essential to the determination of α_λ with respect to light in the kinetic models. It was determined with the use of a Beckmen DK-2 Spectrophotometer.

Total Light Transmitted by the Algal Suspension. Determination of the amount of total light transmitted by the algal suspension was necessary for the experimental determination of, and for comparing the empirical value of, α_t with that computed from individual values of α_λ. To make the determinations, a special rectangular chamber was constructed of 1.5-mm pyrex glass as shown in Figure 29. The length of the chamber was 25 cm; the width, 23 cm; and the depth, 17 mm. In making a determination of total transmittance, a sample of culture from the reactor was placed in the chamber. The chamber with its contents was placed in the same relation to the light source as was that of the algatron reactor. Light from the light source therefore constituted the emitted light. The difference between the light energy entering the sample and that leaving it represented the light absorbed. Light not absorbed, i.e., leaving the sample, represented transmitted light. Incident and transmitted light were measured with a YSI-Kettering Radiometer (Model 65) and a Weston Illuminator Meter (Model 756). The former measures irradiance; the latter, illuminance in terms of foot-candles. The two types of light measurement were made as a means of demonstrating the existence of discrepancies between values for α_t obtained by measurements of irradiance and those by determination of illuminance (cf. Chapter II). The experimental setup is illustrated in Figure 29.

Frequent measurements of light transmittance were made in the experiments concerned with the relation of the kinetics of algal growth to nitrogen concentration to insure the continued presence of light saturation conditions; since it was essential to the success of the experiments that light not be limiting. In these experiments, the transmitted light was measured by placing the probe of the YSI-Kettering Radiometer on the far side of the growth unit from the light source and, of course, with the shielding of the probe needed to keep out scattered and stray light.

Geometrical Distribution of Candle Power of the Light Source. To insure a positioning of the light sources used in the algatron studies which would insure an even distribution of irradiance over the culture surface, a determination was

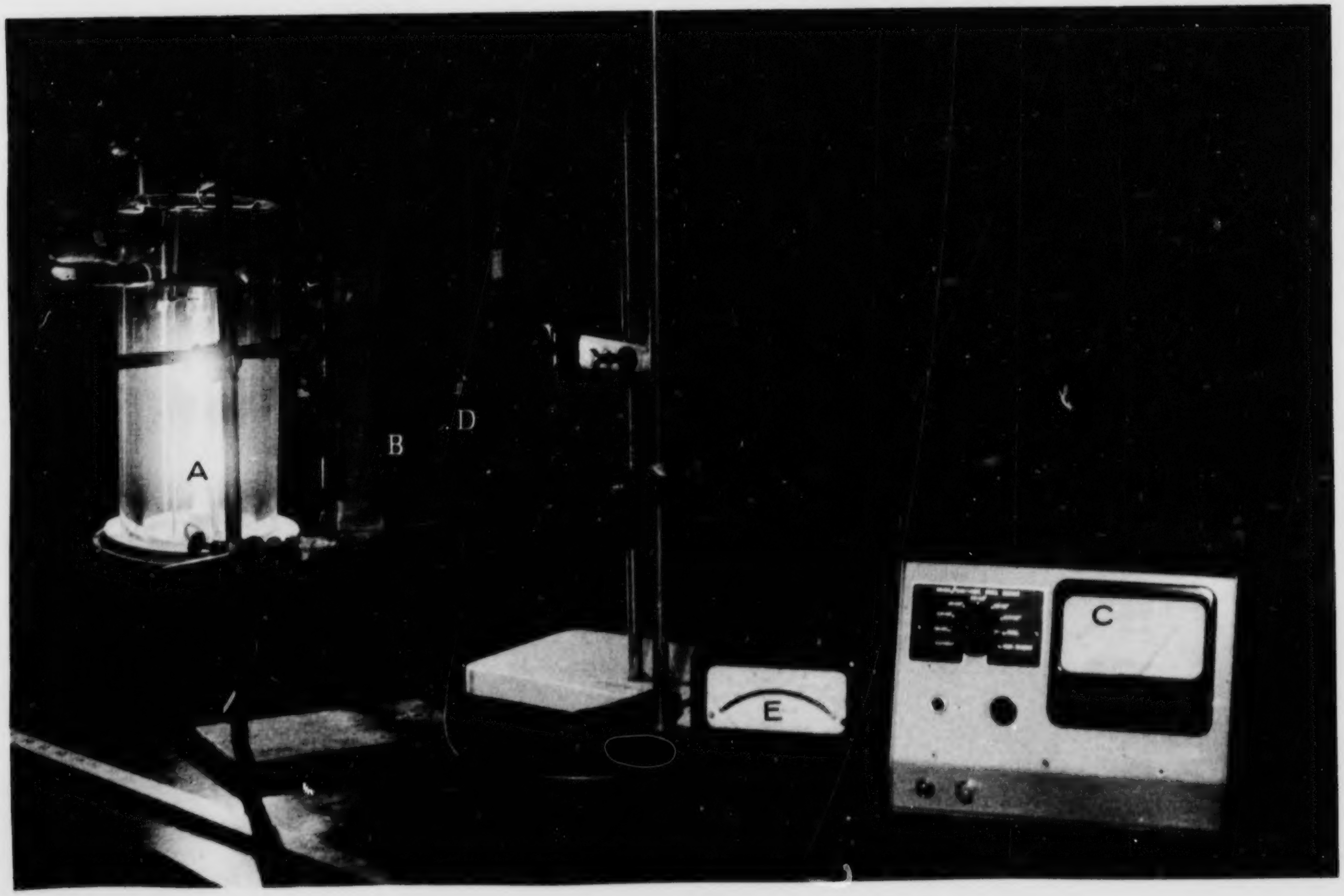

FIGURE 29. ARRANGEMENT FOR THE MEASUREMENT OF TOTAL LIGHT TRANSMITTED BY AN ALGAL SUSPENSION

made of the geometrical distribution of the candle power output of each light source (cf. Figures 53, 54, 57, and 58 in Appendix F). The determination was made with the use of an El-Dorado Photometer (Model 201) and with the light source mounted on a goniometer.

Light Filters. The range of photosynthetically effective spectra was assumed to be between 400 to 700 mμ as is the convention in photosynthetic studies of green algae. Therefore in measuring irradiance, suitable combinations of filters were used to screen out light in the ultraviolet and infrared bands of the spectrum. Since transmittance, absorbence, and reflectance filter curves are not vertical, various combinations of filters were required to measure accurately the photosynthetically sensitive light. The filters were used in the various combinations suggested by Myers [149], and were as follows: a) Fish-Schurman Multi-layer Interference Film Filter Nos. 3024 and 6143, b) Optical Coating Wide-Band Hot Mirror, and c) Schott Color Glass Filters Nos. GG13, WG1, RG695, and RG10. The transmittance curves of the filters are given respectively in Figures 62, 63, and 64 of Appendix G.

SAMPLING AND ANALYSES

Sampling

Samples were taken daily from each growth unit for the determination of various solids measurements, nitrogen and chlorophyll concentrations, and temperature. Samples were taken twice each day on those days in which steady state conditions were about to be reached. Medium contained in the medium reservoir and cultures in the growth units were sampled twice each week for determination of alkalinity. Total chemical analyses of the medium was made occasionally to check on the continued presence of nutrients in optimal concentrations. The size of the samples ranged from 50 to 150 mℓ. The effect of removal of the samples on the reactor materials balance was taken into consideration in all cases.

Solids Determination

The concentration of total dissolved solids, total suspended solids, and volatile suspended solids were determined routinely. The analyses were made according to SERL analytical methods [150]. Algal concentration was assumed to be represented by the concentration of the total suspended solids, since inorganic media were used exclusively. This assumption proved to be justified since the ash concentration of the suspended solids remained within the range of 5.2% to 7.6% – a concentration characteristic of algal organic matter. The J value for the energy content of the algal cells (5.5 cal/mg cellular material) used in the kinetic models is based on the assumption that the total suspended solids are entirely algal in nature. Although the culture was not maintained under bacteria-free conditions, no significant bacterial population was detected in microscopic observations. As it also shows by Ward and Moyer [151], the mass of bacteria associated with actively-growing Chlorella fed by inorganic media is less than 1% of the total algal biomass.

Nitrogen Determinations

Nitrogen determinations were made of the total sample, of its soluble fraction, and of the suspended material (mainly algae and some bacteria) for cross-checking of the results. Nitrate-nitrogen was determined by the phenoldisulfonic acid method [152] whenever chlorides were present in low concentration in the media, and by the brucine method [152] when significant chloride concentrations were present. Nitrite-nitrogen was determined by the diazotization method [152]. Since nitrite-nitrogen in detectable concentrations was present rarely, nitrite determinations were made only infrequently. Ammonia and total unoxidized nitrogen determinations were made according to the A.O.A.C. version of the Kjeldahl method [153].

Chlorophyll Determinations

Chlorophyll content is an indicator of the condition of the algal system, especially in relation to nitrogen starvation. Chlorophylls A and B were determined according to the McKinney method [154].

CRITERIA FOR STEADY STATE CONDITIONS

Steady state conditions were considered to have been attained when the dilution rate (Q/V), algal concentration in the reactor and effluent (C_c), nitrogen concentration in the reactor and effluent (S_{N1}), and nitrogen cellular content (N_c) were ascertained as remaining constant within a certain level for at least three consecutive days. Obviously the nitrogen levels S_{N1} and N_c were determined only in those experiments involving nitrogen. The level of permissible variation depended upon the type of growth unit in use. A maximum variation of ±5.0% was allowed for the turbidostatic units, ±6.0% for the chemostatic growth units, and ±7.5% for the algatron. With each change in growth conditions, it took an average of 42 hours for the culture to reach steady state in the turbidostatic unit and in chemostatic units operated as turbidostatic units at the start of a run. An average of 96 hours was required for steady state conditions to be established in the chemostatic units and in the algatron. A longer period was required for the latter units whenever major changes in operating conditions occurred.

COMPUTATIONS

The theoretical models with respect to light developed in this presentation were programmed by the FORTRAN method and computerized on a 6400 digital computer (Control Data Corp.). Details are given in Appendix H, Programs 1, 2, and 3. The regression and correlation analysis of the logarithmic function of the modified exponential function developed as a part of the experiments involving nitrogen concentration as well as other statistical analysis were made with the use of an IBM 1620 computer (cf. Appendix H, Program 4).

VII. EXPERIMENTAL RESULTS AND DISCUSSION

The experimental work was divided into three major parts: a) experiments concerned with algal growth as a function of light intensity; b) experiments involving algal growth as a function of nitrogen concentration at light saturation; and c) experiments in which both light and nitrogen were limiting. The experiments described under (a) and (c) were conducted with the use of the algatron; and those under (b) with the use of the six 1-liter growth units.

LIGHT AS A GROWTH-LIMITING FACTOR

In the experimental work concerned with light as a growth-limiting factor, two light sources were used in illuminating the algatron: a tungsten filament-halogen lamp (Iodine-Quartz, Sylvania) and a sodium vapor arc lamp (Lucalox, G.E.). Major interrelated variables receiving study under chemostatic conditions were: dilution rate (Q/V), concentration of algal biomass (C_c), and net algal production (P_n). The dilution rate, Q/V of a CSTR-type unit at steady state is equal to the average net specific growth rate, $\bar{\mu}_n$. In all experiments the following light conditions were known (i.e., determined): a) incident irradiance on the culture surface, I_o; b) geometrical distribution of the incident irradiance in the culture surface, $I_o f(h')$, in which h' is the height (cm) of the culture; and (c) the spectral distribution of the light source, $I_o f(\lambda)$.

The results obtained in the experimental work were used to evaluate the theoretical models developed in Chapter II (the model based on energy-balance) and Chapter III (the three macroscopic kinetic models). The theoretical models were transformed to a mathematical form which was used to develop suitable computer programs.

Application of the Theoretical Models to the Algatron

The kinetic models for the prediction of algae production as a function of incident irradiance were transformed for use with the algatron as follows:

a. The spectral light distribution was computed on the basis of relative irradiated energy at 10-mμ increments in the spectral range 400 to 700 mμ. On this basis, 31 values for $I_{\lambda R}$ were obtained. To illustrate: the definition of I_o according to Equation 2-22 was transformed as follows:

$$I_o = \sum_{400}^{700} I_{o\lambda} \qquad (7\text{-}1)$$

in which I_o is the sum of 31 values of $I_{o\lambda}$, each representing a 10-mμ band. Similar techniques were used to replace all of the definite integrals by summation of the increment dλ. In addition to those for $I_{o\lambda}$, values for λ and other functional factors of wavelength, i.e., $I_{d\lambda}$, $I_{\lambda R}$, Q_λ, and α_λ, were related to wavelength bands of 10-mμ and were integrated by the method of summation.

b. On any surface irradiated with artificial light, I_o will vary according to the position of the irradiated surface in relation to the light source and according to the geometric distribution of incident irradiance at the culture surface (cf. Figures 52 and 56). Consequently, values for P_a, P_{a_1} and P_{a_3} for a given model are functions of I_o for a given geometrical area. The total production (i.e., P, P_1, P_2, P_3) in the reactor is the sum of all of the corresponding values for P_a. Since $I_of(h')$ was determined for each centimeter of height of the culture when distributed over the vertical height of the drum (i.e., the algatron in motion), the total production may be given as

$$P = 2\pi\bar{r} \sum_{h'=1}^{h'=30} P_a \tag{7-2}$$

in which $\bar{r}$ is the average radius of the algatron drum. A similar summation was made of the values for P_{a_1}, P_{a_2}, and P_{a_3} according to the model under consideration. It should be noted that in applications in which natural illumination is used, I_o may be assumed to be uniform; hence, the problem of computation is substantially reduced.

c. A unique characteristic of a culture in a rotating algatron is the triangular cross section configuration of the culture. The culture is deepest with respect to the light at the base of the vertical wall of the drum and shallowest at the top. Consequently, depth d at any point on the vertical axis of the culture is $d = f(h')$. The function can be expressed as

$$d(h') = 2.71 - \frac{h'}{s'} \tag{7-3}$$

in which $d(h')$ is the depth at a given point along the vertical axis of the culture, and s' is the slope of the culture surface, i.e., $s = \Delta h'/\Delta d$. The value for s' is equal to the ratio between the centrifugal accelerations imparted to the culture by the rotation of the drum and by terrestrial gravity. In the experiments reported herein, $s' = 15.1$. Obviously cultures grown in stationary conventional growth units would not have a sloped surface, nor would a spinning culture have one under gravity-free conditions (i.e., in space). The complexities involved in computations requiring the inclusion of $d = f(h')$ would not be needed in the two last named applications.

To summarize, algae production P_a, and the average specific growth rate were computed first for a given h', i.e., as a function of the appropriate $I_o(h')$ and $d(h')$. The thirty incremental values of $P_a(h')$ were summed according to Equation 7-2. The practical formulation was derived from the theoretical equations developed in Chapters II and III: Equation 2-24 is rewritten as

$$R_t = \sum_{400}^{700} I_{\lambda R} \; . \tag{7-4}$$

Equation 2-28 is rewritten as

$$I_d(h') = \frac{I_o(h')}{R_t} \sum_{400}^{700} I_{\lambda R} \, e^{-\alpha_\lambda C_c d(h')} \tag{7-5}$$

in which I_d, I_o, and d are functions of h'. The Energy Balance Model given in Equation 2-34 can be rewritten as

$$P_a(h') = \frac{5.645}{J\ 1/\Phi\ R_t}\, I_o(h') \left[\frac{I_s}{I_o(h')} \left(\ln \frac{I_o(h')}{I_s} + 1 \right) \sum_{400}^{700} Q_\lambda\, \lambda\, I_{\lambda R} \right.$$

$$\left. - \frac{I_s}{I_d(h')} \left(\ln \frac{I_d(h')}{I_s} + 1 \right) \sum_{400}^{700} Q_\lambda\, \lambda\, I_{\lambda R}\, e^{-\alpha_\lambda C_c d(h')} \right] \qquad (7\text{-}6)$$

in which P_a is expressed in mg of dry algae per cm^2-day. Limitations discussed in Chapter II concerning situations in which $I_o(h') < I_s$ and $I_d(h') < I_s$ also hold in Equation 7-6.

If Equation 2-35 is written as

$$P_{na} = P_a - 10^{-3} K_d\, C_c\, d(h') \qquad (7\text{-}7)$$

and from Equations 2-36 and 2-37

$$\bar{\mu}_{na} = \frac{10^3 P_{na}}{C_c\, d(h')} \qquad (7\text{-}8)$$

and the values of $P_{na}(h')$ are integrated according to Equation 7-2, then

$$P_n = 191.6 \sum_{1}^{30} P_{na} \qquad (7\text{-}9)$$

and

$$\bar{\mu}_n = \frac{10^3 P_n}{C_c\, V} \quad . \qquad (7\text{-}10)$$

The volumetric net algal production, P_{nv}, which is defined as the net algal production per unit volume of the culture expressed in units of gram of dry algae per day per liter of culture volume can be found as follows:

$$P_{nv} = \frac{P_n}{V} \quad . \qquad (7\text{-}11)$$

The overall light conversion efficiency as defined in Equation 2-2 can be found as

$$E_o = \frac{P_n \times J}{1440 \times 191.6 \sum_{1}^{30} I_o(h')} \quad . \tag{7-12}$$

As stated previously, the Macroscopic Model I results in an equation which is practically identical with that of the Energy Balance Model. Preliminary use of both models showed no significant differences in the models; consequently, it was decided to use Equations 7-6 through 7-10 for both models. The results referring to the equations are designated as P_{a_1}, P_{na_1}, and μ_{n_1} in order to distinguish them from those in Models II and III.

A similar transformation as above may be applied to Models II and III. Thus the following equations for Model II can be formulated from Equations 3-52, 3-53, 7-4, 7-5, 7-7, and 7-10:

$$P_{a_2}(h') = E_m' \, I_s \ln \frac{I_s + I_o(h')}{I_s + I_d(h')} \quad ; \tag{7-13}$$

it can be shown from Equations 2-11, 2-11A, and 2-12 that

$$E_m = \frac{0.00392}{1/\Phi \, R_t} \sum_{400}^{700} Q_\lambda \, \lambda \, I_{\lambda R} \quad . \tag{7-14}$$

And from Equation 3-26

$$E_m' = 262.5 \, E_m \quad . \tag{7-15}$$

Equations similar to those derived for P_{na}, P_n, P_{nv}, μ_{na}, $\bar{\mu}_n$, and E_o in Equations 7-7 through 7-12 can be derived from Equation 7-13 for P_{na_2}, P_{n_2}, P_{nv_2}, E_{o_2}, μ_{na_2}, and $\bar{\mu}_{n_2}$.

Using Equations 3-59, 3-62, 7-5, 7-14, and 7-15, the following equation is derived for Model III:

$$P_{a_3}(h') = E_m' \, I_s \left[\alpha_t(h') \, C_c \, d(h') + E_i\left(\frac{I_o}{I_s}\right) - E_i\left(\frac{I_d(h')}{I_s}\right) \right] . \tag{7-16}$$

In Equation 7-16, $\alpha_t(h')$ is defined as

$$\alpha_t(h') = \frac{1}{d(h') \, C_c} \ln \frac{I_o(h')}{I_d(h')} \quad . \tag{7-17}$$

The values of P_{na_3}, P_{n_3}, P_{nv_3}, μ_{na_3}, $\bar{\mu}_{n_3}$, and E_{o_3} can be found from equations similar to Equations 7-7 through 7-12. The computer programs corresponding to the above equations are given in Appendix H, Programs 1 through 3. The input data for each run included information on the following items: α_λ, I_s, K_d, $1/\phi$, J, s', C_c, $I_o(h')$, $I_{\lambda R}$, and Q_λ. Information used in computing α_λ was obtained by determining light transmission at each 10-mμ wavelength band with the use of a spectrophotometer.

The constant value for I_s was based on data from the literature and it was adjusted to reflect the effect of the temperature at which the algae were grown. In the 27°C experiments with C. pyrenoidosa, I_s was considered to be 0.033 cal/cm^2-min on the basis of data reported by Sorokin et al. [155-158] and Pickett and Myers [149,159]. This value was verified by an estimate of the value of I_s made according to the rewritten form of Equation 3-27, namely, $I_s = \hat{\mu}_x/E_m'$, in which $\hat{\mu}_x$ was estimated on the basis of $\hat{\mu}_{xn}$ in the relation $\hat{\mu}_x = \hat{\mu}_{xn} + K_d$. Repeated determinations of $\hat{\mu}_{xn}$ resulted in values of 2.0 to 2.1 day^{-1}. E_m' was computed from the irradiance data with the use of Equations 7-13 and 7-14. Values for I_s determined according to the rewritten form of Equation 3-27 ranged from 0.032 to 0.034 cal/cm^2-min. This range brackets the value 0.033 assigned to I_s on the basis of reported data in the literature.

In this investigation, the endogenous respiration constant K_d was assumed to be 0.125 day^{-1}. The values for $1/\phi$, J, and s' — constants discussed earlier — were assumed to be respectively 8 einsteins/mole, 5.5 cal/mg, and 15.1. A spectrum of values for the algal concentration C_c was used consisting of 100 mg/ℓ increments extending from 100 mg/ℓ to 6000 mg/ℓ.

Thirty values of $I_o(h')$ were entered for each light source, thirty-one of $I_{\lambda R}$ for each 10-mμ wavelength band, and thirty-one of Q_λ for the corresponding wavelength band. Data on these three characteristics for the Iodine-Quartz lamps and the sodium vapor arc lamp are summarized in Table II. A graphical illustration of these data is given in Appendix F. Data on percent light transmission through the algal suspension as a function of wavelength are shown in Figure 30.

The output data for each model includes information on $P_a(h')$, $P_{na}(h')$, P_n, $\bar{\mu}_{na}$, $\bar{\mu}_n$, E_m, $I_d(h')$, E_o, and other intermediate steps. The computation program was set up on the basis of the use of a turbidostatic control, i.e., as if predetermined values of C_c were maintained throughout each experimental run. Thus for a series of values for C_c, the program was such that the value corresponding to maximum algal net production ($\hat{P}_n$) or P_n, $\bar{\mu}_n$, etc. would be selected. Such a program is possible because the assumptions made in the derivation of the various models were based upon the existence of a fixed relationship between values for P_n, $\bar{\mu}_n$ (i.e., Q/V), and C_c.

Experimental Results as Compared to the Theoretical Models

Light Transmission. Data on percent transmission as shown in Figure 30 were used in computing the extinction coefficient α_λ according to the Beer-Lambert law. A curve showing α_λ as a function of wavelength is presented in Figure 31. The curve illustrates the marked variation in α_λ with wavelength. This variation was one of the reasons which necessitated the incorporation of wavelength distribution in the proposed models.

The light sources used in the principal experiments were also used in measuring the total light transmitted by the algal suspension at various concentrations of algae. The method used in making the measurements is described in Chapter VI and illustrated in Figure 29. The results shown graphically in Figure 32 indicate clearly the decrease in the extinction coefficient with increasing cell concentration. The two curves show the differences between the Iodine-Quartz lamp and the Lucalox sodium-vapor arc lamp with respect to the absolute values of α_t characteristic of the two sources.

TABLE II

IRRADIANCE AND SPECTRAL DISTRIBUTION INPUT DATA

Iodine - Quartz Lamps						Sodium Vapor Arc (Lucalox) Lamp					
λ[a] mμ	T_r %	$I_{\lambda R}$	Q_λ	h' cm	I_o cal/cm^2-min	λ mμ	T_r %	$I_{\lambda R}$	Q_λ	h' cm	I_o cal/cm^2-min
400	50	7.0	0.906	1.0	0.001	400	50	12	0.906	1.0	0.002
410	43	8.3	0.900	2.0	0.007	410	43	12	0.900	2.0	0.003
420	40	9.9	0.833	3.0	0.018	420	40	15	0.833	3.0	0.009
430	38	11.5	0.872	4.0	0.064	430	38	18	0.872	4.0	0.012
440	37	12.8	0.856	5.0	0.082	440	37	18	0.856	5.0	0.076
450	44	14.8	0.833	6.0	0.123	450	44	36	0.833	6.0	0.125
460	48	16.4	0.811	7.0	0.141	460	48	43	0.811	7.0	0.194
470	46	18.0	0.778	8.0	0.150	470	46	17	0.778	8.0	0.226
480	47	19.8	0.750	9.0	0.152	480	47	7	0.750	9.0	0.242
490	53	22.2	0.739	10.0	0.155	490	53	14	0.739	10.0	0.248
500	60	23.4	0.778	11.0	0.157	500	60	90	0.778	11.0	0.258
510	71	25.2	0.817	12.0	0.158	510	71	20	0.817	12.0	0.268
520	80	27.0	0.856	13.0	0.166	520	80	11	0.856	13.0	0.278
530	84	29.0	0.883	14.0	0.168	530	84	15	0.883	14.0	0.287
540	86	31.0	0.911	15.0	0.171	540	86	18	0.911	15.0	0.290
550	88	33.2	0.933	16.0	0.171	550	88	44	0.933	16.0	0.288
560	87	35.5	0.961	17.0	0.169	560	87	82	0.961	17.0	0.287
570	86	37.8	0.978	18.0	0.167	570	86	352	0.978	18.0	0.279
580	84	40.0	0.996	19.0	0.165	580	84	365	0.996	19.0	0.268
590	83	42.3	0.998	20.0	0.160	590	83	220	0.998	20.0	0.265
600	81	44.3	0.998	21.0	0.156	600	81	380	0.998	21.0	0.260
610	79	46.2	0.998	22.0	0.150	610	79	220	0.998	22.0	0.257
620	78	48.6	0.998	23.0	0.142	620	78	125	0.998	23.0	0.255
630	77	51.0	0.998	24.0	0.129	630	77	100	0.998	24.0	0.248
640	76	53.3	0.978	25.0	0.121	640	76	75	0.978	25.0	0.240
650	69	55.5	0.963	26.0	0.110	650	69	66	0.963	26.0	0.234
660	63	58.0	0.958	27.0	0.103	660	63	55	0.958	27.0	0.222
670	52	60.5	0.971	28.0	0.085	670	52	45	0.971	28.0	0.208
680	52	62.7	0.997	29.0	0.062	680	52	35	0.997	29.0	0.190
690	73	65.0	0.889	30.0	0.047	690	73	27	0.889	30.0	0.176
700	86	67.3	0.524			700	86	22	0.524		

[a] See Glossary and text for definition of terms.

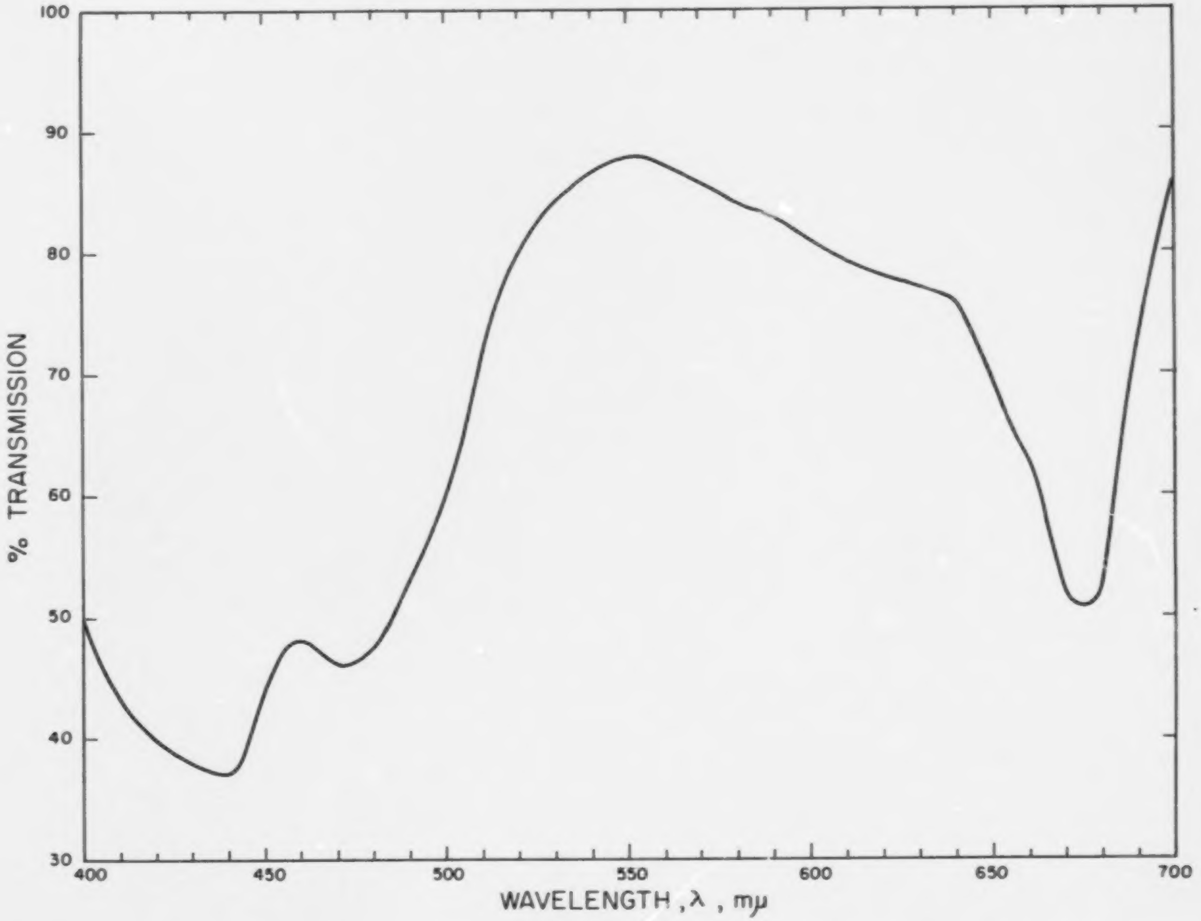

FIGURE 30. LIGHT TRANSMISSION AS A FUNCTION OF WAVELENGTH IN A SUSPENSION OF C. pyrenoidosa

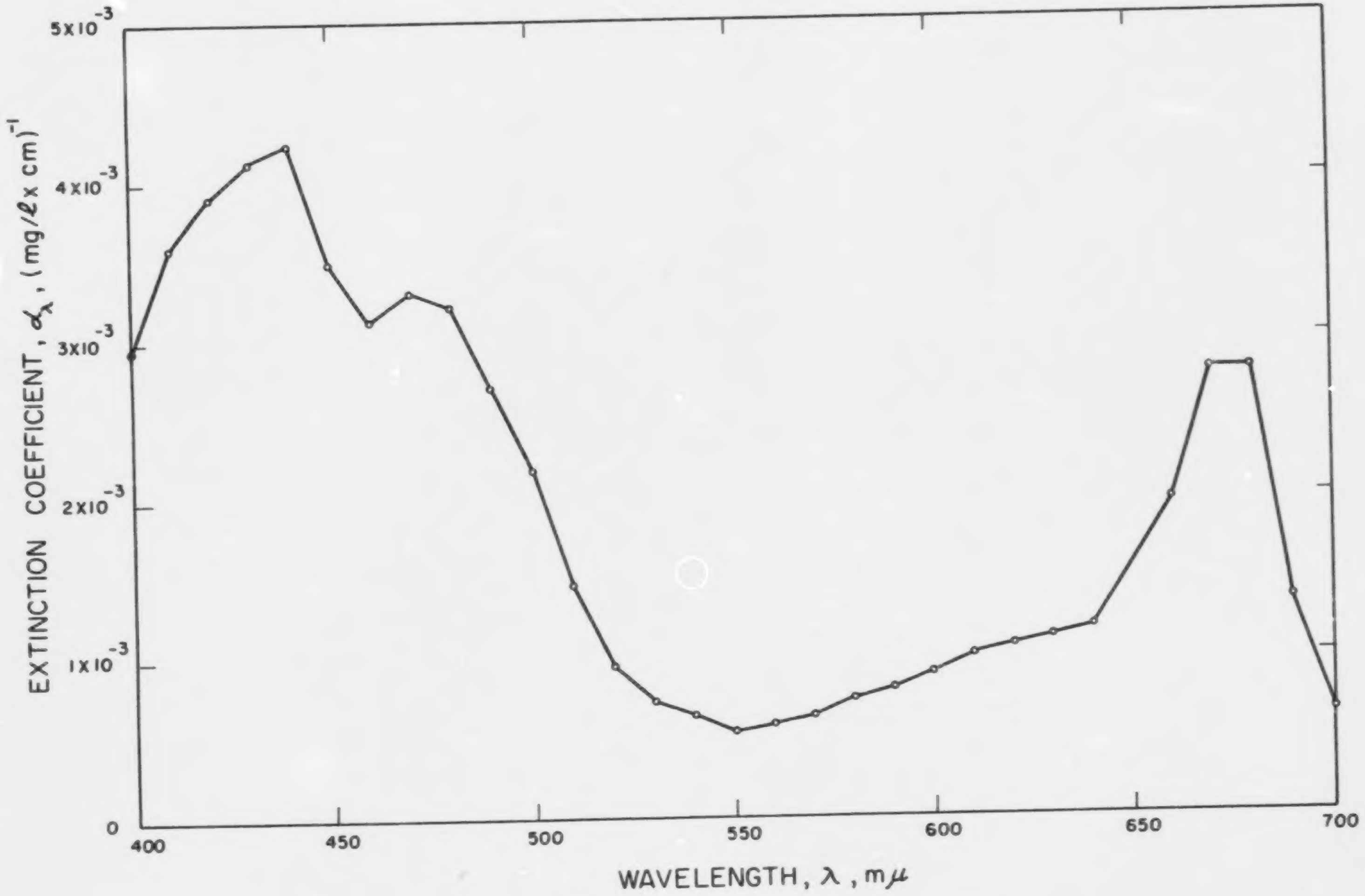

FIGURE 31. THE LIGHT EXTINCTION COEFFICIENT, α_λ, AS A FUNCTION OF WAVELENGTH IN A SUSPENSION OF C. pyrenoidosa

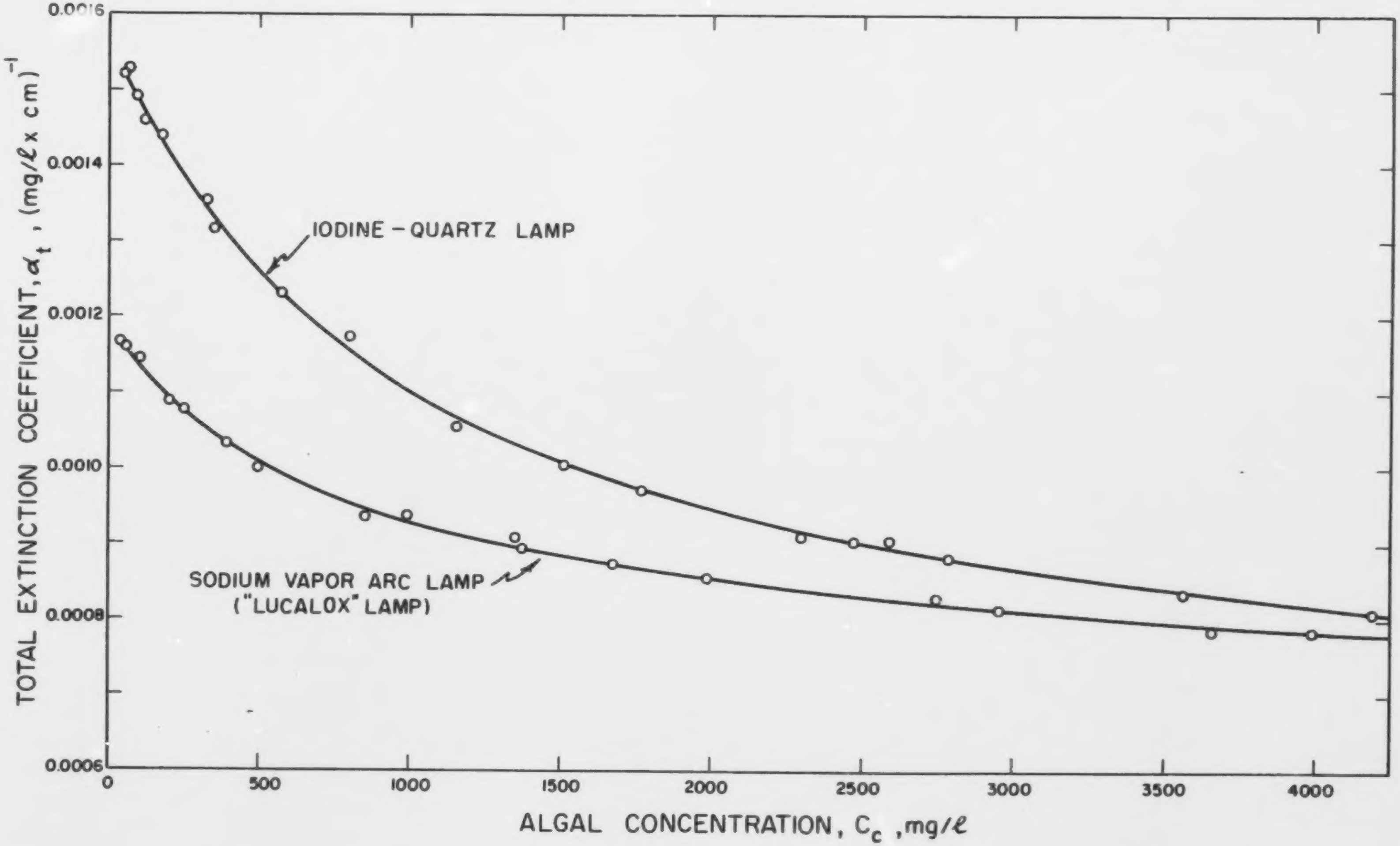

FIGURE 32. TOTAL EXTINCTION COEFFICIENT, α_t, AS A FUNCTION OF CONCENTRATION OF C. pyrenoidosa AT A CONSTANT CULTURE DEPTH OF 1.7 cm

A comparison of the curves shown in Figure 51 (spectral distribution of the Iodine-Quartz lamp) and Figure 55 (Lucalox lamp) presented in Appendix F shows that the emission by the Iodine-Quartz lamp is strongest in the red band (620 to 700 mμ), whereas that by the Lucalox lamp is strongest in the yellow-orange band (570 to 610 mμ). Applying this information to Figures 30 and 31 it becomes evident that the spectral emission of the Iodine-Quartz lamp corresponds to a region of low transmittance by the algal suspension; whereas the spectral emission of the Lucalox lamps coincides with a high spectral transmission region of the algal suspension. When the Iodine-Quartz lamp was used, the integrated total extinction coefficient, α_t, decreased rather sharply with increase in concentration of algae because red light is highly absorbed by an algal suspension. On the other hand, yellow-orange light is transmitted by algal suspensions even at relatively high concentrations of algae; consequently the change in α_t was less abrupt according to the Beer-Lambert law, concentration and depth constitute a multiple ($C_c d$) effect with respect to light transmission, the effect brought about by increase in depth should be comparable to that resulting from an increase in concentration. Because of these facts, the use of a constant α_t, regardless of depth and concentration, inevitably leads to severe discrepancies between theory and practical application realization.

The experiment concerned with total light transmission was conducted to demonstrate the variation in α_t as a function of concentration (or depth), and to demonstrate the advantage of using α_λ in the proposed models.

Algal Growth and Production. The experiments concerned with light as the growth-limiting factor were conducted with the use of the algatron functioning as a chemostat. Algae used in the experiment were of the species *C. pyrenoidosa*. The temperature was maintained at 27°C (±1°C). The medium was the "optimal" SERL nitrate medium.

The dilution rate, Q/V, was predetermined and varied in the course of the experiments, and the concentration of nutrients in the medium was adjusted to suit each dilution rate so as to provide optimum conditions with respect to availability of nutrients. The conditions of complete mixing at steady state were ensured by the design of the algatron. These conditions ensured that Q/V represented the average net specific growth rate of the culture ($\bar{\mu}_n$). The major measured parameters were net algal production of the reactor (P_n), net algal production per liter of culture (volumetric net production, P_{nv}), and algal concentration.

Data collected in experiments in which the Iodine-Quartz lamps were used as the light source are listed in Table III and plotted in Figures 33, 34, and 35. Data from experiments in which the sodium vapor arc lamp (Lucalox) was used are listed in Table III and shown graphically in Figures 36, 37, and 38. The degree of conformity of the experimental data to theory is shown by the families of curves shown in Figures 33 to 38. The bell shape of the curves based on the experimental data is similar to the theoretical curves in Figures 33 and 36, which indicates that the relationship between net production, dilution rate (or $\bar{\mu}_n$), and algal concentration predicted from the kinetic models are reasonably well verified by the experimental data.

Compatability of the Theoretical Models with the Experimental Results

Macroscopic Model I, which is based on the first order-zero order microscopic relationship, generally predicted values for P_n which were much higher than experimental results. However, it predicted the dilution rate at which maximum net production of algae would take place (cf. Figures 33 and 36) more closely than did the other models. Also it appears that Macroscopic Model II, which is based on the rectangular hyperbola microscopic relationship is not compatible with the experimental results.

TABLE III

SUMMARY OF EXPERIMENTAL RESULTS AS COMPARED WITH RESULTS ON THE BASIS OF THEORETICAL KINETIC MODELS OF ALGAL GROWTH WITH RESPECT TO IRRADIANCE

Item*	Current Algatron Prototype							
	Iodine-Quartz Lamps				Sodium Vapor Arc Lamp			
	Actual	Theoretical Model			Actual	Theoretical Model		
		I	II	III		I	II	III
1	2	3	4	5	6	7	8	9
Temperature, C°	27	27	27	27	27	27	27	27
K_d, day^{-1}		0.125	0.125	0.125		0.125	0.125	0.125
E_m		0.266	0.266	0.266		0.276	0.276	0.276
I_s, cal/cm^2-min		0.033	0.033	0.033		0.033	0.033	0.033
$\hat{P}_n$, g/day	19.04	23.58	14.59	18.74	24.45	28.15	18.44	23.46
$\hat{P}_{nv}$, g/liter-day	1.96	2.43	1.50	1.93	2.52	2.90	1.90	2.42
$\hat{P}_{na}$, g/m^2-day	33.11	41.00	25.37	32.59	42.52	48.95	32.07	40.79
C_c at $\hat{P}_n$, mg/ℓ	2420	2680	2600	2590	2740	3800	3570	3580
Q/V or $\bar{\mu}_n$ at $\hat{P}_n$, day^{-1}	0.87	0.90	0.58	0.74	0.92	0.76	0.54	0.67
θ at $\hat{P}_n$, hr	27.6	26.7	41.4	31.6	26.1	31.6	44.4	35.8
E_o at $\hat{P}_n$	0.111	0.137	0.085	0.109	0.079	0.091	0.059	0.075
E_e at $\hat{P}_n$, g/kw-hr	0.79	0.98	0.61	0.78	2.55	2.93	1.92	2.44

*See Glossary and text for definition of terms.

The experimental data generally confirm the Macroscopic Model III (based upon the exponential microscopic model) within a limited range of dilution rates and algal concentrations. A detailed discussion of its applicability follows.

Applicability of Model III. It can be stated that within the practical range of dilution rates and algal concentrations the agreement between experimental and theoretical values based upon Model III is close enough to permit its use in the design and analysis of algal systems. According to Figure 33 (Iodine-Quartz light source), at dilution rates of 1.9 to 0.5 day^{-1}, the net algal production predicted by Model III differed by only ±10% from that obtained experimentally. When the dilution rate was set at 0.74 day^{-1}, for example, the predicted net algal production was found to be 18.7 g/day, or 1.9 g/liter-day. These values differ by only 5% from those obtained experimentally. The agreement between the experimental curve and the theoretical curve was slightly less when the Lucalox lamp was used as the light source. The zone of agreement in this case was from dilution rate of 1.7 day^{-1} to 0.6 day^{-1} (cf. Figure 36).

The degree of compatability between experimental data and those according to Model III with respect to algal concentration as a function of dilution rate is indicated in Figures 34 and 37. Here again the best agreement between the data and the model is in the range of dilution rates of between 1.9 and 0.5 day^{-1}.

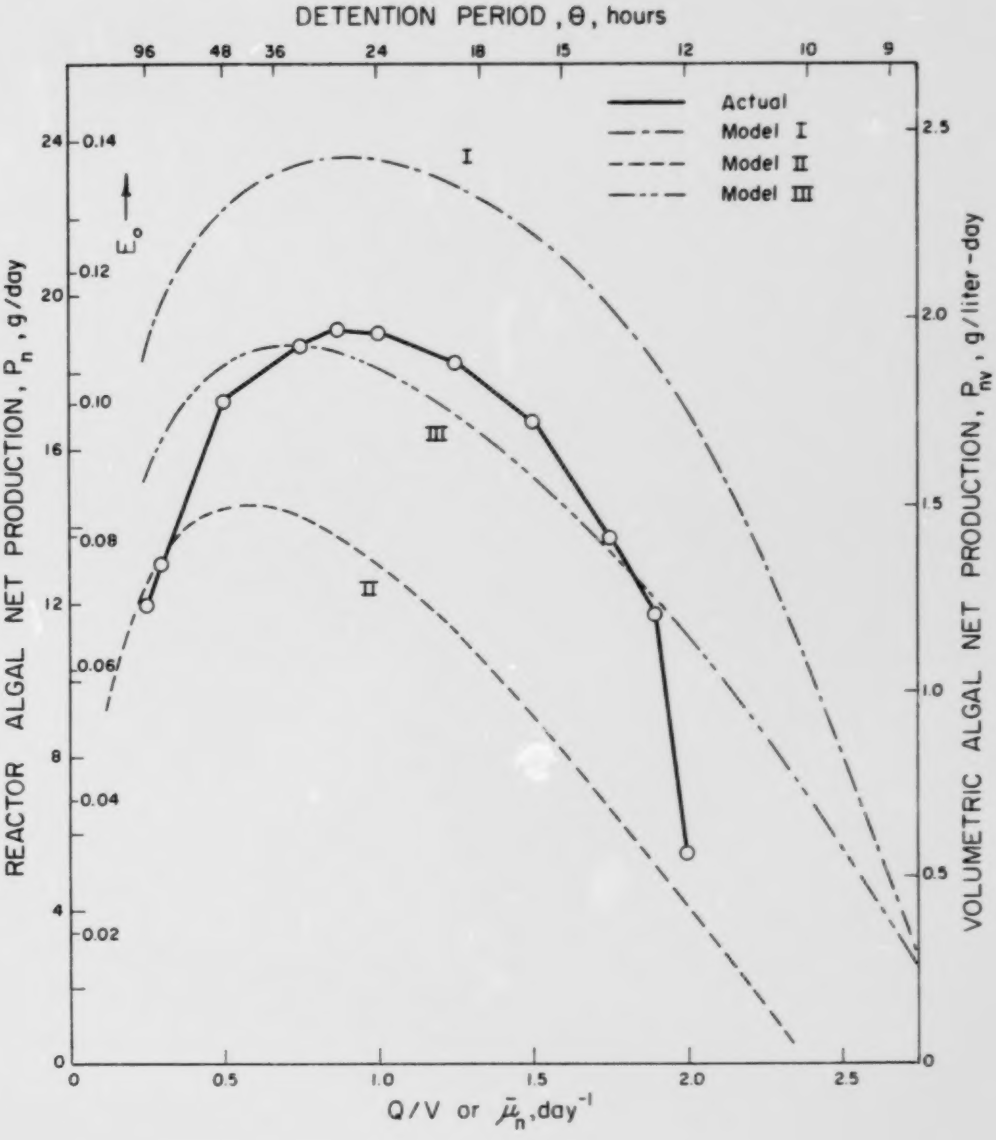

FIGURE 33. ALGAL NET PRODUCTION AS A FUNCTION OF DILUTION RATE (IODINE-QUARTZ LIGHT SOURCE)

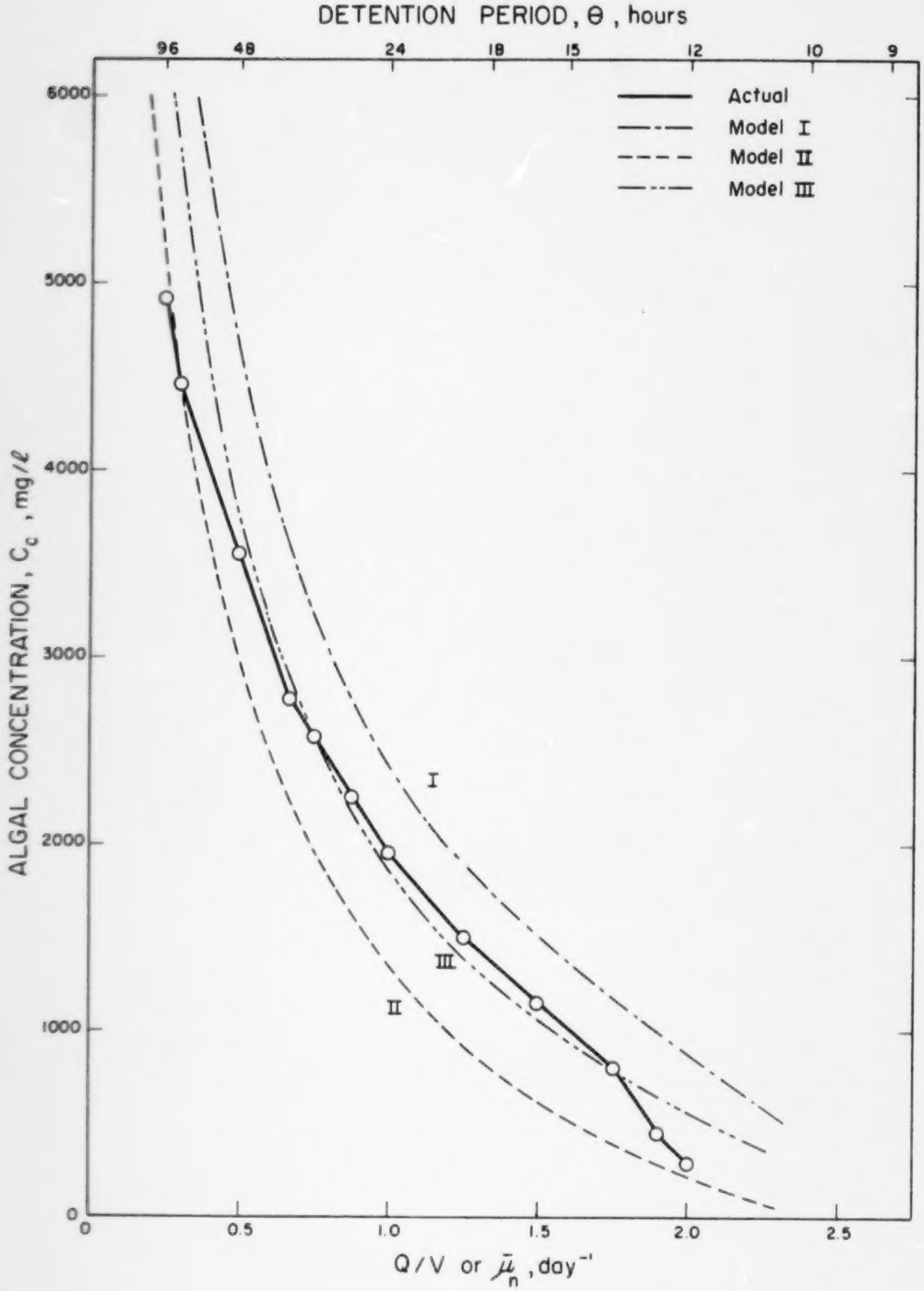

FIGURE 34. ALGAL CONCENTRATION IN THE REACTOR AS A FUNCTION OF DILUTION RATE (IODINE-QUARTZ LIGHT SOURCE)

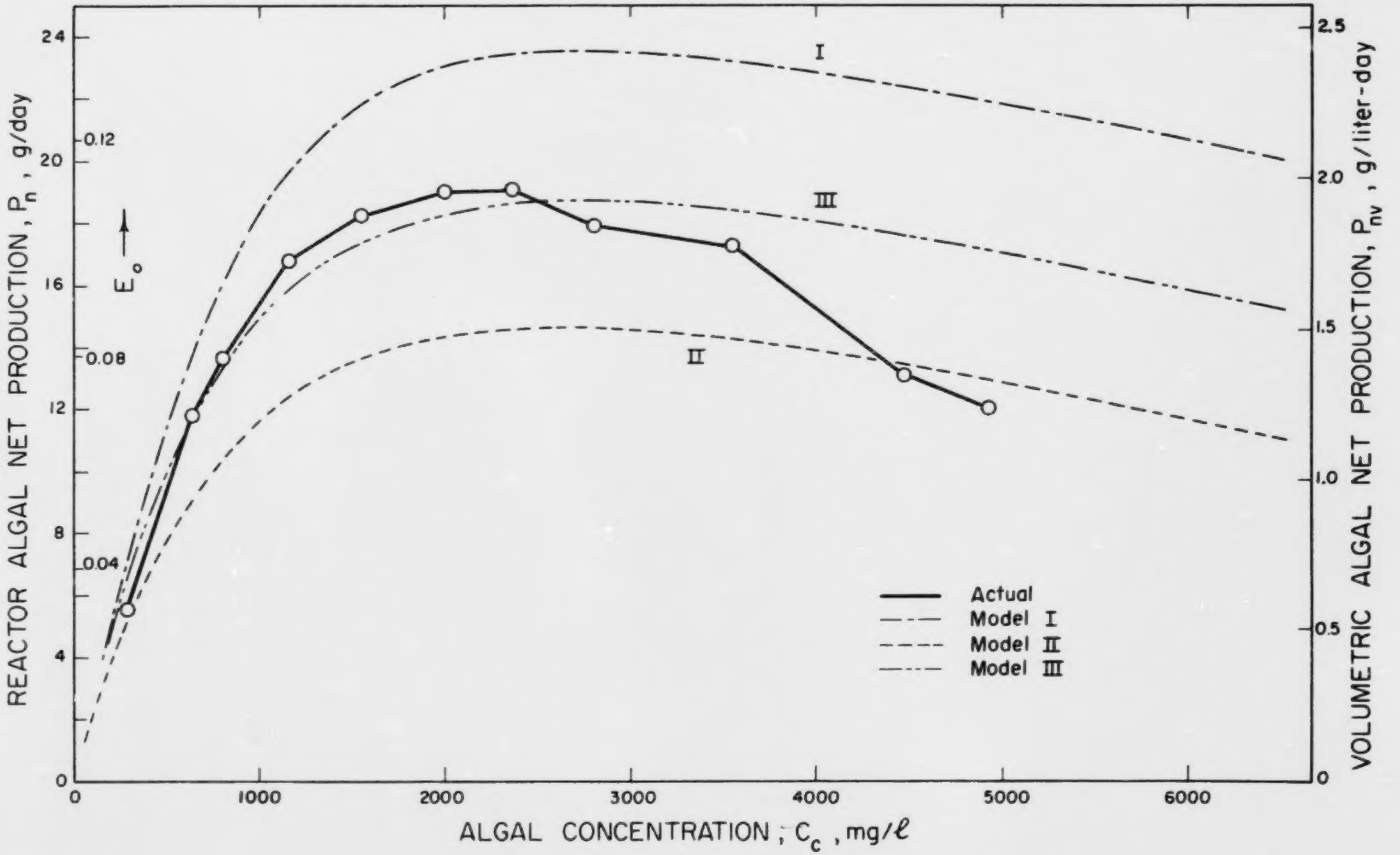

FIGURE 35. ALGAL PRODUCTION AS RELATED TO ALGAL CONCENTRATION (IODINE-QUARTZ LIGHT SOURCE)

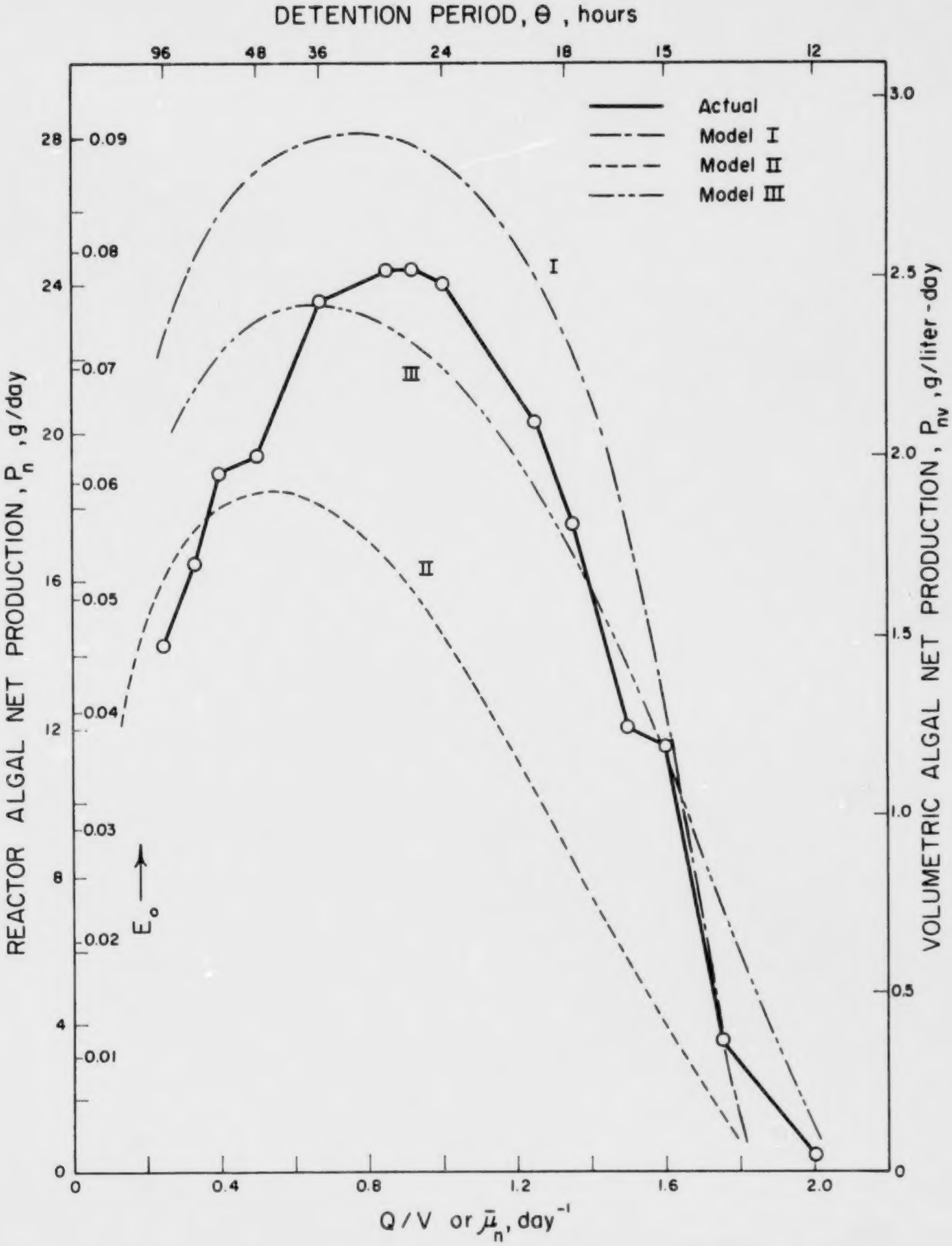

FIGURE 36. ALGAL NET PRODUCTION AS A FUNCTION OF THE DILUTION RATE ("LUCALOX" LAMP AS LIGHT SOURCE)

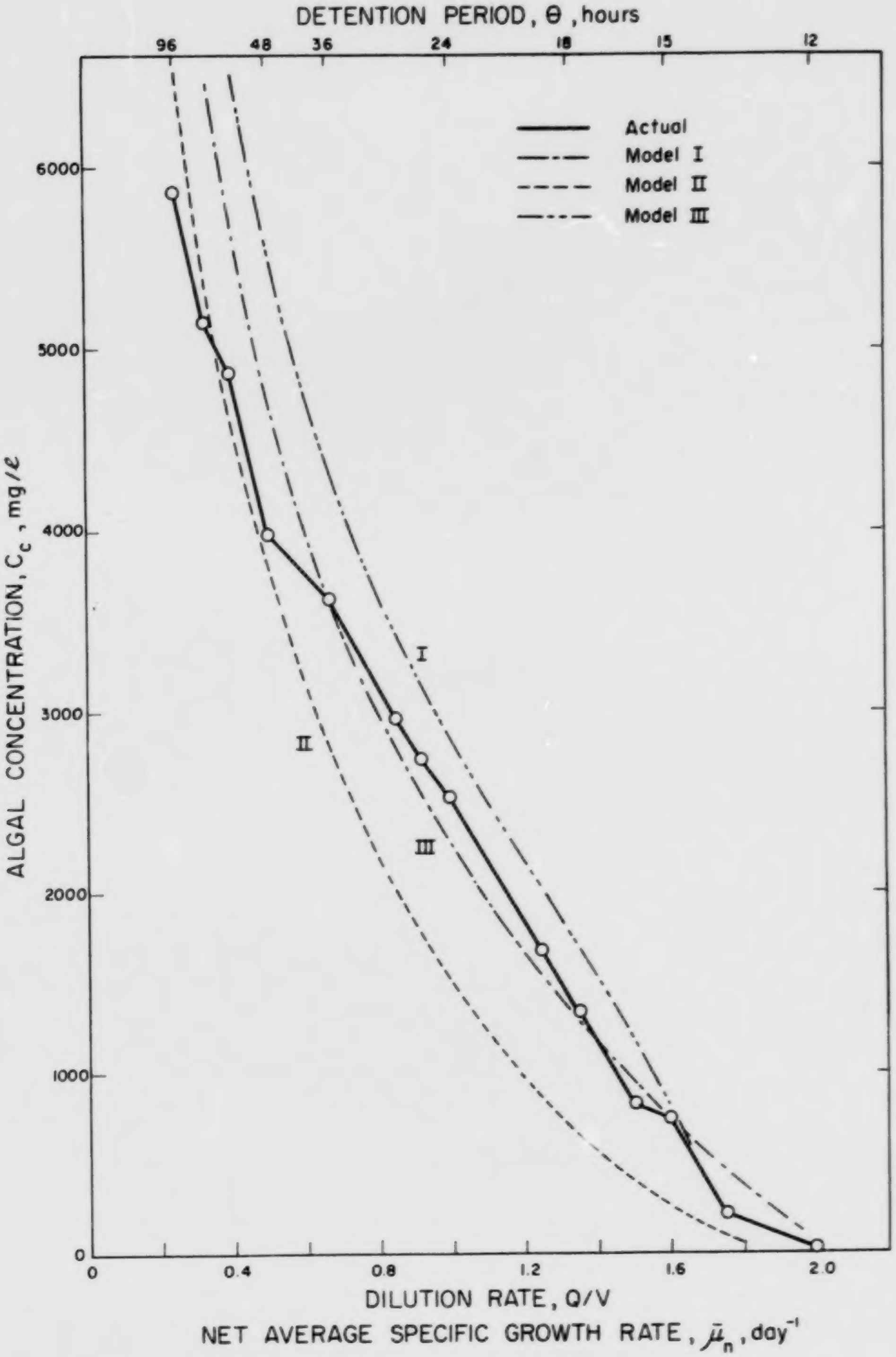

FIGURE 37. ALGAL CONCENTRATION AS A FUNCTION OF THE DILUTION RATE ("LUCALOX" LAMP AS LIGHT SOURCE)

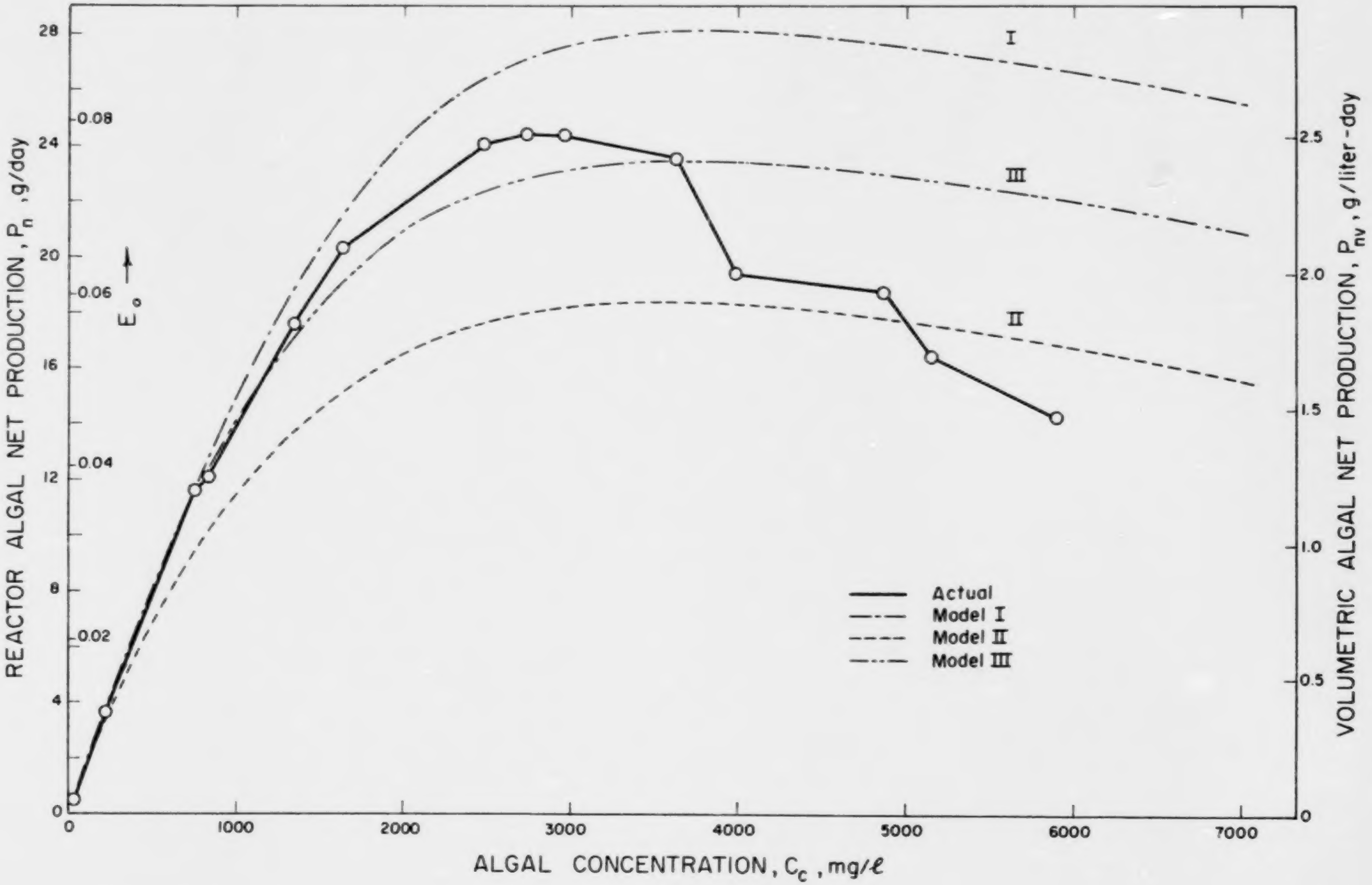

FIGURE 38. ALGAL PRODUCTION AS RELATED TO ALGAL CONCENTRATION ("LUCALOX" LAMP AS LIGHT SOURCE)

The range of applicability of Model III in predicting net algal production as a function of algal concentration is shown in Figures 35 and 38. When the Iodine-Quartz lamps were used as the light source, agreement between the experimental curve and that for Model III was closest within the range of concentrations of 300 mg/ℓ to 3500 mg/ℓ (Figure 35). The range was from 50 mg/ℓ to 3500 when the sodium vapor arc (Lucalox) lamp served as the light source. In interpreting these results, it should be kept in mind that the depth of the culture used in the experiments average only 1.7 cm. Consequently, the zone of agreement would be quite different if the culture were grown in an algae production pond under natural light conditions in which the irradiance, depth, and culture concentrations would be different.

Discrepancies Between the Experimental Data and Model III. A few discrepancies exist between the experimental data and the theoretical Model III. One example is the lower than predicted net algal production rates observed at dilution rates corresponding to algal concentrations of less than 700 mg/ℓ.

Several reasons may be offered to explain the discrepancy in expected net algal production rates at the higher dilution rates. At such dilution rates, the concentration of algae in the suspension is quite low. This low concentration combined with the relatively high intensity of the light source resulted in relatively high light intensities throughout the culture. This particular discrepancy was likely due to experimental error rather than to an inadequacy of the model. Experimental errors and variations in laboratory precision become of increased significance at low algal concentrations. Moreover, at the higher dilution rates, it is difficult to achieve and maintain steady state conditions. Another factor not to be overlooked is that of light inhibition, which may be important in relatively dilute cultures.

It should be noted that according to the theoretical models, a significant net production of algae should take place at dilution rates corresponding to high values $\bar{\mu}_n$. This production is especially noticeable in the theoretical models based on use of the Iodine-Quartz lamp as a light source. A readily apparent reason for the noticeable production predicted by the model for the Iodine-Quartz light source is the fact that when in a thin suspension, algae will selectively absorb light in the red band (cf. Figures 30 and 31). Light in the red band has a high thermodynamic efficiency (E_m). On the other hand, light in the yellow-orange band, which because of its short wavelength has a low thermodynamic efficiency, is transmitted through the culture. Inasmuch as the greater portion on the spectral distribution of the Iodine-Quartz lamp and a small portion of the Lucalox lamp are in the red band, the theoretical models predict higher values for net specific growth in dilute cultures illuminated by the Iodine-Quartz lamp than for those in cultures irradiated by the Lucalox sodium vapor arc lamp. This phenomenon of spectrum selectivity of absorbed light is responsible for the differences which appear between the models for the two types of light source.

A second and rather significant discrepancy is the difference between the decrease in net algal production rates observed in the experiments at low dilution rates and those predicted by the theoretical models. The observed rate of decrease was much greater than the predicted rate. Also, decrease in production was greater with the sodium vapor arc lamp than that observed with other light sources. The sharp decrease observed may be explained on the basis of several factors: 1) The concentration of certain micronutrients present as contaminants from glassware or in the make-up water (one-step distilled water), which may have been great enough at high dilution rates and the accompanying low algal concentration. 2) The CO_2 supply may have been inadequate or unavailable to the cells. Due to design difficulties, the maintenance of CO_2-enriched atmosphere could not be provided in the drum and the CO_2 supply was maintained by injecting it through the internal recirculation system which may have reduced CO_2 availability. 3) Mutual interference, aggravated by the close proximity of cells to one another in a highly concentrated suspension, may have produced localized zones of unfavorable environments. (4) A fourth and probably the most important factor is the sharp increase in average age of the biomass, which is a corollary to the decrease in dilution rate (increase in detention period). In a non-recycle system, the average cell age at steady state is equal to the average hydraulic detention period, θ. It has long been know that photosynthetic activity, along with other cellular activities, decreases with increasing cell age. In work with synchronized algal cultures, Tamiya et al. [87], Nihei et al. [102], and Sorokin et al. [84,160] observed a lower level of photosynthetic activity in older cells than in younger cells exposed to identical conditions of irradiance. This effect was not taken into consideration in the development of the theoretical models because its quantitative influence in terms of reduction in production could not be estimated. 5) Although no herbivores (algae grazers) were observed in microscopic examinations, some may have been present at the longer detention periods.

The discrepancy between the experimental data and theoretical curves based on Model III shown in Figures 33 and 36 also may be due in part to the use of an assumed constant endogenous respiration (decay) rate K_d of 0.125 day^{-1}. The value for $K_d = 0.125\ day^{-1}$ was used because it is the one most widely used for conditions of continuous light. Moreover, the assumption of a constant for K_d other than 0.125 day^{-1} would have resulted only in a vertical shift in the predicted results and it would not have reduced the horizontal spread between the peaks of the two curves, nor bring about a closer agreement in their shapes. The assigning of a constant value to K_d may have been unrealistic in that there is a strong indication that the rate of endogenous respiration, and more importantly the ratio between endogenous respiration and photosynthesis, is not constant. Instead, it is a complex and as yet not fully known function of light intensity and mean "algal age." If K_d is a function of mean "algal age," and the relationship is such that K_d is greater in older cells, at least relative to the rate of photosynthesis, then the theoretical curve for Model III would be shifted in the direction of the curve for the experimental data, and its downward slope at the lower dilution rates would be sharpened. Thus, the discrepancy between the experimental data and the theoretical curve would be decreased.

Light Sources Comparison. As indicated by the data listed in Table III, a comparison between the results obtained with the Iodine-Quartz lamps and those with sodium vapor arc (Lucalox) lamp, shows that in terms of net production, apparently the sodium vapor lamp was the more effective. Furthermore, the higher maximum net production (P_n) attained with the sodium vapor arc lamp occurred at a slightly higher dilution rate and algal concentration than that of the maximum net production obtained with the Iodine-Quartz lamps. As expected, the light conversion efficiency (E_o) in terms of utilization of incident irradiance energy, was significantly higher under the softer light from the Iodine-Quartz lamp than that under the brighter illumination by the sodium vapor arc lamp. On the other hand, if efficiency is based on yield per unit of input electrical energy (E_e), i.e., grams of algae per kw-hr, the efficiency was three times greater with the sodium vapor arc (Lucalox) lamp than with the Iodine-Quartz lamps. A partial explanation is the high degree of efficacy* of the Lucalox lamp and the fact that a relatively large portion of the light from the Iodine-Quartz is in the infrared band of the spectrum and thus unavailable to the algae.

NITROGEN AS A GROWTH-LIMITING FACTOR

Summarized in Figures 39 to 46 and Table IV are the results obtained in the experiments with the chemostatic and turbidostatic one-liter growth units in which nitrogen alone constituted the sole growth-limiting factor. Light intensity was maintained above saturation levels throughout the cross section of the growth unit. Nitrate-nitrogen constituted the nitrogen source, and the algae growth was measured as a function of its concentration.

---

*Efficacy is defined as the efficiency of conversion of electrical energy into irradiance.

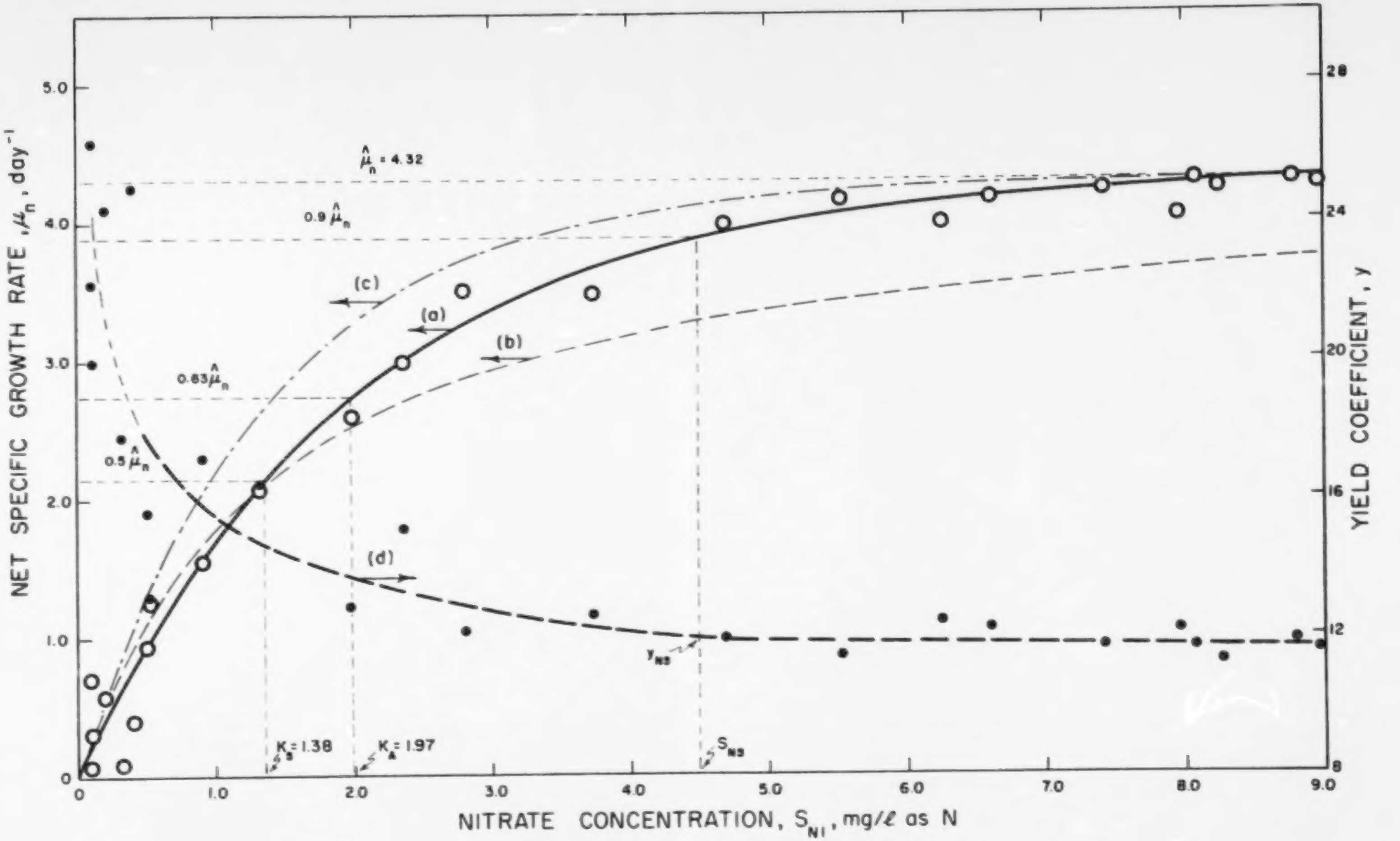

FIGURE 39. ALGAL NET SPECIFIC GROWTH RATE AND YIELD COEFFICIENT AS FUNCTIONS OF NITRATE CONCENTRATION (EXPERIMENT 1 AT 35°C WITH C. pyrenoidosa 71105)

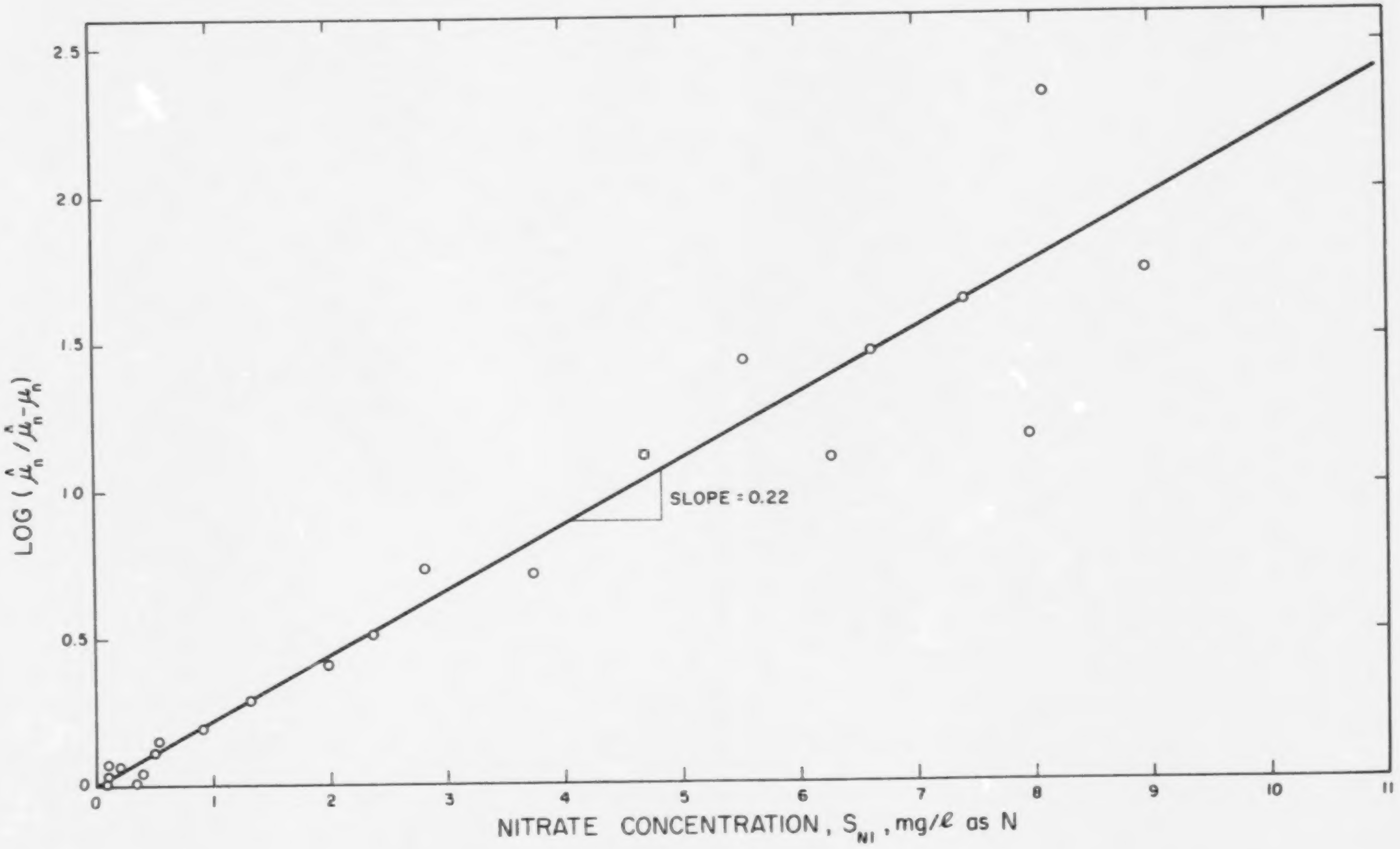

FIGURE 40. REGRESSION ANALYSIS OF THE MODIFIED EXPONENTIAL FUNCTION, USING THE DATA OBTAINED IN EXPERIMENT 1

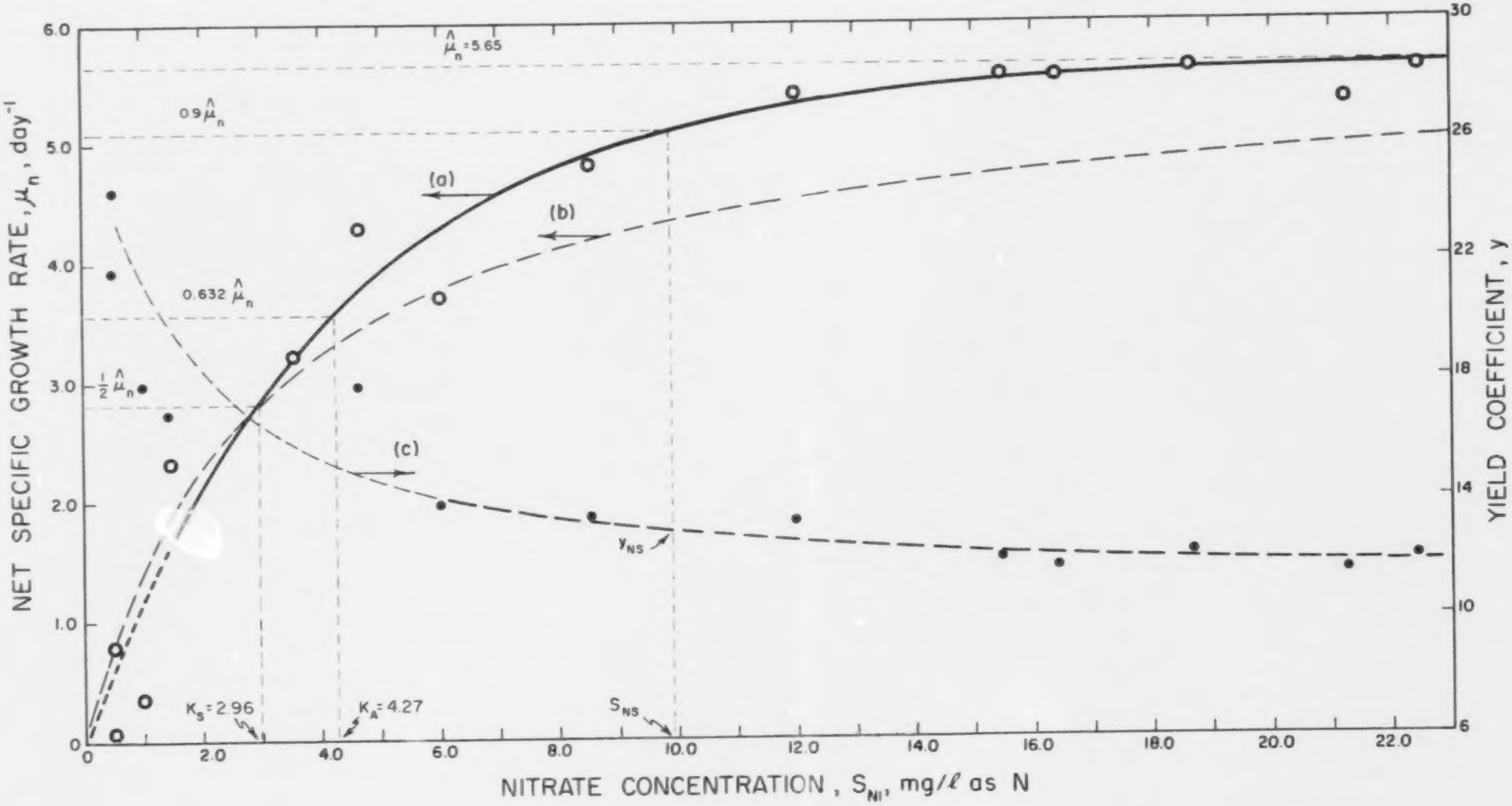

FIGURE 41. ALGAL NET SPECIFIC GROWTH RATE AND YIELD COEFFICIENT AS FUNCTIONS OF NITRATE CONCENTRATION (EXPERIMENT 2 AT 39.2 °C WITH C. pyrenoidosa 71105)

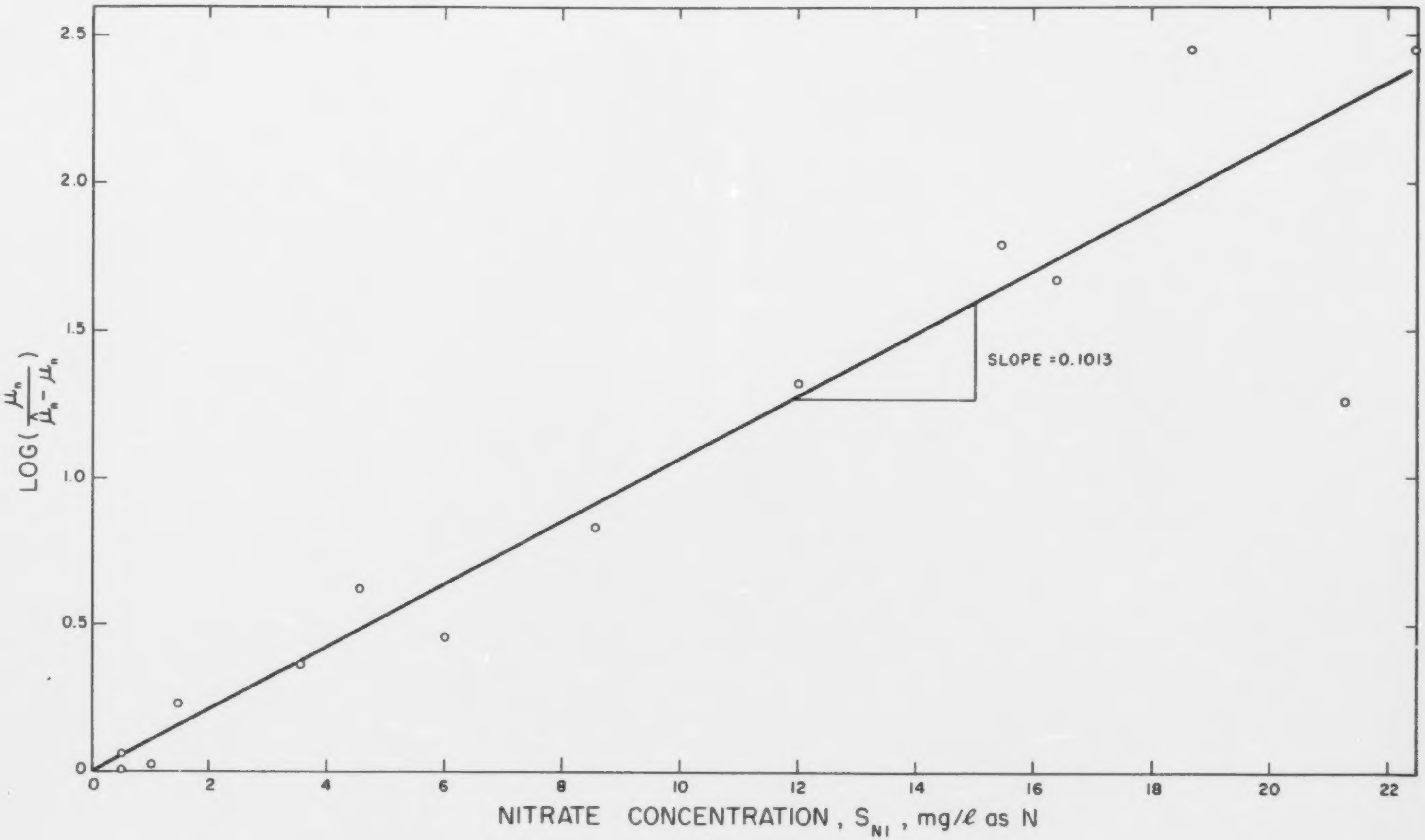

FIGURE 42. REGRESSION ANALYSIS OF THE MODIFIED EXPONENTIAL FUNCTION, USING THE DATA OBTAINED IN EXPERIMENT 2

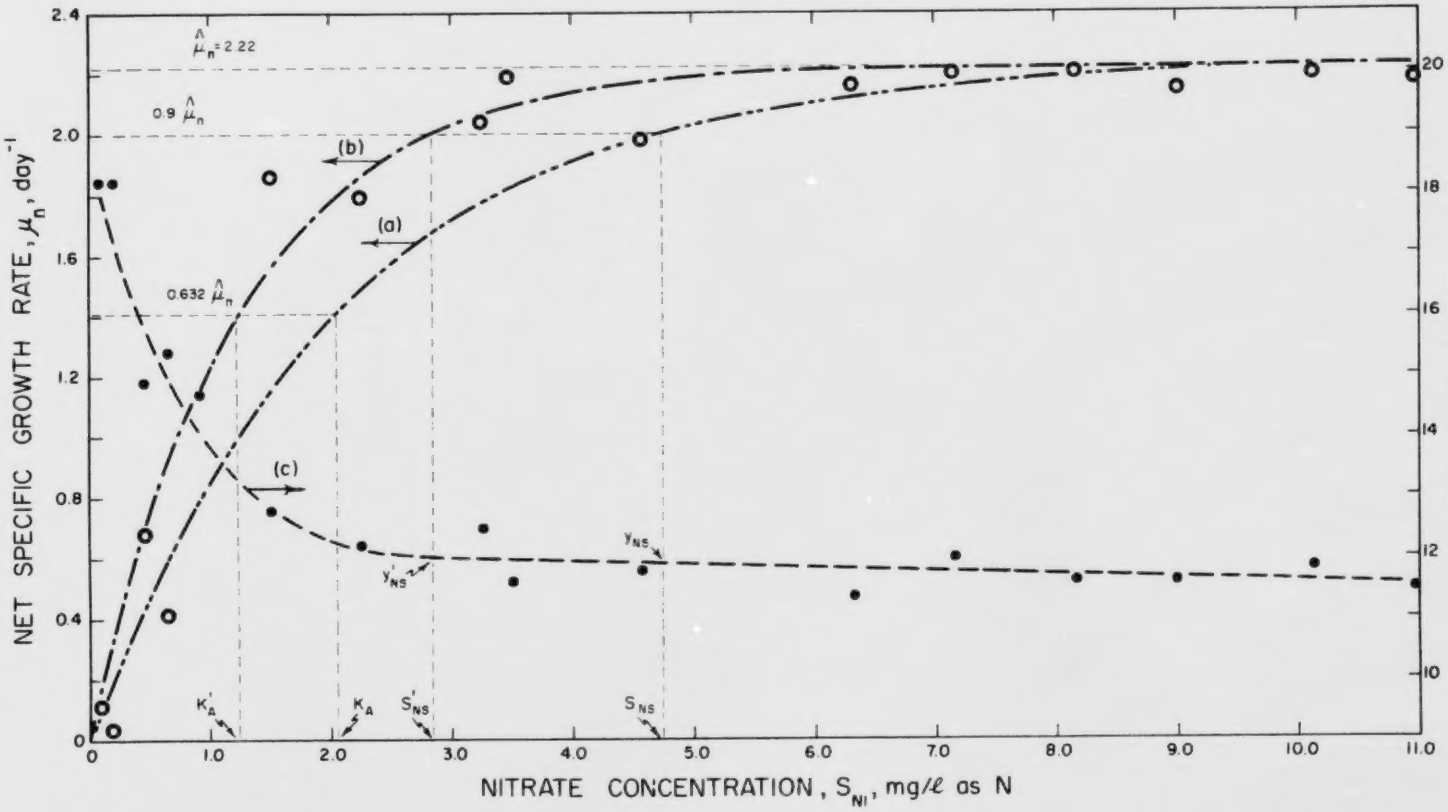

FIGURE 43. ALGAL NET SPECIFIC GROWTH RATE AND YIELD COEFFICIENT AS FUNCTIONS OF NITRATE CONCENTRATION (EXPERIMENT 3 AT 28.5 °C WITH C. pyrenoidosa EMERSON STRAIN)

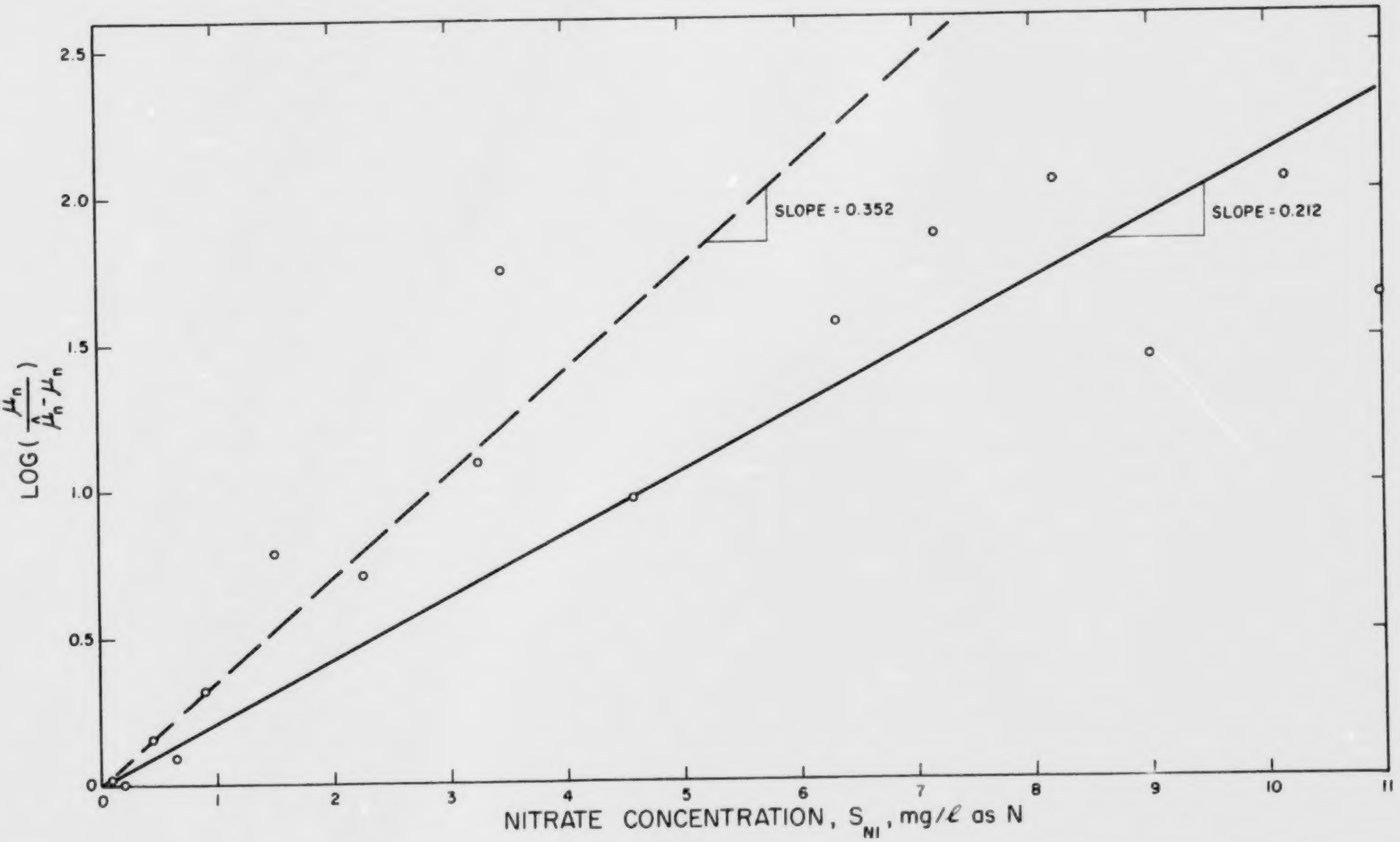

FIGURE 44. REGRESSION ANALYSIS OF THE MODIFIED EXPONENTIAL FUNCTION, USING THE DATA OBTAINED IN EXPERIMENT 3

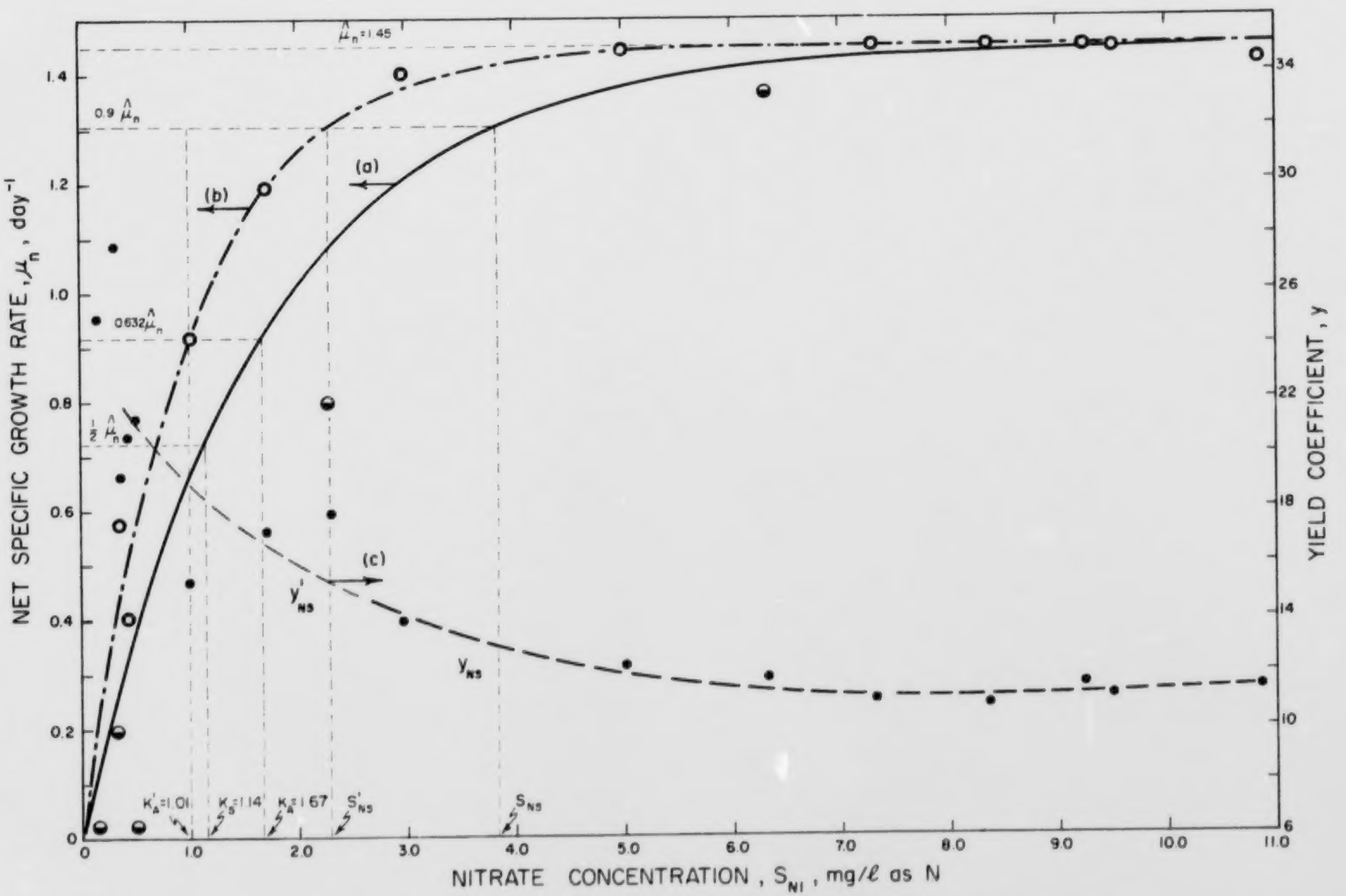

FIGURE 45. ALGAL NET SPECIFIC GROWTH RATE AND YIELD COEFFICIENT AS FUNCTIONS OF NITRATE CONCENTRATION (EXPERIMENT 4 AT 19°C WITH C. pyrenoidosa EMERSON STRAIN)

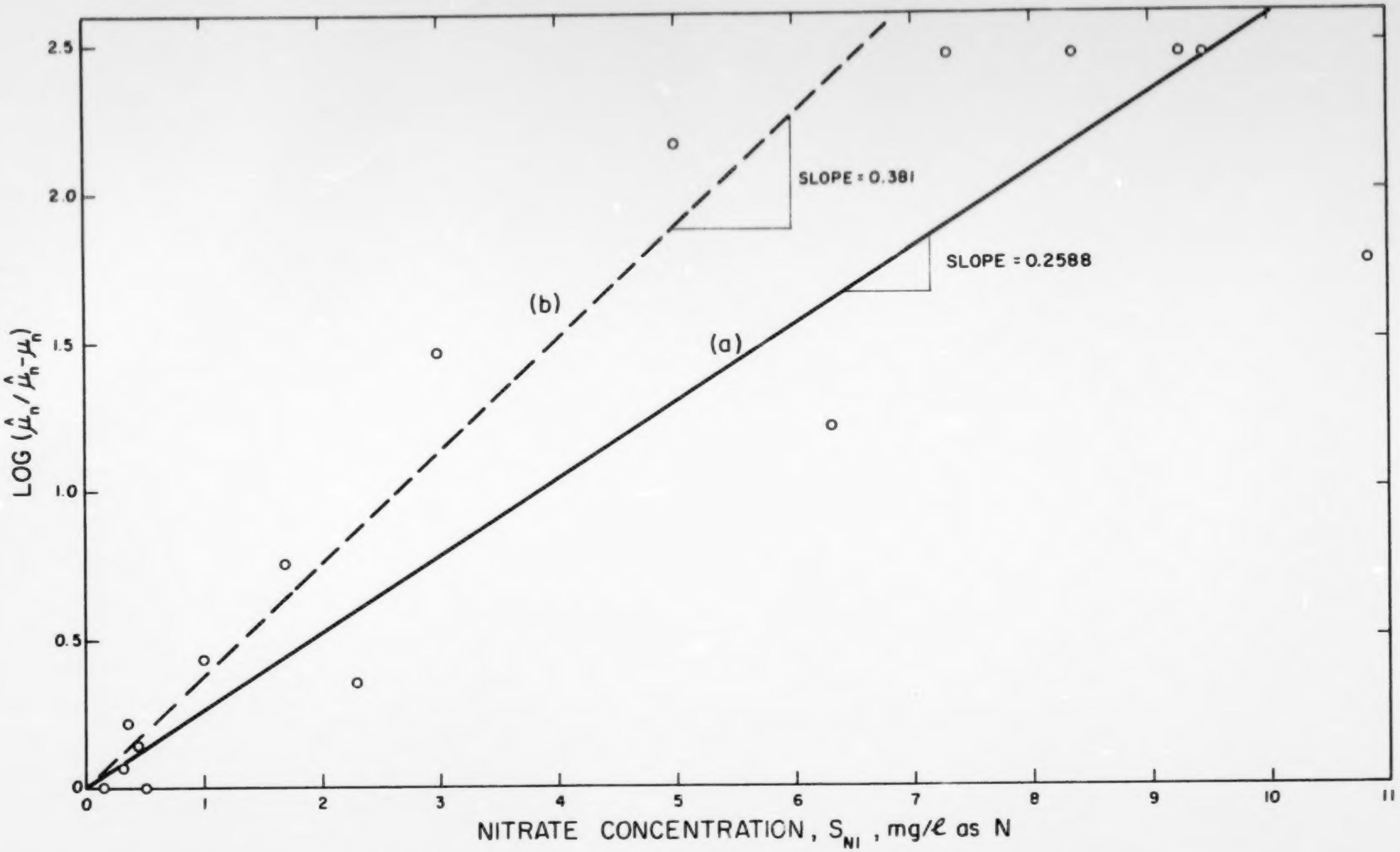

FIGURE 46. REGRESSION ANALYSIS OF THE MODIFIED EXPONENTIAL FUNCTION, USING THE DATA OBTAINED IN EXPERIMENT 4

TABLE IV

A SUMMARY OF KINETIC AND STATISTICAL PARAMETERS OF THE EXPERIMENTS WITH ALGAL GROWTH WITH RESPECT TO NITROGEN CONCENTRATION

Exp. No.	Algae Species	Temp. (°C)	Nitrogen Source	$\hat{\mu}_n$ Observed (day^{-1})	Modified Exponential Function			Michaelis-Menten Function						0.9 $\hat{\mu}_n$ (day^{-1})	S_{NS} (mg/ℓ as N)	Y_{NS}	$\bar{Y}$
					Regression Analysis		Corr. Coef.	Regression Analysis				Corr. Coef.	Estimated K_S (mg/ℓ as N)				
					Slope	K_A (mg/ℓ as N)		$\frac{1}{\hat{\mu}_n}$	Comp. $\hat{\mu}_n$ (day^{-1})	Slope	Computed K_S (mg/ℓ as N)						
1	*C. pyren.* TX 71105	35.0	NO_3^-	4.32	0.220	1.97	0.961	(0.40)[b]	(2.50)	(0.65)	(1.62)	0.603	1.38	3.90	4.50	12.0	11.7
2	*C. pyren.* TX 71105	39.2	NO_3^-	5.63	0.101	4.27	0.933	(-0.37)	(-2.72)	(3.87)	(-1.06)	0.718	2.96	5.10	9.90	13.2	11.8
3	*C. pyren.* Emerson	28.5	NO_3^-	2.22	0.212	2.05	0.880	(1.18)	(0.85)	(1.31)	(1.12)	0.505	1.40	2.00	4.75	11.9	11.7
3A[a]	*C. pyren.* Emerson	28.5	NO_3^-	2.22	0.352	1.23	0.958						0.85	2.00	2.85	12.0	11.7
4	*C. pyren.* Emerson	19.0	NO_3^-	1.45	0.259	1.67	0.900	(-0.88)	(-1.14)	(6.58)	(-7.50)	0.702	1.14	1.30	3.85	13.0	11.2
4A[a]	*C. pyren.* Emerson	19.0	NO_3^-	1.45	0.381	1.01							0.70	1.30	2.30	15.4	11.2

[a] These parameters refer to an alternative best-fit curve in the same experiment.

[b] Those values within parenthesis represent data derived from the regression analysis but which cannot be used as kinetic parameters (see text).

The effect of temperature on the growth of algae with respect to nitrate-nitrogen was also studied.

The major variables measured and reported in each experimental run were: 1) the net specific growth rate μ_n as determined by the dilution rate Q/V of a CSTR-type chemostat or turbidostat at steady state conditions; 2) the yield coefficient, Y, as measured by the nitrogen materials balance; and 3) soluble nitrogen concentration of the culture in the reactor and in the effluent, S_{N_1}.

Due to the fact that $Y = f(S_{N_1})$, it was not possible to estimate the magnitude of the decay rate, K_d, or the gross specific growth rate, μ. It should be noted that as far as algal assimilative removal of nitrogen and/or net algal production are concerned, the value of μ_n is the one of practical significance.

General Patterns

Growth Curves. The general hyperbolic-type relationship between net specific growth rate and concentration of soluble nitrate-nitrogen is indicated in Figures 39, 41, 43, and 45. Since the plotted data points were scattered, it was necessary to use statistical analyses to develop reliable conclusions from the data.

The data on net specific growth rate at the low nitrogen concentrations — the region of "nitrogen starvation" — were so dispersed and inconsistent as to make it extremely difficult to draw any "curve of best fit." The observed net growth rate varied from zero to approximately one-fourth the maximum net specific growth rate without any apparent consistency. In a few runs, growth at the lower nitrogen concentration was greater than that at higher concentrations. This pattern of response differs from the classical microbial growth as a function of concentration and availability of energy source, e.g., bacterial growth in relation to nutrient or organic substrate, and algae in relation to light. In the latter cases, the data points in the lower part of a growth response curve follow a consistent pattern, whereas they have a tendency to be scattered at or near saturation levels of nutrient or substrate.

A possible reason for the apparent inconsistency of the data is the relative inaccuracy of analytical methods at low concentrations, i.e., at the lower end of their range of sensitivity. Perhaps genetic adaptation and natural selectivity exert a significant influence. This is a possibility because the strains of *C. pyrenoidosa* used in the study are not adapted to low concentrations of nutrients. Another possibility is that nitrogen starvation may not affect energy supply; however it may result in damage to the protoplasm of the algal cell and, with increasing severity of starvation, to the chloroplasts, enzymatic structures, and the nucleic acids. Since the extent and effect of the damage differs from cell to cell, the net effect on the growth of the culture as a whole may vary from one experiment to another. A further complicating factor is that damaged cells are in a disadvantageous position with respect to bacterial competition, and may be more susceptible to deficiencies in trace element supply.

The consistency of the data on specific growth rate increased with increases in the nitrogen concentration. Because of the high degree of consistency attained at optimum concentrations of nitrogen, the maximum net specific growth rate, $\hat{\mu}_n$, appears to be a reliable parameter.

In all determinations of $\hat{\mu}_n$, a value was found which proved to be constant for a given strain of algae grown in a medium having an optimum concentration of nutrients at a given temperature. Because of the experimentally demonstrated constancy of the value under a defined set of conditions, and its relation to species and temperature, the maximum specific growth rate can serve as a convenient and reliable parameter with regard to the genetic characteristics of algae and to physical environmental conditions, especially temperature. Furthermore, the value of the parameter $\hat{\mu}_n$ can be drawn directly from the experimental data under optimal conditions and can serve as a parameter in a kinetic model function.

The increasing response in growth rate to an increase in nitrogen concentration is surprisingly sharp. For example, the gap between a nitrogen concentration supporting a growth rate equal to one-fourth the maximum growth rate and that supporting maximum growth rate can be bridged in most cases by an increase in nitrogen concentration (mg/ℓ as nitrogen) of less than one order of magnitude. This relatively sharp response supports the common assumption of the existence of a "critical concentration" of nutrients, i.e., the concentration at which algal growth is triggered in a natural body of water, and above which even a small increase in concentration results in a mass phytoplankton production.

The theoretical curve which best fits the data points obtained in the experiments reported herein with respect to the growth rate of *C. pyrenoidosa* as a function of NO_3-N concentration is the exponential function in its modified form, which is given in Equation 4-14. Apparently, temperature and genetic traits also have a marked effect on the relation between growth rate and nitrogen concentration.

Yield Coefficient. The yield coefficient is defined as the biomass produced per unit of mass of limiting substrate utilized, as determined from the nitrogen materials balance of the system. The yield coefficient is strongly affected by the nitrogen concentration of the medium. The extent of this influence is shown by the curves in Figures 39, 41, 43, and 45 in which the yield coefficient is plotted as a function of nitrogen concentration. The function $Y(S_{N_1})$ has the general configuration of a monotone-decreasing concave curve almost asymptotic to a certain value $\bar{Y}$. The data points for $Y(S_{N_1})$ are quite scattered in the low nitrogen concentrations region of the curve, and even more so as the region of "nitrogen starvation" is approached. The latter scattering stems from the general inconsistency characteristic of data obtained at such nitrogen concentrations.

The general shape of the yield curve resembles that of the growth curves in that at saturation levels of nutrient, the yield coefficient approximates a constant, while Y increases as growth rate decreases. This corresponds to the well-known decrease in cellular nitrogen content under conditions in which nitrogen is limiting. The scattered experimental data and the relative inconsistency of the data from one experimental set to another do not permit the selection of a "best fit" function, nor do they allow any mathematical formulation which would tie $Y(S_N)$ to $\mu_n(S_{N_1})$. However, the data indicate that a linear relationship between nitrogen content of the cells and the prevailing nitrogen concentration in the reactor at levels lower than saturation as observed by Gerloff *et al.* [104,105] for *Microcystis* sp. does not apply to *C. pyrenoidosa*.

Best Fit Kinetic Function

A kinetic function which would best fit the experimental data was sought with methods ranging from trial and error to rigorous statistical analysis. The general hyperbolic type of relationship between the net specific growth rate and the prevailing nitrogen content was observed at the outset, and the first attempt involved the application of the various functions proposed and described in Chapter IV. The rectangular hyperbola as formulated by Michaelis-Menton (Equation 4-8) and the exponential function (Equation 4-13), later modified to the "Modified Exponential Function" (Equation 4-14), became the two likely "best fit" functions.

The Michaelis-Menten Equation. The applicability of the Michaelis-Menten equation to describe the experimental results and the values of its parameters K_s and $\hat{\mu}_n$ were determined in two ways:

1. By best fit (by eye) to the curve based on the experimental data. The value of $\hat{\mu}_n$ was estimated directly from the experimental results. K_s was estimated on the basis of values of S_{N1} corresponding to those of $\mu_n = \hat{\mu}_n/2$ which are approximated from the experimental curve showing specific growth rate as a function of concentration of soluble nitrogen in the medium. The Michaelis-Menten curve was then drawn on the basis of the parameters $\hat{\mu}$ and K_s determined as described above and it was compared visually to the curve based on the experimental data points. This method proved to be moderately successful as will be shown in the section describing the individual experiments.

2. By linear regression analysis, correlation studies and least squares analysis on the reciprocal form of the Michaelis-Menten formula i.e.,

$$\frac{1}{\mu_n} = \frac{1}{\hat{\mu}_n} + \frac{K_s}{\hat{\mu}_n}\frac{1}{S_{N1}} \quad \text{[cf. Figure 13(B)].}$$

Although the regression analysis method is commonly applied in the analysis of bacterial systems, it did not prove suitable in processing the data for determining appropriate constants in the Michaelis-Menten function. In fact, the magnitude of $\hat{\mu}_n$ and K_s obtained from the regression analysis had little relation to the value of $\hat{\mu}_n$ and K_s as determined by visual observation of the data. Consequently, a curve developed by linear regression analysis would bear little resemblance to the best fit curve (by eye) of the data. This discrepancy is shown in Table IV by the difference between the values of $\hat{\mu}_n$ and K_s as drawn from the regression analysis and those of the basis of experimental data.

The regression analysis did not prove suitable for several reasons. a) A large number of data points in the region of nitrogen starvation were quite dispersed. In this region the numerical values of S_{N1} and μ_n were low, thus their reciprocals ($1/S_{N1}$ and $1/\mu_n$) have large numerical values. Moreover, even a slight scattering of the experimental values in this region tend to magnify the extent of the scattering of the values $1/S_{N1}$ and $1/\mu_n$. Thus, the combination of large numerical values and the magnified scattering imparted a tremendous statistical weight in the regression analysis of the experimental data. b) As values of S_{N1} approach the range of saturation, the value of μ_n very closely approaches that of $\hat{\mu}_n$. A plot of the reciprocal values of the experimental data for this region would appear as a crowded assemblage of value points for $1/S_{N1}$ and $1/\mu_n$ on a line nearly parallel to the $1/S_{N1}$ axis at an almost constant value closely approximating that for $1/\hat{\mu}_n$. Further, the numerical values of the reciprocals in this region are relatively small. Thus, the latter data points impart a tenuous statistical significance in the regression analysis.

The Modified Exponential Function. The regression analysis was applied successfully to the logarithmic function $\log \frac{\hat{\mu}_n}{\hat{\mu}_n - \mu_n} = \frac{0.4343}{K_A} S_{N1}$ [cf. Figure 14(B)] to obtain the modified exponential curve best fitting the experimental data, i.e., the parameter K_A. However, its usefulness was decreased somewhat because the data points showed a tendency toward scattering, especially those of the higher values for S_{N1} at which values for μ_n approach those for $\hat{\mu}_n$, and those for $\hat{\mu}_n - \mu_n$ become very small. Because of this tendency, the term $\log \frac{\hat{\mu}_n}{\hat{\mu}_n - \mu_n}$ becomes rather large numerically as shown in Figures 40, 42, 44, and 46. Furthermore, minor scatter in the data for $\mu_n(S_{N1})$ as it approached $\hat{\mu}_n$ caused a relatively high scatter in the values of $\log \frac{\hat{\mu}_n}{\hat{\mu}_n - \mu_n}$. It appears that the values of μ_n approaching those of $\hat{\mu}_n$ (i.e., at relatively high values of S_{N1}) are reliable.

One reason for the relatively successful application of the regression analysis approach in determining the modified exponential function from the experimental data is the fact that the value for $\hat{\mu}_n$ was established reliably through preliminary experiments involving the use of optimal media and was confirmed repeatedly in the course of principal experiments. Thus, only K_A remained to be determined by regression analysis. Furthermore, the restriction that the regression line originates at the origin results in a reduction in regression line parameters. As shown in Figures 39, 41, 43, and 45, the modified exponential equation obtained by regression analysis fits the experimental data well. Moreover, the value for K_A determined by regression analysis was similar to one which could be developed from the value of S_{N_1} corresponding to $\mu_n = 0.63\ \hat{\mu}_n$ with the best fit curve (by eye) for the experimental data.

Recommended Parameters for the Growth Curve

The parameters necessary to describe kinetic functions, namely $\hat{\mu}_n$ and K_s for the Michaelis-Menten equation and $\hat{\mu}_n$ and K_A for the modified exponential function, are summarized in Table IV and are shown in each of the specific growth-rate curves shown in Figures 39, 41, 43, and 45. Two additional parameters which can be useful in practice are S_{NS}, the concentration of growth-limiting soluble nitrogen corresponding to a net specific growth rate which approaches its maximum value $\hat{\mu}_n$, and Y_{NS}, the yield coefficient which corresponds to S_{NS}. To be more specific, the value of S_{NS} was arbitrarily defined as being the concentration of rate limiting nutrient when $\mu_n = 0.9\ \hat{\mu}_n$. The practical significance of the parameter S_{NS}, is that it is the concentration at which near-maximum algal growth and concomitant assimilative removal can be attained and produce a relatively low nitrogen residue in the effluent.

Specific Experiments

In Experiments 1 to 4, NO_3-N was the sole source of nitrogen. Because of ample artificial aeration and photosynthetic oxygenation, no detectable reduction of nitrogen took place in the medium, and thus NO_3-N constituted the sole growth-limiting soluble nitrogenous substrate. A culture of C. pyrenoidosa, strain TX 71105, was used in Experiments 1 and 2 in which the temperature was held at 35°C ± 0.7°C and at 39.2°C ± 0.5°C, respectively, and the Emerson strain of the species in Experiments 3 and 4, in which the temperature was held at 28.5°C (±0.7°C) and at 19°C (±0.7°C), respectively.

Experiment 1. Temperature 35°C. The relation between NO_3-N concentration in the medium and the net specific growth rate μ_n and the yield coefficient Y is shown in Figure 39. Observed and computed growth parameters are listed in Table IV. Growth rates as high as 4.32 day^{-1} were attained frequently. A regression analysis of the exponential function (Equation 4-15), shown in Figure 40 resulted in a K_A parameter of 1.97 mg/ℓ as N. The modified exponential function proved to best fit the experimental data, as is shown by curve (a) in Figure 39. Results were less successful with the use of a regression analysis of the data according to the Michaelis-Menten function. The statistical correlation was poor (cf. Table IV). An attempt was made to plot a best fit curve on the basis of the Michaelis-Menten function by giving $\hat{\mu}_n$ a numerical value of 4.32, and the K_s a value of 1.38 mg/ℓ as N based on the assumption that K_s is equal to S_{N_1} which in turn corresponds to $\hat{\mu}_n/2$. The resulting curve, shown as curve (b) in Figure 39, coincided with the experimental data at the lower end of the concentration (S_{N_1}) scale, but did not fit well at the upper end.

The attempt to graph the function according to Teissler's equation (Equation 4-11) met with greater success. In this plot, the numerical value of 1.38 mg/ℓ was again given to K_s. The result is shown as curve (c) in Figure 39.

Although, as is shown in the figure, curve (c) almost parallels curve (a), it undoubtedly would be preferable to use K_A instead of K_s as in the modified exponential function.

The value for S_{NS} was found to be between 4 and 5 mg of NO_3-N. The high value probably reflects the adaptation of the algal strains used in the study to a substrate relatively rich in nitrogen. However, at a nitrogen concentration of 1.5 mg/ℓ, the net specific growth rate is 2.16 day^{-1} (i.e., $\hat{\mu}_n/2$). These relations show that if an effluent low in nitrogen is desired, a compromise must be made in terms of growth rate. Approximately 12 mg of algae were produced per mg of nitrogen removed (i.e., $Y_{NS} = 12$). This value approximates that of $\overline{Y}$ (11.7) attained at nitrogen saturation. The value of Y increased sharply as the concentration of nitrogen approached the region of nitrogen starvation, as is shown by the slope of curve (d) in Figure 39. The data points also became quite dispersed.

Experiment 2. Temperature 39.2°C. The spread between the data points obtained in Experiment 2 was somewhat greater than was the case in Experiment 1. The $\hat{\mu}_n$ value was repeatedly found to be 5.65 day^{-1}. The modified exponential function was found to best fit with K_A equaling 4.27 mg/ℓ as nitrogen, as is shown by curve (a) in Figure 41. This was found by regression analysis as is illustrated in Figure 42.

The difficulty encountered in Experiment 1 with respect to the regression analysis of the reciprocal Michaelis-Menten equation also arose in Experiment 2. Again using values for $\hat{\mu}_n$ and K_s as estimated from the experimental data, the Michaelis-Menten equation was computed and the results plotted. Curve (b) in Figure 41 is the result. Here again the curve for the Michaelis-Menten equation [curve (b)] ranks with curve (a) in representing the data when the values for S_{N_1} were relatively low. However, the Michaelis-Menten function did not fit well the experimental data at the higher S_{N_1} levels.

Experiment 3. Temperature 28.5°C. Data collected in Experiment 3 are shown graphically in Figure 43. Although the value of 2.22 day^{-1} for $\hat{\mu}_n$ was found in preliminary experiments involving the use of optimal medium, a regression analysis of the data (cf. Figure 44) resulted in two possible values for K_A. Including all of the data in the regression analysis resulted in a K_A value of 2.05 mg of nitrogen/ℓ for the best fit modified exponential function shown as curve (a) in Figures 43 and 44. However, agreement between this curve and the majority of the data points was poor. The second value $K_A = 1.25$ mg N/ℓ was obtained in a regression analysis of data from which a few questionable data were excluded, especially those in which the values for μ_n and $\hat{\mu}_n$ were fairly similar. The resulting curve, curve (b), in Figures 43 and 44 gave a better fit of the experimental data. The variations in yield Y with nitrate concentration [curve (c), Figure 43] are also shown in Figure 44.

Experiment 4. Temperature 19°C. Experimental data on net specific growth rate and yield coefficient as functions of NO_3-N concentration of the substrate are shown in Figure 45. A regression analysis of the data resulted in the regression line plotted as curve (a) in Figure 46. The K_A value was found to be 1.67 mg/ℓ as nitrogen. The modified exponential curve is shown as curve (a) in Figure 45. A modified exponential function with K_A equaling 1.01 was obtained by excluding questionable data. The curve for the function is shown as curve (b) in Figure 45. The deviation of the excluded points from the expected trend may have been due to limiting factors other than nitrogen concentration. Such questionable data are shown by half-full circles in Figure 45. The linear regression of the modified function [curve (b), Figure 46] was found to best fit the "selected" data. Values for S_{NS} proved to be significantly lower than those found at the higher temperatures; while the value for Y_{NS} was slightly higher (as is shown in Table IV).

The Effect of Temperature

In Experiments 1 through 4, the effect of temperature on net specific growth rate and NO_3-N concentration was investigated. The two strains of C. pyrenoidosa, viz., TX 71105 and Emerson, used in these experiments were selected on the basis of tolerance and growth at different temperatures rather than by their response to nutrient. It was assumed, therefore, that both strains possessed similar genetic characteristics with respect to nitrogen requirement.

The effect of the temperature on the net specific growth rate as a function of NO_3-N concentration is shown by the family of curves in Figure 47. The collection of curves in Figure 48 illustrates the effect of temperature on related parameters. The variation in K_A and K_s with temperature is shown in Figure 48(A) and 48(B), respectively. In Figure 48(A), K_A was considered equivalent to S_{N1}, which corresponds to $\mu_n = 0.63\ \hat{\mu}_n$. The curve in Section C of the figure illustrates the effect to temperature on S_{NS}; and that in Section D, the effect of temperature on Y_{NS}. The effect of temperature on S_{N1}, at $\mu_n = 1.0$ day^{-1}; is shown in Section E and at $\mu_n = 2.0$ day^{-1}, in Section F.

The general pattern of the curves in Figure 47 was determined by the variation in $\hat{\mu}_n$ from experiment to experiment. In all cases, $\hat{\mu}_n$ was determined under conditions of light and nitrogen saturation; therefore, the variation is a function of temperature, with the magnitude of $\hat{\mu}_n$ increasing with increase in temperature. This increase reflects the favorable effect of the higher temperatures (within limits of the temperature tolerance of the organism) on light utilization, i.e., on the enzyme complex concerned with irradiance in the photosynthetic apparatus.

Of interest is the fact that the concentration of nitrate needed to maintain a given net specific growth rate increased as the temperature decreased from 35°C to 19°C and as the temperature increased from 35°C to 39.2°C. This is illustrated in Figure 47 as well as in Sections E and F in Figure 48. Furthermore, the high values of net specific growth rate observed at 39.2°C were accompanied by significantly increased requirements with respect to nitrogen. This is evident from Figure 47 as well as from Sections A, B and C in Figure 48 in which the parameters K_A, K_s, and S_{NS} which correspond to relative proportions of $\hat{\mu}_n$ (i.e., $0.5\ \hat{\mu}_n$, $0.63\ \hat{\mu}_n$, and $0.9\ \hat{\mu}_n$, respectively) indicated a sharp increase as the temperature was raised to 39.2°C. Although 39°C may be the optimum temperature for the TX 71105 strain with respect to growth (i.e., photosynthetic conversion of light energy), it is not necessarily so with respect to the utilization of nitrate-nitrogen at relatively low concentrations. The relatively high S_{N1} value corresponding to $\hat{\mu}_n = 1.0$ day^{-1} at 19°C shown in Section E of Figure 48 may be attributed to the fact that the value 1.0 day^{-1} given for μ_n is fairly close to that for $\hat{\mu}_n$. As shown in Section D of Figure 48, the effect of temperature on Y_{NS} was not marked. The high value at 19°C may be an artifact resulting from the scatter of the data points for the yield coefficient obtained in Experiment 4.

NITROGEN AS THE GROWTH-LIMITING FACTOR IN AN OPTICALLY DENSE CULTURE

Experimental work with the algatron system and in which the temperature was held at 27°C (±0.5°C) involved the use of C. pyrenoidosa (Emerson strain) as the microorganism; the SERL nitrate medium; and as a light source, the Sodium Vapor Arc lamp (Lucalox). The concentration of algae was maintained constant at 2680 mg/ℓ (±150 mg/ℓ), while the concentration of nitrogen in the medium was varied according to the experimental conditions. Following each reduction in NO_3-N concentration in the medium, the dilution rate was readjusted until the algal concentration again reached the predetermined value, and steady state conditions were attained. This chemostatic technique proved to be time-consuming inasmuch as after each change in the medium concentration, from two to ten days were needed for the culture to reach steady state. The apparent solution should have been the use of a turbidostatic technique with which a predetermined concentration of algae is automatically maintained and the dilution rate also is automatically adjusted accordingly.

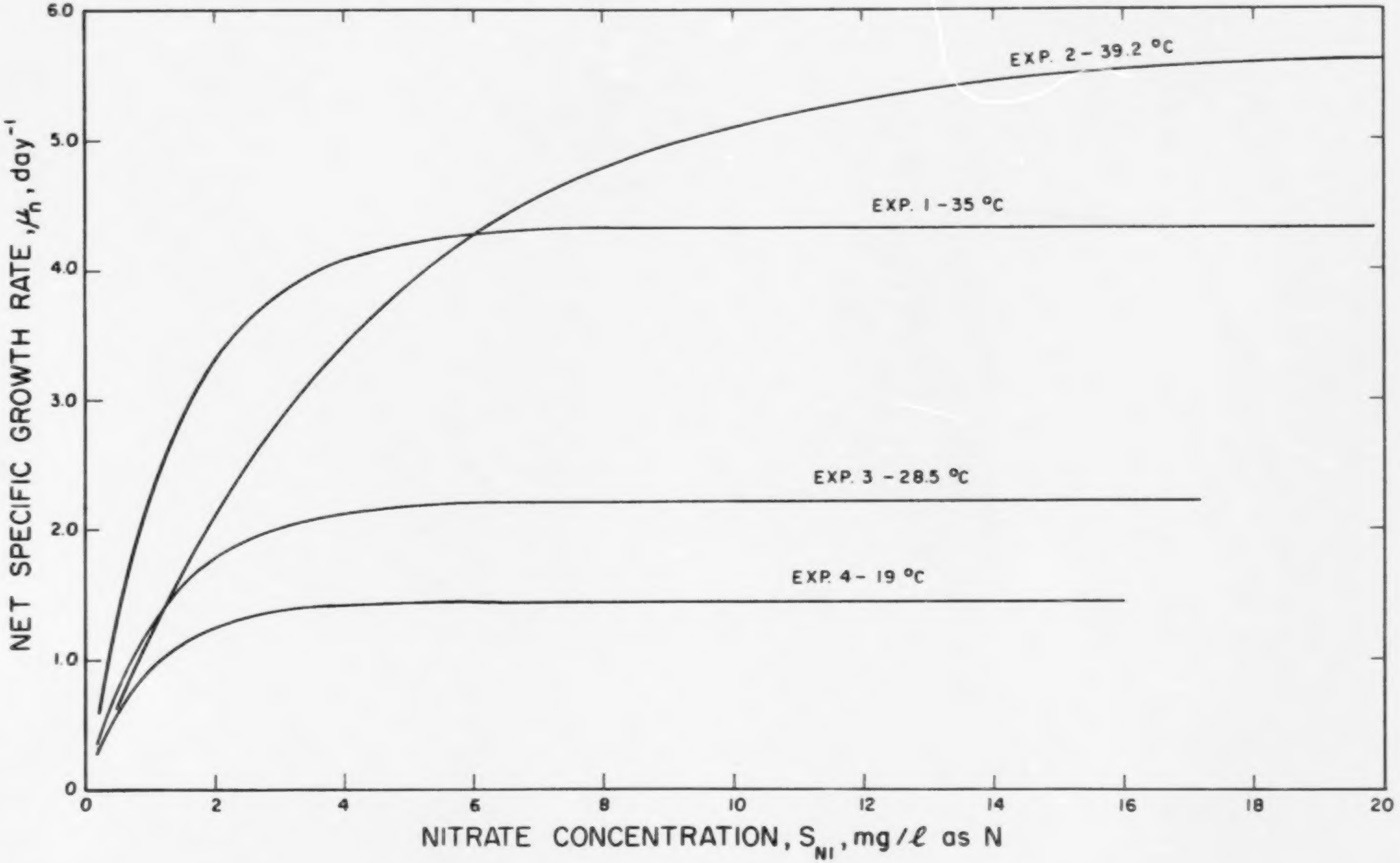

FIGURE 47. THE EFFECT OF TEMPERATURE ON THE NET SPECIFIC GROWTH RATE OF C. pyrenoidosa WITH RESPECT TO NITRATE CONCENTRATION

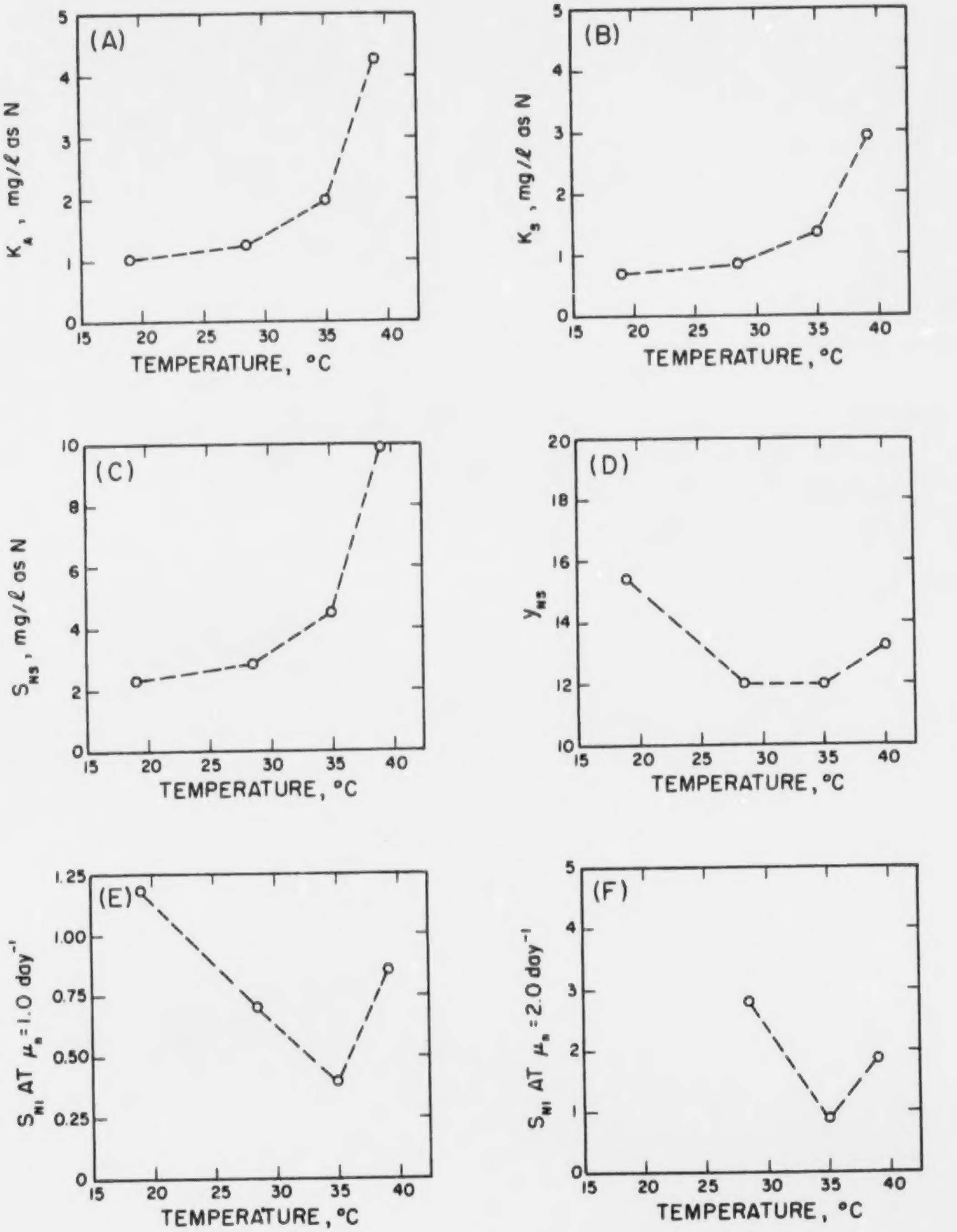

FIGURE 48. THE EFFECT OF TEMPERATURE ON VARIOUS GROWTH KINETIC PARAMETERS OF C. pyrenoidosa WITH RESPECT TO NITRATE CONCENTRATION

Although a turbidostat of this type was used quite successfully with the one-liter growth units, technical and budgetary limitations made impractical its use on the algatron prototype. To evaluate properly the results obtained in these experiments, they should be compared with those obtained in the experiments concerned with light alone and with those concerned with NO_3-N concentrations in which light was maintained at saturation level. In making the comparisons, it should be noted that the experiments concerned with light alone were conducted with the use of the same reactor, light source, and at the same temperature as were those being discussed in this section; whereas those concerned with nitrogen alone were conducted with the use of a different type of reactor (one-liter growth units), a different light source ("Optima" fluorescent lamps), and at a slightly higher temperature (28.5°C). These experiments concerned with nitrogen alone had to be conducted with the use of the one-liter growth units because they had to be done under conditions of light saturation, and as such had to be subjected to conditions more rigidly controlled than would have been possible with the use of the algatron. Moreover, the high intensity of the light source used in the algatron would have exerted a significant inhibitory effect on algal growth in the dilute cultures used in the experiments. As this inhibition is insignificant in optically dense cultures, the algatron could be used without disadvantage in the experiments concerned with nitrogen in dense cultures.

As shown by the curves in Figure 49 and the data listed in Table V, when the NO_3-N concentration approached 5 mg/ℓ, algal net production of the 9.7-liter reactor exceeded 23 grams/day at dilution rates slightly greater than 0.9 day^{-1}. These results approximate those obtained in the experiments concerned with light in which the concentration of nutrients was maintained at an optimum level (cf. Figures 36, 37, and 38). At concentrations of nitrogen ranging from 2 to 5 mg/ℓ, net algal production P_n (as well as P_{nv}) declined gradually. The decrease became abrupt as the nitrogen concentration approached 1 mg/ℓ. At nitrogen concentrations less than 1 mg/ℓ, not only was growth drastically reduced but also the chlorophyll level dropped below 1% and the culture deteriorated, as evidenced by the yellowish cast assumed by the culture. "Cell age" became an important factor in the experiments in which the nitrogen concentration was kept at a low level and detention periods were long. For all practical purposes, growth ceased when the nitrogen concentration fell below 0.3 mg/ℓ.

The results obtained in the experiments with the algatron growth unit cannot be used to evaluate the theoretical approach proposed in Chapter V (cf. Figure 16). According to the simplified theory, nitrogen would be limiting in that cross section of the culture which is sufficiently close to the light source with a high level of light intensity; whereas in the deeper layers, i.e., those farther removed from the light source, light intensity is reduced and consequently light replaces nitrogen as the limiting factor. According to theory, at those concentrations at which nitrogen begins to become limiting, the limiting effect will be manifested only in the well-illuminated (upper) layers; whereas those same concentrations would not be limiting in the deeper layers because their growth already has been limited by lack of light. The theory could be neither proved nor disproved on the basis of results obtained in the algatron because the depth of the culture was not uniform throughout, and the incident irradiance (I_o) varied with the geometry of the culture – as would be expected with a single light source.

Comparison With the Experiment on Growth as a Function of NO_3-N Under Light Saturation (Experiment 3)

Considering the slight difference in temperature (28.5°C and 27°C) between the two experiments and the fact that the reactor was not the same, the significant difference in the results of the two experiments appears noteworthy. A comparison of the curves in Figure 43 (Experiment 3 – Light Saturation) and those in Figure 49(A) (see also Tables IV and V) shows that at equal NO_3-N concentration the average net specific growth rate $\bar{\mu}_n$ in the optically dense culture is less than half the net specific growth rate μ_n observed in Experiment 3 at light saturation. The difference indicates that both nitrogen and light were limiting factors in optically dense culture.

TABLE V

SUMMARY OF EXPERIMENTAL RESULTS ATTAINED WITH AN OPTICALLY DENSE CULTURE IN WHICH NITROGEN WAS LIMITING

S_{N_1}[a] mg/ℓ as N	Q/V or $\bar{\mu}_n$ day^{-1}	P_n g/day	P_{nv} g/liter-day	Chl. %	q day^{-1}	Y
0.11	0.021	0.55	0.06	0.3	0.001	17.20
0.27	0.034	0.88	0.09	0.1	0.002	17.75
0.58	0.146	3.80	0.39		0.009	16.02
0.83	0.115	3.00	0.31	0.5	0.007	16.26
0.92	0.232	6.04	0.62	1.0	0.015	15.03
1.18	0.447	11.62	1.20	1.5	0.033	13.02
1.30	0.552	14.35	1.48	2.3	0.047	11.47
1.80	0.708	18.40	1.90	2.1	0.056	12.18
2.16	0.754	19.62	2.02	1.8	0.062	11.82
2.86	0.808	21.00	2.16	2.5	0.065	12.03
3.50	0.854	22.20	2.29	3.6	0.070	11.91
4.87	0.865	22.50	2.32	3.9	0.074	11.42
5.25	0.892	23.20	2.39	2.5	0.073	11.90
6.93	0.885	23.00	2.37	4.4	0.075	11.51
8.48	0.910	23.65	2.44	3.3	0.081	10.89
9.72	0.912	23.70	2.44	3.0	0.079	11.22

[a] See Glossary and text for definition of terms.

The hyperbolic relationship between the net specific growth rates (μ_n and $\bar{\mu}_n$) and S_{N_1} prevailed generally in both experiments. The fact that the data in Figure 43 (Experiment 3 — Light Saturation) are relatively scattered compared to those in Figure 49(A)(optically dense culture) appears to be due to the low concentrations, the smaller culture volume, and the higher degree of sensitivity of the turbidostatic and chemostatic controls in Experiment 3.

The broken line curve in Figure 49(A) is the result of an attempt to draw a curve for the modified exponential function (Equation 4-14) on the basis of the experimental results by using that value for K_A which corresponds to 0.632 $\bar{\mu}_n$. The value of K_A was found to be 1.46 mg/ℓ as N. The agreement between the curve for the experimental data [solid line in Figure 49(A)] and that for the modified exponential function (broken line) was fairly close so long as S_{N_1} was greater than 1 mg/ℓ. At S_{N_1} values less than 1 mg/ℓ, there was some disparity between the shapes of the two

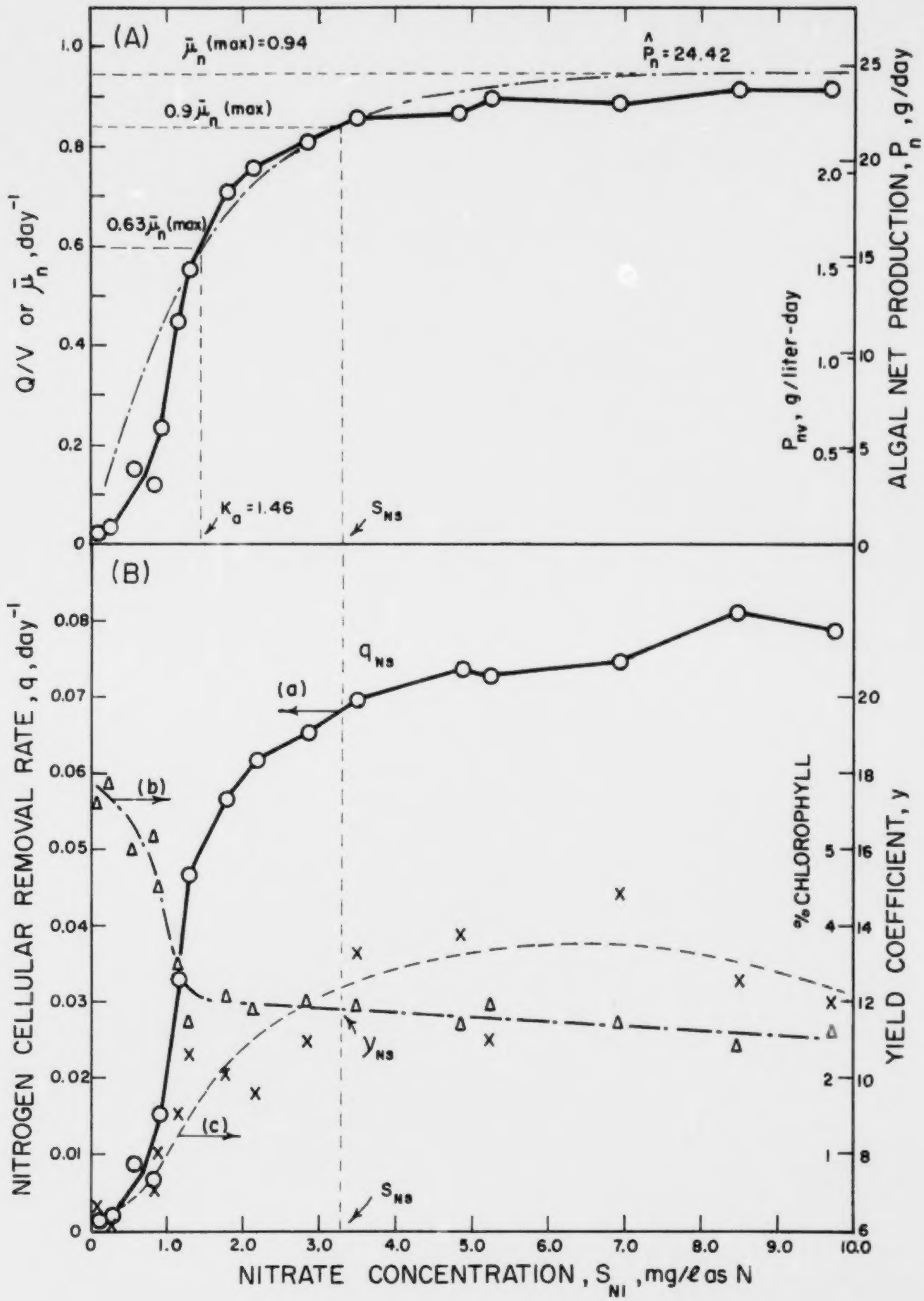

FIGURE 49. NITROGEN CONCENTRATION AS A GROWTH-LIMITING FACTOR IN AN OPTICALLY DENSE CULTURE

curves. The value estimated for K_A in this experiment did not differ greatly from that for K_A in Experiment 3 (Light Saturation). Depending upon the method of data analysis, K_A in Experiment 3 varied 1.23 to 2.05 mg/ℓ as N.

The similarity between the K_A for the two conditions, viz., light saturation and optically dense culture (i.e., light limiting), could cast some doubt as to the validity of the theoretical approach described in Chapter V. According to the theory, the influence of nitrogen as a growth-limiting factor in the deeper layers of the culture should have been decreased by the increasing influence of light as a "co-limiting" factor. If this had been the case, the value for K_A for the optically dense culture would have been lower than that for the culture at light saturation. In the latter situation nitrogen would be the sole growth limiting factor. However, because the observed value of K_A is midway between the two estimated values for the K_A for Experiment 3, no firm conclusion can be drawn concerning the validity of the proposed theoretical approach.

Although the curve based in Equation 4-14 did not fit well the experimental data at the lower values of S_{N_1}, it did fit the experimental data rather well at higher values of S_{N_1}, at which the average net specific growth rate and the net algal production approach their maxima. Moreover, the value of K_A based on this portion of the curve was not significantly different from that for conditions of light saturation. Therefore, it is convenient to describe the relationship between μ_n, P_n, and P_{nv} with respect to S_{N_1} as follows:

$$\bar{\mu}_n' = \bar{\mu}_{n(max)} \left(1 - e^{-S_{N_1}/K_A} \right) \qquad (7\text{-}18)$$

and

$$P_n' = \hat{P}_n \left(1 - e^{-S_{N_1}/K_A} \right) \qquad (7\text{-}19)$$

in which $\bar{\mu}_n'$ and P_n' are respectively the average net specific growth rate and net algal production in an optically dense culture in which nitrogen and irradiance are limiting factors. In this case, both $\bar{\mu}_n'$ and P_n' are functions of S_{N_1} as well as of I_o.

Equations 7-18 and 7-19 are based on an empirical best fit method. However they are applicable only in those situations in which S_{N_1} is above a certain minimum level.

According to Figure 49(A) the empirical approach appears applicable in the range of concentrations which corresponds to $\bar{\mu}_n$, P_{nv}, and P_n values equivalent to more than 50% of their maximum values. This is the range in which most algal systems for biomass production will be operated. Such systems include protein production, life support systems, photosynthetic oxygenation, and nutrient removal systems in which the requirement regarding the quality of the effluent are moderate and when algal biomass production is essential for economical reasons.

Nitrogen cellular removal rate, q, expressed as units of day^{-1} (Equations 4-4 and 4-7) and yield coefficient (on the basis of nitrogen removal, as functions of S_{N_1}) are shown in Figure 49(B) and the data pertaining to the two parameters are listed in Table V. Numerical values were determined by making nitrogen materials balances on the system, i.e., by measuring S_{N_O}, S_{N_1}, and N_c. At nitrogen concentrations less than 1 mg/ℓ, a range of nitrogen starvation as far as C. pyrenoidosa is concerned, the value of Y began to increase, the chlorophyll concentration decreased, and the culture in general began to deteriorate. The increase in Y, which corresponded to a decrease in cellular nitrogen content, was not as sharp as that in Experiment 3 (under light saturation) and the absolute values were slightly lower. Nevertheless, the information is not sufficient to permit a proposal of a particular mathematical formula to describe the function of $Y(S_{N1})$. Thus, q is not directly proportional to $\bar{\mu}_n$ as apparently is the case in bacterial growth [136]. According to Equation 4-7

$$q = \frac{\bar{\mu}_n\ (S_{N1})}{Y\ (S_{N1})}$$

and not enough data are available to determine the general function $q(S_{N1})$. The value of Y varies slightly with S_{N1} (i.e., 11-12) at values of S_{N1} greater than 1.5 mg/ℓ; thus, it may be regarded as a constant for all practical purposes at these concentrations. An estimate of $\bar{\mu}_n(S_{N1})$ can be made according to Equation 7-18 only when the value of S_{N1} is above a certain minimum; therefore it may be concluded that for levels of S_{N1} greater than K_A, the following equation would apply:

$$q = \frac{\bar{\mu}_{n(max)}}{Y}\left(1 - e^{-S_{N1}/K_A}\right) . \qquad (7\text{-}20)$$

Equation 7-20 is approximately the equivalent of Equation 4-19. The value of K_A expressed in mg/ℓ as N, designated as the lower limit for the applicability of Equation 7-20, was selected arbitrarily. A lower limit of applicability could have been set, as for example 0.8 K_A, or any other value at which Y becomes a constant and $\bar{\mu}_n(S_{N1})$ is known.

According to the experimental results, S_{NS} is equal to 3.32 mg/ℓ as N. This is the assumed nitrogen concentration level in the effluent of a CSTR-type algal system in which the algal biomass production is 90% of its maximum attainable level. Thus, at nitrogen concentrations existing in secondary waste treatment effluent (25 to 30 mg/ℓ), an 80% to 90% reduction in nitrogen through assimilation might be expected with an algal system. Any attempt at an additional increase in removal would result in a rather strong reduction in the growth and production of algae and in the nitrogen cellular removal rate, q, as is evident from inspection of Figure 49.

According to experimental results (cf. Figure 49 and Table V), the value of the dilution rate corresponding to 0.9 $\bar{\mu}_{n(max)}$ or 0.9 $\hat{P}_n$ is 0.84 day^{-1}, and q_{NS} and Y_{NS} are 0.068 day^{-1} and 11.9, respectively.

Algal Systems Designed for Assimilative Removal of Nutrients

It is assumed that most practical systems intended for assimilative removal of nutrients would be designed to permit the net algal production to approach its maximum potential. The reason for this requirement is that total mass of the nutrient removed is a function of the mass of algae produced, and that the recovery of the algal biomass is a decisive economical factor in determining the practical feasibility of such a system. A net production which would meet this requirement could be attained only in a relatively optically dense culture in which both light and nitrogen were limiting.

As mentioned previously, the nitrogen concentration in the reactor of S_{NS} must be selected in order to maintain nearly maximum algal growth production and cellular nitrogen removal rates and at the same time permit a reasonably low effluent concentration.

The following steps are part of a simplified method for designing an algal system for the assimilative removal of nitrogen from water having an initial NO_3-N concentration S_{No}, and which involves a CSTR operating at steady state without recycle.

a. The interrelationship between $(C_c d)$, P_n, and Q/V can be established for a range of assumed values of $(C_c d)$ by using Model III and information available on irradiance and spectral distribution. This interrelationship can be plotted in a manner similar to that shown in Figures 33 through 38. Having determined the value of $\hat{P}_n$ in this manner, those for the Q/V, θ, and $(C_c d)$ which correspond to $\hat{P}_n$ can then be used in the design of the desired system.

b. Having determined the value for K_A through experimentation in which light was maintained at saturation, the value for S_{NS} can be determined with the use of Equation 7-19 as follows:

$$S_{NS} = K_A \ \ln\left(\frac{\hat{P}_n}{\hat{P}_n - P_n'}\right) \ ; \qquad (7\text{-}21)$$

with $P_n'/\hat{P}_n = 0.9$,

$$S_{NS} = 2.3 \ K_A \quad . \qquad (7\text{-}22)$$

c. Y can be assumed to be a constant at nitrogen concentrations approximating S_{NS}. (For C. pyrenoidosa, it ranges from 11.0 to 12.5 mg/ℓ of algae produced per mg of nitrogen removed.) The value for C_c in a nonrecycled system can be estimated according to the relationship

$$C_c = (S_{No} - S_{NS}) \ Y \ . \qquad (7\text{-}23)$$

The depth (d) is determined from the product $(C_c d)$ which corresponds to $\hat{P}_n$. The value for q is determined as follows:

$$q = \frac{S_{No} - S_{NS}}{C_c \theta} \quad . \qquad (7\text{-}24)$$

The hydraulic surface loading to be applied is equal to d/θ. The efficiency of nitrogen removal is $S_{No} - S_{NS}/S_{No}$.

To simplify the method, $0.9 \ \hat{P}_n$ is used because of an imposed nitrogen limitation, even though the computed values for $(C_c d)$, Q/V and θ correspond to $\hat{P}_n$. However, using the expedient does not materially affect the accuracy of the method. The method however cannot be used in situations in which S_{N_1} is much lower than S_{NS}.

VIII. CONCLUSIONS

GENERAL CONCLUSIONS

The response of algal systems to various growth-limiting factors can be determined at steady state with continuous-flow algal culture systems. By the use of kinetic models it is possible to evaluate the model and to determine the magnitude of rate constants in the laboratory. The availability of suitable kinetic models and reasonable estimates of the appropriate rate constant permits a rational approach to the design and performance predictions of algal systems.

SPECIFIC CONCLUSIONS

Kinetic Models with Respect to Light Intensity (Irradiance)

Several models which describe the relationship between irradiance and algal growth and production were developed and evaluated. The models incorporated the spectral distribution of the light source as it affects certain essential parameters, viz., thermodynamic quantum conversion and light transmission in an optically dense algal suspension. Each of the models represents the interrelationship existing at steady state conditions between dilution rate, associated algal concentration, and the expected average net specific growth rate and net algal production at a given incident irradiance. The condition which permits algal growth and production at their maximum level can be estimated analytically.

Of the three models developed, the macroscopic model based on the exponential relationship between irradiance and specific growth rate at the microscopic level, (Model III), proved to be the most compatible with the experimental results. Its general formula is:

$$P_{na_3} = E_m' \, I_s \left[\alpha_t \, C_c \, d + E_i \left(\frac{I_o}{I_s} \right) - E_i \left(\frac{I_d}{I_s} \right) \right] - 10^{-3} \, K_d \, C_c \, d \quad . \qquad (8\text{-}1)$$

The net algal production per unit of illuminated culture surface, P_{na_3}, is a function of the thermodynamic light conversion efficiency, E_m'; the light saturation intensity, I_s; the total extinction coefficient, α_t; the algal concentration, C_c; the culture depth, d; and the exponential integral function, E_i, of the ratio between the incident irradiance, I_o, and the transmitted light, I_d, and the light saturation intensity, I_s. A decay rate constant, K_d, is assumed to account for losses caused by endogenous respiration.

The model was found to be applicable for specific ranges of growth rates and algal concentrations. Within the range of growth rates of 1.7 day^{-1} to 0.6 day^{-1} and algal concentrations between 300 and 3000 mg/ℓ, the differences between the values of algal net production predicted by the model and those observed experimentally were less than 10%.

The model was not applicable to dilute algal systems in which a major part of the light is not absorbed by the culture or to situations in which the dilution rates are very low and the concentration of algae reaches very high values.

On the basis of input information on irradiance, spectral distribution, and light transmission by the algal suspension, the model can predict the maximum net production of an algal system. Moreover, estimates can be made of the desired growth rates and the algal concentrations that determine maximum algal net production. A computerized form of the above model was programmed and is given in Appendix H.

Kinetic Model with Respect to Nitrogen Concentration

The modified exponential function appeared to describe best the relationship between the net specific growth rate μ_n, and the NO_3-N concentration, S_{N1}. This function can be written as follows:

$$\mu_n = \hat{\mu}_n \left(1 - e^{-S_{N1}/K_A}\right) \quad . \tag{8-2}$$

The parameter K_A which is equivalent to S_{N1} corresponding to 0.63 of the maximum net specific growth rate, $\hat{\mu}_n$, was adequate to describe the function. Values of K_A were found to range between 1.0 to 2.0 mg/ℓ as N under laboratory conditions. This is a rather high value if compared to algae species indigenous to natural bodies of water. This is likely due to the fact that the strains of C. pyrenoidosa used as the experimental organisms are adapted to relatively rich media.

The relationship between growth and nitrogen concentrations at the very low levels of nitrogen was not clearly defined. However, the relatively strong and rather abrupt drop in net specific growth rate which occurred in the range of concentrations of "nitrogen starvation," supports the principle of controlling algal blooms by keeping the nutrient concentration below a certain level.

The yield coefficient on the basis of nitrogen removal Y was found to vary substantially with the nitrogen concentration S_{N1}.

A sharp increase in Y occurred at low nitrogen concentration levels. At NO_3-N concentrations which limit the specific growth rate to less than one-fourth of its maximum value, i.e., $\mu_n < \hat{\mu}_n/4$, the yield coefficient increased to values as much as 20 mg of algae produced per mg of nitrogen removed. At NO_3-N concentrations which correspond to $\mu_n \geq \hat{\mu}_n/2$, the value of Y approached a constant value of between 11 to 13.

The values of the parameter S_{NS}, which was defined as S_{N1} corresponding to $\mu_n = 0.9\ \hat{\mu}_n$, ranged under ambient temperature conditions between 1.5 and 4 mg/ℓ as N. These values indicate the general range of expected nitrogen concentration levels in the effluent of CSTR-type algal systems in which algal growth is approaching its maximum levels.

A marked effect of temperature on the relationship between algal specific growth rate and NO_3-N concentration and on the various growth parameters was evident. The nitrogen concentration required to maintain a given value of net specific growth rate was lowest at 35°C. A considerably higher NO_3-N concentration was required to maintain the growth of the thermotolerant TX 71105 strain of C. pyrenoidosa at its optimum temperature of 39°C as compared to 35°C.

Kinetic Model with Respect to Both Light and Nitrogen

A semiempirical approach is suggested for the application of the modified exponential function to optically dense culture based upon laboratory results at light saturation conditions. It was found that such functions can describe the relationship between average net specific growth rate or net algal production and nitrogen concentration in a dense culture in which both light and nitrogen are growth-limiting. The average net specific growth rate $\bar{\mu}_n'$ and the net algal production P_n' in an optically dense culture in which both nitrogen and irradiance are limiting factors can be determined by the following equations:

$$\bar{\mu}_n' = \bar{\mu}_{n(max)} \left(1 - e^{-S_N/K_A}\right) \quad (8\text{-}3)$$

and

$$P_n' = \hat{P}_n \left(1 - e^{-S_{N1}/K_A}\right) \quad . \quad (8\text{-}4)$$

K_A can be assumed equal to the value of K_A as determined under conditions of light saturation in which nitrogen is the sole limiting factor. Then $\bar{\mu}_{n(max)}$ and $\hat{P}_n$ can be determined by using the model based on irradiance as described in Equation 8-1.

The applicability of Equations 8-3 and 8-4 is limited to the intermediate and higher levels of nitrogen concentration. As a matter of convenience, the range of its applicability might be given as being above 0.8 K_A.

The use of S_{NS} for S_{N1} in Equations 8-3 and 8-4 makes it possible to simplify the model for the design and performance predictions of algal systems directed at both nutrient removal and biomass production.

The value of S_{NS} was found to be 3.12 mg/ℓ as N which indicates that an effluent of only moderately low concentration of nitrogen can be expected in CSTR-type algal systems in which algal production approaches its maximum level. It can be concluded that only 80%–90% nitrogen reduction can be expected from such a system if the incoming nitrogen concentrations are 25–30 mg/ℓ as N (which are concentrations common in secondary waste effluents). Attempts to significantly reduce the value of S_{N1} in the CSTR-type algal system below S_{NS} would result in a rather sharp decrease in algal net production and in the nitrogen cellular removal rate.

IX. RECOMMENDATIONS

GENERAL

1. The kinetic approach should be used in algal research involving the use of continuous cultures in the study of light intensity, macro- and micro-nutrient concentrations, and other variables.

2. The growth rate of algal species indigenous to natural bodies of water should be investigated with respect to low nutrient concentration.

3. Algal systems based on biomass production such as those used in waste treatment should be designed rationally with due regard to the basic parameters of biological process. Examples of such parameters are specific growth rate, biomass concentration, and the kinetic relationship between growth-limiting factors and biomass propagation.

SPECIFIC

1. A major research effort should be made to establish a satisfactory parameter for algal decay. Rate of endogenous respiration and "decay" by primary algal decomposers and herbivors are essential parameters in arriving at materials balance and quantitative evaluation of algal systems. Effects of light intensity, prolonged darkness, and mean "cell age" on decay rate, and specifically on endogenous respiration, are of prime importance.

2. The adverse effect of excessive propinquity (crowdedness) on algal net production should be investigated. The adverse effect is manifested in a concentration of algae lower than that to be expected at high light intensities.

3. Information should be obtained on the relationship between bacterial and algal populations in algal systems functioning under either controlled and/or natural conditions. Such information is needed for the determination and evaluation of possible symbiotic or antagonistic relations between the two populations. It also is needed for determining the existence and extent of competition between the two populations for available nutrients.

4. Additional research should be conducted on the growth and activity of algal populations in situations in which nutrient concentration is low ("starvation" conditions). Specifically, the growth rate, yield coefficients, and cellular nitrogen content of Chlorella as functions of very low nitrogen concentrations should receive attention. Establishing the function $Y(S_{N_1})$ would lead to an improvement in the kinetic model for algal growth and rate of the assimilative removal of nitrogen as functions of nitrogen concentration.

5. A practical and inexpensive turbidostatic control should be developed for continuous cultures of algae. With the use of a turbidostatic control, maximum efficiency, savings in time, and a high degree of control could be attained in the conduct of experiments involving continuous algal cultures.

APPENDICES

- A. NITRATE MEDIUM
- B. REMARKS ON THE EFFECT OF AUTOCATALYSIS ON THE ORDER OF REACTION IN MICROBIAL PROPAGATION AS COMPARED TO CHEMICAL REACTIONS
- C. THE RECTANGULAR HYPERBOLA FUNCTION AS IT APPLIES TO VARIOUS KINETIC MODELS OF MICROBIAL PROPAGATIONS
- D. THE MATHEMATICAL DEVELOPMENT OF MACROSCOPIC MODEL II
- E. THE MATHEMATICAL DEVELOPMENT OF MACROSCOPIC MODEL III
- F. LIGHT SOURCES
- G. LIGHT TRANSMITTANCE OF VARIOUS FILTERS
- H. COMPUTER PROGRAMS
- I. GLOSSARY

Preceding page blank

APPENDIX A

NITRATE MEDIUM

Myers' nitrate medium is a medium commonly used in practice for the continuous type of algal culture on a laboratory scale. In the experiments reported herein Myers' medium was somewhat modified with respect to chelation of iron and concentration and composition of micronutrients [145]. The formula of the modified Myers' medium is given in Table VI, and that of the micronutrient stock solution, in Table VII.

As was discussed in the text (cf. Chapter VI), the initial low pH level of the modified Myers' medium resulted in prolonged lag period in the growth of algae, thus a further and final modification of the modified Myers' medium had to be made. This was the medium used in the main part of the present investigation. The nitrate medium was then designated as SERL nitrate medium, and its formula is given in Table VIII, and its titration curves along with those of the original medium in Figure 50.

TABLE VI

COMPOSITION OF MODIFIED MYERS' NITRATE MEDIUM

Nutrient	Molar Concentration in Media moles/liter	Preparation	
		Stock Solution moles/liter	Amount ml/liter
KNO_3[a]	$1.2\text{-}3.6 \times 10^{-2}$	1.0	12.0-36.0
KH_2PO_4	0.9×10^{-2}	1.0	9.0
$MgSO_4 \cdot 7H_2O$	1.0×10^{-2}	1.0	10.0
Fe Versenol 120	1.74×10^{-4}	1.0	1.74
Micronutrients	(See Table VII)	(See Table VII)	1.0
$Ca(NO_3)_2$	1.0×10^{-4}	1.0	0.1

[a] Nitrate concentrations vary according to the expected algal yields.

Preceding page blank

TABLE VII

FORMULA OF THE MODIFIED ARNON'S MICRONUTRIENT STOCK SOLUTION [145,161]

Nutrient	Molar Concentration in Media moles/liter	Preparation g/liter in stock solution
H_3BO_3	4.6×10^{-5}	2.86
$MnCl_2 \cdot 4H_2O$	9.2×10^{-7}	1.81
$ZnSO_4 \cdot 7H_2O$	7.7×10^{-7}	0.222
$CuSO_4 \cdot 5H_2O$	3.2×10^{-7}	0.079
MoO_3 (99.5%)	1.0×10^{-7}	0.015
$CoCl_2 \cdot 6H_2O$	1.7×10^{-7}	0.040

TABLE VIII

COMPOSITION OF SERL NITRATE MEDIUM

Nutrient	Molar Concentration in Media moles/liter	Preparation	
		Stock Solution moles/liter	Amount ml/liter
KNO_3[a]	$1.2\text{-}3.6 \times 10^{-2}$	1.0	12.0-36.0
KH_2PO_4	0.6×10^{-2}	1.0	6.0
K_2HPO_4	0.3×10^{-2}	1.0	3.0
$MgSO_4 \cdot 7H_2O$	1.0×10^{-2}	1.0	10.0
Fe Versenol 120	1.74×10^{-4}	0.1	1.74
Micronutrients	(See Table VII)		1.0
$Ca(NO_3)_2$	1.0×10^{-4}	1.0	0.1

[a] Nitrate concentrations vary according to the expected algal yields or experimental needs.

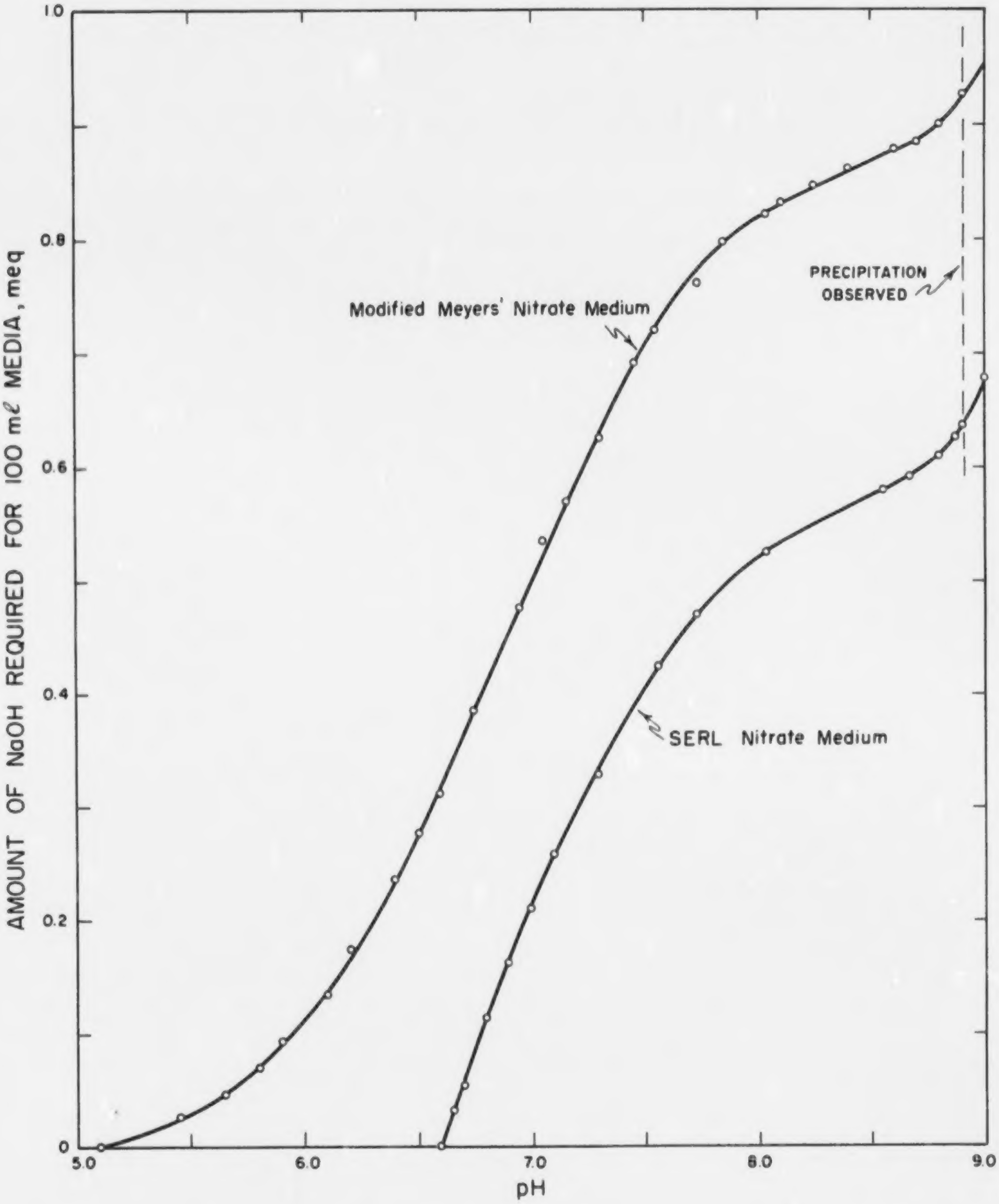

FIGURE 50. TITRATION CURVES OF MODIFIED MYERS' NITRATE MEDIUM AND SERL NITRATE MEDIUM

APPENDIX B

REMARKS ON THE EFFECT OF AUTOCATALYSIS ON THE ORDER OF REACTION IN MICROBIAL PROPAGATION AS COMPARED TO CHEMICAL REACTIONS

The order of reaction as it applies to microbial propagation in respect to growth and growth-limiting substrate can be analogous to the one used in chemical reactions. Thus, if substrate concentration is replaced by light intensity I, then

$$\frac{dC_c}{dt} = -K\frac{d[I]}{dt} \tag{B-1}$$

in which K denotes a light conversion biomass coefficient. Therefore,

$$\boxed{\mu = \frac{dC_c}{C_c\,dt} = \frac{-K\,d[I]}{C_c\,dt}} \quad . \tag{B-2}$$

For a first-order reaction,

$$-K\frac{d[I]}{dt} = k\,[I] \tag{B-3}$$

in which k denotes a constant. However, the "numerical value" of the order of the reaction in microbial propagation will be identical with that of chemical reaction only if the effect of autocatalysis is excluded. This can be done when the concentration of biomass is large enough relative to its change due to growth.

If autocatalysis is excluded and C_c does not change significantly within the particular time scale, then C_c can be regarded as a constant rather than a variable, and

$$-\frac{K}{C_c}\frac{d[I]}{dt} = \frac{k}{C_c}[I] \quad \text{(First-order reaction)} \quad . \tag{B-4}$$

Then from Equation B-2

$$\boxed{\mu = \frac{dC_c}{C_c\,dt} = k'[I]} \tag{B-5}$$

i.e., first-order reaction in respect to growth. On the other hand, if autocatalysis is included, and the relative change of the biomass concentration is significant within the particular time scale, then C_c becomes a variable with respect to time, and

$$-K \frac{d[I]}{dt} = k[I][C_c] \quad \text{(Second-order reaction)} \tag{B-6}$$

and

$$-K \frac{d[I]}{[C_c]\, dt} = k[I] \quad . \tag{B-7}$$

Then using Equation B-2,

$$\boxed{\mu = \frac{d[C_c]}{[C_c]\, dt} = k[I]} \tag{B-8}$$

i.e., first-order reaction with respect to growth as based on a second-order basic reaction.

A "zero-order" description of a nonautocatalytic microbial propagation in effect would be "first order" with respect to an autocatalytic microbial propagation, if one adheres to the meaning of the order of reaction as it is defined for chemical reactions. In describing a nonautocatalytic microbial propagation, C_c is regarded as a constant rather than a variable, and thus

$$-K \frac{d[I]}{dt} = k \quad \text{(Zero-order reaction)} \tag{B-9}$$

and

$$-\frac{K}{C_c} \frac{d[I]}{dt} = \frac{k}{C_c} \tag{B-10}$$

or, according to Equation B-2,

$$\boxed{\mu = \frac{dC_c}{C_c\, dt} = \frac{k}{C_c} = k'} \tag{B-11}$$

i.e., a zero-order reaction with regard to growth and $\mu = k'$. Applying an approach similar to the above to an autocatalytic microbial propagation,

$$-K \frac{d[I]}{dt} = k\ [C_c] \quad \text{(First-order reaction)}$$

and

$$\mu = \frac{d[C_c]}{[C_c]\, dt} = k \tag{B-12}$$

i.e., zero-order reaction with respect to growth based on a first-order basic reaction.

APPENDIX C

THE RECTANGULAR HYPERBOLA FUNCTION AS IT APPLIES TO VARIOUS KINETIC MODELS OF MICROBIAL PROPAGATIONS

BASIC MATHEMATICAL RELATIONSHIPS

Many biological phenomena can be described by the general hyperbolic relationship of the classical "diminishing return" form. This is particularly true with microbial propagations in respect to a growth-limiting factor and also in many cases with respect to time.

The basic hyperbolic equation stems from the general equation of the second degree which can be written as follows:

$$Ax^2 + Bxy + Cy^2 + Dx + Ey + F = 0 \qquad \text{(C-1)}$$

in the case of hyperbolas the following conditions should apply:

$$B^2 - 4AC > 0 \quad . \qquad \text{(C-2)}$$

In a case of a general hyperbola that crosses the origin of the axis y and x and reaches an asymptotic maximum at some value $y = \hat{y}$, it can be shown that Equation C-1 will be transformed to the following general equation:

$$Cy^2 + xy - \hat{y}x + Ky = 0 \qquad \text{(C-3)}$$

where C, $\hat{y}$, and K are the three constant parameters of the general hyperbola.

A simple case of the above hyperbola will be when C = 0 thus:

$$xy - \hat{y}x + Ky = 0 \qquad \text{(C-4)}$$

and

$$y = \frac{\hat{y}x}{K + x} \qquad \text{(C-5)}$$

in which K = x whenever $y = \hat{y}/2$.

Equation C-5 is a rectangular hyperbola and it is analogous to Equations 3-33, 3-34, 3-35, and 4-8.

A different approach to the mathematical definition of the rectangular hyperbola can be as follows: Equation C-1 and C-2 can be developed to a general equation of a hyperbola, namely

$$\frac{x^2}{a^2} - \frac{y^2}{b^2} = 1 \qquad \text{(C-6)}$$

where

$$b = \sqrt{c^2 - a^2} \quad ,$$

$$e = \frac{c}{a} > 1 \quad ,$$

and where a, b, and c are the three parameters of the hyperbola and e is the eccentricity.

It can be shown that in the case of a rectangular hyperbola which crosses the origin of the axis and is asymptotically limited by the line $y = \hat{y}$ which is parallel to the x-axis then $a = b$, $c = \sqrt{2}a$, $e = \sqrt{2}$, and the function has the following form

$$(x + K)\,(y - \hat{y}) = -\,\hat{y}\,K \tag{C-7}$$

which yields

$$y = \frac{\hat{y}x}{K + x} \quad \text{, i.e., Equation C-5} \quad .$$

ENZYME REACTION MECHANISMS BEST DESCRIBED BY THE RECTANGULAR HYPERBOLA FUNCTION

Although the general hyperbolic function can be used to describe many sorts of postulated enzyme reaction mechanisms, it is a rather complicated and inconvenient function. Its simpler form, the rectangular hyperbola, can nevertheless describe a few basic postulated enzyme reaction mechanisms as follows:

Enzyme-Substrate Reaction Mechanism Based On A Simple Surface-Controlled Reaction (Langmuir's Isotherm)

Assuming that the rate of enzyme-substrate complex formation d ES/dt is proportional to the concentration of the substrate [S] times the fraction of free enzyme absorbing sites $1 - \theta'$ while the rate of the destruction of the complex, i.e., the rate of substrate utilization, is proportional to the fraction of occupied enzyme sites, θ', then at steady state

$$k_1\,[S]\,(1 - \theta') = k_2\,\theta' \tag{C-8}$$

which can be transformed to

$$\theta' = \frac{[S]}{k_2/k_1 + [S]} \quad . \tag{C-9}$$

Since θ' is equal to the ratio between the substrate-enzyme complex ES and the total enzyme active surface E_t, then from Equation C-9

$$\frac{[ES]}{[E_t]} = \frac{[S]}{k_2/k_1 + [S]} \tag{C-10}$$

or

$$[ES] = \frac{[E_t][S]}{K + [S]} \quad . \tag{C-11}$$

Assuming that the specific growth rate μ is proportional to ES and the maximum specific growth rate (when $S \rightarrow \infty$) is proportional to E_t, then Equation C-11 yields the following:

$$\mu = \frac{\hat{\mu}\,[S]}{K + [S]} \tag{C-12}$$

which is a rectangular hyperbola similar to Equation C-5 when $\mu = y$ and $S = x$ and obviously Equation C-12 is analogous to Equations 2-34, 3-35, and 4-8.

A slightly different approach based on the dynamic description of a surface controlled reaction is presented by Parsons in his review [99] and it results in a similar expression as Equation C-12.

Consecutive Reaction Mechanism

The rectangular hyperbola can also describe the kinetic function of reaction mechanisms which are not necessarily surface controlled as in the case of photochemical reactions, consecutive chemical reactions, as well as reactions involving enzymes.

Assume the two consecutive reactions as follows

$$C + I \xrightarrow{k_1} C^* \tag{C-13}$$

$$C^* \xrightarrow{k_2} C + D \quad ; \tag{C-14}$$

assume further that reactions C-13 and C-14 are, respectivly, kinetically second- and first-order reactions. Then

$$\frac{d\,[C^*]}{dt} = k_1\,[C]\,[I] \tag{C-15}$$

and

$$-\frac{d\,[C^*]}{dt} = k_2\,[C^*] \tag{C-16}$$

and for the two consecutive reactions,

$$\frac{d\,[C^*]}{dt} = k_1\,[C]\,[I] - k_2\,[C^*] \quad . \tag{C-17}$$

At a steady state

$$\frac{d\,[C^*]}{dt} = k_1\,[C]\,[I] - k_2\,[C^*] = 0 \tag{C-18}$$

or, assuming

$$[C] + [C^*] = [C_t] \quad , \tag{C-19}$$

$$k_1\ [I] \left\{[C_t] - [C^*]\right\} - k_2\ [C^*] = 0 \quad . \tag{C-20}$$

Solving for $[C^*]$,

$$[C^*] = \frac{k_1\ [C_t]\ [I]}{k_2 + k_1\ [I]} \tag{C-21}$$

or

$$[C^*] = \frac{[C_t]\ [I]}{k_2/k_1 + [I]} \quad .$$

Assuming further that the specific growth rate μ is proportional to $[C^*]$ and its maximum value μ is proportional to $[C_t]$, and substituting K for k_2/k_1, then

$$\mu = \frac{\hat{\mu}\ [I]}{K + [I]} \quad , \tag{C-22}$$

which is exactly Equation C-12 if [I] is substituted by [S].

A closer look will show that the assumptions used in this approach are basically analogous to those used in the method given by Parsons [99] in the description of surface-controlled reactions.

APPENDIX D

THE MATHEMATICAL DEVELOPMENT OF MACROSCOPIC MODEL II

Equation 3-51 in Chapter III is

$$P_{a_2} = C_c \hat{\mu}_x \int_{x=0}^{d} \frac{I_o e^{-\alpha C_c x}}{I_s + I_o e^{-\alpha C_c x}} d x \quad . \tag{D-1}$$

Let

$$x' = \alpha x$$

$$d' = \alpha d$$

so that

$$P_{a_2} = C_c \hat{\mu}_x \int_{0}^{d'} \frac{I_o e^{-C_c x'}}{I_s + I_o e^{-C_c x'}} d x' \quad . \tag{D-2}$$

or

$$P_{a_2} = C_c \hat{\mu}_x \int_{0}^{d'} \frac{dx'}{1 + \frac{I_s}{I_o} e^{C_c x'}} \tag{D-3}$$

which may be evaluated by the integral formula [162]

$$\int \frac{dx}{a + b e^{px}} = \frac{x}{a} - \frac{1}{ap} \ln (a + b e^{px}) \quad ,$$

giving

$$P_{a_2} = C_c \hat{\mu}_x \left[x' - \frac{1}{C_c} \ln \left(1 + \frac{I_s}{I_o} e^{C_c x'} \right) \right]_{0}^{d'} \tag{D-4}$$

or

$$P_{a_2} = C_c\, \hat{\mu}_x \left[d' + \frac{1}{C_c} \ln \frac{1 + \frac{I_s}{I_o}}{1 + \frac{I_s}{I_o} e^{C_c d'}} \right]$$

$$= C_c\, \hat{\mu}_x \left[d' + \frac{1}{C_c} \ln \frac{I_o + I_s}{I_o + I_s e^{C_c d}} \right] \quad . \qquad \text{(D-5)}$$

Introducing $e^{-C_c d}$ as a multiplier in the last term,

$$P_{a_2} = C_c\, \hat{\mu}_x \left[d' + \frac{1}{C_c} \ln \frac{(I_o + I_s)\, e^{-C_c d'}}{I_s + I_o e^{-C_c d}} \right]$$

$$= C_c\, \hat{\mu}_x \left[d' + \frac{1}{C_c} \ln \frac{I_o + I_s}{I_s + I_o e^{-C_c d'}} + \frac{1}{C_c} \ln e^{-C_c d'} \right] \qquad \text{(D-6)}$$

$$= \hat{\mu}_x \ln \frac{I_s + I_o}{I_s + I_o e^{-C_c d'}} \quad . \qquad \text{(D-7)}$$

Substituting $d' = \alpha d$ and $\hat{\mu}_x = E_m' I_s$, we arrive at the basic equation of the Macroscopic Model II, namely,

$$\boxed{P_{a_2} = E_m' I_s \ln \frac{I_s + I_o}{I_s + I_o e^{-\alpha C_c d}}} \quad . \qquad \text{(3-72)}$$

APPENDIX E

THE MATHEMATICAL DEVELOPMENT OF MACROSCOPIC MODEL III

Equations 3-57 and 3-58 in Chapter II is

$$P_{a_3} = C_c \, \hat{\mu}_x \int_o^d \left(1 - e^{-(I_o/I_s) \, e^{-\alpha C_c x}} \right) dx \tag{E-1}$$

or

$$P_{a_3} = C_c \, \hat{\mu}_x \, d - C_c \, \hat{\mu}_x \int_o^d e^{-(I_o/I_s) \, e^{-\alpha C_c x}} \, dx \quad . \tag{E-2}$$

Let

$$t' = \frac{I_o}{I_s} e^{-\alpha C_c x} \tag{E-3}$$

so that

$$dt' = - \frac{I_o}{I_s} \alpha \, C_c \, e^{-\alpha C_c x} \, dx \tag{E-4}$$

and

$$dx = \frac{dt'}{\alpha \, C_c \, t'} \quad ; \tag{E-5}$$

then from Equation E-2,

$$\int_o^d e^{-(I_o/I_s) \, e^{-\alpha C_c x}} = \frac{1}{\alpha \, C_c} \int_{(I_o/I_s)}^{(I_o/I_s) \, e^{-\alpha C_c d}} \frac{e^{-t'}}{t'} \, dt' \quad . \tag{E-6}$$

Now,

$$\int_{I_o/I_s}^{\infty} \frac{e^{-t'}}{t'} \, dt' = E_1\left(\frac{I_o}{I_s}\right) \qquad \left(\left| \arg \frac{I_o}{I_s} \right| < \pi \right). \tag{E-7}$$

in which E_1 is the exponential integral which can be solved by performing the integration with the use of appropriate tables; or can be expressed by the following series [93]:

$$E_i\left(\frac{I_o}{I_s}\right) = -\gamma' - \ln\frac{I_o}{I_s} - \sum_{n=1}^{\infty}\frac{(-1)^n\,(I_o/I_s)^n}{n\;n!} \tag{E-8}$$

where γ' is the Euler Constant ($\gamma' = 0.5772\ \ldots$). Similar expressions can be applied to $E_i\left(I_o/I_s\; e^{-\alpha\, C_c\, d}\right)$. Thus, Equation E-6 becomes

$$\int_0^d e^{-(I_o/I_s)\, e^{-\alpha\, C_c\, x}} = \frac{1}{\alpha\, C_c}\left[E_i\left(\frac{I_o}{I_s}\, e^{-\alpha\, C_c\, d}\right) - E_i\left(\frac{I_o}{I_s}\right)\right], \tag{E-9}$$

and substituting this into Equation E-2, we find

$$P_{a_3} = C_c\, \hat{\mu}_x\, d - \hat{\mu}_x\, \frac{1}{\alpha}\left[E_i\left(\frac{I_o}{I_s}\, e^{-\alpha\, C_c\, d}\right) - E_i\left(\frac{I_o}{I_s}\right)\right]\ . \tag{E-10}$$

Substituting $E_m'\, I_s$ for $\hat{\mu}_x$ and rearranging we get then

$$\boxed{P_{a_3} = E_m'\, I_s\left[\alpha\, C_c\, d + E_i\left(\frac{I_o}{I_s}\right) - E_i\left(\frac{I_o}{I_s}\, e^{-\alpha\, C_c\, d}\right)\right]} \tag{E-11}$$

which is identical to Equation 3-59.

APPENDIX F

LIGHT SOURCES

TABLE IX

GENERAL CHARACTERISTICS OF THE LIGHT SOURCES USED IN THE STUDY

Commercial Name of Lamp	Type of Lamp	Power Input Watts	Lamp Code	No. of Lamps Used	Total Initial Lumens per Lamp	Color Temp. (approx.) K^o
Sylvania Iodine-Quartz	Tungsten Halogen	500	IQ 500	2	10,000	3000
G.E. "Lucalox"	High Temp. Sodium Vapor Arc	400	LX 400	1	42,000	
Duro-Test "Optima"	Full-Spectrum Fluorescent	30	FO 30	4		

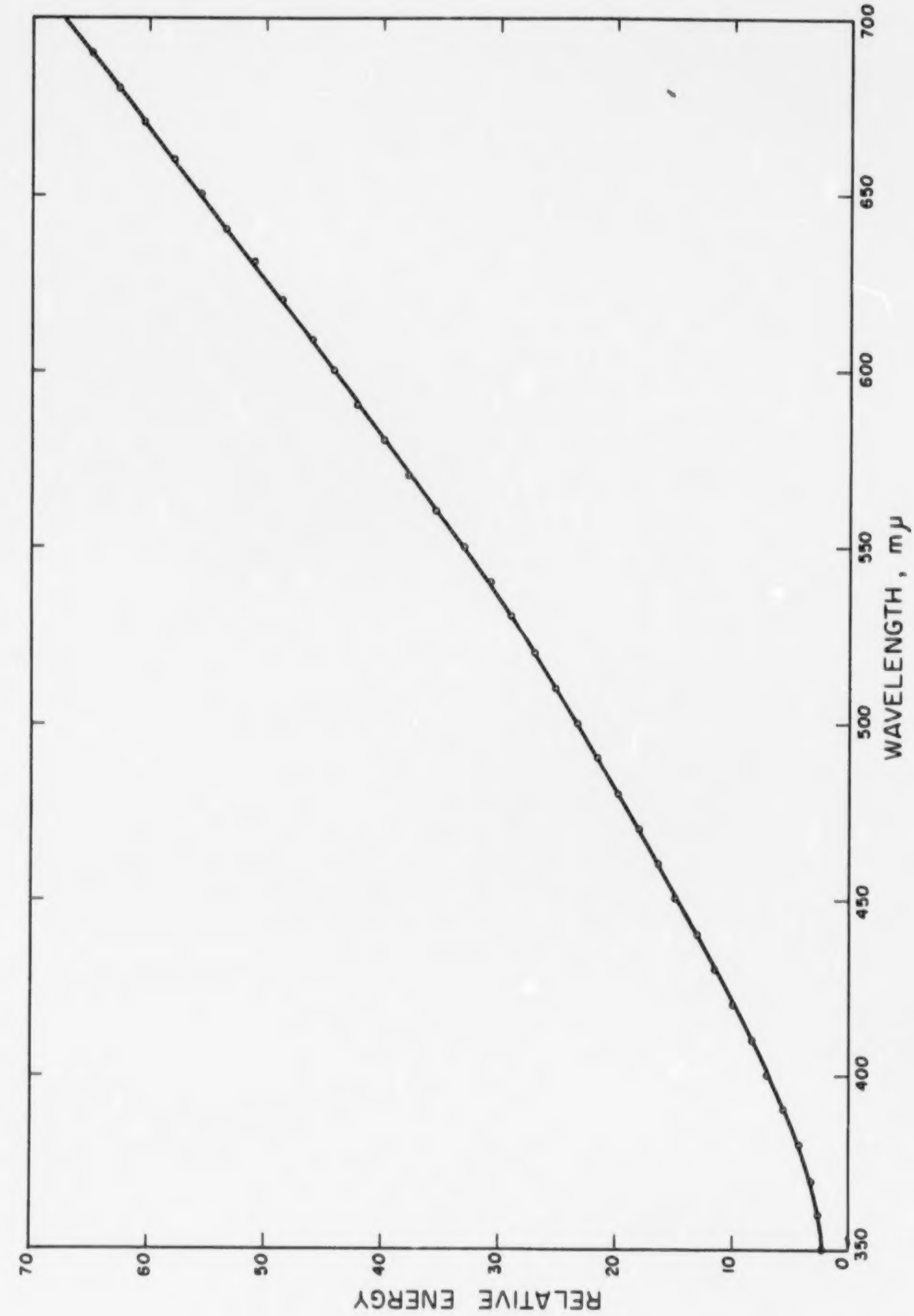

FIGURE 51. SPECTRAL ENERGY DISTRIBUTION OF IODINE-QUARTZ LAMP

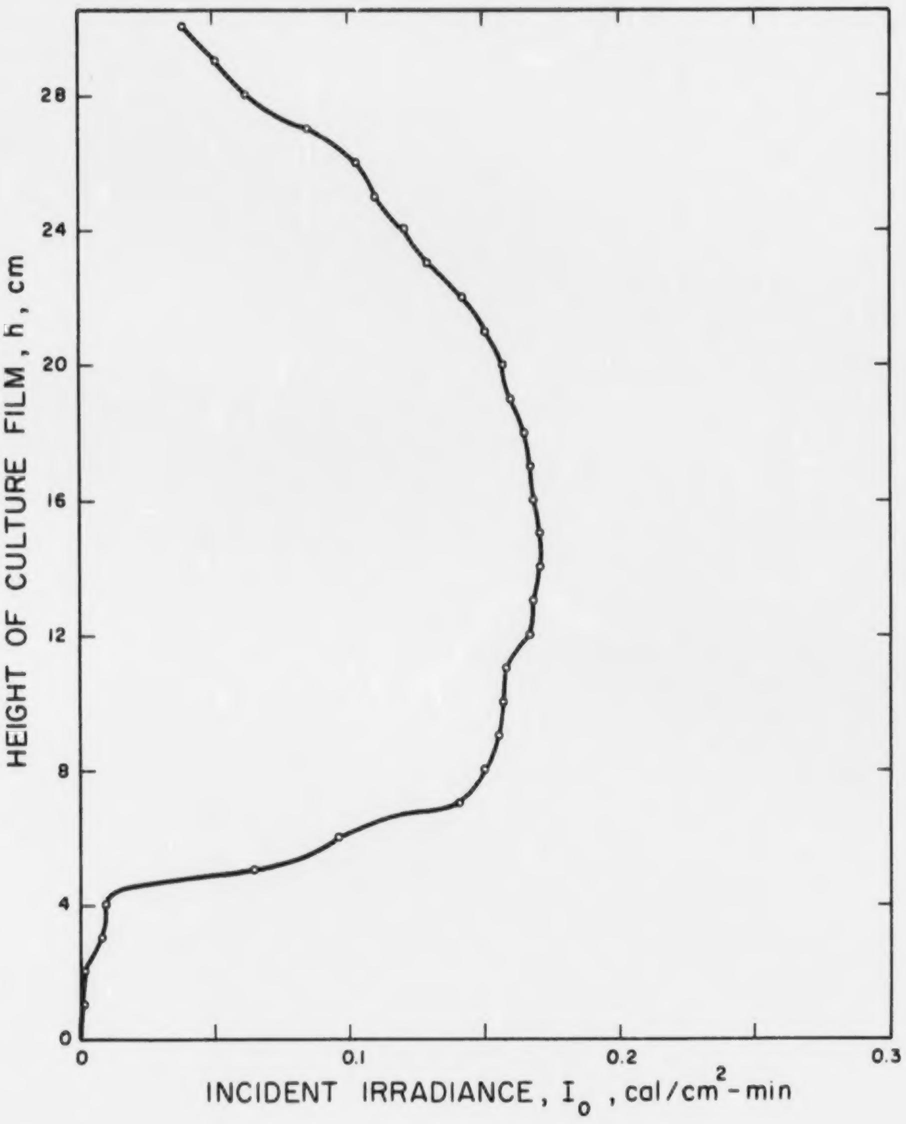

FIGURE 52. INCIDENT IRRADIANCE DISTRIBUTION AT CULTURE SURFACE – IODINE-QUARTZ LAMP

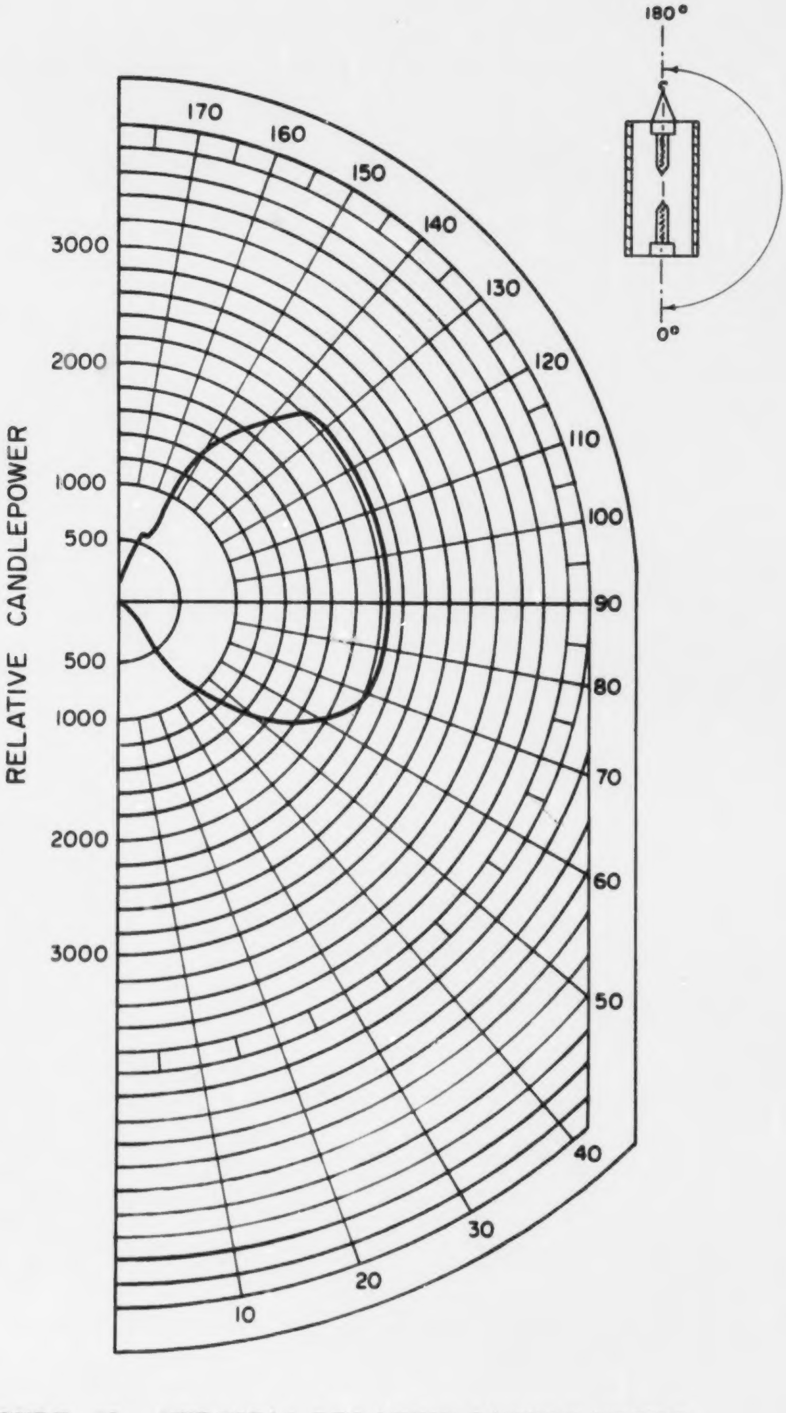

FIGURE 53. VERTICAL RELATIVE CANDLE POWER DISTRIBUTION OF IODINE-QUARTZ LAMPS (WITH WATER JACKET)

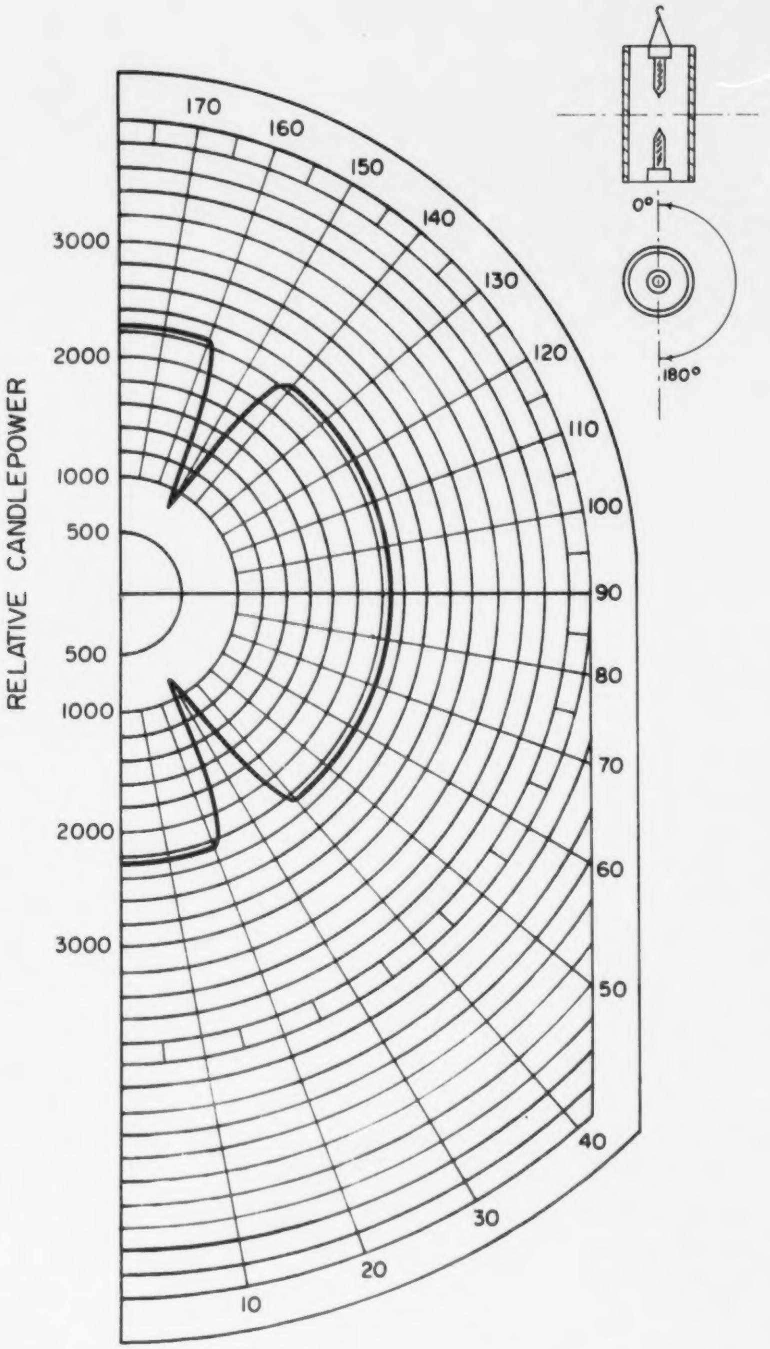

FIGURE 54. HORIZONTAL RELATIVE CANDLE POWER DISTRIBUTION OF IODINE–QUARTZ LAMPS (WITH WATER JACKET)

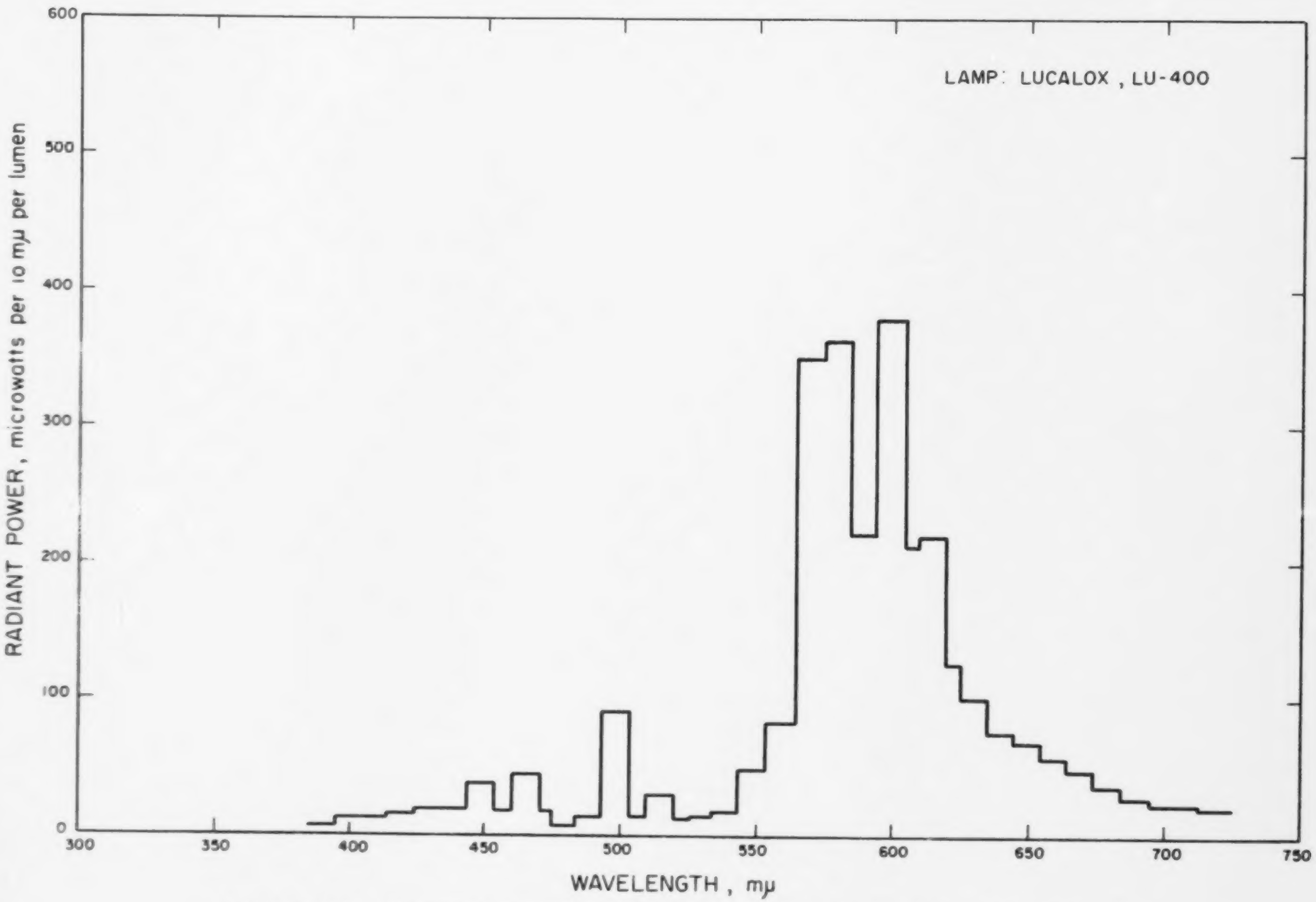

FIGURE 55. ENERGY SPECTRAL DISTRIBUTION OF THE LUCALOX LAMP

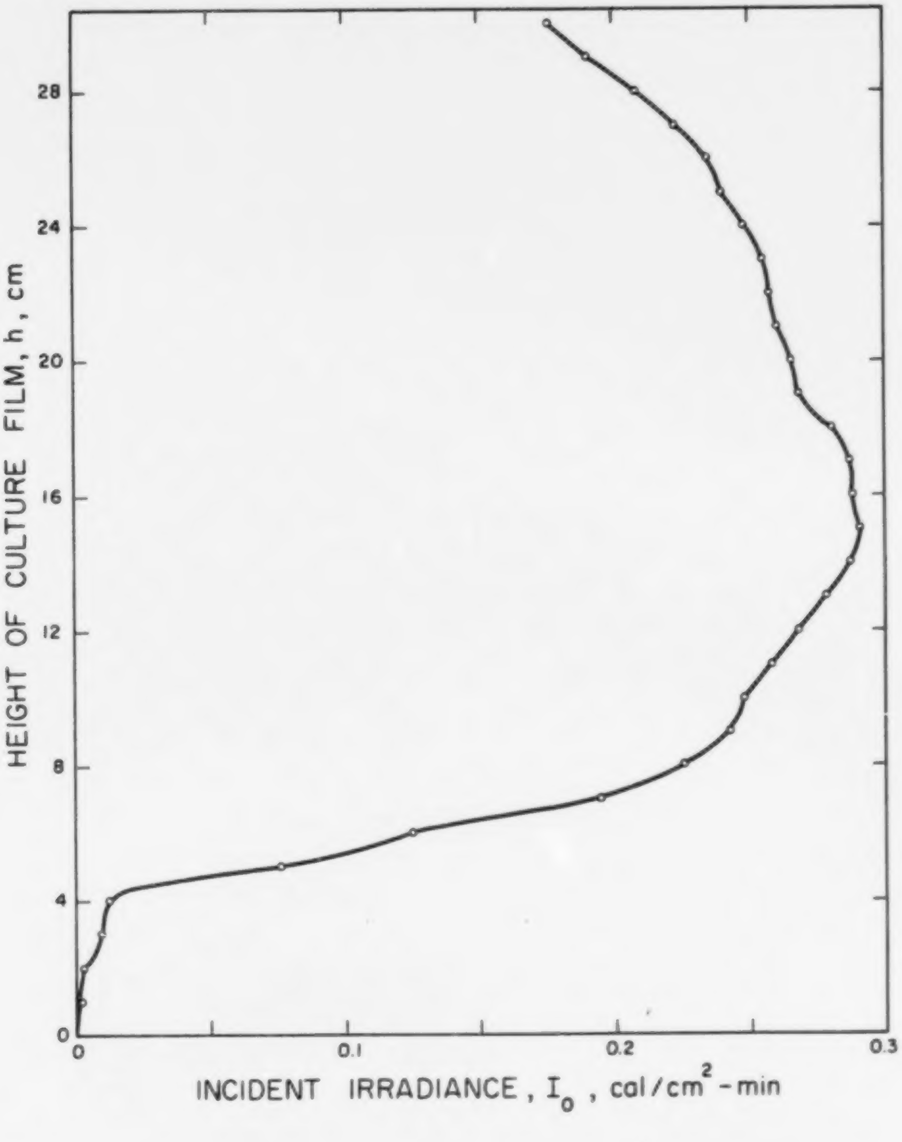

FIGURE 56. INCIDENT IRRADIANCE DISTRIBUTION AT CULTURE SURFACE – LUCALOX LAMP

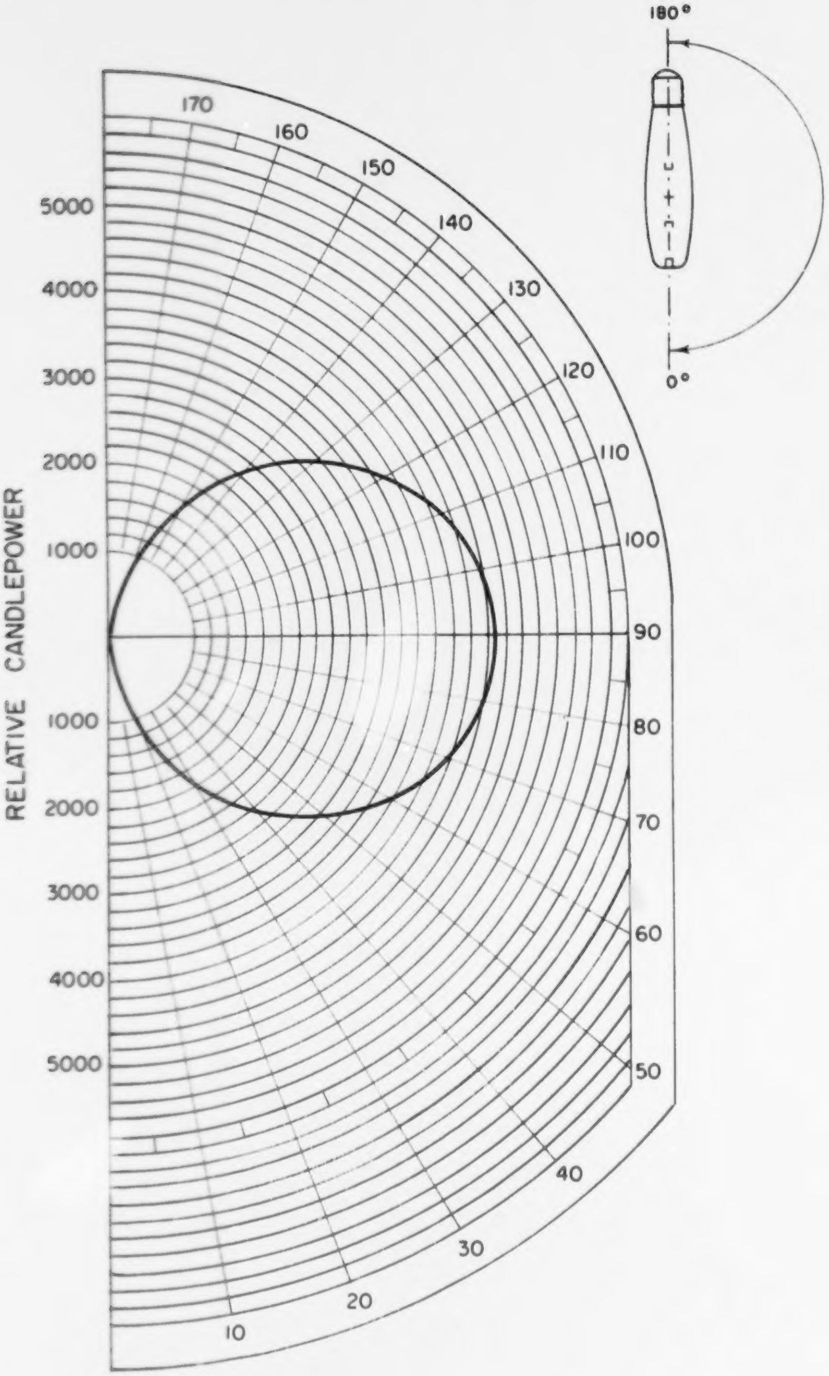

FIGURE 57. VERTICAL RELATIVE CANDLE POWER DISTRIBUTION OF THE LUCALOX LAMP

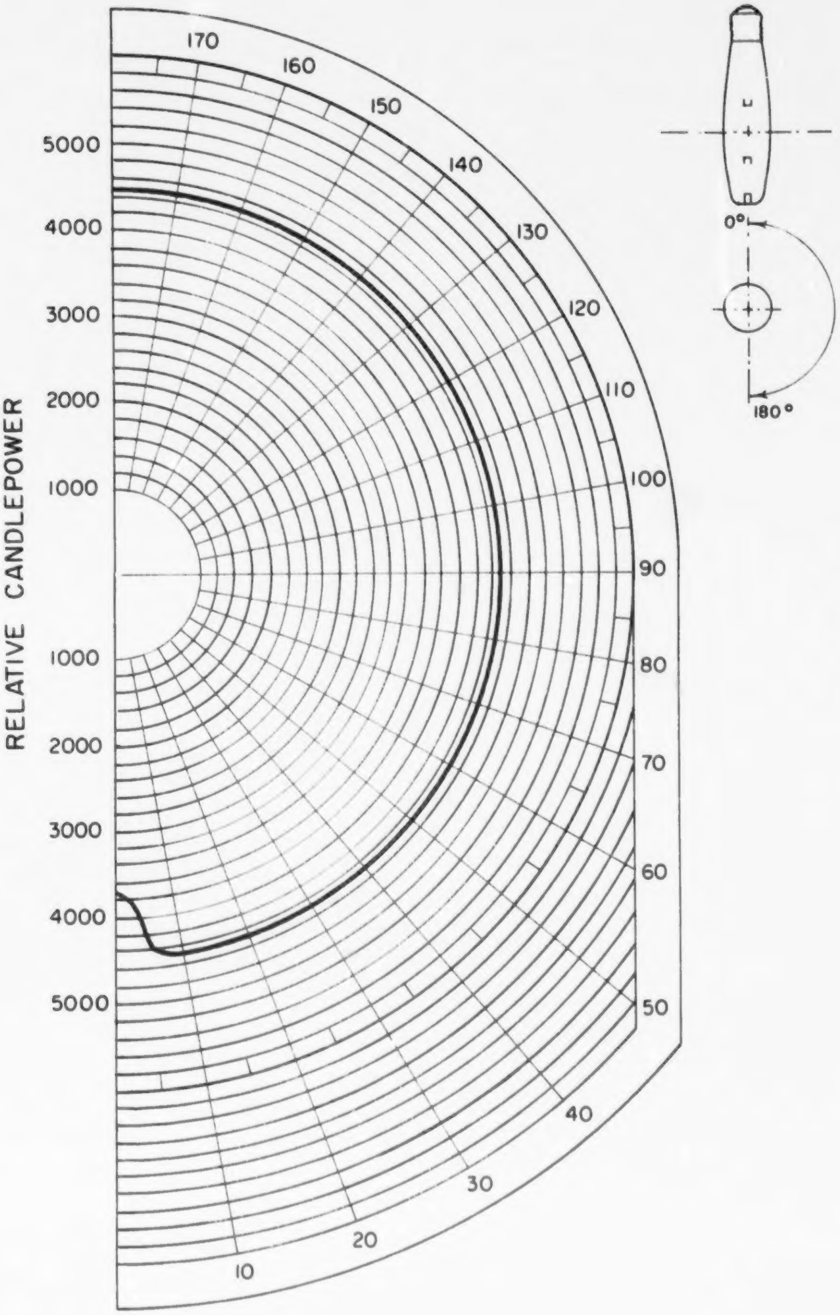

FIGURE 58. HORIZONTAL RELATIVE CANDLE POWER DISTRIBUTION OF THE LUCALOX LAMP

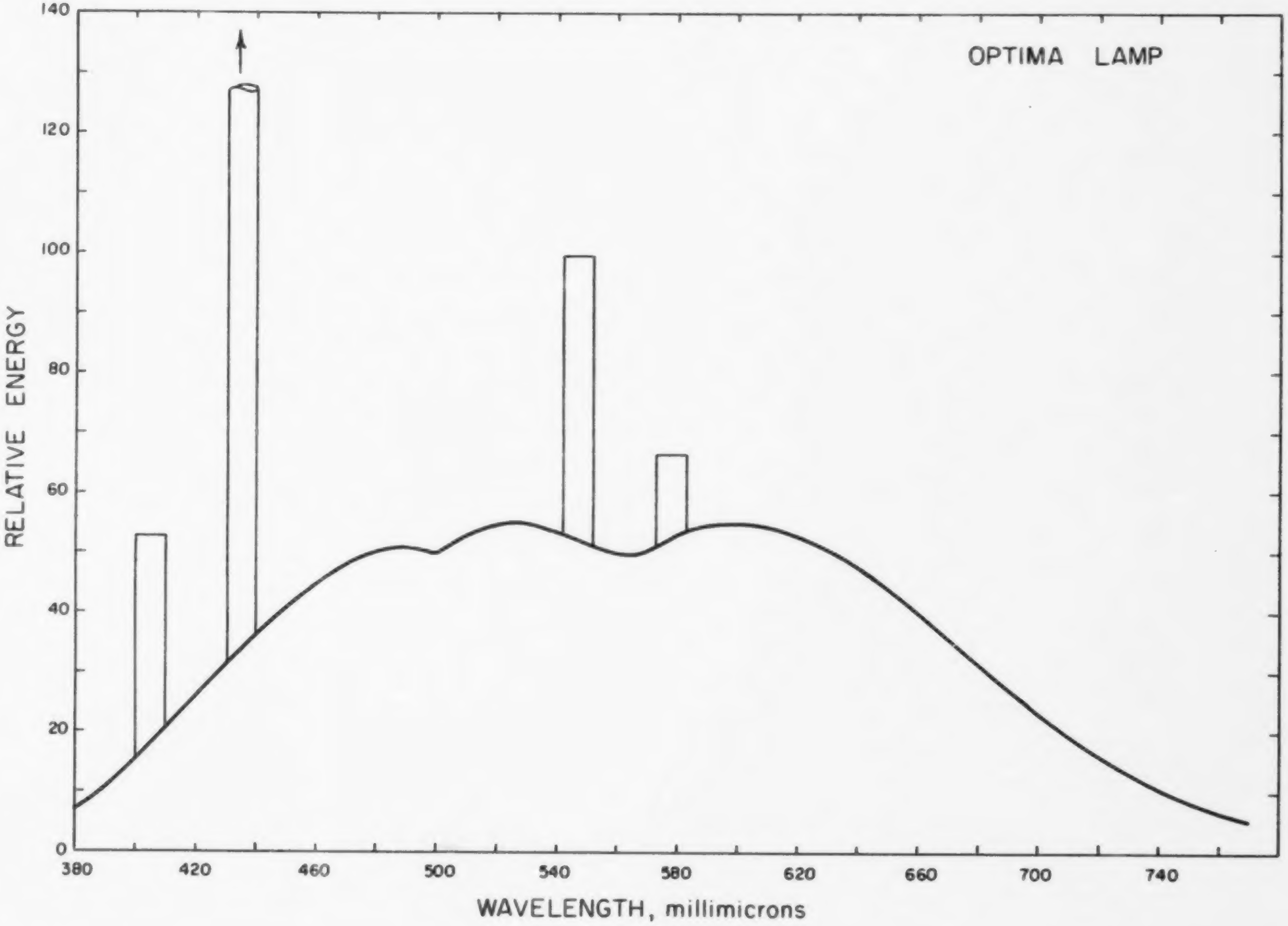

FIGURE 59. RELATIVE ENERGY SPECTRAL DISTRIBUTION OF THE OPTIMA FLUORESCENT LAMP

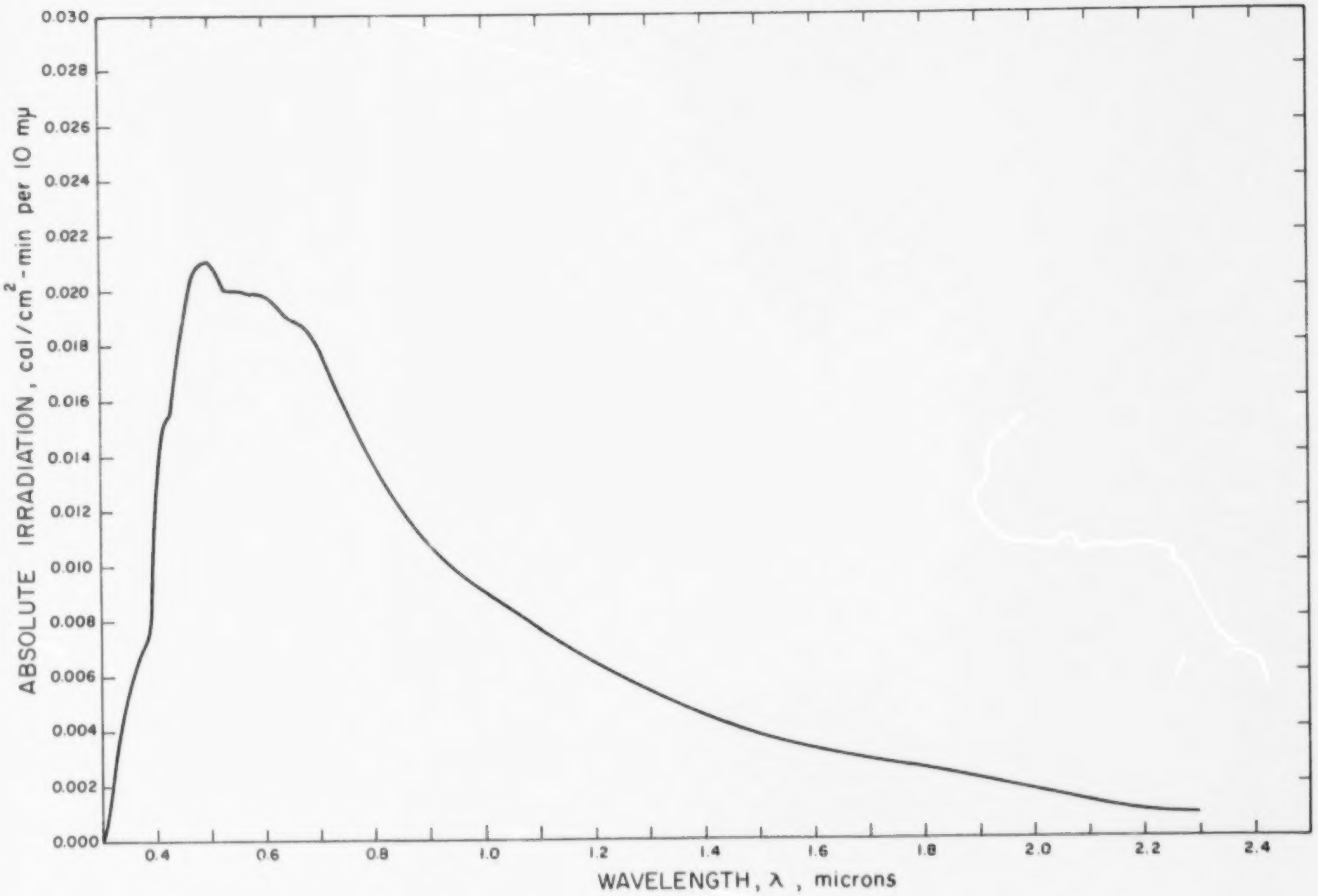

FIGURE 60. ENERGY SPECTRAL DISTRIBUTION OF SOLAR IRRADIATION [148]

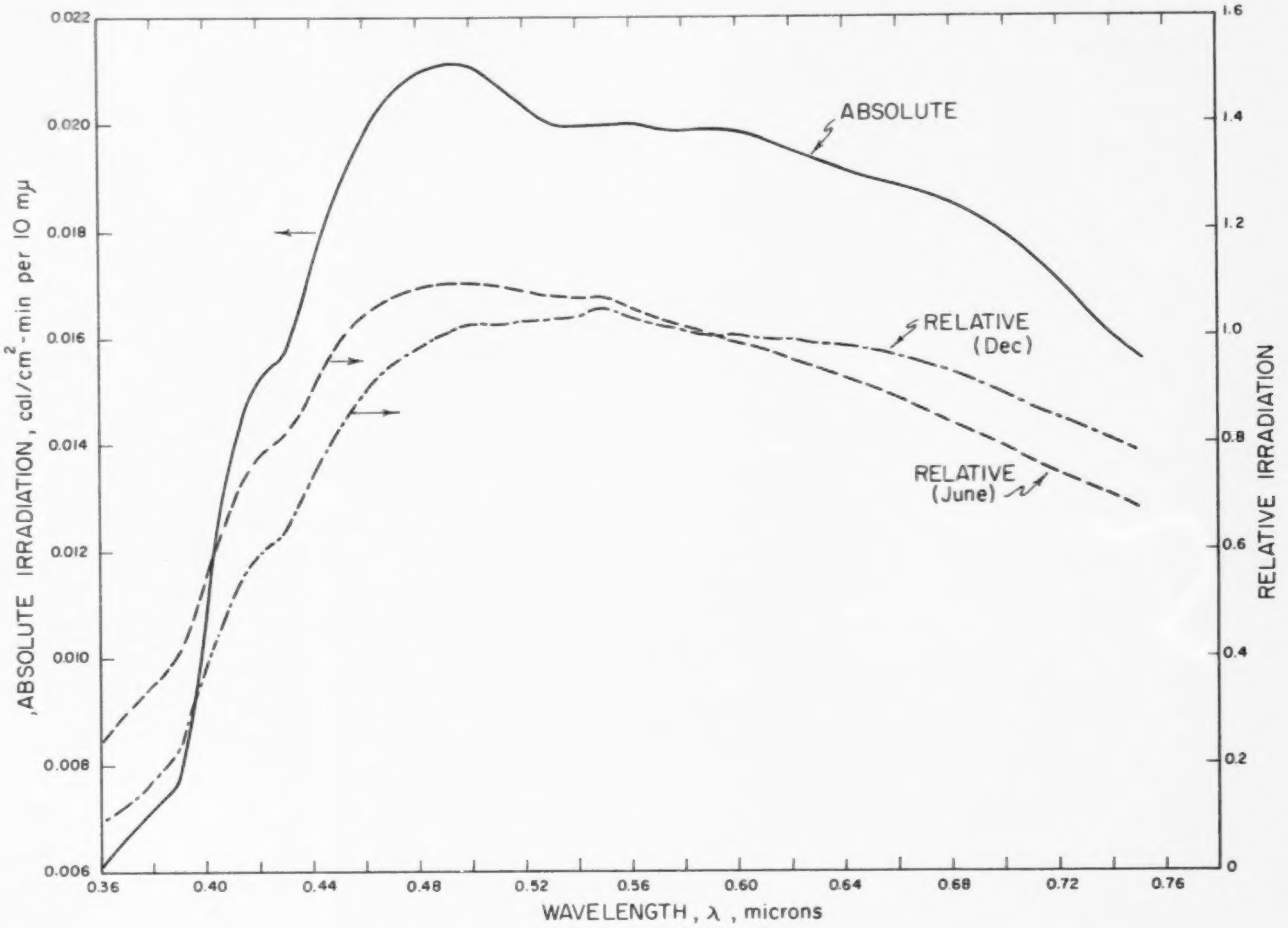

FIGURE 61. ENERGY SPECTRAL DISTRIBUTION OF SUNLIGHT [148]

APPENDIX G

LIGHT TRANSMITTANCE OF VARIOUS FILTERS

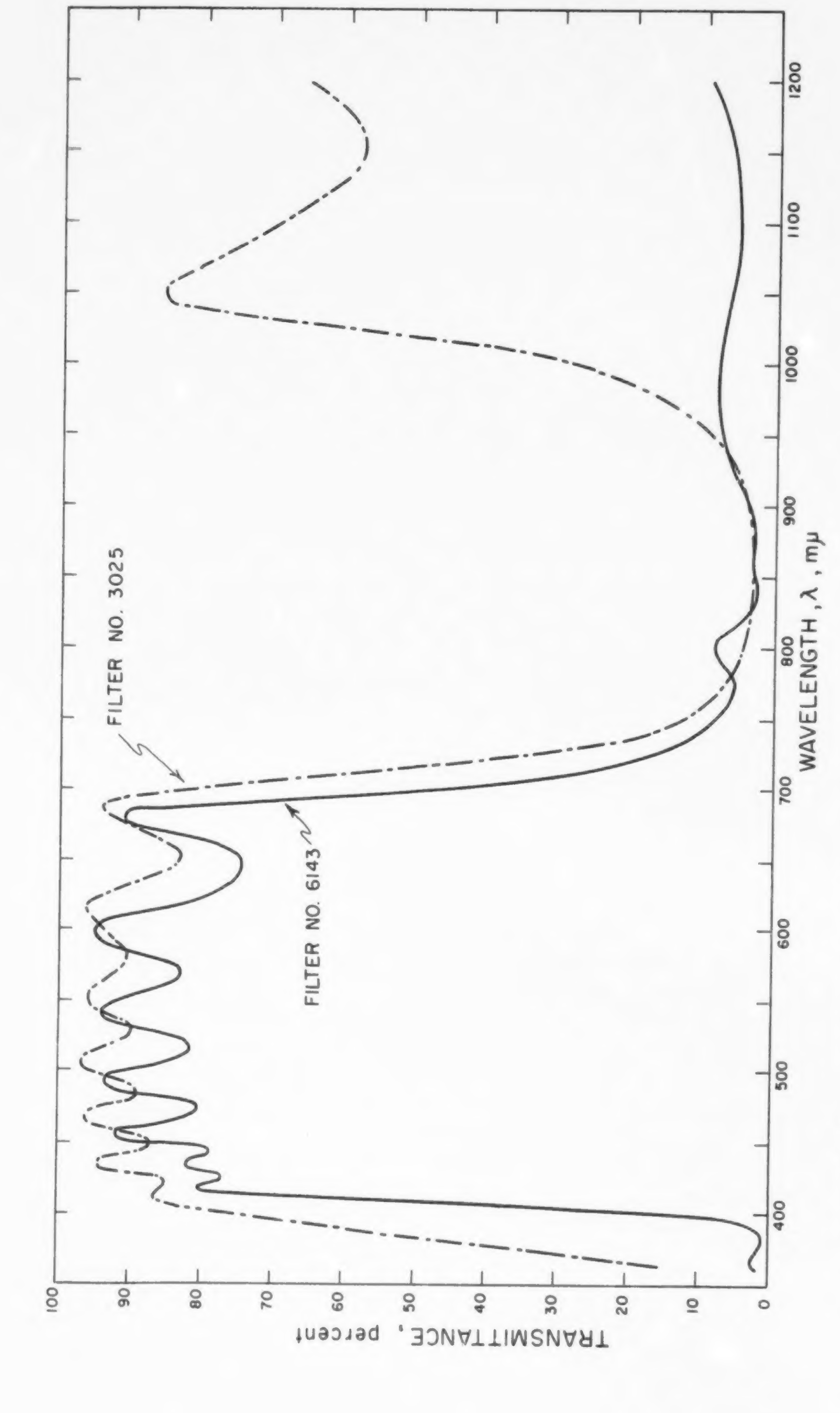

FIGURE 62. SPECTRAL TRANSMITTANCE OF FISH-SCHURMAN MULTILAYER INTERFERENCE FILM FILTERS

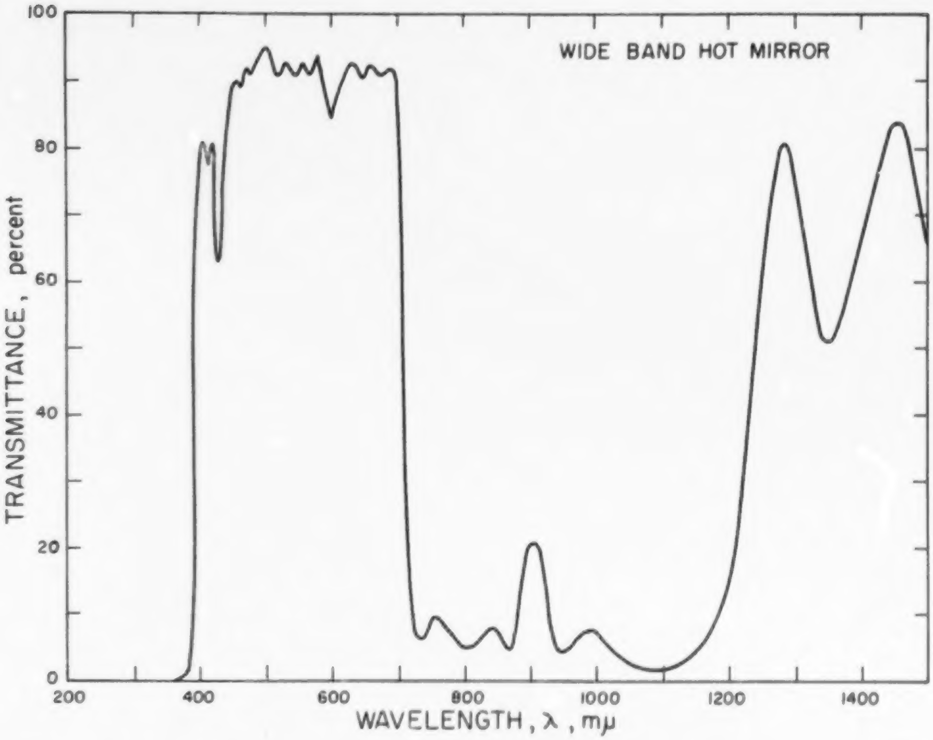

FIGURE 63. SPECTRAL TRANSMITTANCE OF OPTICAL COATING WIDE-BAND HOT MIRROR FILTER

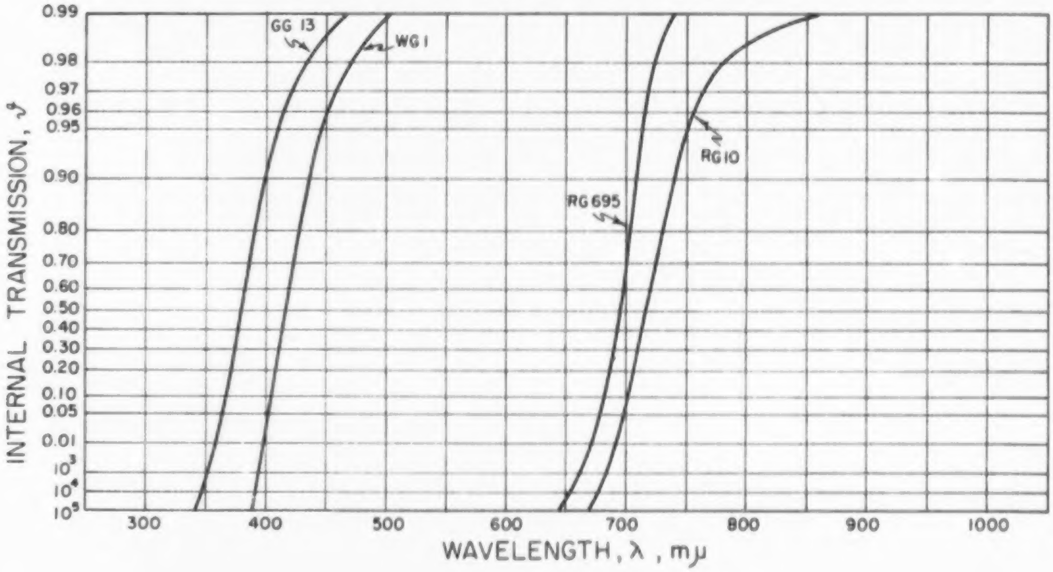

FIGURE 64. SPECTRAL INTERNAL TRANSMISSION OF SCHOTT COLOR GLASS FILTERS

APPENDIX H

COMPUTER PROGRAMS

H-1. COMPUTER PROGRAM FOR THE ENERGY BALANCE MODEL

```
      PROGRAM MAIN(INPUT,OUTPUT)
      DIMENSION  AL(31),APCT(31),ALPH(31),AIOLMR(31),H(31),DH(31),
     1AIOH(31),PH(31),QL(31)
      EQUIVALENCE (APCT(1),ALPH(1)),(H(1),DH(1))
   10 T=0.
      SUM1=0.
      SUM2=0.
      SUM3=0.
      SRHOH=0.
      SPH=0.
      READ 30,NL,NH
   30 FORMAT (2I4)
      PRINT 31,NL,NH
   31 FORMAT (9H1(NL,NH)=,2I4)
      READ 35,PHI
   35 FORMAT (F4.1)
      PRINT 36,PHI
   36 FORMAT (5H0PHI=,F20.10)
      READ 40,AKD
   40 FORMAT (F6.2)
      PRINT 41,AKD
   41 FORMAT (5H0AKD=,F20.10)
      READ 45,CC,CN
   45 FORMAT (2F6.0)
      PRINT 46,CC,CN
   46 FORMAT (9H0(CC,CN)=,2F20.10)
      READ 50,AJ,AIS,X,AG
   50 FORMAT (F4.1,F4.3,F4.1,F6.1)
      PRINT 51,AJ,AIS,X,AG
   51 FORMAT (15H0(AJ,AIS,X,AG)=,4F15.8)
      READ 55,(AL(I),APCT(I),AIOLMR(I),H(I),AIOH(I),QL(I),I=1,NL)
   55 FORMAT (F5.0,2F6.1,F5.1,F7.3,F6.3,45X)
C                                 FIRST CALC ALPH(L),L=1,30 AND D(H),H=1,30
C1                                AND STORE THEM IN THEIR CORR ARRAYS IN CORE
C2                                .NEXT CALC P(H) FOR EACH H BY RUNNING OVER
C3                                THE INDEX L AND STORE IN CORR ARRAY IN
C4                                CORE.FINALLY CALC P BY RUNNING OVER THE
C5                                INDEX H.
      DO 70 I=1,NL
   70 ALPH(I)=(LOGF(100.)-LOGF(APCT(I)))/(X*CN)
      PRINT 72
   72 FORMAT (15H0ALPH(I),I=1,NL)
      PRINT 71,(ALPH(I),I=1,NL)
   71 FORMAT (1H0,F20.10)
      DO 75 J=1,NH
   75 DH(J)=2.71-H(J)/AG
      PRINT 76
   76 FORMAT (13H0DH(J),J=1,NH)
      PRINT 77,(DH(J),J=1,NH)
   77 FORMAT (1H0,F20.10)
      DO 80 I=1,NL
   80 T=T+AIOLMR(I)
C                                 T IS EQUIV TO R ALA SHELEF.
      F1=5.645/(AJ*T*PHI)
      DO 99 J=1,NH
      DO 90 I=1,NL
      E=ALPH(I)*DH(J)*CC
      IF (E-200.) 82,82,81
   81 SUM3=SUM3+AIOLMR(I)*0.0
      GO TO 79
   82 SUM3=SUM3+AIOLMR(I)*EXPF(-ALPH(I)*DH(J)*CC)
   79 SUM1=SUM1+AL(I)*AIOLMR(I)*AIOH(J)*QL(I)
```

```
      IF (F-200.) 89.89.85
   85 SUM2=SUM2+AL(I)*AIOLMR(I)*0.0
      GO TO 90
   89 SUM2=SUM2+AL(I)*AIOLMR(I)*EXPF(-ALPH(I)*DH(J)*CC)*QL(I)
   90 CONTINUE
      SUM33=AIOH(J)*SUM3/T
      PRINT 902.SUM33
  902 FORMAT (7H0SUM33=.F20.10)
C                             SUM33 IS EQUIV TO I SUB D MINUS H ALA SHELEF.
      RHOH=SUM33/AIOH(J)
      PRINT 903.RHOH
  903 FORMAT (20H0RHOH=SUM33/AIOH(J)=.F20.10)
      SRHOH=SRHOH+RHOH
      ALPHT=(LOGF(AIOH(J))-LOGF(SUM33))/(DH(J)*CC)
      PRINT 901.ALPHT
  901 FORMAT (16H0ALPHT(J)=ALPHT=.F20.10)
      IF (AIOH(J)-AIS) 91.91.92
   91 F2=1.0
      GO TO 93
   92 F2=AIS*(LOGF(AIOH(J))-LOGF(AIS)+1.)/AIOH(J)
   93 IF (SUM33-AIS) 94.94.95
   94 F22=1.0
      GO TO 96
   95 F22=AIS*(LOGF(SUM33)-LOGF(AIS)+1.)/SUM33
   96 F3=.001*AKD*CC*DH(J)
      PH(J)=  (F1*(F2*SUM1-AIOH(J)*F22*SUM2)-F3)
      PGH=PH(J)+F3
      PRINT 961.PGH
  961 FORMAT (14H0PGH=PH(J)+F3=.F20.10)
      AMUNMH=1000.*PH(J)/(CC*DH(J))
      PRINT 962.AMUNMH
  962 FORMAT (31H0AMUNMH=1000.*PH(J)/(CC*DH(J))=.F20.10)
      SUM3=0.
      SUM1=0.
   99 SUM2=0.
      PRINT 992.SRHOH
  992 FORMAT (28H0SRHOH=SUM(RHOH(J)).J=1.30.=.F20.10)
      SUML=0.
      DO 990 I=1.NL
  990 SUML=SUML+AL(I)*AIOLMR(I)
      EM=.00392*SUML/(PHI*T)
      PRINT 991.EM
  991 FORMAT (4H0EM=.F20.10)
      DO 100 J=1.NH
  100 SPH=SPH+PH(J)
      P=61.*3.1416*SPH
      PRINT 105
  105 FORMAT (13H0PH(J).J=1.NH)
      PRINT 110.(PH(J).J=1.NH)
  110 FORMAT (1H0.F20.10)
      PRINT 120.P
  120 FORMAT (31H0P=61.*3.1416*SUM(PH(J)).J=1.NH.F20.10)
  130 STOP 00130
      GO TO 10
      END
```

B-[illegible]. COMPUTER PROGRAM FOR KINETIC MODELS I, II AND III

```
      PROGRAM MAIN(INPUT•OUTPUT)
      DIMENSION  AL(31)•APCT(31)•ALPH(31)•AIOLMR(31)•H(31)•DH(31)•
     1AIOH(31)•PH(31)•QL(31)
      EQUIVALENCE (APCT(1)•ALPH(1))•(H(1)•DH(1))
      REAL MUX
      NSETS=0
      READ 5•NS
    5 FORMAT (I2)
      PRINT 6•NS
    6 FORMAT (4HINS=•I2)
      N1=198
      N2=18
      X1=1•0
      X2=15•0
   10 NSETS=NSETS+1
      T=0•
      SUM1=0•
      SUM2=0•
      SUM3=0•
      SRHOH=0•
      SPH=0•
      SAIOH=0•
      SUMLL=0•
      SPH2=0•
      SPH3=0•
      SUML=0•
      READ 20•CONT1•CONT2
   20 FORMAT (2F2•0)
      PRINT 21•CONT1•CONT2
   21 FORMAT (15H0(CONT1•CONT2)=•2F5•0)

      READ 30•NL•NH
   30 FORMAT (2I4)
      PRINT 31•NL•NH
   31 FORMAT (9H0(NL•NH)=•2I4)
      READ 35•PHI
   35 FORMAT (F4•1)
      PRINT 36•PHI
   36 FORMAT (5H0PHI=•F20•10)
      READ 40•AKD
   40 FORMAT (F6•2)
      PRINT 41•AKD
   41 FORMAT (5H0AKD=•F20•10)
      READ 45•CC•CN
   45 FORMAT (2F6•0)
      PRINT 46•CC•CN
   46 FORMAT (9H0(CC•CN)=•2F20•10)
      READ 50•AJ•AIS•X•AG
   50 FORMAT (F4•1•F4•3•F4•1•F6•1)
      PRINT 51•AJ•AIS•X•AG
   51 FORMAT (15H0(AJ•AIS•X•AG)=•4F15•8)
      READ 52•MUX•AKM
   52 FORMAT (F4•1•F6•1)
      PRINT 53•MUX•AKM
   53 FORMAT (11H0(MUX•AKM)=•2F20•10)
      READ 55•(AL(I)•APCT(I)•AIOLMR(I)•H(I)•AIOH(I)•QL(I)•I=1•NL)
   55 FORMAT (F5•0•2F6•1•F5•1•F7•3•F6•3•45X)
      PRINT 56•(AL(I)•APCT(I)•AIOLMR(I)•H(I)•AIOH(I)•QL(I)•I=1•NL)
   56 FORMAT (11H0INPUT DATA•F6•0•2F7•1•F6•1•F8•3•F7•3)
C                                FIRST CALC ALPH(L)•L=1•30 AND D(H)•H=1•30
C1                               AND STORE THEM IN THEIR CORR ARRAYS IN CORE
C2                               •NEXT CALC P(H) FOR EACH H BY RUNNING OVER
C3                               THE INDEX L AND STORE IN CORR ARRAY IN
C4                               CORE•FINALLY CALC P BY RUNNING OVER THE
C5                               INDEX H•
      DO 70 I=1•NL
   70 ALPH(I)=(LOGF(100•)-LOGF(APCT(I)))/(X*CN)
      PRINT 72
   72 FORMAT (15H0ALPH(I)•I=1•NL)
      PRINT 71•(ALPH(I)•I=1•NL)
   71 FORMAT (1H0•F20•10)
      DO 75 J=1•NH
   75 DH(J)=2•71-H(J)/AG
      PRINT 76
   76 FORMAT (13H0DH(J)•J=1•NH)
      PRINT 77•(DH(J)•J=1•NH)
   77 FORMAT (1H0•F20•10)
      DO 80 I=1•NL
   80 T=T+AIOLMR(I)
C                                T IS EQUIV TO R ALA SHELEF•
      DO 990 I=1•NL
      SUMLL=SUMLL+QL(I)*AL(I)*AIOLMR(I)
  990 SUML=SUML+AL(I)*AIOLMR(I)
      FM=•00392*SUML/(PHI*T)
      PRINT 991•FM
  991 FORMAT (4H0FM=•F20•10)
```

```
      DO 993 J=1.NH
  993 SAIOH=SAIOH+AIOH(J)
      PRINT 994.SAIOH
  994 FORMAT (20H0SAIOH=SUM(AIOH(J))=.F20.10)
      FMB=.00392*SUMLL/(PHI*T)
      PRINT 995.FMB
  995 FORMAT (5H0FMB=.F20.10)
      IF (MUX-0.0) 998.996.998
  996 MUX=AKM*FMB*AIS
      PRINT 997.MUX
  997 FORMAT (16H0CALCULATED MUX=.F20.10)
  998 F1=5.645/(AJ*T*PHI)
      DO 99 J=1.NH
      DO 90 I=1.NL
      E=ALPH(I)*DH(J)*CC
      IF (E-200.) 82.82.81
   81 SUM3=SUM3+AIOLMR(I)*0.0
      GO TO 79
   82 SUM3=SUM3+AIOLMR(I)*EXPF(-ALPH(I)*DH(J)*CC)
   79 SUM1=SUM1+AL(I)*AIOLMR(I)*AIOH(J)*OL(I)
      IF (E-200.) 89.89.85
   85 SUM2=SUM2+AL(I)*AIOLMR(I)*0.0
      GO TO 90
   89 SUM2=SUM2+AL(I)*AIOLMR(I)*EXPF(-ALPH(I)*DH(J)*CC)*OL(I)
   90 CONTINUE
      SUM33=AIOH(J)*SUM3/T
      PRINT 902.SUM33
  902 FORMAT (7H0SUM33=.F20.10)
C                                   SUM33 IS EQUIV TO I SUB D MINUS H ALA SHELEF.
      IF (CONT1-1.) 1050.1000.1050
 1000 ARG1=MUX+AKM*FMB*AIOH(J)
      ARG2=MUX+AKM*FMB*SUM33
      PGH2=MUX*(LOGF(ARG1)-LOGF(ARG2))
      PRINT 1005.PGH2
 1005 FORMAT (9H0PGH2(J)=.F20.10)
      PH2=PGH2-.001*AKD*CC*DH(J)
      PRINT 1010.PH2
 1010 FORMAT (8H0PH2(J)=.F20.10)
      SPH2=SPH2+PH2
      AMNMH2=(1000.*PH2)/(CC*DH(J))
      PRINT 1015.AMNMH2
 1015 FORMAT (11H0AMNMH2(J)=.F20.10)
 1050 RHOH=SUM33/AIOH(J)
      PRINT 903.RHOH
  903 FORMAT (20H0RHOH=SUM33/AIOH(J)=.F20.10)
      SRHOH=SRHOH+RHOH
      ALPHT=(LOGF(AIOH(J))-LOGF(SUM33))/(DH(J)*CC)
      PRINT 901.ALPHT
  901 FORMAT (16H0ALPHT(J)=ALPHT=.F20.10)
      IF (CONT2-2.) 1040.1020.1040
 1020 A=AIOH(J)/AIS
      EI1=GINT16(A.X1.N1)
      EI1=EI1+GINT16(X1.X2.N2)
      B=SUM33/AIS
      EI2=GINT16(B.X1.N1)

      EI2=EI2+GINT16(X1.X2.N2)
      PRINT 1021.A.EI1.B.EI2
 1021 FORMAT (3H0A=.F20.10.5H0EI1=.F20.10.3H0B=.F20.10.5H0EI2=.F20.10)
      PGH3=MUX*(ALPHT*DH(J)*CC+EI1-EI2)
      PRINT 1025.PGH3
 1025 FORMAT (9H0PGH3(J)=.F20.10)
      PH3=PGH3-.001*AKD*CC*DH(J)
      PRINT 1030.PH3
 1030 FORMAT (8H0PH3(J)=.F20.10)
      SPH3=SPH3+PH3
      AMNMH3=(1000.*PH3)/(CC*DH(J))
      PRINT 1035.AMNMH3
 1035 FORMAT (11H0AMNMH3(J)=.F20.10)
 1040 IF (AIOH(J)-AIS) 91.91.92
   91 F2=1.0
      GO TO 93
   92 F2=AIS*(LOGF(AIOH(J))-LOGF(AIS)+1.)/AIOH(J)
   93 IF (SUM33-AIS) 94.94.95
   94 F22=1.0
      GO TO 96
   95 F22=AIS*(LOGF(SUM33)-LOGF(AIS)+1.)/SUM33
   96 F3=.001*AKD*CC*DH(J)
      PH(J)=   (F1*(F2*SUM1-AIOH(J)*F22*SUM2)-F3)
      PGH=PH(J)+F3
      PRINT 961.PGH
  961 FORMAT (14H0PGH=PH(J)+F3=.F20.10)
      AMUNMH=1000.*PH(J)/(CC*DH(J))
      PRINT 962.AMUNMH
  962 FORMAT (31H0AMUNMH=1000.*PH(J)/(CC*DH(J))=.F20.10)
```

```
      SUM3=0.
      SUM1=0.
   99 SUM2=0.
      PRINT 992.SRHOH
  992 FORMAT (28H0SRHOH=SUM(RHOH(J)).J=1.30.=.F20.10)
      IF (CONT1-1.) 1120.1100.1120
 1100 P2=61.*3.1416*SPH2
      PRINT 1105.P2
 1105 FORMAT (20H0P2=61.*3.1416*SPH2=.F20.10)
 1120 IF (CONT2-2.) 1150.1125.1150
 1125 P3=61.*3.1416*SPH3
      PRINT 1130.P3
 1130 FORMAT (20H0P3=61.*3.1416*SPH3=.F20.10)
 1150 DO 100 J=1.NH
  100 SPH=SPH+PH(J)
      P=61.*3.1416*SPH
      PRINT 105
  105 FORMAT (13H0PH(J).J=1.NH)
      PRINT 110.(PH(J).J=1.NH)
  110 FORMAT (1H0.F20.10)
      PRINT 120.P
  120 FORMAT (31H0P=61.*3.1416*SUM(PH(J)).J=1.NH.F20.10)
  130 IF (NSETS-NS) 10.131.131
  131 PRINT 132
  132 FORMAT (12H0 END OF JOB)
  133 STOP 00133
      END
      FUNCTION GINT16(XMIN.XMAX.NINT)
      DIMENSION U(8).R(8).T(8)
      IF(NTEST-13579) 1.2.1
    1 NTEST=13579
      U(1)=-9.89400935E-1
      U(2)=-9.44575023E-1
      U(3)=-8.65631202E-1
      U(4)=-7.55404408E-1
      U(5)=-6.17876244E-1
      U(6)=-4.58016777E-1
      U(7)=-2.81603551E-1
      U(8)=-9.50125098E-2
      R(1)= 2.71524594E-2
      R(2)= 6.22535239E-2
      R(3)= 9.51585117E-2
      R(4)= 1.24628971E-1
      R(5)= 1.49595988E-1
      R(6)= 1.69156519E-1
      R(7)= 1.82603415E-1
      R(8)= 1.89450610E-1
    2 Q=XMIN
      XN=NINT
      DQ=(XMAX-XMIN)/XN
      DQ5=DQ*.5
      DO 3 K=1.8
    3 T(K)=DQ5*U(K)
      HINT16=0.
      DO 5 L=1.NINT
      PM=Q+DQ5
      DO 4 N=1.8
      F1=PM-T(N)
      F2=PM+T(N)
      F3=EXP(-F2)/F2
      F4=EXP(-F1)/F1
    4 HINT16=HINT16+(F3+F4)*R(N)
    5 Q=Q+DQ
      GINT16=DQ5*HINT16
      RETURN
      END
```

[illegible] COMPUTER PROGRAM FOR THE GAUSSIAN INTEGRATION OF THE EXPONENTIAL INTEGRAL

```
       PROGRAM  EXPINT (INPUT,OUTPUT,PUNCH)
       EXTERNAL F
      N1=198
      N2=18
      X1=1.0
      X2=15.0
    5 READ 10,X
   10  FORMAT (2E15.8)
       IF (X-15.0) 15,11,11
   11  E=0.0
       GO TO 40
   15  IF (X) 20,20,30
   20  STOP
   30  E=GINT16(X,X1,F,N1)
       E = E + GINT16(X1,X2,F,N2)
   40  PRINT 10,X,E
       GO TO 5
       END
       FUNCTION F(T)
       F= EXP(-T)/T
       RETURN
       END
      FUNCTION GINT16(XMIN,XMAX,F,NINT)
       EXTERNAL F
      DIMENSION U(8),R(8),T(8)
      IF(NTEST-13579) 1,2,1
    1 NTEST=13579
      U(1)=-9.89400935E-1
      U(2)=-9.44575023E-1
      U(3)=-8.65631202E-1
      U(4)=-7.55404408E-1
      U(5)=-6.17876244E-1
      U(6)=-4.58016777E-1
      U(7)=-2.81603551E-1
      U(8)=-9.50125098E-2
      R(1)= 2.71524594E-2
      R(2)= 6.22535239E-2
      R(3)= 9.51585117E-2
      R(4)= 1.24628971E-1
      R(5)= 1.49595988E-1
      R(6)= 1.69156519E-1
      R(7)= 1.82603415E-1
      R(8)= 1.89450610E-1
    2 Q=XMIN

      XN=NINT
      DQ=(XMAX-XMIN)/XN
      DQ5=DQ*.5
      DO 3 K=1,8
    3 T(K)=DQ5*U(K)
      GINT16=0.
      DO 5 L=1,NINT
      PM=Q+DQ5
      DO 4 N=1,8
    4 GINT16=GINT16+(F(PM+T(N)) + F(PM-T(N)) )*R(N)
    5 Q=Q+DQ
      GINT16=DQ5*GINT16
      RETURN
      END
```

H 4. COMPUTER PROGRAM

FOR LINEAR REGRESSION AND CORRELATION OF A LOGARITHMIC FUNCTION

```
 34000320070136000320070249024025119636113001 02
 ZZJOB 5
 ZZFORX51
    N1=0
    AMU=0.
    SN=0.
    AMUT=4.32
    READ 30.N
  30 FORMAT (I4)
  40 READ 50.AMU.SN
  50 FORMAT (2F10.2)
    N1=N1+1
    Y=.4343*LOGF(AMUT)-.4343*LOGF(AMUT-AMU)
    X=SN
    PUNCH 100.X.Y
 100 FORMAT (2F10.4)
    IF (N-N1) 150.150.40
 150 STOP 00150
 180 END
 LINEAR REGRESSION (IN TWO VARIABLES)  -  LEAST SQUARES FIT
 B J SOCKS          DECEMBER 30. 1961.
1 IF(SENSESWITCH1)2.3
2 ACCEPT101.N.M
 GO TO 4
3 READ101.N.M
4 EN=N
 EM=M
 SX=0.
 SY=0.
 SXY=0.
 SX2=0.
 SY2=0.
 DO5I=1.N
 READ102.X.Y
 SX=SX+X
 SY=SY+Y
 SXY=SXY+X*Y
 SX2=SX2+X*X
5 SY2=SY2+Y*Y
 XBAR=SX/EN
 YBAR=SY/EN
 CX2=SX*SX/EN
 CXY=SX*SY/EN
 VX2=SX2-CX2
 VXY=SXY-CXY
 B=VXY/VX2
 A=YBAR-B*XBAR
 C=SXY/SX2
```

```
   R=(((EN*SXY-SX*SY)**2)/((EN*SX2-SX*SX)*(EN*SY2-SY*SY)))**.5
   IF(R)6,7,7
 6 RA=-R
   GO TO 8
 7 RA=R
 8 S2SX=(EN*SX2-SX*SX)/(EN*(EN-1.))
   S2SY=(EN*SY2-SY*SY)/(EN*(EN-1.))
   S2YGX=((EN-1.)/(EN-2.))*(S2SY-B*B*S2SX)
   SYGX=S2YGX**.5
   SB=SYGX/((S2SX*(EN-1.))**.5)
   IF(B)9,10,10
 9 BA=-B
   GO TO 11
10 BA=B
11 T=BA/SB
   IF(T)12,13,13
12 TA=-T
   GO TO 14
13 TA=T
14 DF2=EN-2.
   SEX=((SX2-SX*SX/EN)/(EN-1.))**.5
   SEY=((SY2-SY*SY/EN)/(EN-1.))**.5
   PRINT103
   PRINT104,N
   PRINT105
   PRINT106,A,B
   PRINT107
   PRINT108,C
   PRINT109

   PRINT110,XBAR
   PRINT117,SEX
   PRINT118,SEY
   PRINT111,RA
   PRINT112,SYGX
   PRINT113,SB
   PRINT114,TA
   PRINT115
   PRINT116,DF2
   IF(SENSESWITCH3)16,1
16 SEXM=SEX*EM
   SEYM=SEY*EM
   SGM=SYGX*EM
   DO31I=1,N
   KW=0
   READ102,X,Y
   XD=XBAR-X
   YD=YBAR-Y
   YES=A+B*X
   SDO=Y-YES
```

```
      IF(XD)17,18,18
   17 XD=-XD
   18 IF(YD)19,20,20
   19 YD=-YD
   20 IF(SDO)21,22,22
   21 SDO=-SDO
   22 IF(XD-SEXM)24,24,23
   23 KW=1
      GOTO28
   24 IF(YD-SEYM)26,26,25
   25 KW=1
      GOTO28
   26 IF(SDO-SGM)28,28,27
   27 KW=1
   28 IF(I-1)282,281,282
  281 PRINT119
      PRINT122
  282 IF(KW)29,29,30
   29 PRINT120,I,Y,YD,X,XD,YES,SDO
      GOTO31
   30 PRINT121,I,Y,YD,X,XD,YES,SDO
   31 CONTINUE
      PRINT123
      PRINT124
      GOTO1
  101 FORMAT(I4,I4)
  102 FORMAT(F10.3,F10.3)
  103 FORMAT(/21X,21H  LEAST   SQUARES   FIT)
  104 FORMAT(///5H FOR I4,14H  OBSERVATIONS)
  105 FORMAT(/47H FOR   THE   EQUATION   OF   THE   FORM   Y = A + B X)
  106 FORMAT(/26X,7H Y   =   F10.4,5H     +F10.4,3H  X)
  107 FORMAT(/43H FOR   THE   EQUATION   OF   THE   FORM   Y = C X)
  108 FORMAT(/26X,7H Y   =   F10.4,3H  X)
  109 FORMAT(///24H ADDITIONAL   INFORMATION)
  110 FORMAT(/35X,8H MEAN = F10.4)
  111 FORMAT(/16X,27H CORRELATION COEFFICIENT = F10.7)
  112 FORMAT(/13X,30H STANDARD ERROR OF ESTIMATE = F10.4)
  113 FORMAT(/43H        STANDARD ERROR OF COEFFICIENT,  B  = F10.7)
  114 FORMAT(/23X,20H THE STATISTIC   T = F10.5)
  115 FORMAT(///48H CORRELATION COEFFICIENT AND T ARE BOTH ABSOLUTE)
  116 FORMAT(/25H TABLE SHOULD BE CHECKED F6.0,19H DEGREES OF FREEDOM)
```

```
  117 FORMAT(/16X,27H STANDARD DEVIATION OF X = F10.5)
  118 FORMAT(/16X,27H STANDARD DEVIATION OF Y = F10.5)
  119 FORMAT(///49H ESTIMATION DATA FOR EQUATION RELIABILITY STUDIES)
  120 FORMAT(/I4,F10.4,F10.5,F10.4,F10.5,F10.4,F10.5)
  121 FORMAT(/I4,F10.4,F10.5,F10.4,F10.5,F10.4,F10.5,8H BAD OBS)
  122 FORMAT(///9X,1HY,8X,2HDY,9X,1HX,8X,2HDX,7X,5HY EST,4X,6HDY EST)
  123 FORMAT(///18H CASE IS COMPLETED)
  124 FORMAT(/46H TO PROCESS A NEW CASE, LOAD READER, HIT START)
      END
```

APPENDIX I

GLOSSARY

BOD	Biochemical Oxygen Demand
c	Velocity of Light $[LT^{-1}]$
C_c	Algal concentration in suspension $[ML^{-3}]$
C_{co}	Algal Concentration in the influent $[ML^{-3}]$
Ch	Chlorophyll content
D_R	Loss in production due to respiration and decay $[ML^{-2}T^{-1}]$
d	Depth of algal reactor measured from the illuminated surface $[L]$
E	Quantum energy content; Energy units $[E]$
E_o	Overall light conversion efficiency of photosynthesis
E_e	Algal Conversion Efficiency on the basis of electric energy input
E_1	Exponential integral
E_m	Thermodynamic efficiency of the photosynthetic energy conversion
E_m'	Dimensional thermodynamic light conversion efficiency $[E^{-1}L^2]$
E_q	Quantum efficiency
E_s	Efficiency of light utilization within an illuminated algal suspension
E_T	Total light conversion efficiency
h	Plank's constant $[ET]$
h'	Culture height from the bottom rim of the algatron drum $[L]$
I	Light intensity (irradiance) $[EL^{-2}T^{-1}]$
I_o	Incident light intensity on the illuminated surface (incident irradiance) $[EL^{-2}T^{-1}]$
$\overline{I}_o$	Average incident light intensity on culture surface $[EL^{-2}T^{-1}]$
$I_{o\lambda}$	Incident light intensity of a given wavelength band $[EL^{-2}T^{-1}]$
I_d	Light intensity at depth, d $[EL^{-2}T^{-1}]$
$I_{d\lambda}$	Light intensity at depth d corresponding to a given wavelength band $[EL^{-2}T^{-1}]$
I_s	Light saturation intensity $[EL^{-2}T^{-1}]$

I_x	Light intensity (irradiance) in an incremental depth (dx)
$I_{x\lambda}$	Light intensity corresponding to a given wavelength band at incremental depth (dx) $[EL^{-2}T^{-1}]$
$I_{\lambda R}$	Relative light energy correspond to a given wavelength band
J	Algae chemical energy content $[EM^{-1}]$
K, K_o, K_1 k, k_1, k_n	Constants
K_A	Substrate concentration constant as applied to the "Modified Exponential Function" $[ML^{-3}]$
K_d	Respiration and decay rate constant $[T^{-1}]$
K_s	Substrate concentration constant as applied to the Michaelis-Menten Equation $[ML^{-3}]$
k_d, k_s, k_1, k_2	Various reaction velocity constants
L	Length units
M	Mass units
N_A	Avogadro's Number
N_c	Nitrogen cellular content
n	Number of quanta; any integer
P_a	Gross production of dry algal per unit of illuminated surface per unit of time $[ML^{-2}T^{-1}]$
P_a'	Surface gross production of algae when both light and nitrogen concentrations are limiting $[ML^{-2}T^{-1}]$
$P_{a_1}, P_{a_2}, P_{a_3}$	Gross production of dry algae on the basis of Macroscopic Models I, II and III, respectively $[ML^{-2}T^{-1}]$
P_n	Total algal net production per unit of time $[MT^{-1}]$
$\hat{P}_n$	Maximum algal net production $[MT^{-1}]$
P_n'	Net algal production in an optically dense culture in which nitrogen is limiting $[MT^{-1}]$
P_{na}	Net production of dry algal per unit of illuminated surface per unit of time $[ML^{-2}T^{-1}]$
$P_{na_1}, P_{na_2}, P_{na_3}$	Net production of dry algae on the basis of Macroscopic Models I, II and III, respectively $[ML^{-2}T^{-1}]$
$\hat{P}_{na}$	Maximum algal net production per unit of illuminated area $[ML^{-2}T^{-1}]$
P_{nv}	Algal net production per unit of culture volume $[ML^{-3}T^{-1}]$
$\hat{P}_{nv}$	Maximum algal net production per unit of culture volume $[ML^{-3}T^{-1}]$

Q	Flow rate $[L^3 T^{-1}]$
Q_λ	Relative quantum yield coefficient, accounting for the algal action spectrum of an optically dense culture
q	Substrate cellular removal rate. Mass of nitrogen removed per unit of mass of algae present in the reactor per unit time $[T^{-1}]$
R_t	The sum of the relative energy in the visible range, $\sum_{\lambda=400}^{\lambda=700} I_{\lambda R}$
R_x	Rate of photosynthesis at incremental depth (dx) $[ML^{-2}T^{-1}]$
$\bar{r}$	Average radius of the algatron drum [L]
S_N	Concentration of a nitrogenous compound expressed as N $[ML^{-3}]$
S_{N_1}	Substrate nitrogen concentration (effluent concentration and/or reactor concentration in CSTR-type process) $[ML^{-3}]$
S_{No}	Initial nitrogen concentration (influent concentration) $[ML^{-3}]$
S_{NS}	Nitrogen concentration corresponds to $\mu_n = 0.9\,\hat{\mu}_n$
s'	Slope of culture surface in the algatron
T	Time units
T_r	Percent of light transmission
t	Time
t'	Dummy variable of integration
U	Energy content of a mole of quanta (einstein) [E]
V	Volume of growth unit $[L^3]$
x	Length of light path within algal suspension [L]
x_s	Depth of culture corresponds to I_s [L]
Y	Yield coefficient of nitrogen removal. Mass of algae produced per a unit mass of nitrogen removed
$\bar{Y}$	Average yield coefficient at the range of full growth
Y_{NS}	Yield coefficient as S_{NS}
α	Light extinction coefficient $[M^{-1}L^2]$
α_t	Integrated light extinction coefficient for polychromatic light $[M^{-1}L^2]$
α_λ	Light extinction coefficient for a beam of a particular wavelength $[M^{-1}L^2]$
γ	Fraction of light absorbed by a given algal suspension
γ'	Euler's constant

ΔH	Chemical energy content per mole [E]
θ	Mean residence time or average retention period [T]
λ	Wavelength [L]
$\bar{\mu}$	Average specific growth rate $[T^{-1}]$
$\bar{\mu}_1, \bar{\mu}_2, \bar{\mu}_3$	Average specific growth rates on the basis of Macroscopic Models I, II and III, respectively $[T^{-1}]$
μ_n	Net specific growth rate $[T^{-1}]$
$\bar{\mu}_n$	Average net specific growth rate $[T^{-1}]$
$\hat{\mu}_n$	Maximum net specific growth rate $[T^{-1}]$
μ_N'	Specific growth rate corresponding to a given growth-limiting nitrogen concentration $[T^{-1}]$
$\bar{\mu}_n'$	Average net specific growth rate in an optically dense culture in which both nitrogen and irradiance are limiting
$\bar{\mu}_{n(max)}$	Overall maximum net specific growth rate when irradiance is the sole growth-limiting factor
$\bar{\mu}_{n_1}, \bar{\mu}_{n_2}, \bar{\mu}_{n_3}$	Average net specific growth rate on the basis of Macroscopic Models I, II and III, respectively $[T^{-1}]$
$\bar{\mu}_{na}$	Average net specific growth rate at an incremental surface area $[T^{-1}]$
μ_x	Specific growth rate in an incremental depth (dx) (specific growth rate on the microscopic level) $[T^{-1}]$
$\hat{\mu}_x$	The microscopic maximum specific growth rate $[T^{-1}]$
ν	Wave frequency $[T^{-1}]$
ϕ	Quantum yield: quantum efficiency

REFERENCES

1. Oswald, W. J. "Fundamental factors in stabilization pond design," Proc. 3rd Conference Biological Waste Treatment, Manhattan College, New York, 1960.

2. Wassink, E. C., B. Kok, and J. L. P. Van Oorschot. "The efficiency of light-energy conversion in Chlorella cultures as compared with higher plants," Algae Culture from Laboratory to Pilot Plant. Ed. J. S. Burlew., Publ. 600, Carnegie Inst. of Wash., 1953.

3. Oswald, W. J. and H. B. Gotaas. "Photosynthesis in sewage treatment," Proc. Am. Soc. Civil Engrs., J. Sanit. Engr. Div., 81:1-27, (No. 686), May 1955.

4. Van Oorschot, J. L. P. "Conversion of light energy in algal culture," Mededelingen van de Landbouwhogeschool to Wangeringen, Nederland, 55:225-277, (No. 5), 1955.

5. Gotaas, H. B., W. J. Oswald, and H. F. Ludwig. "Photosynthetic reclamation of organic wastes," The Sci. Monthly, 76:368-378, (No. 6), 1954.

6. Oswald, W. J. and H. B. Gotaas. "Photosynthesis in sewage treatment," Am. Soc. of Civil Engrs., Transactions, 122:73-105, 1957.

7. Oswald, W. J., H. B. Gotaas, C. G. Golueke, and W. R. Kellen. "Algae in waste treatment," Sewage and Ind. Wastes, 29:437-457, (No. 4), 1957.

8. Hintz, H. F., et al. "Nutritive value of algae grown on sewage," J. Animal Sci., 25:675-681, (No. 3), 1966.

9. Hintz, H. F. Private Communication, 1966.

10. Myers, J. "Algal culture," Encyclopedia of Chemical Technology. New York: Interscience Encyclopedia, Inc., 1957.

11. Birge, E. A. and C. Juday. "Plankton, its quantity and chemical composition," The Inland Lakes of Wisconsin. Wisconsin Geol. and Natl. Hist. Survey, Bull. 64, Sci. Series No. 13, 1922.

12. Bush, A. F., J. D. Isherwood, and S. Rodgi. "Dissolved solids removal from waste water by algae," Proc. Am. Soc. Civil Engrs., J. Sanit. Engr. Div., 1961.

13. Eyster, H. C. "Micronutrient requirements for green plants, especially algae," Algae and Man. Ed. D. F. Jackson, Plenum Press, N.Y., 1966.

14. Goldman, C. R. "Micronutrient limiting factors and their detection in natural phytoplankton populations," Primary Production in Aquatic Environments. Ed. C. R. Goldman, Univ. of Calif. Press, 1966.

15. Provasoli, L. "Micronutrients and heterotrophy as possible factors in bloom production in natural wastes," Algae and Metropol. Wastes, USPHS, Publ. No. W61-3, 1961.

16. Guillard, R. R. L. and V. Cassie. "Minimum cyanocolalamin requirements of some marine centric diatoms," Limn. and Oceanog., 8:161-165, (No. 2), 1963.

Preceding page blank

17. Parker, C. D. "Microbiological aspects of lagoon treatment," J. Water Poll. Control Fed., 34:149-161, (No. 2), 1962.

18. Bogan, R. H., O. E. Albertson, and J. C. Pluntz. "Use of algae in removing phosphorus from sewage," Proc. Am. Soc. Civil Engrs., J. Sanit. Engr. Div., SA 5, 86:1-20, 1960.

19. Bogan, R. H. "The use of algae in removing nutrients from domestic sewage," Algae and Metropol. Wastes, R. A. Taft Sanit. Eng. Center, Rept. W61-3, 1961.

20. __________. "Algae aid in sewage nutrient removals," Water and Sewage Works, 108:453-458, 1961

21. Fitzgerald, G. P. and G. A. Rohlich. "An evaluation of stabilization literature," Sewage and Ind. Wastes, 30:1213-1224, 1958.

22. Fitzgerald, G. P. "Stripping effluents of nutrients by biological means," Algae and Metropol. Wastes, R. A. Taft Sanit. Eng. Center, Rept. W61-3, 1961.

23. Oswald, W. J., C. G. Golueke, R. C. Cooper, H. K. Gee, and J. C. Bronson. "Water reclamation, algal production and methane fern in waste ponds," Intern. J. Air and Water Poll., 7:627-648,(No. 6), 1963.

24. Reid, G. W. and J. R. Assenzo. "Culture and harvesting of attached algae grown on domestic sewage," Part I, Water and Sewage Works, 108:248-250, Part II, ibid, 108:264-269, 1961.

25. Reid, G. W., M. J. Wilcomb, G. H. Sullivan, and R. C. Martin. Removal of Nitrogen and Phosphorus by Bio-oxidation Ponds. Progress Rept., Univ. of Okla., Res. Inst., Norman, Okla., 1963.

26. Enebo, L. "Algae protein, state of the art review," paper presented at the Engr. Foundation Res. Conf., Engr. of Unconventional Protein Production, Univ. of Calif., Santa Barbara, August 7-11, 1967.

27. Mitsuda, H. et al. "A new method for obtaining protein isolates from Chlorella algae, torula yeasts and other microbial cells," paper presented at Engr. of Unconventional Protein Production Conf., Santa Barbara, Calif., August 7-11, 1967.

28. Miller, R. L. and C. H. Ward. "Algal bioregenerative systems," Publ. No. SAM-TR-66-11, USAF, Sch. of Aerospace Medicine, Texas, 1966.

29. Oswald, W. J. Personal Communication, Univ. of Calif., Berkeley, 1967.

30. San Joaquin Waste Drain. San Joaquin Valley Drainage Investigation, State of Calif., Dept. of Water Resources, Annual Reports, 1965, 1966. Preliminary Report, 1967.

31. Brown, R. L. Private Communication, San Joaquin Valley Investigation, Fresno, Calif., 1967.

32. Amramy, A. Private Communication, Greater Tel-Aviv Waste Water Reclamation Project, Israel, 1966.

33. Melamed, A. Private Communication, Greater Tel-Aviv Waste Water Reclamation Project, Israel, 1967.

34. Gloyna, E. F. Waste Stabilization Pond Concepts and Experience. Wastes Disposal Unit, Div. of Environ. Health, WHO. Publ. 1-65, 1965.

35. Hermann, E. R. and E. F. Gloyna. "Waste stabilization ponds, III. formulation of design equations," Sewage and Ind. Wastes, 30:963-975, (No. 8), 1958.

36. Marais, B.v.R. and V. A. Shaw. "A rational theory for the desi of sewage stabilization ponds in Central and South Africa," Trans., S. Arf. Inst. Civil Engrs., 3:205, (No. 11), 1961.

37. Marais, B.v.R. "New factors in the design, operations and performance of waste stabilization ponds with special reference to health," Bull. World Health Organiza., 1965.

38. Oswald, W. J. "Light conversion efficiency in photosynthetic oxgenation," Ph.D. Thesis, Algal Res. Project, Sanit. Eng. Res. Lab., Univ. of Calif., Issue No. 6, I.E.R. Series 44, Jan., 1957.

39. _________. "Fundamental factors in stabilization pond design," Advances in Biological Waste Treatment. Ed. W. W. Eckenfelder and J. McCabe. Pergamon Press, 1963.

40. Rabinowitch, E. I. Photosynthesis and Related Processes, Vol. I, Part I. Interscience Publ. Inc., N.Y., 1945.

41. _________. Photosynthesis and Related Processes, Vol. II, Part I. Interscience Publ., Inc., N.Y., 1951.

42. _________. Photosynthesis and Related Processes, Vol. III, Part I. Interscience Publ., Inc., N.Y., 1956.

43. Kok, B. "On the efficiency of Chlorella growth," Acta Botan. Neerl., 1:445-467, 1952.

44. Golueke, C. G. "Over-all light energy conversion efficiency of a high-temperature strain of Chlorella pyrenoidosa," Physiol. Plant., 15:1-9, 1962.

45. Arnold, W. "A calorimetric determination of the quantum yield in photosynthesis," Photosynthesis in Plants. Ed. J. Franck and W. E. Loomis. The Iowa State College Press, 1949.

46. Myers, J. "Use of algae for support of the human in space," Life Sciences and Space Research II. Ed. M. Florlnin and A. Dollfus. Amsterdam: North-Holland Publ. Co., 1964.

47. Miller, R. L. and C. H. Ward. "Algal bioregenerative systems," Atmosphere in Space Cabins and Closed Environments. Ed. K. Kammermeyer, Appleton-Century-Crofts, N.Y., 1966.

48. Handbook of Chemistry and Physics. 47th Ed., The Chemical Rubber Co., 1967.

49. Warburg, O. and E. Negelein. "Uber den Einfluss der Wellenlaenge auf den Energieumsatz bei der Kohlensaeureassimilation," Zeitsch F., Physikal Chem., 106:191, 1923.

50. Emerson, R. and M. S. Nishimura. "The quantum requirement of photosynthesis," Photosynthesis in Plants. Ed. J. Franck and W. E. Loomis, The Iowa State College Press, 1949.

51. Moore, W. E. and B. M. Duggar. "Quantum efficiency of photosynthesis in Chlorella," Photosynthesis in Plants. Ed. J. Franck and W. E. Loomis, The Iowa State College Press, 1949.

52. Rieke, F. F. "Quantum efficiencies for photosynthesis and photoreduction in green plants," Photosynthesis in Plants. Ed. J. Franck and W. E. Loomis. The Iowa State College Press, 1949.

53. Kok, B. "The path of energy in photosynthesis," Encyclopedia of Plant Physiology, Vol. V, Part 1. Ed. W. Ruhland, Springer-Verlag, Berlin, 1960.

54. Bassham, J. A., K. Shibata, and M. Calvin. "Quantum requirement in photosynthesis related to respiration," Biochem. et Biophys. Acta, 17:332-340, 1955.

55. Emerson, R. and C. M. Lewis. "The dependence of the quantum yield of Chlorella photosynthesis on wavelength of light," Am. J. Bot., 30:165-178, (No. 3), 1943.

56. Rabinowitch, E. "Spectral efficiency of photosynthesis," Medical and Biological Aspects of Energies of Space. Ed. P. A. Campbell, Columbia Univ. Press, N.Y., 1961.

57. Bush, V. "Foreword," Algae Culture from Laboratory to Pilot Plant. Ed. J. S. Burlew. Publ. 600, Carnegie Inst. of Wash., 1953.

58. Miller, R. L. and C. H. Ward. "Algal bioregenerative systems," Atmosphere in Space Cabins and Closed Environments. Ed. K. Kammermeyer. Appleton-Century-Crofts, N.Y., 1966.

59. I.E.S. Lighting Handbook. Ed. J. E. Kaufman, Illuminating Eng. Soc., N.Y., 1966.

60. Haxo, F. T. "The wavelength dependence of photosynthesis and the role of accessory pigments," Comparative Biochemistry of Photoreactive Systems. Ed. M. B. Allen, 1960.

61. Syrett, P. J. "Nitrogen assimilation," Physiology and Biochemistry of Algae. Ed. R. A. Lewin, Acad. Press, N.Y., 1962.

62. Myers, J. "Culture conditions and the development of the photosynthetic mechanism,V. Influence of the composition of the nutrient medium," Plant Physiol., 22:590-597, 1947.

63. Tamiya, H. et al. "Kinetics of growth of Chlorella, with special reference to its dependence on quantity of available light and on temperature," Algae Culture From Laboratory to Pilot Plant. Ed. J. S. Burlew, Publ. 600, Carnegie Inst. of Wash., 1953.

64. Myers, J. and J. R. Graham. "On the mass culture of algae, III. Light diffusers; high vs. low temperature Chlorellas," Plant Physiol., 36:342-346, (No. 3), 1961.

65. Willard, H. K. Unpublished data. Re: Variations in Beer-Lambert Absorption Coefficient in Algal Ponds. Univ. of Calif., Berkeley, 1964.

66. Thomas, M. D. and G. R. Hill. "Photosynthesis under field conditions," Photosynthesis in Plants. Ed. J. Franck and W. E. Loomis, The Iowa State College Press, 1949.

67. Cramer, M. and J. Myers. "Effects of starvation of the metabolism of Chlorella," Plant Physiol., 24:255-264, (No. 2), 1949.

68. Kandler, O. and C. Sironval. "Photooxidation processes in normal green Chlorella cells, II. Effects of metabolism," Biochem. et Biophys. Acta, 33:207-215, 1959.

69. Brown, A. H. "The effect of light on respiration using isotopically enriched oxygen," Am. J. Bot., 40:719-729, 1953.

70. Brown, A. H. and G. C. Webster. "The influence of light on the rate of respiration of the blue-green algal anagaena," Am. J. Bot., 40:753-758, 1953.

71. Hoch, G. and O. H. Owens. "Photoreactions and respiration," Photosynthetic Mechanism of Green Plants. Publ. No. 1145, Natl. Acad. of Sci., 1963.

72. Hoch, G., O. H. Owens, and B. Kok. "Photosynthesis and respiration," Arch. Biochem. and Biophys., 101:171-180, 1963.

73. Tsuchiya, H. M., A. G. Fredrickson, and R. Aris. "Dynamics of microbial cell populations," Advances in Chemical Eng., 6:125-206, 1966.

74. Steele, J. H. "Notes on some theoretical problems in production ecology," Primary Productivity in Aquatic Environments. Ed. C. R. Goldman, Univ. of Calif. Press, 1966.

75. Riley, G. A. "Theory of food chain relations in the ocean," The Sea, 2:438-463, Ed. M. N. Hill, 1963.

76. Lumry, R. and J. S. Rieske. "The mechanism of the photochemical activity of isolated chloroplasts, Part V. Interpretation of the rate parameters," Plant Physiol., 34:301-305, 1959.

77. Bassham, J.A. "Photosynthesis: The path of carbon," Plant Biochemistry. Ed. J. Bonner and J. E. Varner, Acad. Press, 1965.

78. Tamiya, H. "Analysis of photosynthetic mechanism by the method of intermittent illumination, II. Theoretical part," Studies from the Tokugawa Inst., 6:43-132, (No. 2), The Tokugawa Inst. for Biol. Res., Tokyo, Japan, 1949.

79. Kok, B. "Photosynthesis in flashing light," Biochem et Biophysiol. Acta, 21:245-258, 1956.

80. Brackett, F. S. "Light intensity and CO_2 concentration as factors in photosynthesis of wheat," Cold Spring Harbour Symp. Quant. Biol., 3:117-135, 1956.

81. Kok, B. and J. A. Businger. "Kinetics of photosynthesis and photoinhibition," Nature, 117:135, 1956.

82. Teissier, G. "Croissance Des Populations Bacteriennes et Quantite D'aliment Disponible," Rev. Sci., Extrait du No. 3208, 1942.

83. Sorokin, C., "The effect of the past history of cells of Chlorella on their photosynthetic capacity," Physiol. Plantarum, 11:275-283, 1958.

84. Sorokin, C. and R. W. Krauss. "Relative efficiency of photosynthesis in the course of cell development," Biochem. et Biophys. Acta, 48:314-319, 1961.

85. Sorokin, C. and R. W. Krauss. "Effects of temperature and illuminance on Chlorella growth uncoupled from cell division," Plant Physiol., 37:37-42, 1962.

86. Tamiya, H. and Y. Chiba. "Analysis of photosynthetic mechanism by intermittent illumination, I. Experiments part," Studies from the Tokugawa Inst., 6:1-42, (No. 2), 1949.

87. Tamiya, H., K. Iwamura, K. Shibata, E. Hase, and T. Nihei. "Correlation between photosynthesis and light-independence metabolism in the growth of Chlorella," Biochimica et Biophysica. Acta, 12:32-40, 1953.

88. Rieske, J. S., R. Lumry, and J. D. Spikes. "The mechanism of the photochemical activity of isolated chloroplasts, Part III. Dependence of velocity on light intensity," *Plant Physiol.*, *34*:293-300, 1959.

89. Miller, R. L. *et al*. "Hydromechanical method to increase efficiency of algal photosynthesis," *I/EC Process Design and Development*, *3*:134-143, (No. 2), 1964.

90. Fredrickson, A. G. *et al*. "Optimum conditions for photosynthesis in optically dense culture of algae," *J. Am. Rocket Soc.*, *31*:1429-1435, 1961.

91. Kamen, M. D. *Primary Processes in Photosynthesis*. Acad. Press, 1963.

92. Powell, C. K. "The motion of algae in turbulent flow." Ph.D. Thesis, Purdue Univ., 1963.

93. Agramowitz, M. and I. A. Stegun. *Handbook of Mathematical Functions*. Dover Publ.,Inc., N.Y., p. 229, *1964*.

94. Fogg, G. E. *The Metabolism of Algae*. Methuen and Co., Ltd., London, 1953.

95. __________. "Nitrogen nutrition and metabolic patterns in algae," *Sym. Soc. Exptl. Biol.*, No. 3, 1959.

96. Krauss, R. W. "Physiology of the fresh-water algae," *Ann. Rev. Plant Physiol.*, *9*:207-244, 1958.

97. Syrett, P. J. "Nitrogen assimilation of green algae (Chlorophyceae)," *Sym. Soc. Gen. Microbiol.*, No. 4, 1954.

98. McKee, H. S. *Nitrogen Metabolism in Plants*. Clarendon Press, Oxford, 1962.

99. Parsons, T. R., K. Stephens, and J. D. H. Strickland. "On the chemical composition of eleven species of marine phytoplankters," *J. Fish Resources*, *18*:1001-1016, 1961.

100. Spoehr, H. A. and H. W. Milner. "The chemical composition of Chlorella effect of environmental conditions," *Plant Physiol.*, *24*:120-144, 1949.

101. Krauss, R. W. "Nutrient supply for large-scale algal cultures," *Scientific Monthly*, *80*:21-28, 1955.

102. Nihei, T., T. Sasa, S. Miyachi, K. Suzuki, and H. Tamiya. "Change of photosynthetic activity of Chlorella cells during the course of their normal life cycle," *Arch. Microbiol.*, *21*:155-164, 1954.

103. Fogg, G. E. "Nitrogen nutrition and metabolic patterns in algae," *Symp. Soc.*, *Exp. Biol.*, *13*:106-125, 1959.

104. Gerloff, G. C. and F. Skoog. "Cell contents of nitrogen and phosphorus as a measure of their availability for growth of Microcystis aeruginosa," *Ecology*, *35*:348-353, (No. 3), 1954.

105. Gerloff, G. C. and F. Skoog. "Nitrogen as limiting factor of growth of Microcystis aeruginosa in Southern Wisconsin Lakes," *Ecology*, *38*:556-561, (No. 4), 1957.

106. Gerloff, G. C. and P. H. Krombholz. "Tissued analysis as a measure of nutrient availability for the growth of angiosperm aquatic plants," *Limn. and Oceanog.*, *11*:529-537, (No. 4), 1966.

107. Nicholas, D. J. D. "Metallo-enzymes in nitrate assimilation of plants with special reference to microorganisms," Sym. Soc. Exptl. Biol., (No. 13), 1959.

108. Jones, R. F. A discussion of paper: "Seasonal cycles and seccession of societies," by G. A. Riley. In Marine Biology II. Ed. C. H. Oppenheimer, Acad. of Sci., N. Y., 1966.

109. Caperon, J. W. "The dynamic of nitrate limited growth of Isochrysis galbana populations,"Ph.D. Thesis., Univ. of Calif., San Diego, 1965.

110. Rodhe, W. "Environmental requirements of fresh water plankton algae," Sym. Bot. Upsalienses, 10:1-149, (No. 1), 1949.

111. Osterlind, S. "Growth conditions of the algae Scenedesmus quadricauda," Sym. Bot. Upsalienses, 10:1-141 (No. 3), 1949.

112. Gerloff, G. C. et al. "The mineral nutrition of Coccohloris peniocystis," Am. J. Bot., 37:835, 1950.

113. Williams, F. M. "Population growth and regulation in continuously cultured algae," Ph.D. Thesis, Yale Univ., 1965.

114. Jewell, W. Private Communication. Stanford Univ., 1968.

115. Ketchum, B. H. "Mineral nutrition of phytoplankton," Ann. Rev. Plant Physiol., 5:55-74, 1954.

116. Fogg, G. E. Algal Cultures and Phytoplankton Ecology. The Univ. of Wis. Press, 1965.

117. ________. "Nitrogen fixation," Physiology and Biochemistry of Algae. Ed. R. A. Lewin, Acad. Press, N. Y., 1962.

118. Neel, J. K. et al. "Experimental lagooning of raw sewage at Fayette, Missouri," J. Water Poll. Control Fed., 33:606-641, 1961.

119. Hermann, E. R. "Stabilization pond as a nitrate reducing reactor," Proc. Am. Soc. Civil Eng., SA 5, 88:1-20, 1962.

120. Golueke, C. G., W. J. Oswald, and H. K. Gee. "Effect of nitrogen additives on algal yield," J. Water Poll. Control Fed., 39:823-834, 1967.

121. Witt, V. M. "Nitrogen and phosphorus removal from secondary sewage plant effluents by algal," Ph.D. Thesis, Univ. of Mich., 1959.

122. Gaur, A. C., W. O. Pipes, and H. B. Gotaas. "Culture of Oscillatoria in organic wastes," J. Water Poll. Control Fed., 32:1060-1065, (No. 10), 1960.

123. Gates, W. E. and J. A. Borchardt. "Nitrogen and phosphorus extraction from domestic waste water treatment plant effluents by controlled algul culture," J. Water Poll. Cont. Fed., 36:443-462, (No. 4), 1964.

124. Monod, J. "The growth of bacteria culture," Ann. Rev. Microbiol., 3:371, 1949.

125. ________. "Recherches sur la Croissance des Culture Bacteriennes," Herman and Cie, Paris, 1942. Ann. Inst. Pasteur, 79:390, 1950.

126. Herbert, D., R. Elsworth, and R. C. Telling. "The continuous culture of bacteria, a theoretical and experimental study," J. Gen. Microbiol., 14:601-622, 1956.

127. Herbert, D. "A theoretical analysis of continuous cultures systems, Continuous Culture of Microorganism, SCI Monograph No. 12, London, p. 21, 1961.

128. Northam, J. I. "The course of bacterial population growth in batch and continuous culture according to the theory of Monod," J. Biochem. Microbiol., Tech. Eng., 1:349, 1959.

129. Wilson, I.S. "Concentration effects on the biological oxidation of trade wastes," Proc. Second International Conf. of Water Poll. Res., London, 1962.

130. Gram, A. L. Reaction Kinetics of Aerobic Biological Processes. Rept. No. 2, IER Series 90, SERL, University of Calif., Berkeley, 1956.

131. Heukelekian, H., H. E. Oxford, and R. Manganelli. "Factors affecting the quantity of sludge production in the activated sludge process," Sewage and Ind. Wastes, 23:945, 1951.

132. Stewart, M. J. Reaction Kinetics and Operational Parameters of Continuous Flow Anaerobic Fermentation Processed. Sanit. Eng. Res. Lab., Publ. No. 4, IER Series 90, Univ. of Calif., Berkeley, June 1958.

133. Agardy, F. J., R. D. Cole, and E. A. Pearson. Kinetic and Activity Parameters of Anaerobic Fermentation Systems. SERL Rept. No. 63-2, Univ. of Calif., Berkeley, February 1963.

134. Andrews, J. F., R. D. Cole, and E. A. Pearson. Kinetics and Characteristics of Multistage Methane Fermentations. SERL Rept. No. 64-11, Univ. of Calif., Berkeley, December 1964.

135. Shea, T. G. Private Communication. Univ. of Calif., 1967.

136. Pearson, E. A. Kinetics of Biological Treatment. Lecture series on Advances in Water Quality Improvement, Univ. of Texas, Austin, 1966.

137. Moser, H. The Dynamics of Bacterial Populations Maintained in the Chemostat. Publ. 614, Carnegie Inst. of Wash., 1958.

138. Kok, B. and J. L. P. Van Oorschot. "Improved yields in algal mass cultures," Acta Bot. Neerlandica, 3:533-546, (No. 4), 1954.

139. Oswald, W. J. "Light conversion efficiency of algae grown in sewage," Trans., Am. Soc. Civil Eng., 128:47-83, (No. 3395), 1963.

140. ________. Light Conversion Efficiency in Photosynthetic Oxygenation. Series 44, (No. 6), Inst. of Eng. Res., Univ. of Calif., 1957.

141. Oswald, W. J., C. G. Golueke, and D. O. Horning. "Closed ecological systems," Proc. Am. Soc. Civil Eng., J. Sanit. Eng. Div., 91:23-46, (No. 4445), 1965.

142. Golueke, C. G., W. J. Oswald, and H. K. Gee. A Study of Fundamental Factors Pertinent to Microbiological Waste Conversion in Control of Isolated Environments. First Tech. Rept., Rept. No. 64-5, Sanit. Eng. Res. Lab., Univ. of Calif., 1964.

143. Shelef, G., C. G. Golueke, W. J. Oswald, and H. K. Gee. A Study of Fundamental Factors Pertinent to Microbiological Waste Conversion in Control of Isolated Environments. Final Rept., Rept. No. 66-8, Sanit. Eng. Res. Lab., Univ. of Calif., 1966.

144. Shelef, G., W. J. Oswald, and C. G. Golueke. Study of a Combined Photosynthetic Waste Reclamation Reactor for Closed Cycle Bioregenerative Life Support. In preparation. Contract No. F 41609-67-C-0002, USAF Aerospace Medical Div., 1967.

145. Bassham, J. A. Private Communication. 1967.

146. Briggs, G. E. and C. P. Whittingham. "Factors affecting the rate of photosynthesis of Chlorella at low concentrations of carbon dioxide and in high illumination," New Physiologist, 51:236-249, 1952.

147. Eyster, H. C. Mineral Nutrient Requirements of Chlorella Sorokiniana in Continuous Pure Culture. Rept. No. SAM-TR-67-40, USAF, Sch. of Aerospace Medicine, 1967.

148. Moon, P. The Scientific Basis of Illuminating Engineering. Dover Publ., Inc., N. Y., 1961.

149. Myers, J. Private Communication. April and August 1967.

150. Jenkins, D. Analytical Methods. Sanit. Eng. Res. Lab., Univ. of Calif., Berkeley, 1966.

151. Ward, C. H. and J. E. Moyer. "Ecologic relationships between bacteria and algae in mass culture," paper presented at the Conf. of Bioregenerative Systems. Sponsored by NASA, Wash. D.C., 15-16 November 1966.

152. Standard Methods for Examination of Water and Waste Water. 12th Ed., Amer. Public Health Assoc., 1965.

153. Official Methods of Analysis of the Association of Official Agricultural Chemists. 9th Ed., Assoc. of Official Agr. Chemists, Wash., D.C., 1960.

154. McKinney, G. "Absorption of light by Chlorophyll solutions," J. Biol. Chem., 140:315, 1941.

155. Sorokin, C. and R. W. Krauss. "Effects of temperature and illuminance on Chlorella growth uncoupled from cell division," Plant Physiol., 37:37-42, 1962.

156. Sorokin, C. "Tabular comparative data for the low and high temperature strains of Chlorella," Nature, 184:613-614, (No. 4686), 1959.

157. ________. "Kinetic studies of temperature effects on the cellular level," Biochem. et Biophys. Acta, 38:197-204, 1960.

158. Sorokin, C. and R. W. Krauss. "The dependence of cell division in Chlorella on temperature and light intensity," Am. J. Bot., 52:331-339, (No. 4), 1965.

159. Pickett, J. M. and J. Myers. "Monochromatic light saturation curves for photosynthesis in Chlorella," Plant Physiol., 41:90-98, (No. 1), 1966.

160. Sorokin, C., "Time course of oxygen evaluation during photosynthesis in synchronized cultures of algae," Plant Physiol., 36:232-239, 1961.

161. Arnon, E. I. "Micro-elements in culture solution experiments with higher plants," J. Am. Bot., 25:322-325, 1938.

162. Handbook of Mathematical Tables. 2nd Ed., The Chemical Rubber Co., p. 320, 1964.